Singlet Oxygen Generation and Photo-oxidation Reactions in Supercritical Fluid Carbon Dioxide

by

Najya Muhammed

BSc (Hons)

A Doctoral Thesis

Submitted in partial fulfilment of the requirement

for the Award of

Doctor of Philosophy

at Loughborough University

To my late Dad who passed away just a few week after submitting my thesis, Additionally to my grandmother and Cousin, Tatu Saburi and Mahmoud Salim aka Henry for all the love and the best educational support any child could ever be given.

Acknowledgements

First of all I would to thank Allah (SWT) for having made everything possible by giving me strength and courage to complete this work.

My deepest gratitude then goes to my supervisor Dr. David Worrall for his unselfishness continuous guidance, encouragement and support throughout this research, much appreciated. Thanks also to Ustadh Ali Samuel for giving me the best introduction to the world of chemistry during my high School. Also my sincere thanks to all the chemistry lecturers for continuing to ensure that I received the best knowledge in this field. Special thanks to Dr Siân Worrall for her help, suggestions and useful discussions. I would also like to thank Will Simpson, for his contribution with some of the data in this thesis.

I also would like to thank my parents for all their love and support especially my mum, throughout my educational journey. I also thank my brother Babli for his love and mostly the financial incentives which have always come in handy especially for my love of food. I would also like to express my sincere appreciation to my aunt and uncle especially Rukiya for believing in me so much more than I could believe in myself to further my education to the highest ranks. Thanks also to the rest of my very big family for their support and the humour which really did take me through the tough times of my life. And thanks to my newly acquired family (Fatma et al) in UK for accepting me and making me feel as if I have always been part of her family from day one.

I would also like to acknowledge the EPSRC for financial support. And to my fellow researchers and friends at Loughborough for their advice and friendship including, Aisha, Shabana, Lina, James and Ian.

Lastly I would like to thank all the chemistry departmental auxiliary staffs who really formed the backbone of my research as without them it would not have been easy to order chemicals or even run some technical equipments and last but not least I would like to thank everyone and anyone that I may have forgotten to mention.

CONTENTS

Abstract

Oxygen is remarkable in that it has a triplet ground state, a $^3\Sigma_g$ state, with its first two excited states being of singlet multiplicity ($^1\Delta_g$ and $^1\Sigma_g^+$, lying 94 kJ mol^{-1} and 158 kJ mol^{-1} above the ground state, respectively). Relaxation of the singlet state to the ground state is consequently spin forbidden, resulting in a long lifetime for singlet oxygen. Singlet oxygen is a highly reactive species and is responsible for oxidative damage in a number of systems. In this study, singlet oxygen quantum yields, Φ_Δ, have been measured at varying temperatures and pressures, as a function of oxygen concentration, in supercritical fluid carbon dioxide.

Φ_Δ values were measured in supercritical carbon dioxide and anthracene relative to perinaphthenone as a standard sensitiser, for which Φ_Δ is 0.95 ± 0.05 and is suggested to be insensitive to changing solvent[1]. Due to the chemical and biological importance of singlet oxygen quenching in conventional solvents has been studied in depth[2], although few studies have been made in supercritical fluid carbon dioxide[3-5] and indeed these have not reported quantum yields. High-pressure cell design presents unique challenges in this area, and by utilising near-IR detection techniques and carefully controlled sample geometries coupled with extensive and equipment sample characterisation it is possible to determine reliable quantum yield values of less than one, which in previous studies[6] were found to be greater than one.

Using perinaphthenone as a reference sensitise in supercritical carbon dioxide, at 44.5 °C and 200 kg m^{-2} at an absorbance range of 0.1 to 1, singlet oxygen quantum yields of anthracene obtained in supercritical carbon dioxide ranged from approximately 0.21 to 0.85, (based on perinaphthenone $\Phi_\Delta = 0.95$). Further work was also done to establish if a systematic variation with concentration, pressure and temperature exists.

Flavins such as Lumiflavins, Roseoflavin etc were studied, these compounds are very important in photobiological studies as further studies of their quantum yields and fluorescence quenching were then investigated which eventually were then used as sensitisers on the formation of juglone . Their triplet-triplet spectra were also recorded.

Photooxidation conversion of 1,5-dihydroxynaphthalene to Juglone was followed by using super critical carbon dioxide as a solvent and looking at the influence of pressure and temperature on the rates. This study made it possible to carry out the synthesis using super critical carbon dioxide and this was further proven with IR and NMR spectra in comparison to the original spectra of the pure Juglone.

There were no obvious trends of the relationship between temperature and pressure but there was a clear increase of rate of formation on Juglone with increase of pressure.

References

1. R.Schmidt, C. Tanielian, R. Dunsbach and C. Wolff, *J Photochem. Photobiol A: Chem* **1994** ;79:**1-2** 11

2. R. Schmidt, *Photochem. Photobiol.* **2006** ;82(5): 1161

3. D.R.Worrall, A.A. Abdel-Shafi, F.Wilkinson, *J. Phys. Chem.A* **2001**; 105: 1270.

4. M. Okamoto, T. Takagi, F. Tanaka, Chem. Lett. **2000** ;12: 1396.

5. A.A. Abdel-Shafi and D.R. Worrall, *J Photochem. Photobiol A:* Chem. **2007** ;**186:** 263

Glossary of Terms

λ = Wavelength (metres)

ν= Frequency of radiation, no. of complete cycles per second (Hz)

c = Speed of light in a vacuum (2.998×10^{8} m s^{-1})

h = Planck's constant (6.63×10^{-34} Js)

N_A = Avogadro's number (6.023×10^{23} mol^{-1})

l = Pathlength through the solution (cm)

ε = Decadic molar absorption coefficient (l mol^{-1} cm^{-1})

k_{obs} = Observed rate constant (s^{-1})

k_d = Decay rate constant (s^{-1})

σ, σ^*= Sigma bonding and antibonding, respectively

π, π^* = Pi bonding and antibonding, respectively

Ψ = Wavefunction

M = Spin multiplicity

IC = Internal conversion

ISC = Intersystem crossing

VR = Vibrational relaxation

τ_r^0 = Natural lifetime of a species

Φ_T = Triplet quantum yield

Φ_Δ = Singlet oxygen quantum yield

SCF= Supercritical fluid

$ScCO_2$ = Super critical carbon Dioxide

$^1\Sigma_g^+$ = Second excited singlet state of oxygen

$^1\Delta_g$, = First singlet excited state of oxygen (singlet oxygen)

$^3\Sigma_g^-$ = Ground state oxygen

η = Viscosity

Abs = Absorbance

I_0 = Incident light/ radiation intensity

I = Transmitted light intensity

c = Concentration (mol l^{-1})

k_q^T = Triplet quenching rate constant (l mol^{-1} s^{-1})

k_q^S = Singlet quenching rate constant (l mol^{-1} s^{-1})

[Q] = Concentration of quencher (mol l^{-1})

ΔG_{CET} = Free enthalpy change for complete energy transfer

E_{CT} = Energy of charge transfer state

F = Faradays constant (9.6485×10^4 Coulomb mol^{-1})

E_T = Triplet energy

E_a = Activation energy (kJ mol^{-1})

R = Ideal gas constant (8.3145 J K^{-1} mol^{-1})

ρ = Density (g cm^{-3})

V = Volume (m^3)

M_r = Molecular mass (g mol^{-1})

DHDN = 1,5-Dihdroxy Naphthalene

RB = Rose Bengal

MB = Methylene Blue

AcN = Acetonitrile

Anth = Anthracene

Sens = Sensitiser

All = Alloxazine

Chapter 1

Introduction

1.0 Introduction

1.1.1 Photochemistry

Photochemistry as the name suggests is the study of chemical changes initiated by light energy[1], usually absorption of the ultraviolet and visible regions of the electromagnetic spectrum. The Grotthus-Draper Law states that only the radiation actually absorbed by the reacting system can initiate reaction and a more satisfactory version of the Stark-Einstein law states that if a species absorbs radiation, then one particle is excited for each quantum of radiation absorbed.

The frequency, wavelength and energy of light are related by the Planck's law equation (equation 1.1) which refers to the primary photochemical process of a species, in which photons of radiation of specific frequency ν had associated with them a fixed energy E. These processes may induce secondary reactions including chain reactions consuming many further molecules of the starting material without the need for more light.

$$E = h\upsilon = \frac{hc}{\lambda} \qquad \textbf{1.1}$$

Where h = Planck's constant (6.63×10^{-34} Js)

c = Velocity of light (2.998×10^{8} ms^{-1})

λ = Wavelength (m)

υ = Frequency of radiation (Hz)

Accordingly photons can also be calculated using a linear relationship between energy per mole E and wavelength λ as shown in equation 1.2;

$$E = \frac{Nhc}{\lambda} \qquad \textbf{1.2}$$

Where N = Avogadro's number (6.023×10^{23} mol^{-1})

c = Velocity of light in a vacuum (2.998×10^{8} ms^{-1})

λ = Wavelength (m)

When a photon passes close to a molecule there is an interaction between the electrical field associated with the molecule and the electric field associated with the radiation. This interaction may not result in a permanent change in the molecule, but it is possible for an interaction to occur in which the photon is absorbed by the

molecule, thus changing its electronic structure. This occurs when the molecule absorbs a quantum of radiation whose energy corresponds to a transition within the molecule. In terms of molecular orbitals this means a change in the occupation of states from the ground to an excited state. The energy of the photon may not match exactly the energy difference between the lowest vibrational levels of the ground and excited state of the absorbing molecule, the energy of the photon may be in excess. When this occurs an upper vibrational level in the excited state is initially populated but quickly loses its energy to relax back down to the lowest vibrational level.

1.1.2 Beer Lambert Law

The absorption of an appropriate photon of light can cause a molecule to form an electronically excited state which may possess different electronic and nuclear properties to the ground state. The Beer Lambert law is a linear relationship between absorbance and concentration of an absorbing compound. As shown in equation 1.3, it is used to describe the fraction of light absorbed by a solution of low concentration (homogeneously absorbing system) of absorber at a given wavelength.

$$A = \varepsilon c l = \log_{10} \frac{I^o}{I} \qquad 1.3$$

Where A is the measured absorbance of a given molecule at a frequency ν related to concentration c (mol l^{-1}), I^0 and I are the intensities of the incident and transmitted light intensities respectively, at a pathlength l of l (cm), ε is the molar absorption coefficient (l $mol^{-1}cm^{-1}$), hence this relationship shows the amount of light absorbed per unit concentration.

1.1.3 Electronic Structure of Molecules

The electrons in a molecule occupy molecular orbitals; together with wavefunctions these can be used to describe the positions of electrons in a molecule. One molecular orbital is a bonding orbital and the other is an antibonding orbital. The bonding molecular orbital is more stable than the initial atomic orbitals and the antibonding molecular orbitals are of higher energy than the initial atomic orbital and therefore less stable. There are five types of molecular orbitals which have been distinguished, σ and π bonding, σ* and π* antibonding and n, non-bonding.

Molecular orbitals are often formulated from linear combinations of the valence shell atomic orbitals, as shown in the figure 1.2:

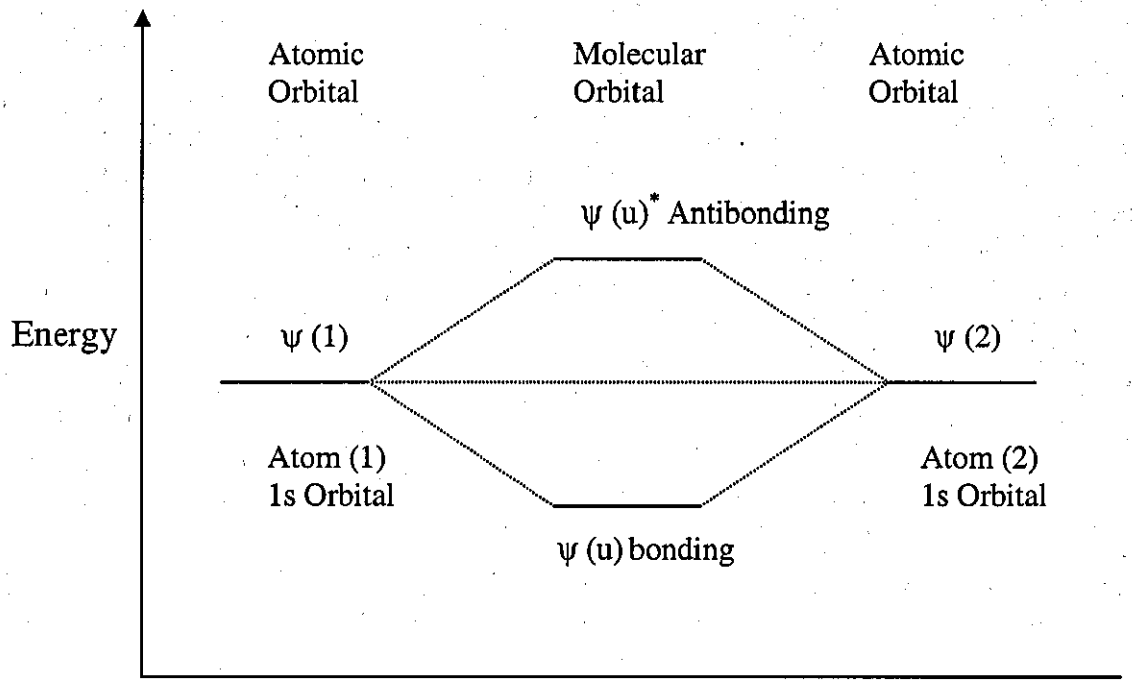

Figure 1.2: Energy levels of s-s atomic and molecular orbitals

Wavefunctions $\Psi(x, y, z)$ are often used to represent the spatial properties, momentum and energy of states. The modulus of the square of the wavefunctions can be used to define the electron probability density, the probability of finding electrons in given configurations is then equal to multiplying $\Psi(x, y, z)^2$ by the volume concerned (dx, dy, dz). Wavefunctions describe the energy state and can be separated into electronic and vibrational components denoted by ϕ or χ respectively.

1.1.4 Pauli's exclusion principle

Pauli's exclusion principle states that no two electrons in an atom can have identical quantum numbers, which means that each orbital may hold a maximum of two electrons whose spin must be paired. These orbitals can be in the form of: bonding (σ or π), non bonding (n) and anti-bonding (σ^* or π^*) which are of lower, equal and higher energy respectively than the atomic orbitals from which they are constructed. Orbitals which are symmetric about the internuclear axis are designated σ and σ^* and have high electron density for bonding orbitals along the molecular axis. Whilst

π orbitals are formed if 2px or 2py orbitals are mixed and n orbitals if non bonding valence shell electrons are present. All of these orbitals have different relative energies as shown in figure 1.3 and transitions induced between these levels by the absorption of a photon leading to an excited state. n → π*, π → π*, n → σ* and σ → σ* are common transitions in organic compounds and some of these transitions can produce a singlet or a triplet state (see section 1.15).

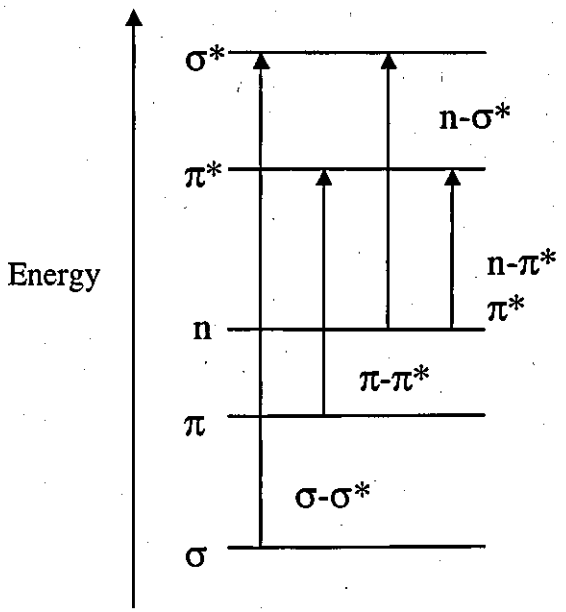

Figure 1.3: Relative energies of the different transitions

Wavefunctions Ψ(x, y, z) are often used to represent the spatial properties, momentum and energy of states. The quantum aspect of a system can be represented using wavefunctions ψ (x, y, z) which is defined by the Schrödinger equation as shown below:

$$-\frac{\hbar^2}{2m}\frac{d^2\psi(x)}{dx^2}+\frac{\omega^2 m}{2}x^2\psi(x)=E_n\psi(x) \qquad \textbf{1.4}$$

ψ = Schrödinger wavefunction

Where E_n = energy eigenvalue

dx^2 = position (x, y, z)

h = Planck constant (6.63×10^{-34} Js)

m = Mass (Kg)

E = Energy (J)

V = Potential energy (J)

1.1.5 Spin multiplicity

The spin multiplicity is defined as M = 2S+1, where S is the vector total spin quantum number from each electron. For spin paired electrons S will be equal to zero whilst for two electrons with parallel spins S will be one. Each electron in a molecule has a spin quantum number of ½ which can either correspond to spin magnetic quantum numbers m_s= ½ and m_s= -½ these two orientations depend on the electron's alignment with respect to a specified axis. Therefore M = 1 for a singlet and 3 for a triplet state, by using a symbol S_0 to denote a singlet ground state and excited state singlets by S_1, S_2, S_3 etc with the subscript denoting increasing energy. Triplet states follow the similar pattern with T_1 being usually the lowest triplet state and increasing in energy as T_2, T_3, T_4 etc

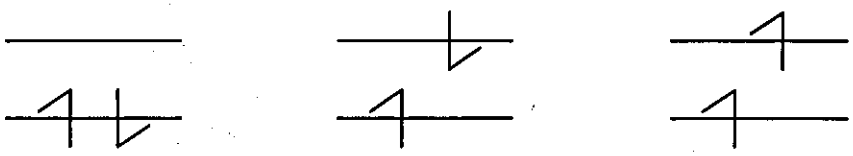

Ground State Singlet (spin paired S=0) | Excited State Singlet (spin preserved S=0) | Excited State Triplet (spin inverted S=1)

Figure 1.4: Representation of spin orientation in singlet and triplet excited states

Since the Pauli exclusion principle states that an orbital can never have more than two electrons in it (i.e. that no two electrons can have the same set of quantum numbers), electrons occupying the same orbital must have paired spins in the form of m_s= ½ and m_s= -½. According to Hund's rule there are two ways of arranging electrons within a set of degenerate orbitals but keeping the repulsion between the energy to a minimum:

- electrons will occupy different orbitals whenever energetically possible
- two electrons occupying degenerate orbitals will have parallel spins in their lowest energy state

Therefore as most molecules in their ground state contain an even number of electrons, the electrons will be spin paired and hence the ground state will be a singlet state. Electron repulsion is minimised where spins are parallel, so consequently triplet states have lower energies than their corresponding singlet states and a promotion of an electron from the ground state can give rise either to an

excited singlet or an excited triplet. Accordingly the triplet ground state is T_0 and the excited triplets are T_1, T_2 etc. Not many molecules have a triplet ground state, one of the few molecules that does is molecular oxygen, due to the lone pair of electrons in its outer shell which occupy separate, degenerate orbitals.

Selection rules may be used to establish whether a transition between two states is likely to occur. There are 3 types of selection rules; transitions are usually referred to as either allowed or forbidden

- **Spin selection rule**: The radiative transition should take place with no change in the total electron spin, i.e. $\Delta S = 0$.
- **Orbital symmetry selection rule:** Relating to diatomic and linear molecules. Transitions involving a large change in the orbital angular momentum are forbidden, therefore electron should occupy the same region of space after light absorption, i.e. $\Delta L = \pm 1$.
- **Orbital overlap rule**: for a transition to be allowed there must be a good spatial "overlap" between the orbitals of the state involved, hence π to π^* is allowed whereas n to π^* is not.

1.1.7 Electronic Transitions

1.1.7 Franck-Condon Principle

The Franck-Condon principle states that 'since electronic transitions are much faster than nuclear motion, electronic transitions occur most favourably where the nuclear structure of the initial and final states are most similar'. Hence, the more vibrational wavefunctions level overlap the more likely the transition will happen and this is determined by the probability of finding a nucleus at a given internuclear distance in a given vibrational level v, for each vibrational level (v) there are v+1 maxima, and the transition is most likely to occur from a v maximum in the lower state vertically upwards to the v' level in the upper state having the best overlap. Each state has vibrational levels associated with it and each vibrational level has a wavefunction associated with it, as the vibrational levels increase the number of nodes increases.

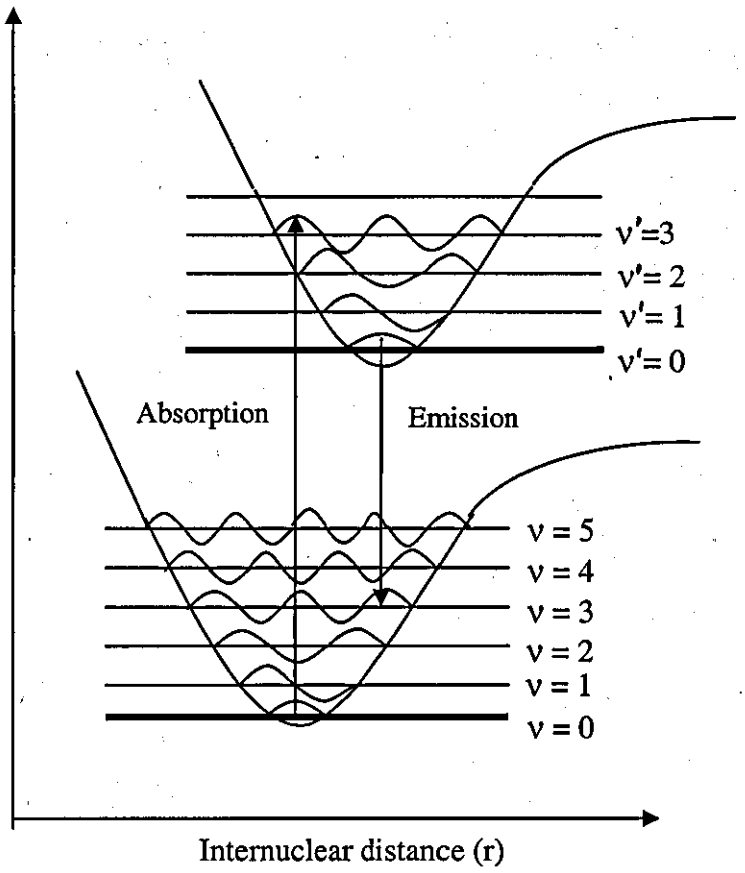

Figure 1.5: Diagram illustrating the Franck-Condon principle

For a given vibrational level v, there will be v + 1 maxima and v nodes between the maxima for the vibrational wavefunction of the particular vibrational level. From the energy diagram the best vibrational overlap for absorption is between v = 0 to v = 3, corresponding to the highest intensity, the same rationale is applied to the emission process. According to the Boltzmann distribution, at room temperature the majority of molecules in the lower electronic energy state are located in the lowest vibrational energy level of that state, hence the most favoured transitions occur from $v'=0$.

1.2 The Jablonski diagram

There are a number of pathways available for the dissipation of energy and deactivation of the excited state. The Jablonski diagram can be used to show the electron excited states and transitions between the states of molecules used to represent the electronic excited states and the fundamental processes that occur from such states. Excited states are defined in terms of the total spin angular momentum.

Since S_0 is the singlet ground state and S_1, S_2, S_3 etc are the electronically excited singlet states, increasing in energy. Applying the same rationale to triplet states, T_0 is the triplet ground state and T_1, T_2 etc are the electronically excited triplet states. Each state has vibrational and rotational levels associated with it.

Radiative processes involve the emission of electromagnetic radiation (photons) from a molecule to return to the ground state.

Non-radiative processes involve a transition between states of either the same or different multiplicity, to return to the ground state without the emission of electromagnetic radiation. The principal transitions are as follow:

- Singlet to singlet and triplet to triplet absorptions preserve spin orientation and are therefore spin allowed, and consequently correspond to strong transitions.
- Singlet to triplet absorption requires spin flip and is spin forbidden, consequently such transitions are of low intensity

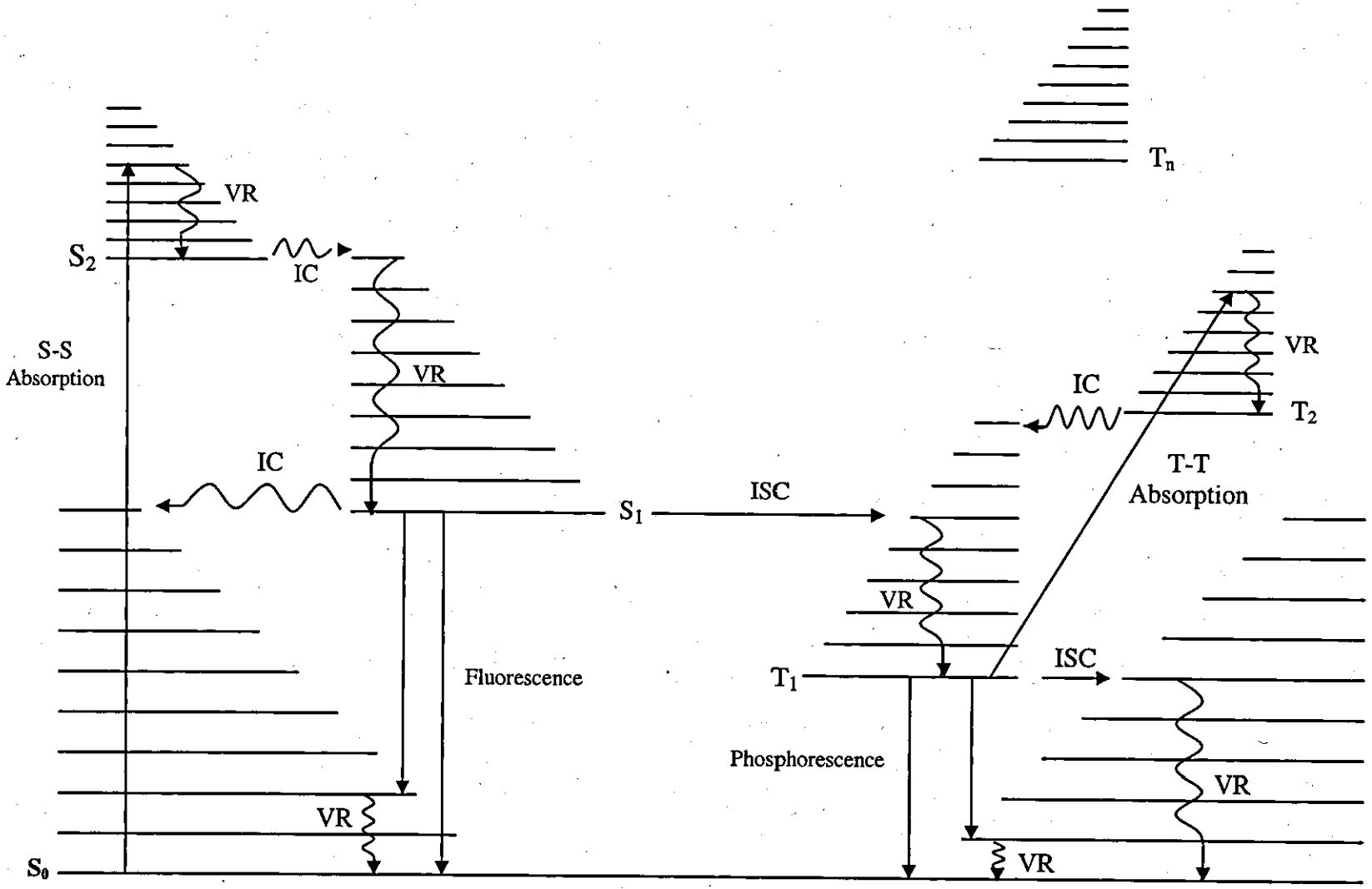

Figure 1.6: The Jablonski Diagram illustration for singlet and triplet states

1.2.1 Singlet State

Absorption conventionally occurs from the singlet ground state to the singlet excited state as shown in figure 1.6; a higher level than S_1 may be initially populated, but from here rapid vibrational relaxation occurs to populate the lowest electronically excited state, S_1. The transitions can be described as radiative or non radiative and can be spin allowed or spin forbidden. From here there are 3 main intramolecular possibilties[2]:

1. **Fluorescence:**

$$^1A^* \longrightarrow {}^1A + h\upsilon \qquad 1.5$$

Fluorescence usually occurs from the lowest vibrational level in the singlet state and is a relatively fast transition, since it is spin allowed, occurring on timescales of the order of 10^{-10} to 10^{-6} s^{-1}. This is a radiative transition which is spin allowed since it occurs between states of like multiplicity. There are two types of fluorescence, prompt and delayed. Prompt fluorescence occurs from the excited singlet state to the singlet ground state following absorption from S_0 to S_1. Kasha's rule states 'the emitting electronic energy level of a given spin multiplicity is the lowest excited energy level of that multiplicity'. However there are a few exceptions to this rule, fluorescence in both azulene [3, 4] and thioketones[5] has been shown to occur from S_2.

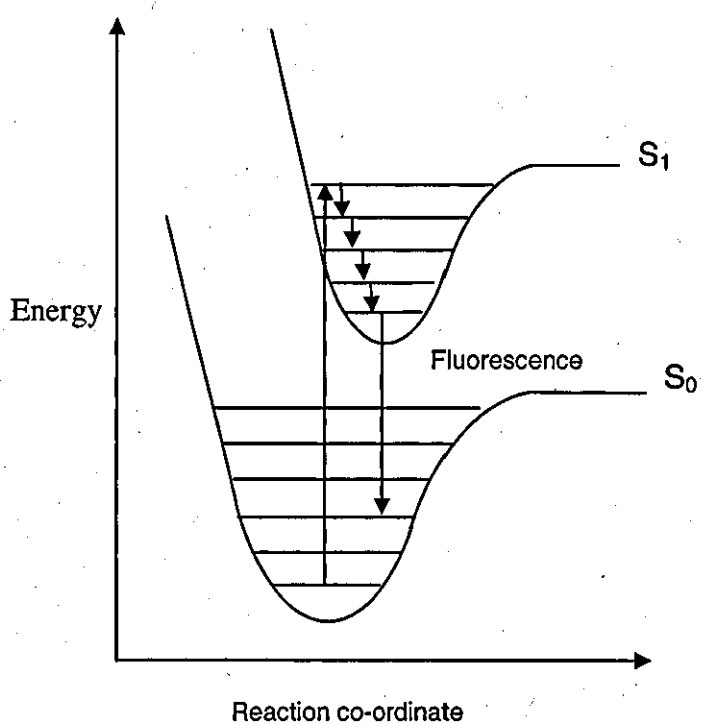

Figure 1.7: Absorption and subsequent fluorescence illustration from the singlet state

2. **Internal Conversion, IC:**

$$^1A^* \longrightarrow {}^1A + \text{heat} \qquad \textbf{1.6}$$

Non-radiative decay from the first singlet excited state to the singlet ground state (e.g. liberation of heat). Electronic energy in one state is converted to vibrational energy in a lower state. The rate of internal conversion is dependent on the energy gap between the two states involved, the larger the energy gap the slower the transition due to decreasing Frank-Condon factors.

3. **Intersystem Crossing, ISC:**

$$^1A^* \longrightarrow {}^3A^* \qquad \textbf{1.7}$$

This process occurs between states of different spin multiplicities i.e. it is a non-radiative transition from the first singlet excited state to the first triplet excited state, this transition is of low probability as it involves a change in spin multiplicity, and is spin forbidden. This could be seen in on the Jablonski diagram in figure 1.6; if intersystem crossing occurs from the excited singlet state the triplet state will be populated.

1.2.2 Triplet State

For intersystem crossing to occur from the excited singlet state, the triplet state will be populated, deactivation of the triplet state then occurs from the lowest vibrational level of the T_1 triplet state. Since relaxation from the first excited triplet state involves a change in spin multiplicity, triplet states are long lived, microseconds to milliseconds, relative to singlet states which have lifetimes of the order of nanoseconds. Consequently the triplet state has a lower energy than the singlet state, due to the repulsive nature of the spin-spin interaction between electrons of the same spin. Promotion of an electron from the ground state can give rise to either an excited singlet (spin orientation preserved), or an excited triplet (spin orientation inverted) as could be seen on figure 1.6. From the triplet state there are two main possibilities:

1. **Phosphorescence:**

$$^3A^* \longrightarrow {}^1A + h\upsilon \qquad \textbf{1.8}$$

Phosphorescence is the decay from the triplet state to the singlet ground state *via* the emission of a photon. It is a radiative transition of lower energy than fluorescence, its spin forbidden nature results in the radiative lifetime of phosphorescence being

long; this allows diffusional quenching of the triplet state by solvent molecules and other triplets to compete efficiently with phosphorescence. As it is a radiative transition between states of differing spin multiplicity, but occurs due to the effect of spin orbit coupling. It is a transition from the lowest lying triplet state to the singlet ground state via the emission of a photon. Its spin forbidden nature ($\Delta S=0$), results in the radiative lifetime of phosphorescence being long, this allows diffusional quenching of the triplet state by solvent molecules and other triplets to compete efficiently with phosphorescence. The typical radiative relative lifetimes for both fluorescence and phosphorescence are shown in table 1.1 below:

Transition	Typical radiative lifetimes
τ_r^0 ($S_1 = {}^1(\pi, \pi^*)$)	10^{-9}s
τ_r^0 ($S_1 = {}^1(n, \pi^*)$)	10^{-6}s
τ_r^0 ($S_1 = {}^3(n, \pi^*)$)	10^{-2}s
τ_r^0 ($S_1 = {}^3(\pi, \pi^*)$)	10s

Table 1.1: Typical radiative relative lifetimes of fluorescence and phosphorescence

2. Intersystem Crossing (ISC):

Non-radiative decay from the triplet state to the singlet ground state involves a change in spin multiplicity and is a radiationless transition between states of differing multiplicity. The transition is of low probability as it involves a spin inversion, but the transition is made possible by the effect of spin orbit coupling. The shortest lifetime is on the singlet π, π^* transition since this process is spin allowed and does not involve a change in orbital configuration in comparison to the slower n, π^* transition as this transition involves a change in orbital configuration. Whilst the triplet lifetimes are much longer because relaxation to the singlet ground state is spin forbidden as this transition involves a change in spin. However, the n, π^* transition is faster than the π, π^* transition in triplet states, despite the change in orbital configuration which also explains spin orbit coupling.

1.2.3 Triplet-Triplet Annihilation

The process of triplet-triplet annihilation can be represented as;

$$^3M^*(T_1) + {}^3M^*(T_1) \longrightarrow M(S_0) + {}^1M^{**}(S_1) \longrightarrow 2M(S_0) + h\nu_f \qquad 1.9$$

Triplet-triplet annihilation (TTA) can be determined[2] and also occurs when two excited triplets collide and redistribute their energies *via* an entity X, whereby X is the encounter complex which then decomposes and resulting in the promotion of one triplet to the singlet excited state S_1. Whilst S_1 decays non-radiatively to the singlet ground state S_0, *via* intersystem crossing as seen in figure 1.6. Once back in the excited singlet state (S_1), emission occurs with the same rate constant as prompt fluorescence. Delayed fluorescence is governed by the spin probabilities and forms one molecular entity in its excited singlet state and another molecular entity in its electronic ground state, referred to as P-type, from pyrene, whilst the thermally activated delayed fluorescence involving back intersystem crossing, referred to as E-type, from eosin. This only occurs when the S_1-T_1 gap is small enough for thermal energies to populate S_1 from T_1. This type of delayed fluorescence exhibits the same lifetime as triplet state decay and occurs with an intensity that is proportional to the exciting light intensity.

The following scheme describes the pathway leading to the triplet-triplet annihilation (TTA):

$$S_0 \xrightarrow{h\nu} S_1 \qquad \text{Absorption}$$

$$S_1 \xrightarrow{k_{isc}} T_1 \qquad \text{Intersystem crossing}$$

$$T_1 + T_1 \longrightarrow X \qquad \text{Triplet-Triplet Annihilation}$$

$$X \longrightarrow S_1 + S_0 \qquad \text{Back Intersystem Crossing}$$

$$S_1 \xrightarrow{k_f} S_0 + h\nu \qquad \text{Delayed fluorescence}$$

Scheme 1.1: Mechanism of delayed fluorescence via triplet – triplet annihilation

The radiative or natural lifetime of a species τ_r^0 – either fluorescence or phosphorescence can be defined by the following equation

$$\tau_r^0 = \frac{1}{k_r} \qquad \textbf{1.10}$$

k_r is the radiative rate coefficient which is related to the Einstein coefficient for spontaneous emission. The measured fluorescence (τ_f) or phosphorescence (τ_p)lifetime will generally be shorter than the radiative lifetime owing to further contributions to the decay of the excited state via either internal conversion (IC) or intersystem crossing (ISC), so the singlet and triplet lifetimes are given by the following equation:

$$\tau_f = \frac{1}{(k_f + k_{isc} + k_{ic})} \qquad \textbf{1.11}$$

or

$$\tau_p = \frac{1}{k_p + k_{isc}}$$

The quantum yield of fluorescence (Φ_f) or phosphorescence (Φ_p) can be given by the following equations respectively:

$$\Phi_f = \frac{k_f}{k_f + k_{isc} + k_{ic}} \qquad \textbf{1.12}$$

$$\Phi_p = \frac{k_p}{k_p + k_{isc}} \Phi_T \qquad \textbf{1.13}$$

Where Φ_T is the triplet quantum yield

k_p is the phosphorescence constant

k_f is the fluorescence constant

k_{isc} is the intersystem crossing constant

k_{ic} is the internal conversion constant

1.2.4 Spin orbit coupling

This coupling arises because an electron experiences a magnetic field due to the motion of the nucleus, due to a relation between angular momentum and the strong nuclear force. This occurs for the protons and neutrons moving inside the nucleus,

leading to a shift in their energy levels in the nucleus shell model. The magnetic field is often strong enough to cause spin flipping of the electron, and so to conserve total angular momentum (spin and orbital) this results in the electron changing orbital. When a molecule has heavy atoms present strong interactions occur between the spin angular momentum and the orbital angular momentum of the electron, i.e. spin orbit coupling. Atoms with high atomic numbers give more spin orbit coupling, the higher the charge the greater the coupling and this is due to the fact that spin orbit coupling depends on interaction with the nucleus. Xenon, iodides and bromides are often used to enhance spin forbidden transitions either as intramolecular (substituents) or intermolecular quenching agents. Since pure singlet or pure triplet states do not exist, this leads to forbidden transitions to occur, as singlets have some triplet character and also triplets have some singlet character due to coupling between spin and orbital angular momentum as shown in the equations below:

$$\psi_T = \psi^0_T + \lambda_x \psi_{sx} \qquad \textbf{1.14}$$

$$\psi_s = \psi^0_s + \lambda_y \psi_{Tx} \qquad \textbf{1.15}$$

Where ψ_T and ψ_s are the wavefunctions describing triplet and singlet states respectively, the superscript 0 denotes pure states and λ_x and λ_y are fractions less than one.

Decay from the triplet (n, π^*) excited state to the ground state involves both spin flip and a change in orbital configuration, whereas relaxation to the ground state from the excited state (π, π^*) triplet requires just spin flip.

1.3 Intermolecular processes

Energy transfer conserves energy through an exciting molecule losing its energy, and transferring the excited energy to another molecule, creating the ground state of the donor and excited state of the acceptor. The transfer of energy from an electronically excited donor (D*) to an acceptor (A) is often referred to as quenching of D* by A and can be summarised as follow:

$$D^* + A \rightarrow D + A^* \qquad \textbf{1.16}$$

Where D is the ground state of the donor and A* is the electronically excited acceptor.

Radiative (trivial) or non radiative energy transfer involves a specific interaction of D* and A as shown in equation 1.16, of which there are two types.

i) Long range coulombic energy transfer

ii) Short range electron energy transfer

1.3.1 Radiative energy transfer

Radiative energy transfer involves the absorption of the emission of light (fluorescence or phosphorescence) from the donor molecule followed by the absorption of the emitted photon by the acceptor:

$$D^* \rightarrow D + h\upsilon \qquad \textbf{1.17}$$

$$h\upsilon + A \rightarrow A^* \qquad \textbf{1.18}$$

This can only occur if there is an overlap between the emission spectrum of the donor with the absorption spectrum of the acceptor. The emission from the donor is not influenced by the presence of the acceptor furthermore the molecules do not need to be in close proximity.

In an energy transfer experiment the quenching of emission of D* and its replacement by emission of A will be observed. Although the photon is absorbed by D, A becomes excited. Processes arising from A* are said to be sensitised processes. When the donor and acceptor are identical the energy transfer is referred to as migration.

Energy transfer mechanisms are usually classified according to the initial spin multiplicity of D* and final spin multiplicity of A*, for example the following process is known as triplet-triplet energy transfer.

$$^3D^* + A \longrightarrow D + {}^3A^*$$

Electronic energy transfer and paramagnetic catalysed intersystem crossing is the mechanism by which oxygen quenches excited states.

1.3.2 Non-radiative energy transfer

This involves the emission of a specific photon from the excited molecule, of which there are two types: coulombic and collisional energy transfer

- ***Coulombic energy transfer***: This process occurs between a well separated donor-acceptor, as the donor can induce a change in the acceptor at a distance. This only occurs if there is sufficient superposition of the electronic and nuclear vibrational levels in both donor and acceptor. The oscillation of the excited electron in the donor induces an oscillation in the highest energy electron in the acceptor.
- ***Collisional energy transfer:*** This occurs when the donor and acceptor atoms are sufficiently close together to allow their respective electron clouds to overlap allowing an exchange of electrons to take place. The excited electron from the donor molecule transfers into the LUMO of the acceptor molecule, simultaneously an electron from the HOMO of the acceptor molecule is transferred to the corresponding orbital. Triplet-triplet energy transfer usually occurs via a collisional mechanism, due to the low extinction coefficient of the $S_0 \rightarrow T_1$ transition, on which the coulombic mechanism is dependent.

1.4 Fluorescence Quantum yield

Fluorescence Quantum yield Q can be defined as the ratio of the numbers of photons emitted through fluorescence to the number absorbed and can be represented mathematically:

$$Q = \frac{Photons_e}{Photons_a} \qquad \textbf{1.19}$$

The subscripts e and a represent emission and absorption respectively.

It can also be represented by the relative rates of the radiative and non radiative pathways, which deactivate the excited states:

$$Q = \frac{k_r}{k_r + \Sigma k_{nr}} \qquad \textbf{1.20}$$

where the subscripts r and nr, correspond to the rates of radiative and non radiative processes respectively.

Determination of the relative quantum yield is generally accomplished by a comparison of the wavelength intensity of the unknown samples with the common standard known like Rhodamine, cresyl violet, fluoresceine[6] etc.

Fluorescence quantum yields from acquired data can be calculated using the following equation:

$$\Phi x = \left(\frac{A_s}{A_x}\right)\left(\frac{\int_b^a (x)_x dx}{\int_b^a (x)_s dx}\right)\left(\frac{\eta_x}{\eta_s}\right)^2 \Phi_s \qquad \textbf{1.21}$$

Φ = Fluorescence quantum yield

$\int_b^a (x)_x dx$ = Area under corrected emission curve

A = absorbance

η = Refractive index of solvent used

Subscripts s and x refer to the standard and unknown samples respectively

1.5 Quantum Yield of Singlet Oxygen Production

The quantum yield of sensitized production of singlet oxygen, Φ_Δ, is given by the sum of the contributions arising from oxygen quenching of the lowest excited singlet state (S_1) and the lowest excited triplet state (T_1) of the sensitiser;

$$\Phi_\Delta = \Phi_\Delta (S_1) + \Phi_\Delta(T_1) \qquad \textbf{1.22}$$

Singlet oxygen (discussed in detail in chapter 3) is thus produced with varying efficiency due to quenching of both triplet and singlet states. The quantum yields of production of singlet oxygen $^1O_2$ ($^1\Delta_g$) have been reported for a number of compounds in a variety of solvents. Rate constants for quenching of singlet, k_q^S, and triplet states k_q^T, by oxygen and the fraction of triplet states quenched which produce singlet oxygen, f_Δ^T, have been shown to depend on several factors including; excited state energy, nature of the excited state, redox potential of the excited state and nature of the solvent[7-11].

1.5.1 Quenchers

Quenchers are substances which accelerate the decay of an electronically excited state to the ground state or to a lower electronically excited state, which may be summarised by the equation below:

$$M^* + Q \rightarrow M'$$

Where M* = Excited state of a molecule

M' = Ground state of a molecule

Q = Quencher

Quenching is the process of deactivation of an excited molecular entity intermolecularly by an external influence (quencher), or intramolecularly by a substituent through a non-radiative process. When the external environment (quencher) interferes with the behaviour of the excited state after its formation the process is referred to as dynamic quenching. Common mechanisms include energy, charge or electron transfer. The quenching process occurs in many different mechanisms and is induced by many different substances as mentioned previously, but oxygen is universal hence it is necessary to reduce the concentration of the dissolved oxygen to the minimum by degassing or deoxygenating. Fluorescence quenching of organic molecules in solutions by various quenchers like bromobenzene, iodopropane, halide ions, metal ions, oxygen etc have been shown to follow the Stern-Volmer relations. But in some cases, it has been observed that the experimental results show a deviation from a linear Stern-Volmer plot[12]. This deviation is attributed to various processes like

- Chemical Reaction
- Association (excited complexes)
- Proton transfer
- Heavy atom quenching
- Electron transfer
- Paramagnetic Catalysed intersystem crossing
- Electronic energy transfer

1.6 Stern-Volmer kinetics relationship

This term applies broadly to variations of quantum yields of photophysical processes or photochemical reactions like fluorescence or phosphorescence, usually with the concentration of a given quencher reagent. The process for measuring quenching constants of compounds is by using the Stern-Volmer equation which simply states that the reciprocal of fluorescence yield is proportional to the quencher concentration. A linear relationship should be observed when plotting I^0/I vs. [Q] from the equation below and the slope will be $k_q \tau_0$ which is known as the Stern-Volmer constant, with an intercept of 1.

$$\frac{I^0}{I} = 1 + k_q \tau_0 [Q] \qquad \textbf{1.23}$$

I^0 = Initial peak intensity of the fluorescence without a quencher

I = Intensity peak of fluorescence with a quencher

k_q= Quenching Constant (l $mol^{-1}s^{-1}$)

τ_0= Lifetime of the excited state in the absence of the quencher Q (s)

[Q]= Concentration of the quencher (mol l^{-1})

The Stern-Volmer equation predicts a linear dependence of $\frac{I^0}{I}$ on quencher concentration, at least if the quenching constant is a true constant. The existence and magnitude of the quenching constant, however, can be understood in terms of the competing processes of fluorescence and quenching, namely,

$$A \xrightarrow{h\nu} A^*$$

$$A^* \xrightarrow{\tau_0^{-1}} A$$

$$A^* + Q \xrightarrow{K} A + Q \qquad \textbf{1.24}$$

Using the notion that I is proportional to the steady state concentration of A, gives

$k_q = k\tau_0$

Since the fluorescence lifetime is independent of the quencher concentration, a linear relationship should be observed when using a Stern-Volmer equation, there have been cases when deviations[13-14] from the Stern-Volmer linearity have been observed and a non linearity was seen for both positive and negative curvature. Both positive curvature and negative curvature have been observed.[15-17]. Negative curvature involves a decrease in k_q and is associated with a change in the absorption and fluorescence spectrum of the fluorophore[16]. Deviations from the Stern-Volmer equation in such reactions have been explained by the existence of multiple fluorescing states [15] or by a compound formation.[16] On the other hand, a variety of quenching reactions have been reported which exhibit positive curvature in Stern-Volmer plots, yet which show no evidence of multiple excited states or molecular association. For example, the oxygen quenching of perylene in dodecane[18] shows a large positive curvature, even though there is no detectable change in the absorption spectrum of perylene up to oxygen concentrations of 1 M. Several explanations of positive derivations from Stern-Volmer behaviour have been advanced. The one most commonly used is that a 'static" quenching mechanism is important at higher quencher concentrations. The static quenching mechanism is a slight variation on the theme of molecular association. According to Frank and Wawilow[19] it involves interactions with quenchers that are within a sphere of action of the fluorophore at the moment of excitation. However, the quenching of anthracene fluorescence by oxygen or sulphur dioxide[17] leads to a sphere of action with a radius of 30 Å, which is at odds with the fact that these quenching reactions are collisional rather than resonant. Consequently, Bowen and Metcalf[17] gave another interpretation of static quenching involving the quencher-fluorophore pairs that "are in juxtaposition at any instant". These pairs appear in the Bowen- Metcalf scheme as if they were molecularly associated with an equilibrium constant K. This type of association leads to the expression

$$\frac{I^0}{I} = (1+k[Q])\ (1+k_q\tau_0[Q]) \qquad \textbf{1.25}$$

A third kind of explanation of positive curvature is due to Noyes [20-21]. Their work is based on the assumption that the quenching reactions are rapid, and so are under diffusion control. Using the Smoluchowski theory they calculate a dependence of k_q on quencher concentration arising from time-dependent effects. This theory depends

only on an encounter radius and a mutual diffusion constant, the same parameters used to explain the low quencher concentration experiments.

1.7 Diffusion controlled reactions

The lingering of one molecule near another on account of the hindering presence of solvent molecules is often referred to as the cage effect. Such an encounter pair may accumulate enough energy to react even though they do not have enough to do so when first formed

Consider a bimolecular reaction between two different species, A and B in solution.

$$A + B \underset{k_{-d}}{\overset{k_d}{\rightleftharpoons}} [A \text{---} B] \xrightarrow{k_p} P \qquad \textbf{1.26}$$

The reaction can be considered in terms of the formation and dissociation of an encounter complex.

If the rate of formation of products is greater than the rate of dissociation of the encounter complex, $k_p >> k_{-d}$, the reaction is said to be fully diffusion controlled and $k_{obs} = k_d$. Conversely, where the rate of dissociation of the encounter complex is greater than the rate of formation, $k_{-d} >> k_p$, the reaction is said to be in the pre-equilibrium region and $k_{obs} = Kk_r$.

If a reaction is diffusion controlled the rate of reaction cannot exceed the rate the molecules can diffuse together to react. Therefore the reaction rate is determined solely by the rate of encounter and is limited by the rate of diffusion.

1.8 Laser Flash Photolysis

This is a powerful technique for qualitative and quantitative study of rapid reactions, triplet states, and isomerisation reactions to identify reactive intermediates in photochemical systems; it was initially developed in the 50s by Norrish and Porter[22]. Commonly, an intense excitation pulse of short duration from a laser or less common by a flash lamp is used to produce a concentration of a transient species which can be monitored by measuring the changes in the amount of light transmitted. At a short interval of time after the generating pulse the system is analysed by observing emission or absorption characteristics. The decay or production of the transient absorption or emission at one particular wavelength is

monitored or the absorption or emission spectrum of the transient is recorded at given times after the exciting pulse.

1.8.1 Lasers

Laser is an acronym for Light Amplification by the Stimulated Emission of Radiation. All lasers consists of a lasing material (solid, liquid or gas), two mirrors one of which is partially reflective to allow laser light through and the other one is totally reflective, and also there has to be an excitation mechanism which pumps energy into the active medium by one or more of three basic methods; optical, electrical or chemical

The main properties of laser light which makes it unique from conventional light are the following:

- **Coherence:** All the emitted photons bear a constant phase relationship with each other in both time and phase
- **Directionality:** laser light is highly directional, with low divergence; easily allowing the beam to be focused on a specific point.
- **Monochromaticity:** Laser light is concentrated in a very narrow range of wavelengths

For laser action to occur a lasing medium is "pumped" to get the atoms into an excited state or molecules in the case of dye lasers. Typically, very intense flashes of light or electrical discharges pump the lasing medium and create excited-state atoms. The atoms are excited to a level that is two or three levels above the ground state. This increases the degree of population inversion: which is the number of atoms in the excited state versus the number in ground state. Once the lasing medium is pumped, the laser cavity contains a collection of atoms with some electrons in the excited levels. Just as the electron absorbed some amount of energy to reach this excited level, it can also emit energy in the form of photons (light energy). The photon emitted has a very specific wavelength that depends on the state of the electron's energy when the photon is released. The photon that any atom releases has a certain wavelength that is dependent on the energy difference between the excited state and the ground state. If this photon encounters another atom that has an electron in the same excited state, stimulated emission can occur. The first photon can stimulate or induce atomic emission such that the subsequent emitted photon vibrates with the same frequency and direction as the incoming

photon. The other key to a laser is a pair of mirrors, one at each end of the lasing medium. Photons, with a very specific wavelength and phase, reflect off the mirrors to travel back and forth through the lasing medium. In the process, they stimulate other electrons to make the downward energy jump and can cause the emission of more photons of the same wavelength and phase.

1.8.2 Population Inversion

Since the atoms are excited to a level that is two or three levels above the ground state, normally for two energy levels, u (upper) and l (lower), with energies εu and εl and population N_u and N_l. Normally the distribution of population of molecules among their various energy states will be biased towards the ground state according to Boltzmann equation

$$\frac{N_u}{N_i} = \exp\frac{-(\varepsilon_u - \varepsilon_l)}{kT} \qquad 1.27$$

Where this equation gives the ratio of the number of particles in the upper (u) and lower (l) energy levels and k denotes the Boltzmann constant which has a value of 1.38×10^{-23} J K^{-1}. A larger population in the upper level results in stimulated emission dominating, whilst if there are more in the lower state, absorption dominates. Population inversions are impossible in two level systems because the probability for absorption and for spontaneous emission is exactly the same, hence it will not be able to achieve a situation where the higher energy state is more populated than the lower energy state. Nonetheless three and four level systems can achieve inversions much more easily and consequently are used in laser systems. The ruby laser (crystalline aluminium oxide doped with chromium) is an example of a three level system as shown in section 1.8.5. The absorption of a photon of energy equal to the difference between ε_u and ε_l as shown in the equation below will result in the promotion of an electron from the lower to the upper level.

$$\nu = \varepsilon_u - \frac{\varepsilon_l}{h} \qquad 1.28$$

This excited electron will relax back to its ground state through a relaxation pathway, either by spontaneous or stimulated emission.

1.8.3 Stimulated Emission

$A^* + h\nu \rightarrow 2h\nu + A$ ------ stimulated emission

A sample can emit energy spontaneously or as a result of stimulus acting on the molecule. For stimulated emission to occur the energy of the light directed into the system must have a photon of energy that exactly matches the gap between the excited state and the lower energy state. The light emitted will be of the same frequency as the supplied radiation. The stimulated emission will occur in the direction of the stimulating beam, unlike spontaneous emission, which is random. This is then amplified in intensity.

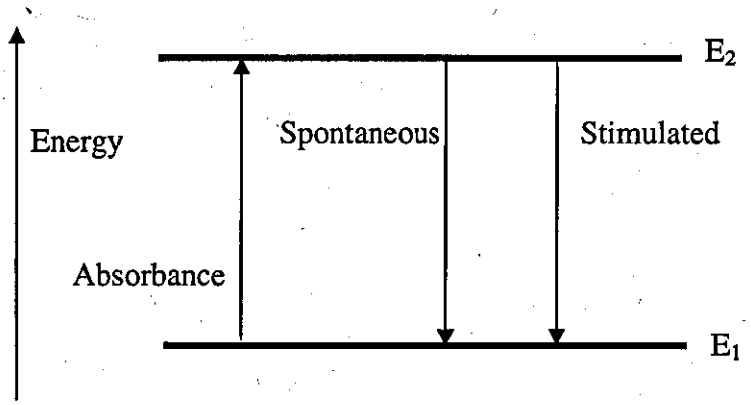

Figure 1.9: Representation of the three radiative processes that can occur in a 2 level system

1.8.4 Spontaneous emission

This is a random process when an atom (or a laser ion in a gain medium) is excited into a higher-lying energy level, e.g. by absorption of a photon, it may after some time spontaneously return to its ground state, or to some intermediate energy level, by releasing the energy in the form of a photon, and occurs without the involvement of additional photons. As spontaneous emission is a random process, the product is incoherent light waves, which are out of phase with each other in both time and space.

1.8.5 Types of excited state level system

1. **Three level system:** In a three level system the excitation source leads to a population of energy level 2, which then rapidly converts to energy level 1. The transition from energy level 1 to level 0 occurs infrequently, and so level 1 achieves a much higher population than level 0, and a population inversion is achieved.

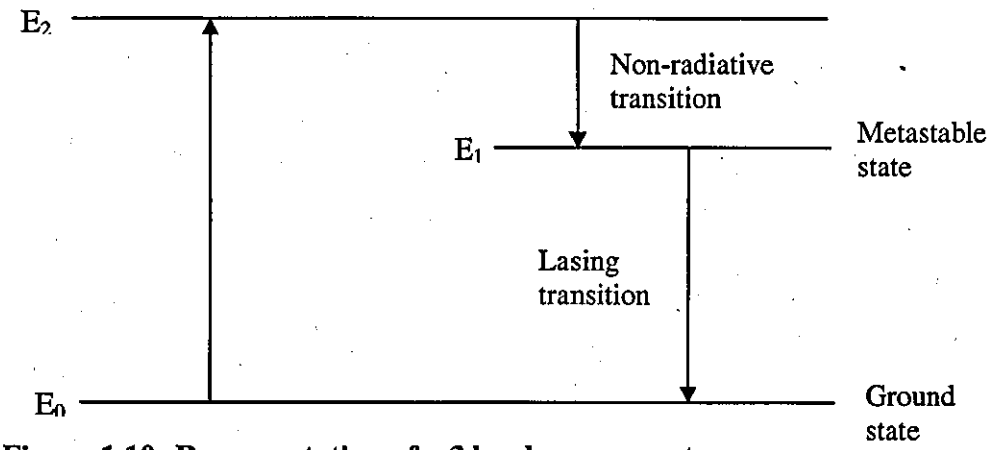

Figure 1.10: Representation of a 3 level energy system

An example of a 3 level laser is the Ruby laser, and it is doped with Cr_2O_3. The Cr_3^+ ions are excited to an upper state E_2 by an intense flash of light. Rapid relaxation occurs to the E_1 state, the atom remains in the E_1 state for long periods, before dropping down to the ground state by spontaneous emission, hence the term metastable state. In a three level laser the method of obtaining a population inversion between the middle and the ground state is inefficient. This is because the middle state is effectively empty at the start of the pumping as a result of the Boltzmann distribution, at least half the population of the ground state molecules must be pumped into the middle level before a population inversion is achieved.

2. **Four level systems:** Four level lasers eliminate the problem associated with a 3-level system, since in three level lasers half of all the particles must be excited into level 1 before inversion is achieved, which leads to inefficient energy transfer from the pump to the amplified beam.

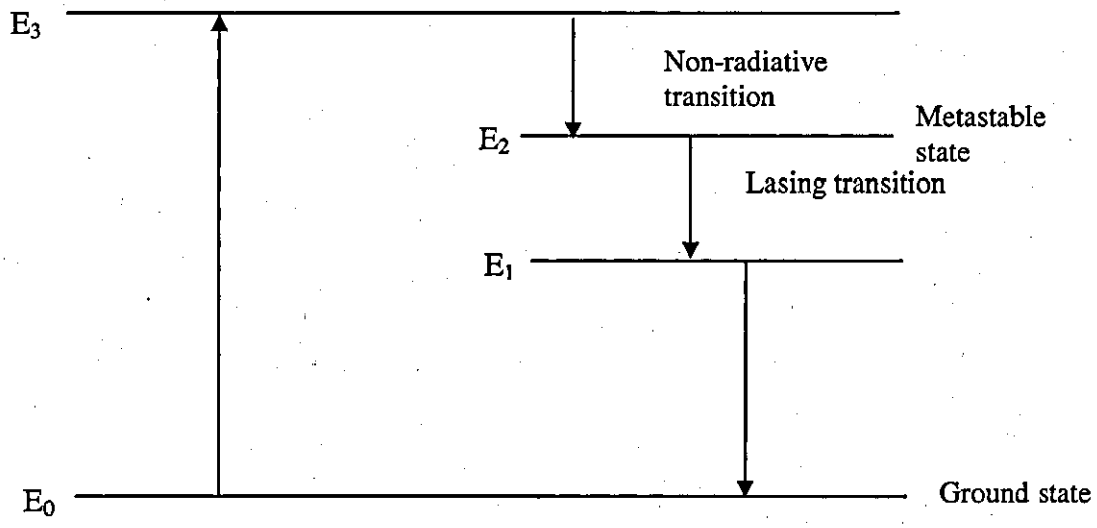

Figure 1.11: A schematic presentation of a four level laser system

In a four level laser atoms in the ground state E_0 are pumped into the E_3 level. They relax to the metastable state E_2 non-radiatively. The atoms then descend to the E_1 state and then drop to the E_0 state, since the lasing transition takes place between these two states (E_2 and E_1), a comparatively small population is required in E_2 to sustain laser action

1.8.6 The optical cavity

The laser pulse is allowed to build up between two mirrors which are partially reflecting, the beam is then suddenly diverted out of the cavity. In addition to sustaining the laser the optical cavity must be resonant at the wavelength of radiation, must sustain laser action and improve the spatial and temporal coherence of any output beam. This technique can generate high power pulses. The fixed cavity length means maximum amplification is only achieved for light waves which exhibit nodes at the mirrors satisfying the so called standing wave condition:

$$\lambda = \frac{2d}{n} \qquad \textbf{1.29}$$

Where d is the cavity length and n is the number of half wavelengths contained within length d. This places quite severe restrictions on the form of the wave and the frequencies of radiation, but a number of modes which will satisfy this are waves called axial or longitudinal cavity modes as this places quite severe restrictions on the form of the wave and the frequencies of radiation.

1.8.7 Axial/Longitudinal Modes

These are modes which oscillate along the length/axis of the cavity consist of a large number of frequencies given by:

$$\nu = \frac{nc}{2d} \qquad 1.30$$

Where n is the number of half wavelengths contained in length d and c is the speed of light. The quality of a laser can be defined by the mean frequency divided by the distribution width. The occurrence of more than one axial mode results in an increase in the output bandwidth.

1.8.8 Transverse modes

The laser cavity is considered to amplify light travelling down the optical axis of the laser hence a photon travelling at right angles to this axis may cause stimulated emission, but will not be amplified to form a laser beam because there will not be enough gain to overcome its losses. These reflect the intensity distribution across the output mirror, and arise due to beams following off-axis paths between the two cavity mirrors. If a photon is only slightly off axis the wave may be able to zigzag between mirrors enough times producing sufficient gain to overcome its losses, resulting in a complicated intensity distribution across the output mirror. Transverse modes are normally described using the notation TEMpq where p and q describe the number of intensity minima across the laser beam in perpendicular directions, as shown below

TEM_{00} TEM_{10} TEM_{20} TEM_{21}

Figure 1.12: Transverse modes in laser cavity

Where TEM stands for Transverse Electric and Magnetic fields. These are the waves which propagate through the laser cavity oscillating along the axis of the laser (axial or longitudinal cavity modes) and slightly off axis (transverse modes). Ideally lasers are operated in TEM_{00} which corresponds to a Gaussian intensity profile.

1.8.9 Q-switching

Q-switching is a technique by which a laser can be made to produce a pulsed output beam by increasing the peak power of the laser and reduce pulse length. In Q-switching a shutter is placed in the cavity (the distance between the two mirrors), when the shutter is closed reflection between the mirrors is prevented. The quality factor of the laser cavity can also be expressed as:

$$Q = \frac{2\pi\nu_0 \text{ (energy stored in mode)}}{\text{Energy lost per second from mode}} \qquad 1.31$$

ν_0 is the resonant frequency

The quality Q-factor of a laser can rapidly be improved after allowing the population inversion to keep building up to well over its normal level by preventing laser action and then Q-switching to abruptly depopulate it. This results in a very fast increase in photon density inside the cavity, leading to a rapid reduction in the population inversion through stimulated emission producing a short intense pulse of radiation. This action is called Q-switching as the system suddenly switches from a high cavity loss (low Q) to low loss (high Q), all the energy accumulated in the inversion is released as a short and giant pulse. Techniques of Q-switching can either be chemical, mechanical or optical between the laser rod and the totally reflecting mirror in the cavity.

1.8.9.1 Pockels cells

Pockels cells are the basic components of electro-optic modulators, used for Q switching lasers which is a device consisting of an electro-optic crystal (with some electrodes attached to it) through which a light beam can propagate, thus acts as a voltage-controlled waveplate. Absorption of laser radiation produces heating of the electrooptic crystal which degrades the laser performance and behaviour of an electro-optic Q-switch in high-average- power laser is presented. This could form a large increase in output energy stability achieved by employing a switching voltage pulse of the special temporal shape to the Pockels cell. The phase delay in the crystal (Pockels effect) can be modulated by applying a variable electric voltage.

1.8.10 Xenon arc lamp

Xenon arc lamps used as analysing sources in photochemistry are managed at pressures of approximately twenty atmospheres to give an output which is continuum. If operated at lower pressures the lamps generate an output composed of distinct wavelengths which correspond to the emissive transitions in the excited atoms. Such lamps are operated with DC power supplies, and are mounted vertically with the larger anode above the smaller cathode, with typical anode-cathode separations in the range 2 to 4mm. The output is a smooth continuum with some weak lines superimposed in the visible region and some stronger lines in the near infra-red region. Arc lamps with input powers ranging from 150 to 1000 watts are typically used as analysing sources in photochemical investigations.

References

1. Sergei MB and Weisman RB. *Journal of Physical Chemistry A* **2000**; 104: 7711-7714.
2. Beer, M., Longuet-Higgins, HC., *J. Chem. Phys.*, **1995;** 1390-1391.
3. Huber, J.P., Mahaney, M., *Chem. Phys. Lett.*, **1975;** 30: 410-412.
4. Atkins, P.W., Physical Chemistry, Fifth Edition, Oxford University Press, (1997), chapter 17 and 27.
5. Povrozin, Y., Terpetsching E. Measurement of Fluorescence Quantum Yields on ISS Instrumentation Using Vinci. *Innovation in Fluorescence.* http://www.iss.com/resources/yield.html accessed on 20/05/07.
6. Abdel-Shafi AA, Wilkinson F. *J. Phys Chem A* **2000**; 104:5747-5757.
7. Wilkinson F, McGarvey DJ, Olea AF. *J.Am.Chem.Soc.* **1993**; 115:12144-12151.
8. Abdel-Shafi AA, Worrall DR. *J. Photochem and Photobio A-Chem.* **2005;** 172: 170-179.
9. Wilkinson F, McGarvey DJ, Olea AF *J.Phys.Chem.* **1994**; 98:3762-3769.
10. Wilkinson F, Olea AF, McGarvey DJ, Worrall DR. *Journal of the Brazilian Chemical* Society **1995**; 6:211-220.
11. Boaz H, Rollefson GK. *J.Am.Chem.Soc.* **1950**; 72:3435-3443.
12. Keizer J. *J. Am. Chem. Soc.* **1982;** 105:1494-1498
13. Peak D, Werner TC, Dennin RM, Baird JK. *J.Chem.Phys.* **1983**; 79:3328-3335.
14. Rollefson G.K. and Boaz H., *J. Phys. Colloid Chem.*, **1984;** 52, 518-527.
15. Boaz H. and Rollefson *G.* K., *J. Am. Chem. Soc.*,**1950;** 72,3435-3443
16. Bowen E. J. and Metcalf W. S., *Proc. R. Soc. London Ser. A,* **1951**; 206, 437 - 447.
17. Lakowicz J. R. and Weber *G., Biochemistry,* **1973;** 12, 4161-4170.
18. Frank I. M. and Wawilow S. I., *Z.Phys.,* **1931;** 69,100-110 .
19. Noyes R. M., *J. Am. Chem. Soc.,* **1957**; 79, 551-555.
20. Noyes R. M., *J. Phys. Chem.* **1961;** 65,763-765.
21 Noyes R. M., *Prog. React. Kinet.,* **1961;** 1, 131-160.
22. Porter G., Nobel Lecture: Flash Photolysis and some of its applications, *science, 1968,* 160: 1299-1307.

Chapter 2

Supercritical Fluid Carbon Dioxide

2.0 Supercritical fluids

Supercritical fluids (SCFs) are highly compressed gases which combine properties of gases and liquids in an intriguing manner and are phases created when substances are at conditions of temperature and pressure above their critical point. The critical point represents the highest temperature and pressure at which the substance can exist as a vapour and liquid in equilibrium. Every stable compound has a triple and critical point[1] and any gaseous compound becomes supercritical when compressed to a pressure higher than the critical pressure (P_c) above its critical temperature (T_c).

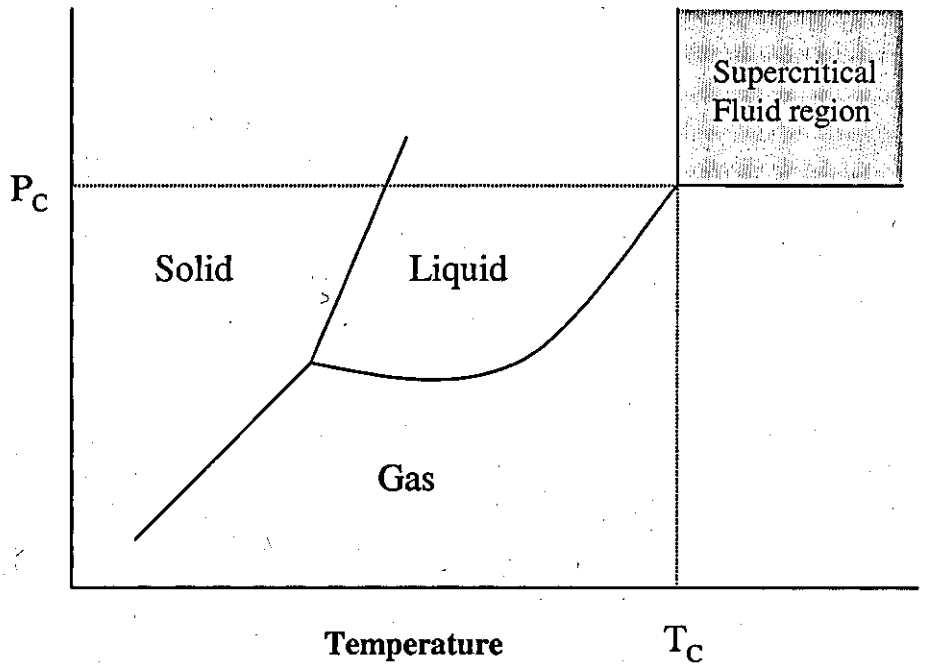

Figure 2.1: Phase diagram of a typical material

SCFs are of considerable interest as solvents due to their physical properties such as density and viscosity can be influenced significantly by changes in temperature and pressure. This could be seen through the effects of fundamental solvent properties on the rates of reactions without changing the chemical identity of the solvent[2]. Properties of supercritical fluids are different from those of normal fluids and are tuneable simply by changing properties such as temperature and pressure, without changing the chemical nature of the solvent, in particular the density and viscosity change drastically at conditions close to their critical point[3-4]. The properties of SCF's are frequently described as being intermediate between those of a gas and a

liquid, as the nature of SCF's arises from the gaseous and liquid phases merging together to become indistinguishable at the critical point. In addition, supercritical fluids mix perfectly with gases, giving them a huge advantage over conventional liquid solvents in gas-liquid reactions. Supercritical fluids have densities and diffusivities similar to liquids but viscosities comparable to gases as seen in table 2.1.

Mobile Phase	Density (kg m^{-3})	Viscosity (poise)	Diffusivity (cm^2 sec^{-1})
Liquid	800 – 1000	0.3 - 2.4 ($x10^{-2}$)	0.5 - 2.0 ($x10^{-5}$)
SCF	100 - 900	0.2 - 1.0 ($x10^{-3}$)	0.1 - 3.3 ($x10^{-4}$)
Gas	~1.0	0.5 - 3.5 ($x10^{-4}$)	0.01 - 1.0

Table 2.1: Comparison of fluids to gases and liquids[2]

Not all properties of supercritical fluids are intermediate between those of gases and liquids; compressibility and heat capacity for example are significantly higher near the critical point than they are in normal liquids or gases or even in the supercritical state further from the critical point[5]. Energy transfer studies have shown to proceed at the expected diffusion controlled limit, and therefore not affected by increased local densities and local compositions that exist in the SCF region[6-7].

Although the properties of a compound may change drastically with pressure near the critical point, most of them show no discontinuity and the changes start gradually rather than with a sudden onset, when the conditions approach the critical point.

Many types of bimolecular reactions including fluorescence quenching have been examined in SCF solvents[8-11] as they are particularly attractive as reaction media due to: increased mass transfer, elimination of the need for multiphase reactions, ease of separation of products or unused reactants, slower deactivation of catalysts, dramatic pressure effects on rate constants and changes in selectivities.

Increased diffusion rates are observed in the supercritical region, diffusivities are greater than they are in liquids since the SCF has a lower fluid density and is more

like a gas. Diffusion coefficients are sensitive functions of pressure and temperature in the supercritical region.

The possibility of using SCFs as tuneable solvents not only for extraction but for chemical reactions is one of the many interesting features associated with their application in modern synthesis.[12-18].

2.1 Solubility of SCFs

The solubility of naphthalene in supercritical carbon dioxide is shown below in Figure 2.2.

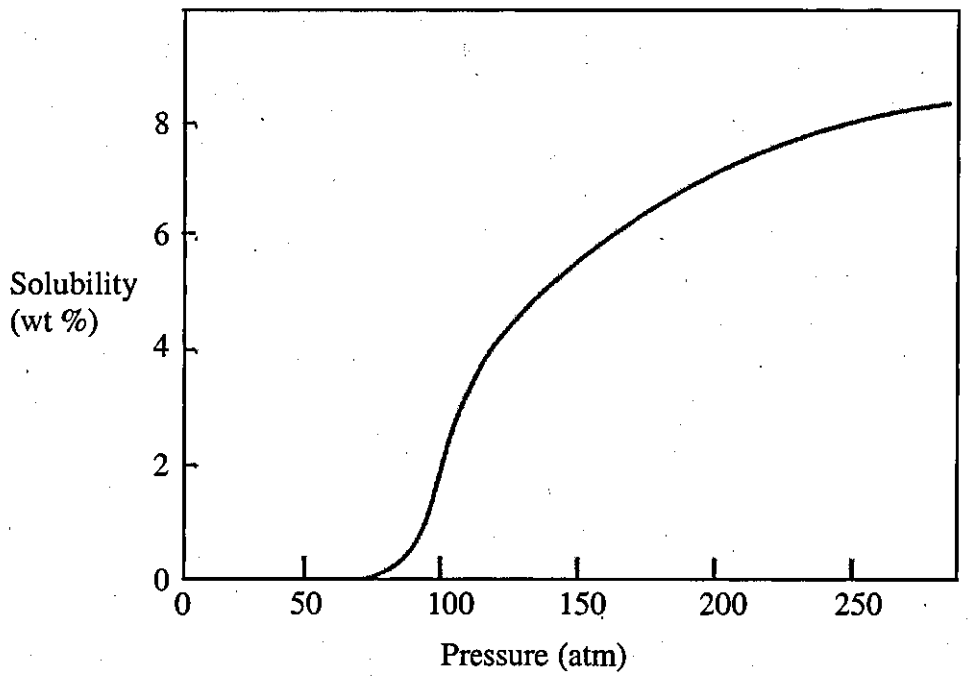

Figure 2.2: The solubility of naphthalene in supercritical fluid carbon dioxide[19-20].

As expected at low pressures the solubility is very low and as the pressure is increased to above the critical pressure of carbon dioxide (72.9 atm), solubility increases.

The solubility behaviour shown here is the basis of almost all supercritical fluid extraction/separation processes[21-25]: soluble components are extracted from a substrate by a supercritical fluid, and the extracted components that have been dissolved in the supercritical fluid are precipitated out when the pressure is reduced.

The solubility of compounds in supercritical fluids has possibly been the most extensively investigated area of SCF research [26-29]. The efficacy of a supercritical

fluid as a solvent for a particular solute can be elucidated from solubility data. Binary solubility data are useful in determining the selectivity of a supercritical fluid for a particular solute, since the solubility of an individual solute in an SCF may not be the same as the solubility in a multi-component system.

The solubility of a component is predominantly influenced by the following factors; nature of the SCF solvent, chemical functionality, the operating conditions.

2.4.1 Supercritical Fluids as Solvents

It is common to express the solubility of a material in a supercritical fluid in terms of the mole fraction of the solute and the ability of supercritical fluids to dissolve substances arises from the highly non-ideal behaviour of pure SCFs. Under supercritical conditions solubility is enhanced by several orders of magnitude above that predicted by the ideal gas law[30]. The solubility enhancement of a component particularly in the vicinity of the critical point is determined mainly by the augmentation in density of the SCF.

The solubility of a given solute also depends on the type of supercritical fluid as shown in Table 2.2. Under the conditions shown, fluoroform has the highest mass density; however it displays the lowest affinity for naphthalene.

Solvent (SCF)	**Solubility (mole fraction)**	**Density (g ml^{-1})**
Ethane	4.70×10^{-2}	0.39
Carbon dioxide	2.42×10^{-2}	0.81
Fluoroform	1.17×10^{-2}	0.92

Table 2.2: Variation of solubility with solvent[3]

This variation in solubility of naphthalene in different supercritical fluids indicates that there are varying degrees of intermolecular interaction between the solid and SCF, which can be explained in terms of solvent polarity. The overall effect of solvent polarity on the solubility of naphthalene for example, follows the same solubility rule as in liquids, of, "like dissolve like". Naphthalene is a non-polar solid

and hence is most soluble in non-polar supercritical ethane. Carbon dioxide is fairly non-polar, but behaves less as a non-polar solvent than ethane, due to its quadrupole moment[31] and fluoroform is the most polar solvent due to the fluorine atoms which are electron withdrawing.

Hence, it is preferable to employ non-polar solvents for aromatic hydrocarbons, however, for polar solids the effect of solvent polarity is not as simple.

Generally non-polar SCFs exhibit lower affinities for polar solutes, but the maximum solubility of a polar solute does not necessarily occur in the most polar SCF, for example, carbon dioxide is a better solvent for benzoic acid than fluoroform[32]. Polar SCFs may exhibit greater potential for polar molecules when they contain functional groups, thereby increasing the level of intermolecular interaction with the solvent. For example, fluoroform can be considered a good a solvent for amino containing compounds, as a result of hydrogen bonding between the amino group and the acidic proton in fluoroform.

The addition of co-solvents can have large effects on solubilities in SCFs. Addition of a co-solvent usually increases the density of a supercritical fluid and since solubility increases exponentially with density this can have a significant effect on solubilities. It is common to add small amounts of co-solvents to supercritical fluids, to increase the solubilities of heavy organic solutes. In such cases the co-solvents are chosen to have size and interaction energies (Lennard-Jones parameters) intermediate between those of the SCF and the solute [33]. Consequently, the solute would be preferentially solvated by the co-solvent. At high densities the local composition is similar to that of the bulk but at lower pressures, the density is lower and hence there is more free volume, the local volume can be more than ten times that of the bulk value. The local density around a dissolved solute in compressed gases and SCFs is expected to be greater than in the bulk. In the presence of an attractive co-solvent, the local environment around the solute will be enriched with the co-solvent, with this phenomenon being much more pronounced at lower pressures.

2.4.2 Chemical Functionality of the Solute

In a given SCF the difference between solid solubilities depends mainly on two factors, the solid vapour pressure and intermolecular interactions between the solvent and solute. Solubilities of individual solids can vary significantly but

differences between enhancement factors are less significant, which indicates that the solid vapour pressure exerts the greatest influence on solubility. The types of functional groups present in their chemical structures affect the degree of intermolecular interactions between the solvent and solute, for example it is possible to increase the solubility of organic compounds in supercritical carbon dioxide by fluorinating the compound. Differences in solubilities of solids can be explained in terms of structural features, which limit or enhance solubility. The addition of a functional group to the parent compound generally reduces solubility.

The solubility of a number of organic compounds in dense carbon dioxide has been examined [34]. They report that among structural features which greatly influence the solubilities in carbon dioxide, such as chain length and branching, the extent and particular structural features which affect the solubility are specific to certain types of compounds, for example;

a) Alcohols: Chain length, branching, and nature (primary secondary or tertiary).
b) Hydrocarbons: Type and substituents on the rings.
c) Ethers: Chain length, aromaticity and nitrogen containing functional groups.
d) Amides and aromatic amines: Extent of N-alkyl substitution and type of alkyl group.
e) Amines: Nature (primary, secondary and tertiary) and basicity.
f) Nitro-compounds: Type and position of substituents, number of nitro groups and aromatic nuclei.

2.4.3 Temperature and Pressure Effects

Increasing pressure generally leads to an increase in solubility since the density of the SCF increases. It is necessary to consider both the density of the supercritical fluid and the vapour pressure of the solute when evaluating the effect of temperature. Although an increase in temperature causes a decrease in SCF density it also leads to an increase in solute vapour pressure, as a result solubility usually increases with temperature, however retrograde vaporisation has been known to occur near the critical point of the SCF. Retrograde vaporisation is where a decrease

in solute solubility is observed with isobaric increases in temperature, this trend and crossover phenomena have been studied by several groups[35,36].

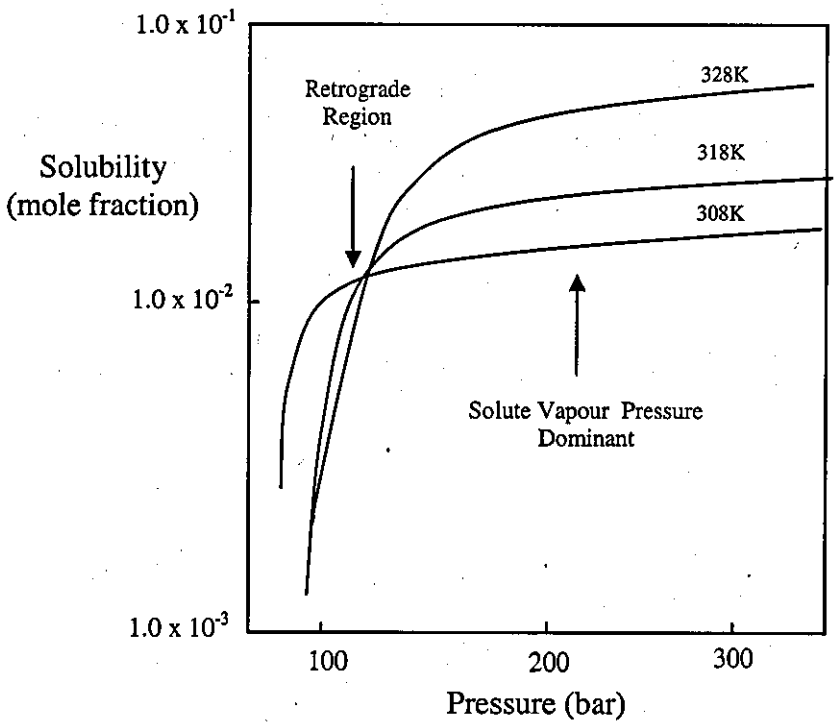

Figure 2.5: Solubility of naphthalene in supercritical carbon dioxide [36]

Solubility isotherms usually intersect within a narrow range of pressure, Figure 2.5. For any two isotherms, the point of intersection, or crossover pressure, represents a change in the temperature dependence of solubility

The solubilities of naphthalene, biphenyl and phenanthrene in supercritical carbon dioxide were reported to decrease with increasing temperature, between 308 and 328K, which was found to be in good agreement with previous studies[37-38]. In contrast to their findings Miller and Hawthorne reported a continuous increase in the solubility of some organic molecules in supercritical carbon dioxide, with increasing temperature at constant pressure[39]. They found that increasing pressure resulted in an increase in solubility, particularly of anthracene. They found that while increasing density at a constant temperature generally increases solubility,

increasing density at constant pressure, by lowering the temperature was found to lower solubility.

Phase behaviour is important since bringing reagents into the same phase allows them to react more effectively. Secondly phase behaviour can be important in separation of a product in a reaction, terminating the reaction at an intermediate stage or pushing a reversible reaction to completion. It is also important to determine the critical temperature, T_c, of the multi-component reaction mixture in order to know whether the system is a liquid, below T_c or an SCF, above, T_c. Although the difference in behaviour in passing below the critical temperature is not dramatic, as the temperature moves below T_c the medium becomes less compressible and loses the characteristic of a supercritical fluid[40].

2.5 Activation Volume

Chemical reactions in solution are generally accompanied by changes in volume, known their reaction volumes[41]. The activation volume is interpreted according to the transition state theory, as the difference between the partial molar volumes of the transition state and the sums of the partial volumes of the reactants at the same temperature and pressure.

Changes in viscosity have been known to affect the activation volume; prominent among them are those reactions that are diffusion limited[42]. Activation volumes have been studied in the liquid state for sometime but relatively little is known about activation volumes in supercritical fluids.

Consider the following diagram;

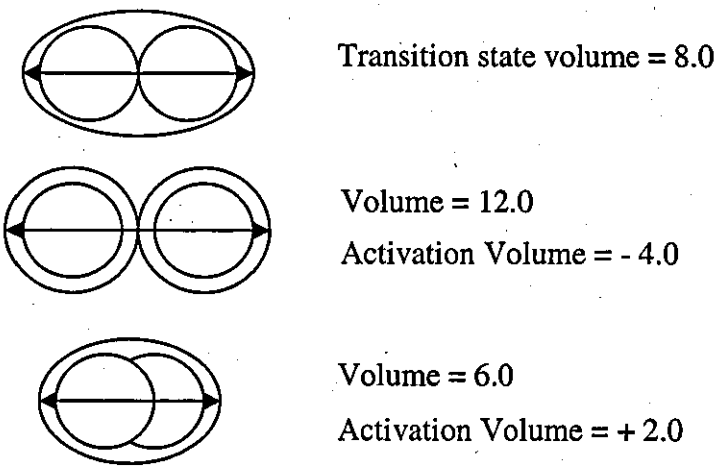

Figure 2.6: Diagram to illustrate the theory of activation volume

In order to react, the molecules must get within certain proximity of each other, known as the transition state volume, Figure 2.6. To reach this volume work either has to be done by the solvent to push the molecules together, or by the molecules to move further apart, thus doing work on the environment.

Partial molar volumes in liquids are only a few cm^3mol^{-1}, they can be very large and negative in SCFs, and as a result the pressure effect on the reaction rate constant can be very significant. Partial molal volumes of solutes in supercritical fluids were reported to be small and positive at high pressures, but large and negative at low pressures in the highly compressible near-critical region. This was true for all the solutes studied[43] in both supercritical carbon dioxide and supercritical ethylene.

2.1 Reasons for using supercritical fluids

Supercritical fluids can act in a variety of ways to affect reaction rates.

A) ***Increased diffusion rates:*** Diffusion co-efficients are sensitive functions of temperature in the supercritical region. The rate constant for a diffusion controlled reaction can be modelled using the Stokes Einstein based Debye equation, which states that bimolecular reaction rate constants are governed by $8RT/3\eta$, where η is the solution viscosity. This equation predicts that a reaction in supercritical fluid carbon dioxide for example should increase by a factor of approx 2.5 over a small range at 308K. Diffusivities are greater than they are in liquids since supercritical fluids have a lower fluid density and are more gas like[39].

B) ***Increased reactant solubilities:*** Formation of organo-metallic species in supercritical fluids could take place in a single phase supercritical solution compared to its normal multi-phase system operation. Since the solubility of nitrogen and hydrogen are so high in many SCFs, synthesis of a variety of previously unknown dinitrogen and dihydrogen organo-metallic species were possible[43]. Solubility of model compounds in supercritical fluids investigated by measuring solubility of naphthalene in supercritical carbon dioxide [19-20].

C) ***Facilitated separation:*** The solubility of solutes in SCF's is strong functions of temperature and pressure in the compressible region near the critical point. In

synthetic applications, there are no problems with separation of solvent; products may easily be separated downstream by simply reducing the pressure or adjusting the temperature of the fluid

D) Pressure effect on the rate constant: In terms of the transition state theory, the reactants are in thermodynamic equilibrium with a transition state. Once the transition state complex is formed it proceeds directly to products. In supercritical fluids the pressure effect on the reaction rate constant reflects the relative strengths of the intermolecular interaction between the reactant and the transition state with the SCF solvent.

E) Changes in Selectivities: In a situation where several parallel or competing reactions can take place, the thermodynamic pressure effect on each of the individual rate constants may be different i.e. the activation volumes are not equal for all the reactions. As a result increased pressure may favour one reaction over the others. In this way one may be able to control or enhance selectivities for the desired product by operating at the required temperature and pressure

F) Effects of local densities: Theories which support the idea of local densities greater than the bulk around a solute in a supercritical fluid solution have been proved and, one of these is the molecular dynamics studies[44], which clearly demonstrates that in an attractive mixture the environment around a solute molecule is continuously enriched with solvent relative to bulk conditions. Very importantly they point out the dynamic nature of the cluster, which loses its identity in a few picoseconds.

G) ***Effects of local compositions:*** Another possible effect on the reaction rate in an SCF is the changes in the local concentrations of reactants. Studies[21] have shown that in the compressible region near the critical point the local concentration of a co-solvent around a solute molecule could be as high as seven times that of the bulk.

2.2 Supercritical Fluid Carbon Dioxide

Supercritical carbon dioxide has a critical temperature of 31.3 °C and a critical pressure of 7.4 MPa and is very attractive as it is: largely inert in many reactions,

abundant, recyclable, inexpensive, non-flammable, easily scaleable, non-toxic and environmentally benign.

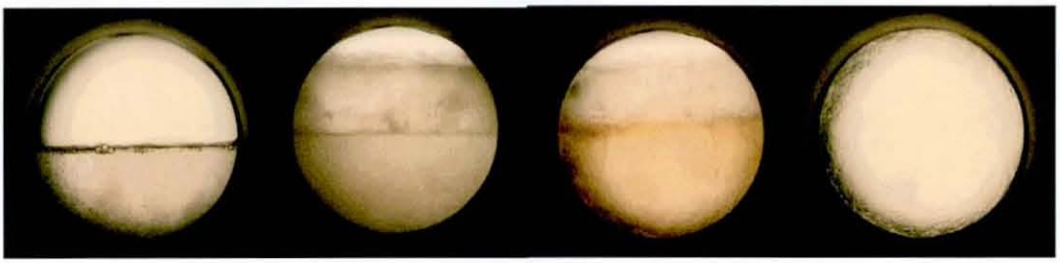

1 2 3 4

Figure 2.2: Stages of the formation of supercritical carbon dioxide[45]

1: The separate phases of the carbon dioxide are easily observed.

2: Upon heating the phase boundary begins to diminish

3: Further heating causes the gas and liquid densities to become similar.

4: T_c and P_c have been exceeded and supercritical fluid is observed.

It has a high solubility for non-polar organic compounds, with a maximum solvent strength comparable to that of hexane[46]; it can easily be modified by the addition of modifiers / co-solvents such as methanol or acetonitrile. Additions of co-solvents have been studied for a variety of supercritical fluid solvents[47-49].

Its viscosity is very low near the critical density and increases steeply with increasing pressure, hence is a suitable solvent for the study of the contribution of diffusion to energy transfer by the collisional or exchange mechanism. Although the solvation power of supercritical carbon dioxide is similar to that of hexane, it can easily be modified by the addition of modifiers such as methanol or Acetonitrile. Aside from carbon dioxide there are several other compounds that are commonly considered for use as supercritical solvents, the most common of which are given in Table 2.2. Supercritical xenon is also used because of a number of reasons; its easily accessible critical parameters (T_c = 16.6 °C, P_c = 5.8 MPa), of all the elements, xenon shows one of the highest spin orbit coupling constants (6080 cm^{-1})[47] makes it an ideal 'heavy atom' containing solvent[50].

Compound	Critical Temperature (°C)	Critical Pressure (MPa)	Critical Density (kg m^{-3})
CO_2	31.3	7.4	467.6
C_2H_4	9.2	5.1	214.2
C_2H_6	32.2	4.9	207
C_5H_{12}	196.6	3.4	232
NH_3	132.3	11.3	225
$CClF_2$	96.1	5.0	523.8
CHF_3	25.9	4.8	525
H_2O	373.9	22.1	322
Xe	16.6	5.8	1100

Table 2.2: Common compounds employed as supercritical fluids

2.3.1. Local Density Augmentation

Supercritical fluids have density fluctuations near the critical point which is known as local density augmentation (also termed 'local density enhancement'), which rises from the solute-solvent attraction. Evidence suggests that in supercritical mixtures there is a difference in the local and bulk environment of a solute molecule[51].

Conventionally this is thought to occur as a result of clustering of solvent molecules around the solute molecule through solvent solute interactions[52] hence, giving regions of higher and lower densities which are observed. However further research has shown that it is not caused by the solute, but by the pre-existing near critical fluctuations in the solvent. Therefore there would be higher solubility of the solute in the more dense regions of the solvent.

It is well known that density inhomogeneities exist, regions of higher density surrounded by regions of lower density[53].

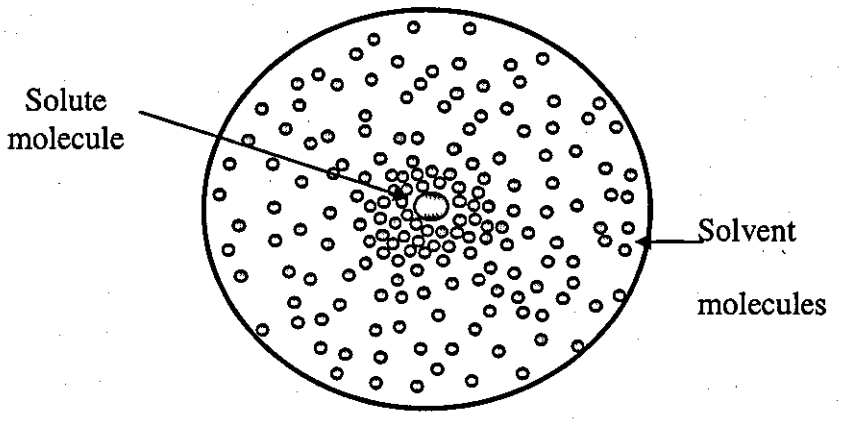

Figure 2.3: Schematic illustration of enhanced densities observed in the near critical region

The way in which the distribution of local densities found around an atom varies as the critical point is approached has been examined [54] and found that the mean local density enhancements arises as a necessary and direct consequence of the long-range density inhomogeneities present in such fluids.

Shifts of electronic spectra with density have been used to provide a simple means of monitoring local densities in supercritical fluids. The extent of density augmentation depends markedly on temperature, being most pronounced in the region of high fluid compressibility, research shows augmentation is relatively insensitive to solute-solvent interactions[55]. Although there seem to be a correlation between the strength of solvent-solute interactions and the extent of augmentation, unidentified characteristics contributed to the observed behaviour.

2.4 Applications of Supercritical Fluids

There are many different areas supercritical fluid can be used, such as extraction, photochemistry, chromatography, food and pharmaceutical chemistry and many more. As supercritical fluids are being investigated to replace organic solvents as they are more environmentally friendly.

2.4.1 Supercritical Fluid Extraction

Supercritical fluid extraction can be used in almost every area of chemical industry, pharmaceuticals, foods, natural products, bio molecules, pesticides, fuels and polymer additives [56-60]. Supercritical carbon dioxide is used regularly in extraction processes as it is non toxic and non flammable which lead to it being approved by the Food and Drug Administration (FDA) for uses within the food and

pharmaceutical industries. Some of the most common extraction process using supercritical carbon dioxide in industry is the extraction of caffeine from coffee [61], the extraction of hops for beer production and the extraction of nicotine from tobacco.

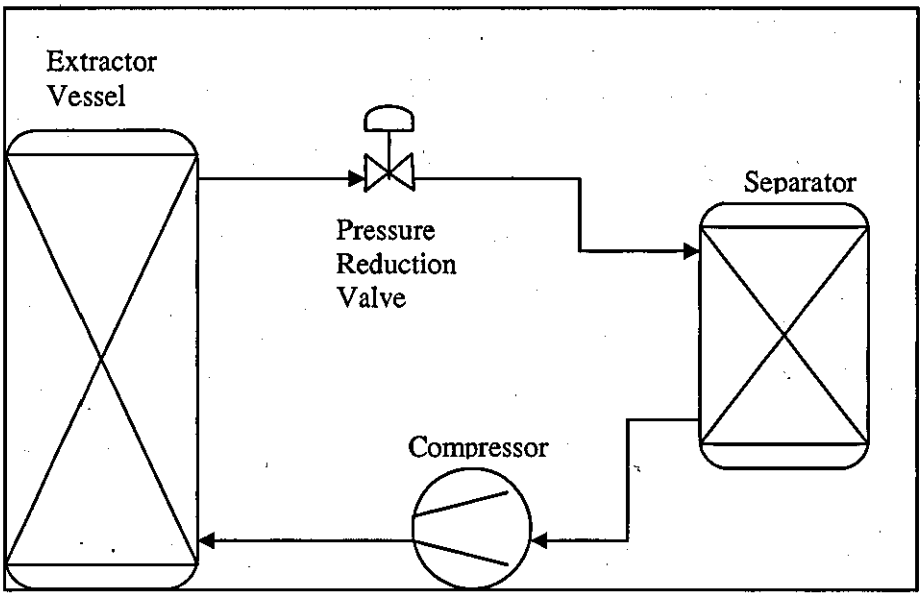

Figure 2.4: Schematic diagram of a simplified supercritical fluid extraction process [56].

The supercritical fluid extraction process involves placing the mixture into an extraction vessel. Carbon dioxide is then heated and compressed passed its critical point. Then a pressure reduction valve is opened to begin the carbon dioxide flow. Part of the mixture will be dissolved into the carbon dioxide and carried off into a separator. In the separator the temperature and pressure is reduced and therefore the solvating power of the carbon dioxide is reduced. Everything dissolved in the carbon dioxide begins to precipitate out and is collected. The carbon dioxide is then recompressed and heated to be recycled back through the system [56].

As supercritical fluids require high pressures; novel high pressure systems have been designed and built, which has to allow a continuous flow of a supercritical fluid solution through high pressure spectroscopic cells[57]. The equipment enables the production of the supercritical fluid and then the mixing with the modifiers. Supercritical fluids are normally used in conjunction with a modifier and have been found that modified supercritical carbon dioxide as a suitable reaction media for

photochemical reactions. This was investigated by looking at the triplet-triple energy transfer between anthracene and azulene as well as between benzophenone and naphthalene. The results showed that in modified supercritical carbon dioxide energy transfer proceeds at a greater fraction of the diffusion-controlled rate constant than in the pure modifier solution [58].

Supercritical xenon has also been used in photochemistry, where it is being used is looking at the singlet state of oxygen. It has been found that the relative lifetime of the singlet sate is shorter in supercritical xenon than in other solvents, this is due to the heavy atom quenching of the singlet state by the xenon atom [64-65].

2.4.2 Dry Cleaning

Carbon dioxide can be used as substitute for the dry-cleaning solvents currently used. These solvents are potentially toxic and environmentally harmful. The most commonly used dry-cleaning solvent, perchloroethylene (PER), is suspected to be carcinogenic. Carbon dioxide (CO_2) is a viable alternative for these solvents. Carbon dioxide is non-toxic, non-flammable, ecologically sound, and available on a large scale. Therefore, it can serve as a permanent alternative for hydrocarbon solvents. An additional advantage of using CO_2 is that the fabrics will be dry after washing, because the carbon dioxide evaporates from the fabrics during depressurization of the cleaning-vessel. Therefore, no additional drying step is needed; in addition it is non-toxic, non-flammable, ecologically sound, and available on a large scale. A disadvantage of CO_2 is its limited ability to dissolve polar molecules. However, the characteristics of CO_2 can be modified by the addition of miscible, polar compounds; these are called co solvents. In supercritical fluid extraction, short chain alcohols, for example methanol[66] and ethanol[67-68] are often used as co-solvent.

References

1. Kajimoto O. *Chem. Rev.* **1999**; 99:355-390
2. Noyori R. *Chem.Rev.* **1999;** 99: 353-354.
3. Roek DP, Kremer MJ, Roberts CB, Chateauneuf JE, Brennecke JF. *Fluid Phase Equilib.* **1999** ;160:713-722
4. Morita A, Kajimoto O. *J.Phys.Chem.* **1990;** 94:6420-6425.
5. Polikhronidi NG, Batyrova RG, Abdulagatov IM, Magee JW, Stepanov GV. *The Journal of Supercritical Fluids,* **2005,** *33,* 209-222
6. Petsche IB, Debenedetti PG, Mohamed RS. *J.Chem.Phys.* **1989;** 91:7075-7084.
7. Worrall DR, Wilkinson F. *Journal of the Chemical Society-Faraday Transactions.* **1996;** 92:1467-1471.
8. Bauza R, Ríos A, Valcárcel M. *Analytica Chimica Acta* **2001**; 450: 1-11.
9. Brunner G. *Journal of Food Engineering* **2005**; 67: 21-33.
10. Bernardo-Gil, M. G.; Lopes, I. M. G.; Casquilho, M.; Ribeiro, M. A.; Esquível, M. M.; Empis, J. *The Journal of Supercritical Fluids* **2007**; 40: 344-348.
11. Erkey, C.; *The Journal of Supercritical Fluids* **2000**; 17: 259-287.
12. Zagrobelny, J. Betts, T.A. Bright, F.V. *J. Am. Chem. Soc.* **1992** ;114: 5249-5259.
13. Bernardo-Gil, M. G.; Lopes, I. M. G.; Casquilho, M.; Ribeiro, M. A.; Esquível, M. M.; Empis, J. *The Journal of Supercritical Fluids* **2007**; 40: 344-348.
14. Bhattacharjee, P.; Singhal, R. S.; Tiwari, S. R. *Journal of Food Engineering* **2007**; 79: 892-898.
15. Gomes, P. B.; Mata, V. G.; Rodrigues, A. E. *The Journal of Supercritical Fluids* **2007**; 41: 50-60.
16. Iwai, Y.; Okamoto, N.; Ohta, S.; Arai, Y.; Sakanishi, K. *The Journal of Supercritical Fluids* **2007**; 40: 227-231.

17. Nakagawa, T.; Yamanaka, S.; Urakawa, H.; Kanji Kajiwara; Hayashi, S. *Journal of Molecular Structure: THEOCHEM* **1999**, *458*, 275-283.
18. Brennecke, J.F., *Supercritical Fluid Engineering Science*, Chapter 16, **1993**; 201-209.
19. http://dwb4.unl.edu/Chem/CHEM869J/CHEM869JLinks/www.phasex4scf.com/scf.htm. accessed on 21.09.08
20. http://www.phasex4scf.com/supercritical_fluids/about_supercritical fluids.htm accessed on 21.09.08
21. Poliakoff, M.; Howdle, S. M.; Healy, M.A.; Whalley, J.M. *Proc. Internat. Symposium. on Supercrtical Fluids*, ed. M. Perrut, Soc. Chem. Franc., **1988**; 967-971
22. Hanny, J. B.; Hogarth, J., Proc. R. Soc. Section A, 29 (**1879**), 324
23. Gu, M.; Li, Q.; Zhou, S.; Chen, W.; Guo, T. *Fluid Phase Equilibria,* **1993**, *82*, 173-182.
24. Marceca, E.; Schäfer, G.; Hensel, F. *The Journal of Chemical Thermodynamics,* **1996**, *28*, 647-666.
25. Marshall, W. L.; Gill, J. S.; Slusher, R. *Journal of Inorganic and Nuclear Chemistry,* **1962**, *24*, 889-897.
26. Johnston, K. P.; Ziger D. H.; Eckert, C. A., *Ind. Eng. Chem. Fundam.*, 21, **1982**, 191-197.
27. Bamberger, T.; Erickson, J. C.; Cooney, C. L., *J. Chem. Eng. Data*, 33, **1988**, 327-333.
28. Zhang, X.; Gao, L.; Liu, Z.; He, J.; Han, B., J. *Supercritical fluids*, 23, **2002**, 233-237.
29. Bartle, K. D.; Clifford, A. A.; Jafar, S. A.; *J. Chem. Soc. Faraday Trans.*, 86, **1990**, 855-860.
30. Hannay, J. B.; Hogarth, J., *Proc. R. Soc.*, Section A, *29*, **1879**, 324-328.
31. McHugh, M. A.; Krukoni, V. J., *Supercritical Fluid Extraction, Principles and Practice,* Butterworths, Boston, **(1986),** Chapter
32. Schmitt, W. J.; Reid, R. C., *J. Chem. Eng. Data*, 31, **1986**, 204-212.
33. Brennecke, J. F.; Chateauneuf, J. E., *Chem. Rev.*, **99**, (1999), 433-452.

34. Dandge, D. K.; Heller, J. P.; Wilson, K. V., *Ind. Eng. Chem. Prod. Res. Dev.*, 24, **1985,** 162-166.

35. Forster, N. R.; Gurdial, G. S.; Yun, J. S. L., *Ind. Eng. Chem. Res.*, 30, **1991,** 1956-1960.

36. Johnston, K. P.; Barry, S. E.; Reed, N.K; Holcomb, T. R., *Ind. Eng. Chem. Res.*, 26, **1987,** 2372-2377.

37. Suoqi, Z.; Renan, W.; Guanghua, Y., *J. Supercritical Fluids*, **8, 1995,** 15-19.

38. McHugh, M. A.; Paulattis, M. E.; *J. Chem. Eng. D*ata, **25, 1980,** 326-329.

39. Miller, D. J.; Hawthorne, S. B., *Anal. Chem.*, **67, 1995,** 273-283.

40. http://www3.interscience.wiley.com/cgibin/booktext/117875396/BOOKPDFSTART accessed on 30.09.80

41. Qin, J.; Eyring, M.; van Eldik, R.; Johnston, K. P.; Goates, R. S.; Lee, M.L., *J. Phys. Chem.*, 99, **1995,** 13461-13466.

42. Noble, W.J.; Asano, T., *J. Phys. Chem. A.*, 105, **2001,** 3428-3429.

43. Eckert, C. A.; Ziger, D. H.; Johnston, K. P.,; Kim, S., *J. Phys. Chem.*, 90, **1986,** 2738-2746.

44. Petsche, D.Y.; Debendetti, P.G., *J. Phys. Chem.*, 91; **1989**: 7075-7084.

45. http://www.chem.leeds.ac.uk/people/cmr/whatareSCF.html. Accessed on 10/10/08

46. Ikushima Y, Saito N, Arai M, Arai K. Bull. Chem. Soc. Jpn., 64, **1991,** 2224-2229.

47. Ekart, M. P.; Bennett, K. L.; Ekert, S. M.; Gurdial, G. S.; Liotta, C. L.; Eckert, C. A, *AICHE J.*, **39,** (1993), 235-241.

48. Lemert, R. M.; Johnston, K. P., *Ind. Eng. Chem. Res.*, 30, **1991,** 1222-1231.

49. Worrall, D.R.; Wilkinson, F., *J. Chem. Soc., Faraday Trans.*, 92, **1996,** 1467-1471.

50. Abdel-Shafi, A.A., Wilkinson, F. and Worrall, D.R. *Chemical Physics Letters* 343 (3-4), **2001**, 273-280.

51. Aizawa T,Kanakubo M, Ikushima Y, Richard L. Smith, JR. *Fluid Phase Equilibria* 219, **2004,** 37–40.

52. Wu RS, Lee LL, Cochran HD. *Ind. Eng. Chem. Res.*, **1990**, *29*, 6, 977-988.

53. Knutson BL, Tomasko DL, Eckert CA, Debenedetti PG, Chialvo A. A. *ACS Symposium Series*, **1992**, *488*, 60-72.

54. Tucker, S.; Goodyear, G.; Maddox, M. W., *J. Phys. Chem. B.*, 104, **2000**, 6248-6257.

55. Marconelli, M.; Lewis, J. E.; Biswas, R.; *Chem. Phys. Lett.*, 310, **1999**, 485-494.

56. Fermamdez-Prini, R., Pure and Applied Chem., 67, **1995**; 519-526.

57. Hanny, J. B.; Hogarth, J., *Proc. R. Soc. Section A*, 29, **1879**; 324-326.

58. Wang L., Yang B., Du X., C. Yi, *Food Chemistry* 108, **2008**; 737-741.

59. Okamoto H., Danjo K. *Advanced Drug Delivery Reviews*, 60, **2008**; 433-446

60. Smith R. M., J. *of Chromatography A 856,* **1999**; 83-115.

61. Okamoto M., Wada O., Tanaka F., Hirayama S., *J. Phys. Chem.* A **2001**; 105: 566-572.

62. Kubo M., Takizawa T., Wakia C., Matabagsi N., Nukahar M., *J Chem. Phys.* 121, **2004,** 960

63. Desimone J. M., Tumas W (Eds) Oxford University Press. ISBN 0-19515483-5, **2003.**

64. Abdel-Shafi, A. A.; Wilkinson, F.; Worrall, D. R. *Chemical Physics Letters* **2001**, *343*, 273-280.

65. Abdel-Shafi, A. A.; Worrall, D. R. *Journal of Photochemistry and Photobiology A: Chemistry* **2007**, *186*, 263-269.

66. Kersch C., Roosmalen van M.J.E. Woerlee, G..F. Witkamp, G..J. *Ind. Eng. Chem. Res.* 39, **2000**; 4670-4672.

67. Teberikler, L. Koseoglu, S. Akgerman, A. *J. Am. Oil Chem. Soc.* 78, **2001**; 115-120.

68. Cocero M.J., Calvo L., *J. Am. Oil Chem. Soc.* 73 **1996**; 1573-1578.

Chapter 3

Singlet Molecular Oxygen

3.0 Singlet Molecular Oxygen

3.1 Introduction

Oxygen is unique among homonuclear diatomic molecules, in that its ground state has two unpaired 'p' electrons, i.e. it is paramagnetic. In the ground state the lowest energy configuration corresponds to the presence of the two electrons in degenerate π_g^* (antibonding) molecular orbitals. Since the electrons are of the same spin the ground state has triplet multiplicity denoted by the spectroscopic symbol $^3\Sigma_g$ or ($^3\Sigma_g^-$) and has zero angular momentum about the internuclear axis. It exists as a triplet in its ground state and quenching of excited states by molecular oxygen produce the excited singlet states of oxygen, $^1\Sigma_g^+$ and $^1\Delta_g$, which lie 158 kJmol^{-1} and 94 kJmol^{-1}, respectively, above the $^3\Sigma_g^-$ ground state; there are two possible configurations of the electrons in the π_g^*;

- The electrons are spin paired in the same orbital leading to a doubly degenerate state, $^1\Delta_g$.
- The electrons are spin paired in different orbitals leading to a singly degenerate state, $^1\Sigma_g^+$.

Whilst the $^1\Sigma_g^+$ is often formed initially, electronic to vibrational energy transfer swiftly occurs to deactivate this state to the metastable and highly reactive $^1\Delta_g$ state, which is the vigorous species in many important photo-processes and which is more commonly known as singlet oxygen. The lifetime of the $^1\Delta_g$ state is prolonged and therefore reactivity of singlet oxygen is observed almost entirely from this state. Owing to the forbidden nature of intersystem crossing linked with absorption, transitions are seldom seen by direct excitation, but are seen by energy transfer from both triplet and singlet excited states of other molecules. With the exception of the first two degenerate antibonding π_x and π_y orbitals, all molecular orbitals are doubly occupied.

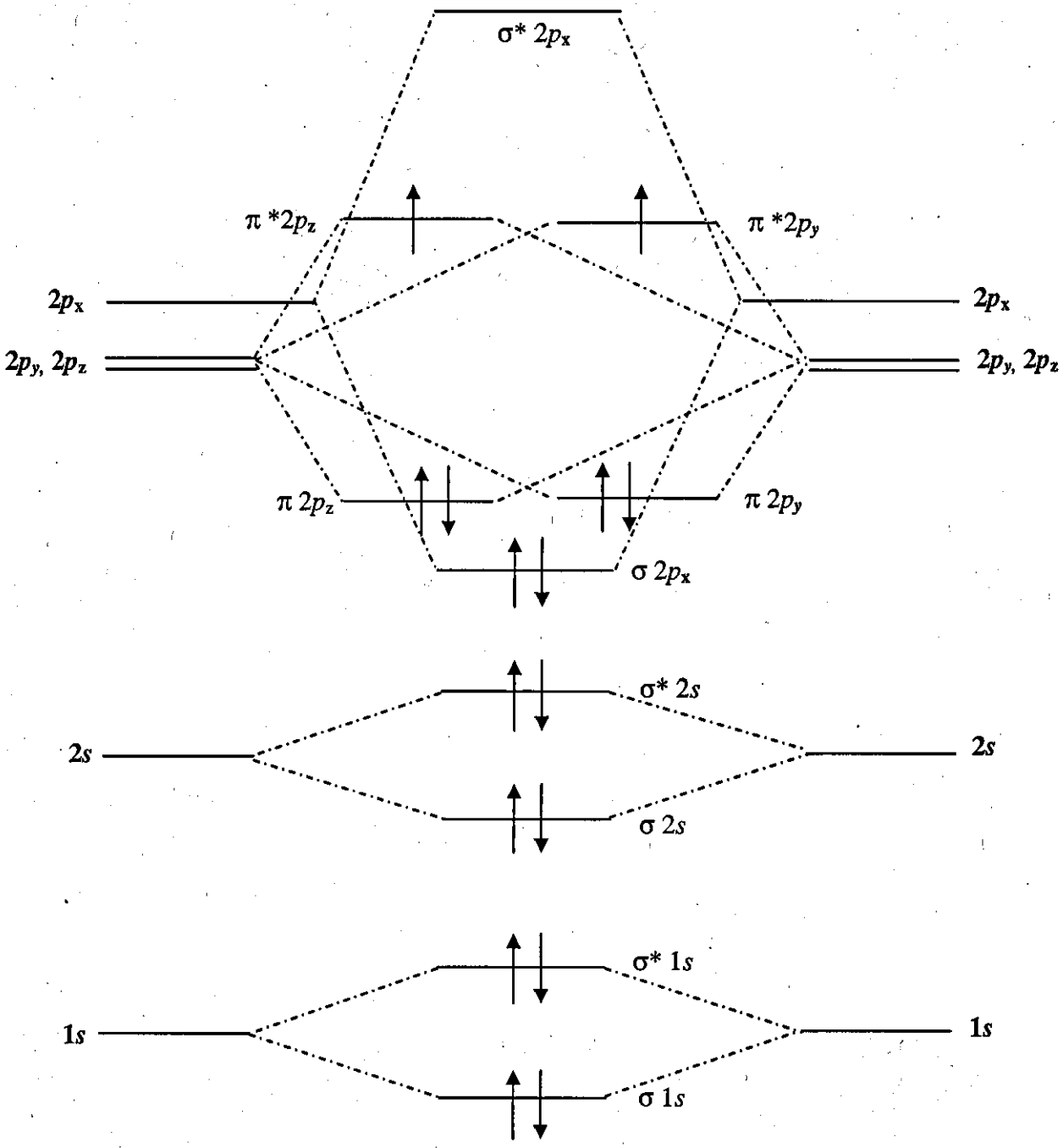

Figure 3.1: Energy pattern for homonuclear diatomic molecular oxygen

From the eight electrons in the oxygen, it is only the six electrons found in π orbitals that are of interest. Four of these electrons fill the degenerate bonding π_x and π_y orbitals and two electrons half fill the degenerate antibonding π^*_x and π^*_y orbitals.

The two electrons in the ground state occupy different orbitals to yield a $^3\Sigma_g$ state[1]. It is the arrangement of the two electrons in the antibonding π orbitals that determine which of the three low lying states shown in Figure 3.3 is produced.

The electrons in the ground state occupy different orbitals to yield a $^3\Sigma_g^-$ state[2].

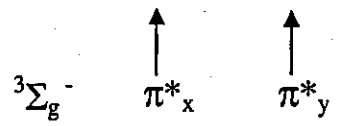

The two electrons in the $^1\Sigma_g^+$ state are paired and also occupy different orbitals;

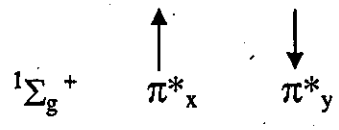

Analysis of the orbital wave function indicates that both electrons are spin paired in the same orbital for the $^1\Delta_g$ state, this component is responsible for the interesting reactivity of singlet oxygen, represented by;

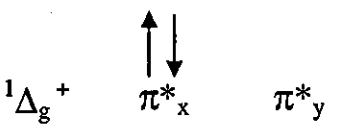

The other component of the $^1\Delta_g$ state can be represented by;

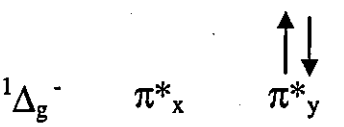

The electron occupancy of the ground state and lower excited singlet states are shown in Figure 3.2.

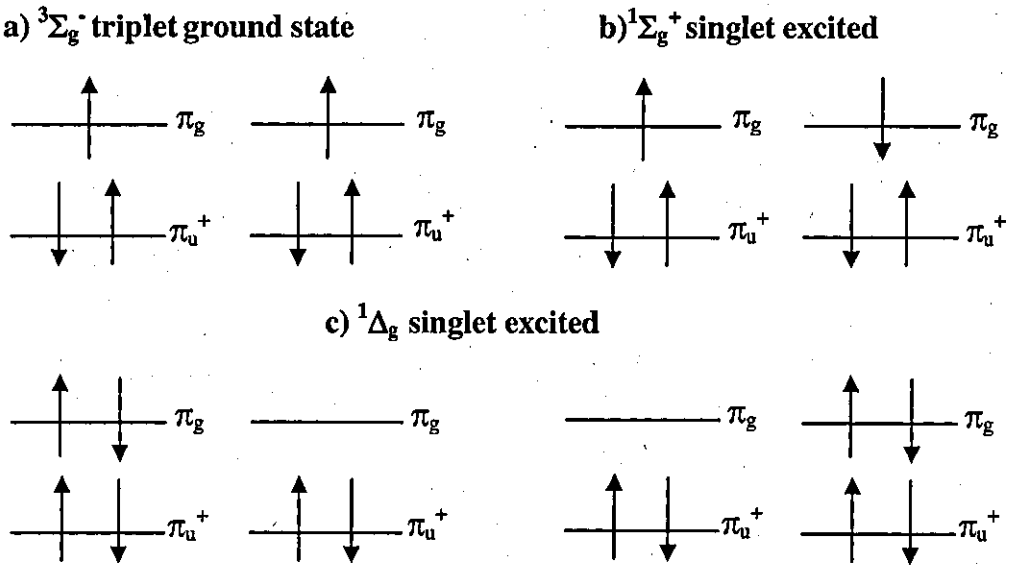

Figure 3.2: Occupation of molecular orbitals in ground state and the two lowest excited states of oxygen

The radiative lifetime of singlet oxygen $^1\Delta_g$ in the gas phase is ~ 64mins and the lifetime of $^1\Sigma_g^+$ is ~ 10 sec, but in solution the lifetime of the $^1\Delta_g$ is considerably shorter, this is due to the interaction of the solvent[2] and also due to the energy transfer to the ground state of the sensitiser as the energy of the triplet state of the sensitiser is lower than the excited state of singlet oxygen. As a result of high energy laser excitation it is possible to produce lifetimes which are shorter than expected, due to multiphoton processes producing species which can quench singlet oxygen. Collisions with other molecules can shorten lifetime in two ways:

- by inducing an electric dipole transition at the same wavelength
- by inducing a radiationless transition to the ground state

3.2 The Lifetime of Singlet Oxygen

Although the electronic transitions $^1\Delta_g \longleftarrow {}^3\Sigma_g^-$ and $^1\Sigma_g^+ \longleftarrow {}^3\Sigma_g^-$ are highly forbidden, but isolated molecules of oxygen in the $^1\Delta_g$ state spontaneously undergo a transition to the ground state, principally through the transition:

$$O_2(^1\Delta_g) \longrightarrow O_2(^3\Sigma_g^-) + h\nu \qquad 3.1$$

3.3 Production of Singlet oxygen

a) Chemical Generation: Some of the chemical reactions used in the generation of singlet oxygen ($^1\Delta_g$) are:

i) Decomposition of hydrogen peroxide, caused by reaction of hydrogen peroxide with the hyperchlorite anion or hyperbromite anion[3]

$$H_2O_2 + ClO^- \longrightarrow O_2(^1\Delta_g) + Cl^- + H_2O \qquad \textbf{3.2}$$

ii) Reaction of potassium superoxide with hypochlorite

iii) Thermal decomposition of the ozonide of triphenyl phosphite

b) Microwave Generation / Gas Phase Discharge

Radiofrequency discharge tubes have been utilised as a convenient source of singlet oxygen, for spectroscopic studies. When an electric discharge, most commonly microwave radiation is passed through oxygen gas in a gaseous flow system, singlet molecular oxygen ($^1\Delta_g$ and $^1\Sigma_g^+$), atoms and ozone are produced, which can be removed *via* reaction with mercury vapour, when the merging gases are bubbled through solutions containing oxidizable substrates, the singlet oxygen $^1\Sigma_g^+$ state is rapidly quenched to give the singlet oxygen $^1\Delta_g$ state[4].

c) Photosensitization

The production of singlet oxygen *via* photosensitisation involves the following steps:

1) Absorption of light by the photosensitiser itself
2) Formation of the sensitiser triplet state
3) Trapping of the triplet state by molecular oxygen within its lifetime
4) Energy transfer from the sensitiser to molecular oxygen

Quenching of the excited singlet state S_1 by ground state oxygen may give rise to the first triplet state T_1, which may then itself be quenched by ground state oxygen and produce singlet oxygen[5].

d) Sensitised Production by Pulsed Radiolysis

Passing a high energy electron beam through liquid benzene produces excited states in high yield. Since the lifetimes of singlet and triplet states of benzene are only of

the order of a few nanoseconds, quenching by dissolved oxygen produces little singlet oxygen. However, in the presence of a triplet energy acceptor, e.g. naphthalene, energy transfer occurs from triplet benzene to produce triplet naphthalene, this is in turn quenched by oxygen, producing singlet oxygen.

e) Direct Absorption by O_2 ($^1\Delta_g$)

This method is less frequently utilised to sensitise singlet oxygen also known as dimol emission.

$$2O_2\ (^3\Sigma_g^-, {}^3\Sigma_g^-) \longrightarrow 2O_2^*\ (^1\Delta_g, {}^1\Delta_g) \qquad \textbf{3.3}$$

Generation of singlet oxygen is achieved by irradiation with a Nd:YAG laser of Freon solutions subjected to high pressures of oxygen using the simultaneous transition of oxygen.

3.4 Singlet Molecular Oxygen Detection

3.4.1 Time Resolved Infra-Red Luminescence

There are two possible approaches to utilising phosphorescence of singlet oxygen as a detection method:

- Pulsed excitation of the solution of interest.
- Steady-state illumination and detection.

IR luminescence can be measured and monitored at ~1270 nm to determine the lifetime of singlet oxygen in most solvents. Following pulsed excitation the logarithm of phosphorescence intensity is plotted as a function of time and the slope gives the decay rate constant or data is fitted to a single exponential. The measured rate constant will be the sum of the intrinsic rate constant for deactivation in that particular solvent, k_d, and any bimolecular quenching rate constants, k_q, multiplied by quencher concentration, [Q].

$$k_{obs} = k_d + k_q\,[Q] \qquad \textbf{3.4}$$

Steady state phosphorescence measurements have also been employed to determine quenching constants using the Stern-Volmer equation;

$$\frac{I_0}{I} = 1 + \frac{k_q[Q]}{k_d} \qquad \textbf{3.5}$$

By measuring the steady state phosphorescence intensity I, as a function of quencher concentration.

3.4.1 Thermal Lensing

Thermal lensing is a technique that determines the alteration in the refractive index of a medium as a result of the temperature rise in the path of a laser beam absorbed by the medium which is ideal for probing the decay rates of excited states, which do not have favourable spectroscopic properties for using conventional absorption or emission techniques. The absorption of energy in a laser pulse gives rise to local temperature changes in gases and liquids. This local heating effect leads to a change in density and refractive index, which causes the system to act as a diverging lens. Non-radiative transitions from excited states release energy, which cause these local heating effects. Time resolved thermal lensing due to this release of energy could be used to measure lifetimes of singlet oxygen in the range 0.1 to 100 μs, by probing with a another continuous laser source, which is deflected by the thermal lens. The dynamic range of time resolved thermal lensing is determined by two factors; the acoustic transit time of the heat across the laser beam, determined by the velocity of sound in the medium, and the thermal recovery time of the medium. Time resolved thermal lensing could also be used to measure quantum yields of singlet oxygen and in addition the time profile of heat generation could be used to yield the lifetime of singlet oxygen[13]

3.5 Singlet Oxygen Applications

Ground state molecular oxygen is well known to be highly reactive and essential to life. However, excited states of oxygen have been found to be involved in photosensitised oxidations, photodynamic inactivation of viruses and cells[6], photo-carcinogenesis[7] and in the photo-degradation of dyes and polymers. The following are some of the processes mediated by singlet oxygen:

3.5.1 Photodynamic therapy

Photodynamic therapy (PDT) is a potential method used in the treatment of cancer[6-7] through the use of drugs (photosensitisers) that are activated by light. It is used in conjunction with chemotherapy for treatment of malignant tumours and involves

utilising the interaction of an inert dye, light and oxygen. The most widely used drugs are a water soluble red powder consisting of a mixture of metal-free porphyrins[7-8].

3.5.2 Photohaemolysis

Photohaemolysis refers to the opening of red blood cell (RBC) membranes and release of haemoglobin, induced by exposure to light[9-10]. Exposure of animals to sunlight after ingestion of plants containing the natural pigment hypericin (HY) leads to inflammation, ulceration, and infection, and in severe cases, convulsions and death. Studies have shown that photohaemolysis by hypericin is indicated by singlet oxygen.

3.5.3 Atmospheric pollution

Polycyclic aromatic hydrocarbons (PAHs) are a class of organic pollutants released in the atmosphere by natural sources, (*e.g.* volcanoes) and many types of man-made sources, (*e.g.* automobile exhausts) and absorb sunlight in the UV-A region (320-400 nm). Singlet oxygen generated in the lower atmosphere by the action of sunlight on PAHs may be involved in causing atmospheric pollution and smog[11]. Production of $^1O_2$ ($^1\Delta_g$) by photosensitisation is favourable owing to the high triplet yields and long lifetimes of the triplet states. In addition to the direct reactions of singlet oxygen with biological substrates, PAHs react with $^1O_2$ ($^1\Delta_g$) to form unstable dioxetanes and endoperoxides which are potential candidates for biological damage[12].

3.7 Deactivation of Singlet Oxygen

Deactivation of singlet oxygen $^1O_2$ ($^1\Delta_g$) in solution may occur using radiative or non-radiative transitions to the triplet ground state, or using quenching of the singlet excited state.

i) Radiative Decay

Radiative decay of singlet oxygen involves emission from the excited state to the triplet ground state.

$$O_2(^1\Delta_g) \longrightarrow O_2(^3\Sigma_g^-) + h\nu \qquad \textbf{3.6}$$

The decay of singlet oxygen is known to be significantly affected by the nature of the solvent in which it is dissolved [13]

ii) Non-Radiative Decay

Is a pathway which is highly dependent upon the molecular structure of the solvent, the transition being forbidden due to the dielectric dipole. The radiative lifetime may be as long as 64 minutes in the gas phase[14].

iii) Quenching

Deactivation of singlet oxygen can be accomplished by either physical or chemical quenching. In both cases similar intermediates may be involved in the reaction or quenching paths.

3.8 Chemical quenching processes

Chemical quenching of singlet oxygen involves reaction of singlet oxygen with substrate molecules to form an oxidised chemical species; this can be through autooxidation, or dye sensitised photooxidation of a substrate.

3.9 Physical quenching processes

There are a number of mechanisms for the physical quenching of singlet molecular oxygen which are as detailed below:

- **Quenching by Solvent**

The greater the solvent absorption at 7880cm^{-1} (1270nm), the shorter the singlet oxygen lifetime although it is known that the lifetime of singlet oxygen varies considerably with solvent[2], indicating that direct conversion of the singlet oxygen electronic excitation energy into vibrational energy in the solvent, is a dominant factor in determining the rate of decay. The lifetime of singlet oxygen varies considerably with solvent, which indicates that direct conversion of the singlet oxygen electronic excitation energy into vibrational energy, in the solvent, is a dominant factor in determining the rate of decay. Consequently in solvents that possess combination bands which have appreciable absorption in this region, such as water, hydrocarbons and alcohols, the singlet oxygen lifetime is very short, being approximately a few tens of microseconds.

In solvents such as freons and perdeuterated solvents, the positions of the infra-red absorption frequencies do not facilitate such energy transfer and therefore singlet oxygen lifetimes are longer, ranging from hundreds of microseconds to milliseconds. However, theories which only consider the infra-red properties of the solvent are not very successful at predicting the singlet oxygen lifetime in a given solvent. Hence, other solvent properties must be considered.

- **Charge Transfer Quenching**

This reaction involves interaction between the electron deficient singlet oxygen molecules with electron donors to give a charge transfer complex.

$$^1O_2\,(^1\Delta_g) \rightleftharpoons [D^{\delta+}\ldots O_2{}^{\delta-}]^1 \rightleftharpoons [D^{\delta+}..O_2{}^{\delta-}]^3 \longrightarrow D + {}^3O_2 \qquad \textbf{3.7}$$

There have been shown to be correlations between the rate constants for physical quenching of singlet oxygen and the ionisation potential of a number of aliphatic and aromatic amines, giving further support to the partial charge transfer proposal[15]. There are two factors which determine the rate constants for quenching by amines: one is the ionisation energy, the quenching rate increasing with decreasing ionisation potential supporting the charge transfer mechanism, the other is steric factors, and the quenching rate is seen to decrease with increasing steric hindrance to the amino nitrogen[15].

- **Quenching by Energy Transfer**

The absorbed energy which is released by an excited molecule can be quenched through transfer of the excitation energy to another molecule. The quenching of singlet oxygen in fluid media *via* the energy transfer mechanism has been documented for a number of compounds, this mechanism of quenching is the reverse of the reaction by which singlet oxygen is formed, which involves formation of triplet quencher and ground state oxygen as shown below

$$^1A + {}^1O_2{}^* \rightleftharpoons [^1A....{}^1O_2]^* \rightleftharpoons {}^3A^* + {}^3O_2 \qquad \textbf{3.8}$$

3.10 Electron Transfer Quenching Mechanisms

Electron Transfer Quenching Mechanisms are divided in two:

- ***Quenching Via Encounter Complexes***: Excitation of the sensitiser usually takes place before formation of the encounter complex. In this case transfer of the electron occurs during the lifetime of the collision complex, the charge transfer species which is immediately formed is known as a "contact ion pair" (CIP). The collision complex can separate slightly, undergo electron transfer, and generate a "solvent separated ion pair" (SSIP), subsequently solvent molecules rapidly stabilise contact ion pairs and solvated ion pairs. Thus a contact ion pair may be separated by a solvent molecule and be converted into a solvent separated ion pair and conversely a solvent separated ion pair may convert to a contact ion pair[16].

- **Quenching *via* Exciplexes:** The term exciplex refers to an excited state complex formed by the combination of two non-identical moieties, atoms or molecules in the excited state . Exciplexes are characterised by strong binding energies, partial charge transfer on each reactant molecule, and large dipole moments, which reflect the degree of charge transfer[17]. An encounter complex can rapidly form an intermediate, if the interaction between the reactants is strong before proceeding to products, which may have a sufficiently long lifetime to undergo light emission. Such intermediates are termed exciplexes.

3.11 Quenching by Ground State Oxygen

Molecular oxygen is an efficient quencher of electronically excited states and in most cases quenching by oxygen is so efficient that the reaction rate is believed to be diffusion limited. When quenching of an excited state takes place, excitation energy may be transferred to oxygen, resulting in the formation of the first excited singlet state of the oxygen molecule; the second may be generated initially depending on the energy of the donor. The literature reported quenching rate constants vary significantly from compound to compound[19-23].

Quenching of singlet states of molecules can occur if the excited singlet lifetime is sufficiently long or a high concentration of oxygen is present. Quenching occurs by

collisional spin allowed energy transfer generating singlet oxygen, if the energy gap between singlet and triplet states in the donor is large enough[18].

$$^1M^* + {}^3O_2\,(^3\Sigma_g^-) \longrightarrow {}^3M^* + {}^1O_2^*\,(^1\Delta_g) \qquad \textbf{3.9}$$

Which is followed by spin allowed catalysed intersystem crossing;

$$^1M^* + {}^3O_2\,(^3\Sigma_g^-) \longrightarrow {}^3M^* + {}^3O_2\,(^3\Sigma_g^-) \qquad \textbf{3.10}$$

In the case of quenching of triplets, quenching occurs either by collisional spin allowed energy transfer[20];

$$^3M^* + {}^3O_2\,(^3\Sigma_g^-) \longrightarrow {}^1M + {}^1O_2^*\,(^1\Delta_g) \qquad \textbf{3.11}$$

or by spin allowed catalysed intersystem crossing;

$$^3M^* + {}^3O_2\,(^3\Sigma_g^-) \longrightarrow {}^1M + {}^3O_2\,(^3\Sigma_g^-) \qquad \textbf{3.12}$$

3.11.1 Diffusion Controlled Reactions

Encounters between reactants in solution occur in a different manner from encounters in gases. Reactant molecules need to make their way through the solvent and as a result their encounter frequency is considerably less than in a gas[24].

Consider the following bimolecular reaction;

$$A + B \underset{k_{-diff}}{\overset{k_{diff}}{\rightleftharpoons}} [A\text{---}B] \xrightarrow{k_p} P \qquad \textbf{3.13}$$

The reaction can be considered in terms of the formation and dissociation of an encounter complex. If the rate of formation of products is greater than the dissociation of the encounter complex, $k_p >> k_{diff}$, the reaction is fully diffusion controlled and $k_{obs} = k_{diff}$. Conversely, where rate of dissociation of the encounter complex is greater than the rate of formation of products, $k_{diff} >> k_p$, the reaction is considered to be in the pre-equilibrium region.

If a reaction is diffusion controlled the rate of reaction cannot exceed the rate the molecules can diffuse together to react. Therefore the reaction is determined solely by the rate of encounter and is limited by the rate of diffusion.

It is often claimed that a quenching reaction is diffusion controlled if the rate constant exceeds a value of approximately 10^{10} l mol^{-1} s^{-1}, or sometimes even a value smaller than this. It is important that a clear distinction is made between fully diffusion-controlled reactions and nearly diffusion controlled reactions, since in the latter case the quenching efficiency is less than unity. Quenching of excited states of many organic molecules by oxygen is considered to be diffusion controlled, to determine the fraction that is diffusion controlled it is necessary to consider the spin statistics.

3.11.2 Singlet Excited States Interaction with Ground State Oxygen

The most extensive studies in conventional solvents have been carried out on excited singlet state interactions of aromatic hydrocarbons with ground state molecular oxygen[25-28]. Experimental rate constants for a large number of molecules have been obtained from Stern-Volmer plots of the effect of oxygen concentration on the fluorescence intensity, and by measuring the fluorescence lifetimes in the absence and presence of oxygen. Singlet excited state lifetime measurements have been found to yield quenching rate constants, k_q^S, which are shown to be diffusion controlled[25, 27-28]. The quenching rate constants of the S_1 state in non-viscous solvents have been reported to be of the order of 10^{10} mol l^{-1} s^{-1}, close to the rate constant for diffusion control, calculated by the Debye equation[29]

$$k_{diff} = \frac{8RT}{3\eta} \times 10^3 \qquad 3.13$$

However, this expression has often faild in experiments where a change in temperature and solvent results in a change in viscosity. Furthermore may also be inappropriate for oxygen since assumptions are made about the molecular radii.

High pressure studies have clearly demonstrated that fluorescence quenching by oxygen of the S_1 state of a number of meso-substituted anthracene derivatives is diffusion controlled in nature, from the pressure induced solvent viscosity dependence at constant temperature[27-28]. Okamoto studied the fluorescence quenching of 9, 10-dicyanoanthracene (DCNA) by oxygen, in liquid and supercritical carbon dioxide at 25°C and 35°C respectively as a function of pressure[25]. The quenching rate was found to below diffusion control and increased

with increasing pressure in both systems. The plots of $\ln k_q$ against pressure were approximately linear in liquid CO_2, whereas in supercritical CO_2 quenching rates increased rapidly in the lower pressure region and monotonically with further increases in pressure. In an earlier study Okamoto and co-workers[26] investigated quenching of another derivative of anthracene, 9-dimethylanthracene (DMEA), and found it to be nearly diffusion controlled and to possess a positive activation volume. The quenching rate constant for DCNA was reported to be significantly smaller than that for DMEA. They explained this in terms of the electronic nature of the substituents, since DCNA has an electron withdrawing group and DMEA has an electron donating group.

Studies[27] on the effect of pressure on quenching of the S_1 state of pyrene in non-polar solvents found that the rate constant for quenching k_q^S, decreased significantly with increasing pressure due to increasing viscosity. Hence it was thought that the quenching by oxygen may involve an encounter complex pair $^1(MO_2)^*$, with singlet spin multiplicity, Scheme 3.5.

$$^1M^* + O_2\,(^3\Sigma_g^-) \underset{k_{-diff}}{\overset{k_{diff}}{\rightleftharpoons}} {}^1(M\,O_2)^* \xrightarrow{k_{ic}} {}^3M^* + O_2\,(^3\Sigma_g^-)$$

$$^1M^* + O_2\,(^3\Sigma_g^-) \underset{k_{-diff}}{\overset{k_{diff}}{\rightleftharpoons}} {}^1(M\,O_2)^* \xrightarrow{k_{et}} {}^3M^* + O_2\,(^1\Delta_g)$$

Scheme 3.5: Formation of an encounter complex of singlet multiplicity during singlet state quenching by oxygen

3.11.3 Triplet Excited State Interaction with Ground State Oxygen

In what is widely regarded as the seminal work in this field, Porter and co-workers reported on the mechanism of oxygen quenching of electronic excited states of aromatic hydrocarbons[30-31]. They demonstrated the importance of spin statistical factors in the quenching of triplet states by oxygen.

Essentially the spin states of the donor and acceptor can be combined in any way to give those of products provided there is no change in total spin[32].

Porter and Kearns[30, 33] initially investigated the quenching mechanism of aromatic hydrocarbons, Algar and Stevens[34] proposed the spin statistics for triplet state quenching by molecular oxygen, Scheme 3.6.

$$^3S^* + {}^3O_2 \underset{k_{-1}}{\overset{^1/_9 k_1}{\rightleftharpoons}} {}^1[S\text{---}O_2]^* \xrightarrow{k_{et}} {}^1S + {}^1O_2^* \quad 1$$

$$\underset{k_{-2}}{\overset{^1/_3 k_2}{\rightleftharpoons}} {}^3[S\text{---}O_2]^* \xrightarrow{k_{isc}} {}^1S + {}^3O_2 \quad 2$$

$$\underset{k_{-3}}{\overset{^5/_9 k_3}{\rightleftharpoons}} {}^5[S\text{---}O_2]^* \quad 3$$

Scheme 3.6: Different pathways for triplet state quenching by oxygen

Where k_{et} and k_{isc} denote; the rate of formation of products *via* energy transfer and intersystem crossing respectively, and k_1, k_2 and k_3 are all the same.

According to the spin statistical factors, two interacting triplets give rise to nine possible encounter complexes; five quintet states, three triplet states and one singlet state, all of equal probability. If all three steps were occurring then the quenching constant would be equal to the diffusion constant.

For triplet-triplet encounters there are no spin allowed products for a quintet state, therefore the maximum rate constant is $^4/_9$ of the diffusion controlled value (route 1 and 2 respectively). Of the two possibilities energy transfer to oxygen (route 1) is more favourable, because it is spin allowed and paramagnetically induced. The formation of products from the triplet state (route 2) is spin allowed but has poor Franck-Condon factors; hence this route is rendered less favourable.

Aromatic hydrocarbons with low triplet energy, E_T, between 30 and 42 kcal mol^{-1}, showed that the rate constant for triplet quenching (k_q^T) was limited to approximately one ninth of the diffusion controlled rate constant [30-31] and the quenching of triplet states with high triplet energies, where $E_T > 42$ kcal mol^{-1}, gave rate constants which were less than $^1/_9 k_{diff}$. Such observations led to the suggestion

that k_q^T reflected quenching solely *via* route one, Scheme 3.6, and was therefore limited to a maximum value of $^1/_9\, k_{diff}$.

Deviations to lower values were considered to arise as a consequence of both decreasing Frank-Condon factors with increasing triplet energy and hydrocarbon dependent symmetry factors that effectively decreased the relative magnitude of k_1 with respect to k_{-1}[30-33]. Quenching *via* the triplet encounter complex was predicted to be negligible due to the highly unfavourable Franck-Condon factors for the more exothermic process, giving ground state products leading to $k_{-2} >> k_2$[34]. The fact that k_q^T was experimentally limited to $^1/_9\, k_{diff}$ confirmed the lack of involvement of route 2 Scheme 3.6, at room temperature.

Studies have shown that rate constants[35], which were greater than $^1/_9\, k_{diff}$, and in some cases which approached $^4/_9\, k_{diff}$, could be explained in terms of both singlet and triplet encounter complexes decaying efficiently to form products.

The encounter complex in this study involves high energy triplet states of carbonyl and amine molecules with oxygen having a degree of charge-transfer character. The charge transfer state lies at lower energies than the locally excited triplet states, in which case processes one and two in Scheme 3.6 may involve transitions to these states. The scheme proposed in the study, which includes inter-system crossing between charge transfer states of singlet and triplet multiplicity is shown in Scheme 3.7.

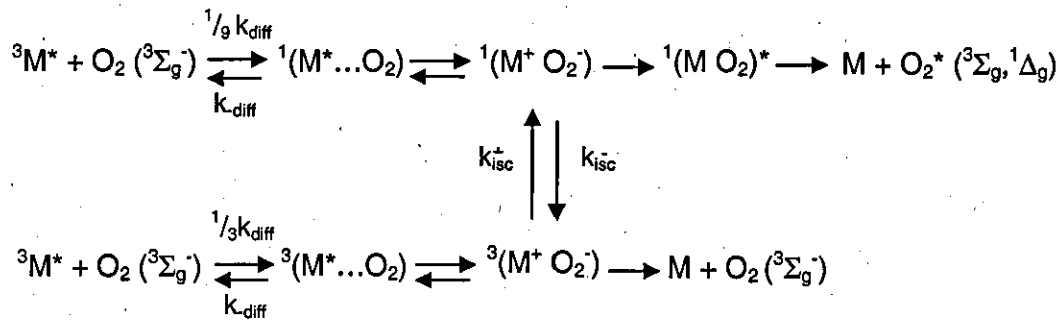

Scheme 3.7: Spin statistical mechanism involving inter-system crossing between charge transfer states

Generally, because the application of high pressure can significantly change solvent viscosity without having to change temperature or solvent, studies performed at high pressures provide information for quenching with nearly and fully diffusion controlled rate constants. Systems with high[36] k_q^T at 0.1 MPa, reported the rate of quenching decreased monotonically with increasing pressure, whereas for those with lower k_q^T at 0.1MPa, the pressure dependence of k_q^T showed a maximum.

They found that the triplet energy dependence of k_q^T decreases as pressure increases and found k_q^T to be almost independent of triplet energy at higher pressures ≥ 400 MPa.

3.12 Singlet Oxygen Quantum Yields

The quantum yield of sensitized production of singlet oxygen Φ_Δ is given by the sum of the contributions arising from oxygen quenching of the lowest excited singlet state (S_1) and the lowest excited triplet state (T_1) of the sensitiser;

$$\Phi_\Delta = \Phi_\Delta (S_1) + \Phi_\Delta(T_1) \qquad 3.14$$

Singlet oxygen is thus produced with varying efficiency due to quenching of both triplet and singlet states. The quantum yields of production of singlet oxygen ($^1\Delta_g$) have been reported for a number of compounds in a variety of solvents[37-40].

Rate constants for quenching of singlet, k_q^S, and triplet states k_q^T, by oxygen and the fraction of triplet states quenched which produce singlet oxygen, f_Δ^T, have been shown to depend on several factors including; excited state energy, nature of the excited state, redox potential of the excited state and nature of the solvent[30,41-44].

There has been considerable recent interest in the factors which determine oxygen quenching of excited states and the efficiency of formation thereby of singlet oxygen[41-44]. However, despite recent interest over the last few decades, the mechanism by which oxygen quenches the excited states of organic molecules remains poorly understood[40-43]. It is well known that singlet oxygen ($^1\Delta_g$) is frequently produced as a consequence of these quenching interactions. However, it is abundantly clear that the yield of singlet oxygen and the quenching rate constants vary considerably depending on the nature of the excited state being quenched and on the solvent or micro-environment[40-53].

Studies have shown that oxygen quenching of the lowest[56] excited singlet state of eight aromatic hydrocarbons induces intersystem crossing with high yield in toluene, they found that this yield drops when acetonitrile is used as a solvent. The fraction of singlet states quenched by oxygen which yield triplet states, with or without singlet oxygen production, f_T^{O2}, was found to be ≥ 0.9 in all cases in

toluene, but decreased to give values in the range of 0.55 to 0.9 in the polar solvent acetonitrile.

The fraction of excited triplet states arising due to oxygen quenching of the excited singlet states of nine aromatic hydrocarbons were measured in acetonitrile and values were reported to be between 0.36 and 1.0[47], whilst another study measured f_T^{O2} values for anthracene and eight of its derivatives, which were found to vary from approximately 0.6 to 1.0 in acetonitrile[43]; however in cyclohexane these same derivatives had f_T^{O2} values of unity[41]. The quenching of various aromatic hydrocarbons in a variety of solvents was investigated[49] which reported mixed first and second order decay kinetics of singlet oxygen, as a result of the oxygen quenching of certain aromatic triplet ketones. The second order contribution was thought to have been as a result of a bimolecular reaction between singlet oxygen and a long lived species, formed due to oxygen quenching. Low values were obtained for the efficiency of singlet oxygen generation which could be due to competition between formation of singlet oxygen and a biradical species (Figure 3.7), as a result of branching of the singlet encounter complex.

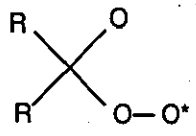

Figure 3.7: Diagram of biradical species

Such a biradical species, of unspecified multiplicity, was originally proposed by Quinkert as an intermediate in the light induced oxidation of methanone[52].

The factors affecting the efficiency of singlet oxygen production were elucidated by studying oxygen quenching of a range of meso-substituted anthracenes in cyclohexane[51], and Singlet oxygen production efficiency from the singlet state ranged from zero to unity. However, singlet oxygen production from the triplet state was found to be unity in all cases. This observation was explained in terms of dependency of the efficiency of formation on the triplet encounter complex $^3(T_2...^3\Sigma)$. They postulated that the complex dissociates to give ground state oxygen and the T_2 state of the separated anthracene derivative, which dissipates its excess energy by internal conversion to the T_1 state, the dissociation of the $^3(T_1...^3\Sigma)$

complex subsequently produces singlet oxygen. They also reported values for a range of substituted biphenyls[21, 51] and naphthalenes[52] in acetonitrile, benzene and cyclohexane. The f_{Δ}^{T} values showed pronounced sensitivity to the oxidation potential of the derivatives and to solvent polarity. An increase in polarity and in oxidation potential of the derivative resulted in an increase in the quenching rate.

Studies[53] of the rate constants for formation of the $^1\Delta_g$, $^1\Sigma_g^+$ and $^3\Sigma_g^-$ states of molecular oxygen for a series of nine benzophenones of varying oxidation potential, showed almost constant triplet energy. Weaker charge transfer effects were observed for T_1 (n, π^*) benzophenones compared to those obtained for T_1 (π, π^*) biphenyls. Quenching of T_1 (n, π^*) and T_1 (π, π^*) sensitisers were proposed to proceed *via* two different channels, each capable of producing the three lowest lying states of molecular oxygen[53], Scheme 3.8.

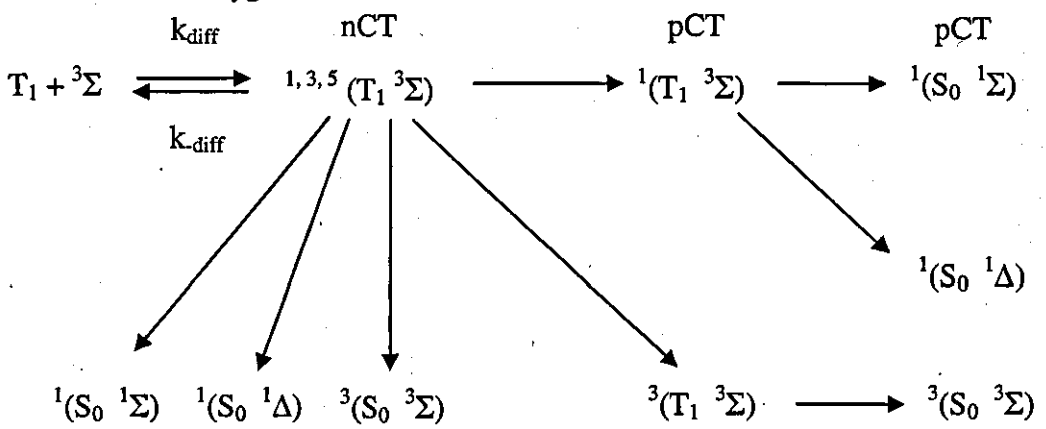

Scheme 3.8: Schematic to illustrate the different pathways for partial and non charge transfer quenching

The effect of heavy atom-containing sensitisers on the singlet oxygen generation efficiency was investigated and it was found that in the case of π,π^* triplets (tetrahalo-p-benzoquinones and haloanthracences), introduction of heavy atoms had practically no influence on the singlet oxygen generation efficiency[54]. However, for n,π^* triplets (haloacetophenone), the S_{Δ} values decreased sharply with increasing number of heavy atoms, due to the intersystem crossing between singlet and triplet states in an encounter complex. This assumption was based due to the π,π^* triplet sensitisers intersystem crossing from the triplet state to the singlet state of the encounter complex with oxygen, being faster than dissociation of the triplet encounter complex to ground state sensitiser and oxygen, $^3\Sigma_g^-$.

A further study of the solvent effects on the singlet oxygen quantum yield[55] reported that for carbonyls, the quenching rate constant and singlet oxygen generation efficiencies are independent of polarity and viscosity of the solvent, with few exceptions, and therefore the assumption that $k_q^T \sim {}^1/_9\, k_{diff}$ for estimating quenching by the energy transfer mechanism does not hold. However, singlet oxygen efficiencies did increase in alcohols; they explained this trend in terms of specific solvation of the triplet carbonyls by alcohols, which resulted in a decrease in the deactivation rate constant of the triplet encounter complex to the ground state, and an increase in the contribution of energy transfer to quenching[56-58].

Worrall and Abdel-Shafi[59] reported rate constants for quenching by molecular oxygen of excited singlet and triplet states, k^S_q and k^T_q , respectively, of some aromatic hydrocarbons in acetonitrile. The fraction of excited singlet states quenched by oxygen; which result in triplet states, f^S_T , are in the range of 0.25–0.85. and the efficiencies of singlet oxygen production during oxygen quenching of the excited singlet and triplet states, f^S_Δ and f^T_Δ, respectively, were also measured. Values of f^S_Δ were shown to be 0.28±0.05 for 1,2;5,6-dibenzanthracene, pyrene, fluoranthene, 1,11- benzoperlyene and perlyene while values of f^T_Δ cover the range of 0.25–1.0. Additionally recent studies[59] have shown that the photosensitized generation and subsequent decay of singlet oxygen in supercritical fluid xenon; as a function of pressure and temperature found that the rate constant for quenching of singlet oxygen by ground state oxygen, k_q^O , increases as the pressure increases and decreases as the temperature increases. At 298 K, the value of k_q^O increases from (1.27 to 1.76)×10^3 dm^3 mol^{-1} s^{-1} as the pressure increases from 9.8 to 39.2 MPa; at 355 K the values of k_q^O drop to 6.2×10^2 and 1.54×10^3 dm^3 mol^{-1} s^{-1} at these same pressures. It has also been found that the fractional contribution of the oxygen quenching to the overall singlet oxygen decay rate increases with increasing pressure, although showing greater variations at high temperatures, and decreases with increasing temperature.

References

1. Rabek, J.F. Ranby, B. *Photochem. Photobiol.* **1978**; 28:557-570.
2. Hurst, J.R. Schuster, G.B. *J.Am.Chem.Soc.* **1983**; 105:5756-5760.
3. Kearns, D.R. *Chem.Rev.* **1971**; 71:395-427.
4. Rossbroich, G. Garcia, N.A. Braslavsky, S. E. *Journal of Photochemistry* **1985**; 31:37-47.
5. Matheson, I.B. Lee, J. *Chemical Physics Letters* **1972**; 14:350-351.
6. Paba, V. Quarto, M. Varriale, L. Crescenzi, E. and Palumbo, G. *Journal of Photochemistry and Photobiology B: Biology*, **2001;** *60,* 87-96.
7. Walther M, Delaney T, Smith P, Friauf W, Thomas G, Shawker T, Vargas M, Choyke, P. Linehan, W. Edward, H. Abraham, *et al. Urology*, **1997**; 50: 199-206.
8. Madan, V. Loncaster, J. Allan, D. Lear, J. Sheridan, L. Leach, C and Allan, E. *Photodiagnosis and Photodynamic Therapy*, **2005**; 2: 273-281.
9. Misra, R. B. Bajpai, P. K. Joshi, P. C and Hans, R. K. *Food and Chemical Toxicology*, **2001;** 39: 11-18.
10. Traynor, N. J. Johnson B. E. and Gibbs N. K. *Toxicology in Vitro*, **1996;** 10: 619-624.
11. Mcdow S, Vartiainen M, Sun Q, Hong Y, Yao Y and Kamens R. *Atmospheric Environment*, **1995;** 29: 791-797.
12. Toyooka T and Ibuki Y. *Environmental Toxicology and Pharmacology*, **2007**; 23: 256-263.
13. Scurlock, R.; Nonell, S.; Braslavsky,S.; Ogilby, P. *Phys. Chem.* **1995;** *99:* 3521-3526.
14. Matheson IB, Lee J. *J.Am.Chem.Soc.* **1972**; 94:3310-3314.
15. Asahi T, Mataga N. *J.Phys.Chem.* **1991;** 95:1956-1963.
16. Schmidt R. *J. Phys. Chem.* **2006;** 110:5990-5997.
17. Munroe, B. M., *J. Phys. Chem.*, **1977**; 81: 1861-1864.
18. Okamoto M, Tanaka F, Hirayama S. *J. Phys. Chem. A* **1998;** 102:10703- 10709.
19. Grewer C, Brauer HD. *J.Phys.Chem.* **1993;** 97:5001-5006.
20. Baltrop, J. A.; Coyle, J. D., John Wiley and Sons, *Principles of Photochemistry*, **1978**, Chapter 4, 116.

21 Grewer, C.; Brauer, H. D., *J. Phys. Chem.*, **1994**; 98: 4230-4235.

22. Sciano, J. C.; Nau, W. M., *J. Phys. Chem.*, **1996**; 100: 11360-11367.

23 Wilkinson, F.; Abdel-Shafi, A. A., *J. Phys. Chem. A.*, **1999**, 103: 5425-5438.

24. Abdel-Shafi, A. A.; Wilkinson, F.; Worrall, D. R., *J. Photochem. Photobiol. A,* Chem., **2001**; 142: 133-143.

25. Okamoto, M.; Tamai, T.; Tanaka, F., *J. Phys. Chem. A,* **2003**, 107: 1284-1289.

26. Atkins, P.W., *Physical Chemistry*, Fifth Edition, Oxford University Press, **1977**; chapter 17 and 27.

27. Okamoto, M.; Yamada, K.; Nagashima, H.; Tanaka, F., *Chem. Phys. Letts.*, **2001**; 342**:** 578-582.

28. Okamoto, M.; Wada, O.; Tanaka, F.; Hirayama, S., *J. Phys. Chem.* A, **2001**, 105: 566-572.

29. Okamoto, M.; Tanaka, F., *J. Phys. Chem. A.* **2002**; 106: 3982-3990.

30. Tanaka, F.; Fukuta, T.; Okamoto, M.; Hirayama, S., *Phys. Chem. Chem. Phys.*, **2004**; 6:1219-1228.

31. Murov, S.L.; Carmichael, I.; hug, G.L., *Handbook of Photochemistry*, Second edition, Marcel Dekker, **1993**; 207.

32. Gijzeman, O. L. G.; Kaufman, F.; Porter, G., *J. Chem. Soc., Faraday Trans. II*, **1973**; 69: 721-726.

33. Petterson, C.K.; Porter, G.; Topp, M.R., *Chem. Phys. Letts.*, **1970;** 7: 612.

34. Cox, A, Kemp, T.J., *Introductory Photochemistry*, McGraw-Hill Book Co. **1970**; p21.

35. Kearns, D. R.; Stone, A. J., *J. Chem. Phys.*, **1971**; 55: 3383-3389.

36. Stevens, B., Algar, B. E., *J. Phys. Chem.*, **1968**; 72: 2582-2587.

37. Garner, A.; Wilkinson, F., *Chem, Phys. Lett*, **1977**; 45: 432-435.

38. Gorman, A A.; Lovering, G.; Rodgers, M. A. J., *J. Am. Chem. Soc.*, **1978**; 100: 4527-4532.

39. Schweitzer, C. Schmidt, R. *Chem. Rev.*, **2003**; 103**:** 1685 - 1758 and references therein.

40. Saltiel, J. B. Atwater, W. *Adv. Photochem.*, **1988;** 14; 1-90, and references therein.

41. Redmond, R. W. Gamlin, J. N. *Photochem. Photobiol.*, **1999**; 70: 391- 475, and references therein.

42. Stevens, B.; Marsh, K. L.; Baltrop, J. A., *J. Phys. Chem.*, **1981**; 85: 307-312.

43. Wilkinson, F; McGarvey D.J.; Olea, A., *J. Am.Chem.Soc.*, **1993**; 115: 12144-12151.

44. Kikuchi, K.; Sato, C.; Watabe, M.; Ikeda, H.; Takahashi, Y.; Miyashi, T., J. *Am. Chem. Soc.*, **1993**; 115: 5180-5184.

45. Wilkinson, F.; Abdel-Shafi, A. A., *J. Phys. Chem. A.*, **2000**; 104: 5747-5757.

46. Olea, A. F.; Wilkinson, F., *J. Phys. Chem.*, **1995**; 99: 4518-4524.

47. McGarvey, D. J.; Szekeres, P. G.; Wilkinson, F., *Chem. Phys. Lett.*, **1992**; 199: 314-319.

48. Potashnik, R.; Goldschmidt, C. R.; Ohalanghi, M., *Chem. Phys. Lett.*, **1971**; 9: 424- 428.

49. Sato, C.; Kikuchi, K.; Okumara, K.; Takahashi, Y.; Miyashi, T., *J. Phys. Chem.*, **1995**; 99: 16925-16931.

50. McLean, A. J.; McGarvey, D. J.; Truscott, T. G.; Lambert, C. R.; Land, E. J., *J. Chem. Soc., Faraday Trans.*, **1990**; 86: 3075-3080.

51. Gorman, A.A; Rodgers, M. A. J., *J. Am. Chem. Soc.*, **1986**; 108: 5074-5078.

52. Quinkert, G., *Pure Applied Chem.*, **1964**; 9: 607-621.

53. Wilkinson, F.; Abdel-Shafi, A. A, *J. Phys. Chem. A.*, **1997**; 101: 5509-5516.

54. Wilkinson, F.; McGarvey D. J.; Olea, A., *J. Phys. Chem.*, **1994**; 98: 3762-3769.

55. Schmidt, R.; Mehrdad, Z.; Schweitzer, C., *J. Phys.Chem. A.*, **2002**; 106: 228-235.

56. Darmanyan, A. P.; Foote, C. S., *J. Phys. Chem.*, **1992**; 96:3723-3729.

57. Darmanyan, A. P.; Foote, C. S., *J. Phys. Chem.*, **1993**; 97: 5032-5035.

58. Abdel-Shafi, A. A.; Worrall, D. R. *Journal of Photochemistry and Photobiology A Chemistry* **2005**, *172*, 170-179.

59. Abdel-Shafi, A. A.; Worrall, D. R. *Journal of Photochemistry and Photobiology A: Chemistry* **2007**, *186*, 263-269.

Chapter 4

Experimental

4.0 Experimental

4.1 Compounds and Solvents

3-Methyl-riboflavin-tetra acetate (3 TARF)[1], Iso-6,7-riboflavin (1R), 3-benzyl riboflavin (BR)[1] and Lumiflavin (Lf)[1], 6,9 Mall (6,9-methyl alloxazines) are samples donated by Prof. Marek Sikorski Adam Mickiewicz University in Poland. Anthracene (Aldrich, <99%), 9-methylanthracene (Aldrich <99%), 9,10-dichloroanthracene (Aldrich <99%), cyanoanthracene (Aldrich <99%), Naphthalene (Aldrich <99%), Benzophenone (Aldrich<99%), 5-hydroxy-1-4-naphthoquinone (Aldrich), 1,5-dihydroxynaphthalene (Aldrich 97%), Methylene Blue (Aldrich), Tris (2,2-bipyridyl) ruthenium II chloride hexahydrate, Rose Bengal (Aldrich<90%), .

Acetonitrile (Aldrich HPLC grade <99%), Methanol (Aldrich HPLC grade <99%), Ethanol (Aldrich grade <99%), Distilled Water, Cyclohexane (Aldrich grade <99%), Bromobenzene (Aldrich grade <99%), 1-iodopropane (Aldrich grade <99%), Hexane (Aldrich HPLC grade<99%), carbon dioxide (BOC), oxygen (BOC).

4.2 Ground State Absorption

Absorption spectra of all ground state samples were recorded using either an HP8453 UV-Visible spectrophotometer or a Perkin-Elmer Lambda Bio 40 UV-Vis spectrophotometer. Samples were measured by using the solvent used to dissolve the compound in as a blank as the spectrum for Anthracene shown in figure 4.1.

4.2.1 Ground State Absorption Spectra in SCF Cell

All Ground state absorption spectra in the cell were recorded using ocean optics fibre and a 250 W xenon arc lamp as a continuous source. Methanol is initially introduced to the cell as the background measurement, pressurised to 50 MPa and the lamp intensity recorded. The lamp intensity profile is then recorded with the sample in the cell and absorbances were recorded.

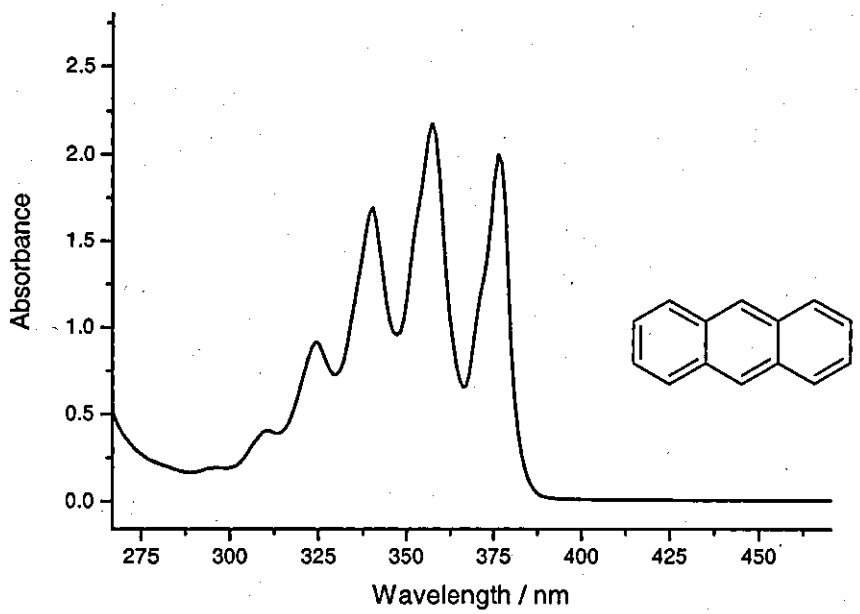

Figure 4.1: Ground state absorption spectrum of [Anthracene] = 3.5 x 10^{-4} mol l^{-1}

4.3 Fluorescence Measurements

Fluorescence measurements were made by using Spex Fluoromax Spectrofluorimeter. Samples were measured in solution and the Spectrofluorimeter was set to monitor at the required range of wavelength and all the values were recorded with the excitation wavelength of 355 nm, as shown in figure 4.2.

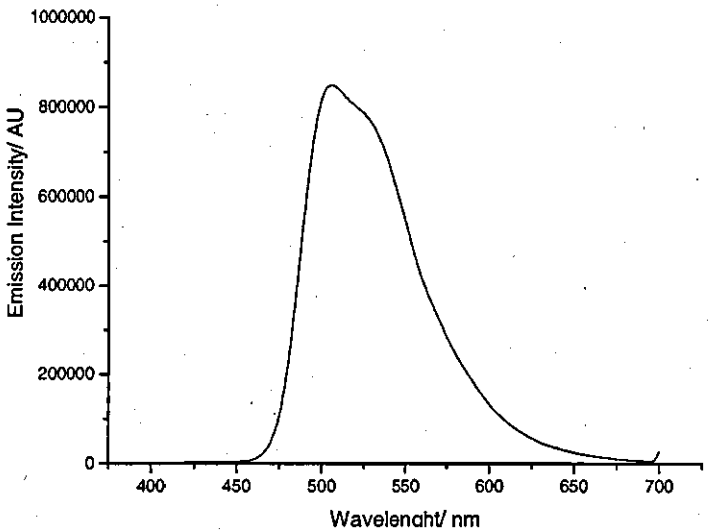

Figure 4.2: Fluorescence spectrum of Lumiflavin in acetonitrile between the ranges of 330-700 nm

4.4 Deoxygenation for laser flash photolysis

All the samples were deoxygenated through nitrogen bubbling; this was done by transferring the solution into a cuvette and sealing the top by fitting a rubber septum. A tube is fitted with a needle to the nitrogen gas cylinder which allows it to be bubbled and another needle is placed on the rubber septum to allow displaced gases to escape. The solution is concentrated with nitrogen for approximately 15 mins, prior to measurements.

4.5 Laser Flash Photolysis

This is a powerful technique for studying qualitative and quantitative rapid reactions, triplet states, isomerisation reactions and to identify reactive intermediates in photochemical systems. Commonly, an intense excitable pulse of short duration from a laser or a flash lamp is used to produce a concentration of a transient species which can be monitored by measuring the changes in the amount of light transmitted. At a short intervals of time after the generating pulse the system is analysed by observing emission or absorption characteristics. The decay or production of the transient absorption or emission at one particular wavelength is monitored or the absorption or emission spectrum of the transient is recorded at given times after the exciting pulse. This is achieved using a Lumonics Hyper HY200 Q-switched Nd:YAG laser with a pulse duration of 8 ns. The energy per pulse is approximately 7 mJ per pulse whilst the wavelength used for the photochemical investigations is achieved using the third harmonic at 355 nm of the fundamental laser wavelength at 1064 nm. The excitation energy was attenuated using solutions of sodium nitrite in water. The analysing beam was obtained from a 250 W xenon arc lamp (Optical Radiation Corporation). Appropriate filters of were used to cut off any unwanted wavelengths and neutral density filters were employed to reduce the intensity of the lamp beam.

4.5.1 Time Resolved Flash Photolysis Measurements

The Q-switched Lumonics HyperYAG HY200 (Lumonics) was used as the excitation source and the analysing light from the Xenon arc lamp was collected and focused into a monochromator and photomultiplier tube (Hamamatsu R928). An accelerating voltage was applied to the photomultiplier tube using a Fluke 415B high voltage power

supply, the signal from the multiplier was then transferred to a digital oscilloscope (Tektronics 2432A) and interfaced to the computer via an AT-GPIB interface card (National Instruments). The sequence and timing events of this system were controlled by a home built analogue delay generator which sends out a clock pulse every 1.65 ns, which triggers the computer and sets up two delays; one to trigger the opening of the shutters and the other to fire the laser. The computer enables the relevant shutters, ready to be triggered by the delay generator and arms the oscilloscope. The 1064 nm wavelength from the laser is set to trigger the oscilloscope by leakage through the end cavity mirror and is detected using a photodiode. On receipt of this signal the oscilloscope triggers, digitises and transfers the data from the photomultiplier to the computer where it is first displayed on the screen and then saved. The whole cycle takes less than 1.6 ns and is repeated on receiving the next clock pulse until the baseline; transient absorption, emission and topline are recorded.

Topline: Neither of the shutters is open, this gives the signal with zero analysing light
Baseline: The arc lamp shutter is open and the solution is monitored in an unexcited state without any scattered light
Emission: The laser shutter is open but the arc lamp shutter is closed; this gives a trace of emission by the excited state and any scattered light.
Absorption: Both the arc lamp and laser shutters are open; the arc lamp monitors the sample after the laser has excited it. This trace shows the absorption of the solution due to the excited species present. This trace may be negative which could be due to loss of ground state molecules that absorbs at this wavelength, or due to large emission by the excited state.

4.6 Methods

4.6.1 Fluorescence Quenching Measurements

Lumiflavin (Lf) in acetonitrile was used as a standard, since the quantum yield of fluorescence was given as 0.16[1]. Lf was dissolved in Acetonitrile to obtain an absorbance of ≤ 0.1 at 355 nm excitation wavelength and emission of around 365-600

nm, the solution was then placed in a cuvette, sealed and degassed (see section 4.4) for approximately 15 mins. Fluorescence spectra of the compounds were then measured and integration measurements were then calculated using MicroCal Origin.

3-Methyl-riboflavin-tetra acetate (3TARF), 3-benzyl riboflavin (BR) and iso-6,7-riboflavin (1R), were dissolved in methanol and an increasing amount of bromobenzene (quencher) was added to maintain an absorbance of ≤ 0.1 at the excitation wavelength of 355 nm, the solutions were then placed in a cuvette, sealed and degassed for approximately 15 minutes. UV ground state absorbances of the samples were then measured at the excitation of 355 nm and the fluorescence spectra recorded for the emission of 365 – 600 nm. Fluorescence spectra measurements of the samples were recorded in a similar way to the Lf in Acetonitrile and the areas under curve were obtained and recorded and values of fluorescence quenching were obtained using the Stern-Volmer equation as discussed in section 4.3.3

4.6.2 Fluorescence Quantum yield measurements

The samples were dissolved in different solvents to obtain an absorbance of ≤ 0.1 at 355 nm, the solutions were then placed in a cuvette, sealed and degassed for approximately 15 mins. The fluorescence spectrum using an excitation wavelength of 355 nm was then obtained and measurements of area under curve were then calculated using MicroCal origin programme.

4.6.3 Determination of the Triplet-Triplet spectra

Triplet triplet absorption spectra were obtained using laser flash photolysis – see section 4.5. In some cases (with the Flavins) varying amounts of bromobenzene (BrBz) were added to the solutions in order to increase their triplet yield. The samples were placed in a cuvette and degassed for 15 mins. The triplet state was produced using a 355 nm pulsed excitation from a frequency tripled Lumonics HY200 Nd:YAG laser. Data was typically gathered over the wavelength range 350 nm - 600 nm.

4.6.4 Determination of Triplet Quantum yields using Bromobenzene (BrBz)

Anthracene and varying amounts of BrBz were placed in a cuvette and degassed. The anthracene triplet state was produced using a 355 nm pulsed excitation from a

sensitiser) was used as a standard and also used in the quantitative measurements of the relative amounts of fluorescence and of the relative initial triplet state absorption using flash excitation in the presence and absence of bromobenzene as a quencher. Anthracene triplet-triplet absorption is around 420 nm which was chosen as the analysing wavelength. Flash excitation of the anthracene ground state was achieved at 355 nm laser excitation and the triplet-triplet absorption intensity measured. The amount of anthracene stock solution used was constant with increasing amounts of bromobenzene and the values recorded using the equation below:

$$\frac{F'}{F} = \left(\frac{D_T \, F'}{D_T{}^0 F} - 1 \right) \Phi_T + 1$$

F' = Fluorescence intensity in the absence of a quencher

F = Fluorescence intensity in the presence of a quencher

D_T^0 = Absorbance of the triplet state in the absence of a quencher

D_T = Absorbance of the triplet state in the presence of a quencher

Φ_T = Triplet quantum yield

4.6.5 Fluorescence Lifetime measured using single Photon Counting

A single photon counting technique was used to measure fluorescence decays using a Model 199 fluorescence decay time spectrometer (Edinburgh Instruments). Excitation of the samples was with a nitrogen filled flash lamp at 337nm. A solution of anthracene in methanol was placed in a cuvette as a reference, and the solution was then purged with nitrogen for 10 mins and then placed on the holder of the photon counting and the counting was started. After the count of the reference has been done then the sample of the flavins solution was purged with nitrogen and placed on the holder and then the count was started. For oxygen quenching studies the samples were purged with the nitrogen and oxygen ratios. The photon counts obtained which are the electric pulses from the monochromator were then fed into a discriminator and pulses with amplitudes higher than a given threshold value are counted. Photon Counting is a technique which is used to measure extremely low light fluxes; a flash lamp which uses nitrogen was used. Two photomultipliers were used to convert light into an electrical signal and the photon which passes through the window of the (photo multiplier tube) PMT.

4.6.6 Sample Preparation for the SCF set up/system

The apparatus used to prepare the supercritical fluid solutions has been described in detail elsewhere [2-5]. CO_2 (BOC, 58 MPa) is liquefied by chilling to −5 ^{0}C and the resulting liquid CO_2 is then pumped using an HPLC pump (Jasco model PU-980) through stainless steel tubing into a home-built pressure cell. The tubing is heated to the desired temperature in a gas chromatograph oven (Pye Unicam), and the cell is electrically heated using a home-built temperature controller. The cell temperature, typically controlled in these experiments to ±1 K, is monitored using a K series thermocouple and the pressure monitored using the pressure transducer in the HPLC pump head. Samples were introduced into the cell as Acetonitrile or methanol solution of the desired concentration. The solution was placed in the cell, and the solvent removed with a slow flow of oxygen gas whilst heating the cell.

Pressures ranged from 100 - 300 MPa, and were monitored using the pressure transducer in the HPLC pump head. Temperatures ranged between 300 K and 330 K and the tubing is heated using a gas chromatograph oven. The solution of the desired compound concentration in methanol or acetonitrile was pumped into the cell from the reservoir using a HPLC pump (JASCO model PU 980) and absorption measurements were taken as detailed in section 4.2.1. The set up which was home built is shown in figure 4.3, using $scCO_2$ as baseline for measuring absorption using supercritical carbon dioxide was done. Once the solution is in the cell the, solvent was removed by purging it with a steady flow of oxygen at 200 cm^3 min^{-1} for approximately 10 mins whilst heating the cell electronically using a home built temperature controller. The tubing is heated using a gas chromatograph oven, Figure 4.4.

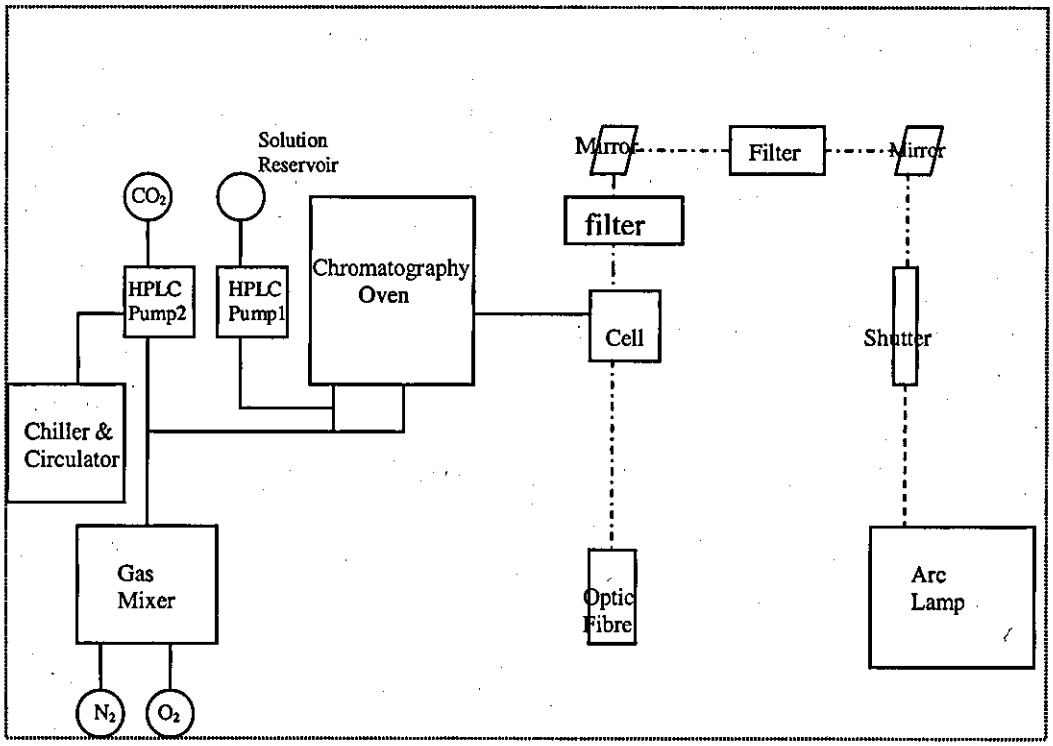

Figure 4.3: Geometry of apparatus used for absorption measurements using an optical fibre

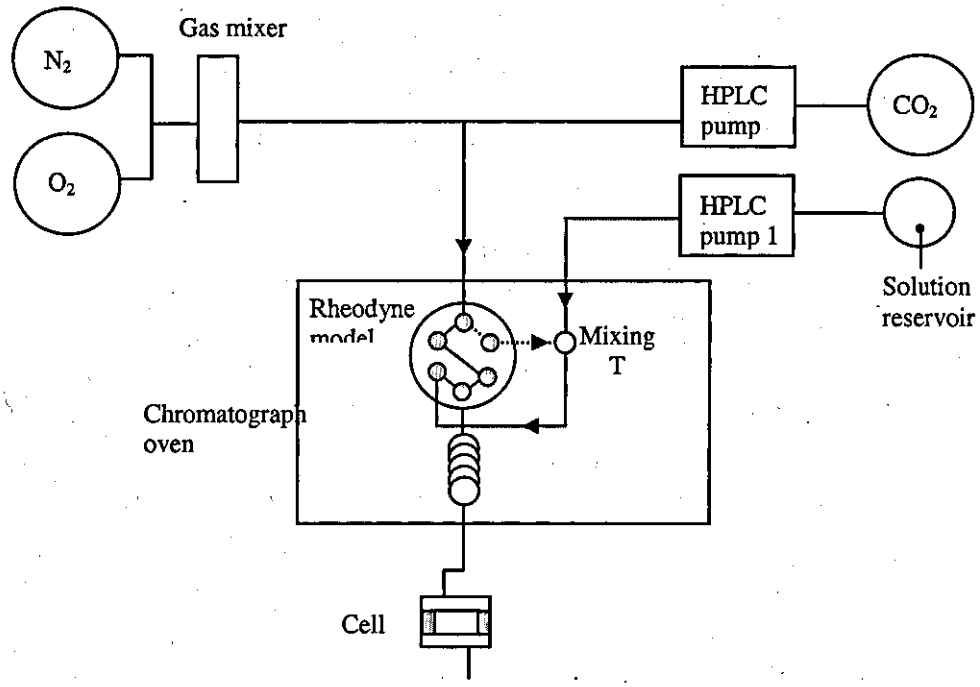

Figure 4.4: Schematic diagram of SCF preparation system

4.6.7 Singlet Oxygen Detection in SCF

Utilising near-IR detection techniques it was possible to measure the phosphorescence of singlet oxygen at 1270 nm. Quantum yield values were measured in supercritical carbon dioxide for anthracene relative to perinaphthenone as a standard sensitiser, known to be insensitive to changing solvent, for which quantum yield is 0.95 ± 0.05[6]. The quantum yield can be obtained from a plot of luminescence by fitting a plot of singlet decay versus time, with a single exponential affording the luminescence intensity and the decay rate constant. Experiments were performed as a function of laser energy and fitting a plot of singlet oxygen luminescence intensity versus laser energy with a straight line. The experimental setup was designed such that it was possible to measure the absorbance in the cell for each sensitiser allowing the mismatched ground state absorbances to be accounted for and corrected using the following equation.

$$\frac{m_u}{m_s} = \frac{\Phi_{\Delta u}}{\Phi_{\Delta s}}\left(\frac{1-10^{-A_s}}{1-10^{-A_u}}\right)$$

m_u = Gradient of unknown (Anthracene)

m_s = Gradient of sensitiser (Perinapthenone)

A = Absorbance

Φ_Δ = Singlet oxygen Quantum yield

Where the subscript u and s represents unknown and sensitiser: Anthracene and Perinapthenone respectively.

The absorbance of the solution was initially determined using the USB 2000 optic fibre as shown in figure 4.3 and then after the absorbance measurements were taken then the detector is placed at the same position and then the singlet oxygen detector was placed as shown in figure 4.5. Excitation of the sensitizer was with the third harmonic of a Lumonics hyperYAG HY200 Nd:YAG laser (355 nm, 8 mJ per pulse, 8 ns FWHM). The excitation energy was attenuated using aqueous sodium nitrite solution. Detection of $^1O_2(^1\Delta_g)$ was with an EO-980P liquid nitrogen cooled germanium photodiode detector (North Coast Scientific), with a 1270 nm interference filter interposed between sample and photodiode to isolate the singlet oxygen phosphorescence and to reduce detection of laser scatter and sensitizer emission. Data capture was with a 250 MS/s digitising oscilloscope (Tektronix 2432A) and data analysis were done using MicroCal Origin 6.1. After taking the singlet oxygen measurements, the USB 2000 optic fibre is placed back again and a further absorbance measurement was taken to ensure that the solution was consistent with the measurement taken immediately before the singlet oxygen measurements.

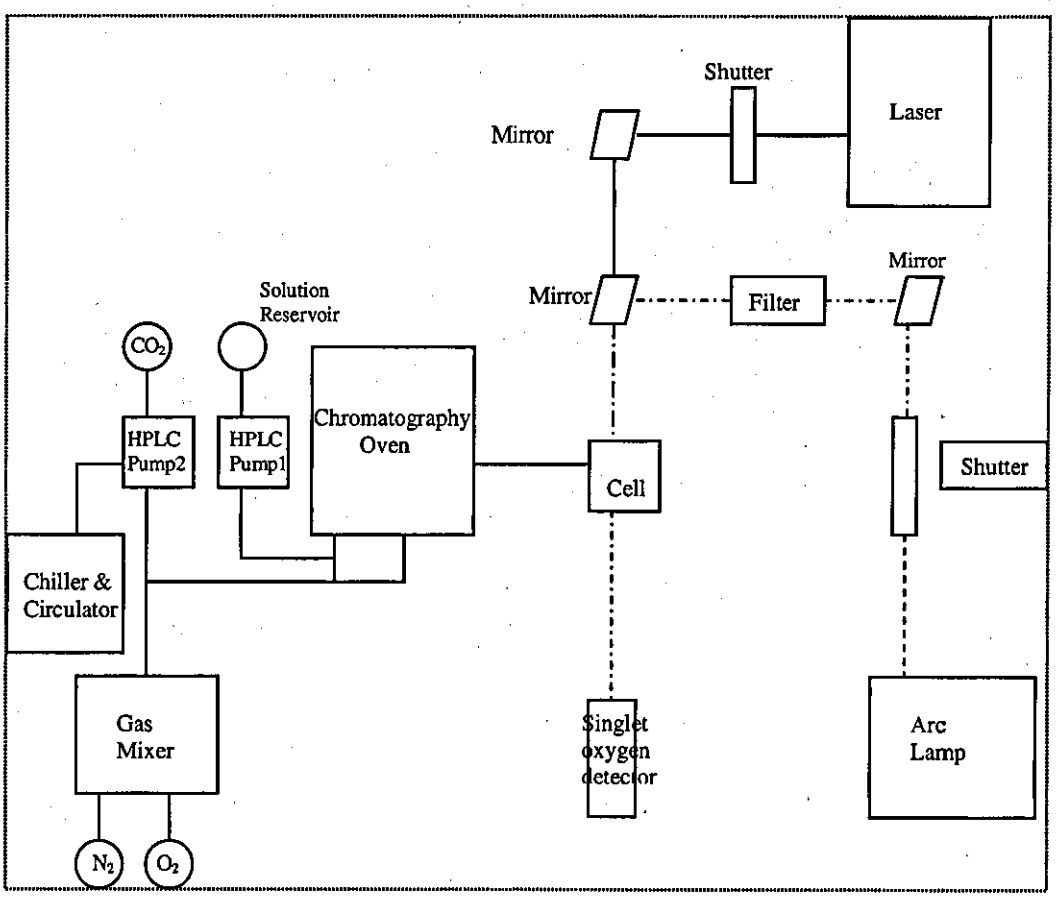

Figure 4.5: Geometry of apparatus used for singlet oxygen detector

4.7 Juglone production

The synthesis of Juglone using different types of sensitiser and different conventional solvents as well as scCO$_2$ solvents was studied. Photooxygenation of 1,5-dihydroxynaphthalene (dhdn) was studied with light to form 5-hydroxy-1,4-naphthoquinone (juglone). The reaction of singlet oxygen with 1,5-dihydroxynaphthalene is an example of a photo-Diels Alder reaction ([4+2]-cycloaddition), in which dhdn functions as diene and singlet oxygen as a dienophile.

The photooxidation of 1,5-dihydroxynaphthalene in both conventional solvents and supercritical carbon dioxide was carried out using the set-up shown in Figure 4.3. A xenon lamp (150W, Light Support) was used for the irradiation. The measurement of the absorption spectra and production of scCO$_2$ are described in sections 4.2.1, 4.6.6 and 4.6.7. The sensitisers used in the production of Juglone included Methylene Blue (MB),

Rose Bengal (RB) and anthracene (Anth) whilst the various solvents used were acetonitrile, methanol and $scCO_2$. The lamp intensity of the blank (Methanol) was recorded initially; the methanol was then flushed out of the cell using oxygen gas. Once the methanol was removed, the solution of interest was introduced into the cell, as described in Section 4.6.6, and the solvent was removed by flushing a steady stream of oxygen gas through the cell. Liquid carbon dioxide was then pumped into the cell to the initial pressure (typically 100 MPa) and the system heated to the desired temperature, the absorbance of the lamp through the cell was then recorded.

The set up is similar to the section 4.6.5 and 4.6.7 with a few adjustments from the filter being moved to reduce radiation from light. To prevent irradiation of compounds (around 400-450 nm) a coloured light filter (filter A) was used (orange, > 490 nm) positioned as shown in figure 5.6. For monitoring purposes, an optical fibre (Ocean Optics USB 2000, with Ocean Optics Spectrasuite software) was used to measure absorbance. Neutral density light filters (filter B) was used after the cell to decrease the light intensity at the spectrometer; this was optimised for the region of interest, i.e. 400-450 nm which was monitored at the 420nm wavelength for every minute, for the first five minute and then for every five minutes for the remaining half an hour. Add in monitoring times and wavelength

Methylene blue is one of the sensitisers which has shown great success to use in the production of Juglone, it has shown to work tremendously well in various studies[6-9] by using different solvents, although it is insoluble in hexane, it was found that it was soluble in $scCO_2$.

The absorbance measurements of anthracene in supercritical carbon dioxide were performed by removing the solvent from the cell by flowing oxygen at a flow rate of 200 cm^3 min^{-1} for 5 mins whilst heating the cell at a temperature of 318 K and then pressurising the cell with carbon dioxide to 200 MPa.

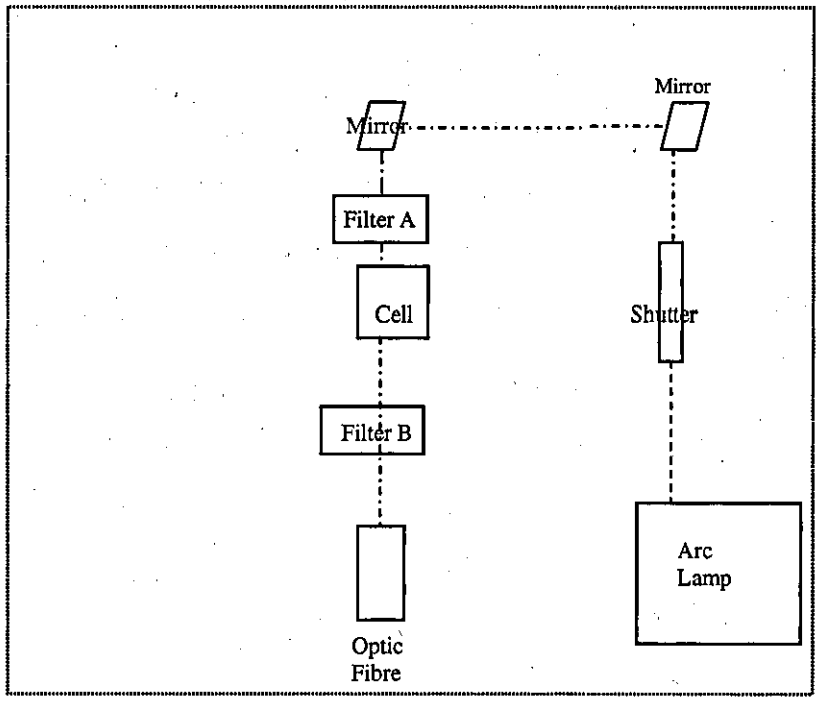

Figure 4.6: Schematic representation of reaction set-up for Juglone formation

References

1. Worrall, D.R.; Wilkinson, F.; *J. Chem. Soc. Faraday Trans.* **1996**;92: 1467-1471.
2. Worrall, D.R.; Abdel-Shafi, A.A.; Wilkinson, F. *J. Phys. Chem.A* **2001** 105: 1270-1276.
3. Abdel-Shafi, A.A.; Wilkinson, F.; Worrall, D.R.; *Chem. Phys. Lett.***2001; 343**: 273-280.
4. Abdel-Shafi, A.A.; Worrall, D.R.; *J. Photochem. and Photobio A*: **2007** ;186: 263-269
5. Schmidt, R.; Tanielian, C.; Dunsbach C. R. and Wolff, C. *J Photochem. Photobiol A: Chem.***1994;** 79:1-2

Chapter 5

Equipment Validation

5.0 Validation of the relationship between the Absorption set ups: In-situ Ocean Optic USB 2000 *vs* HP8453 Spectrophotometer

The purpose of this chapter is to characterise the equipment through absorbance measurements in order to obtain correct values of singlet oxygen quantum yields. It was from validating this equipment that correct values were obtained for singlet oxygen quantum yields for anthracene as compared to the previous study[1] which reported very high values in super critical carbon dioxide fluid.

5.1 Experimental Set up

All experiments were carried out in the set-up as shown in section 4.6.6 for both conventional solvent and $scCO_2$. A comparison between the absorption determined using the HP8453 UV-Visible or a Perkin-Elmer Lambda Bio 40 UV-Vis spectrophotometers and the $scCO_2$ cell were done as shown in figure 5.1.

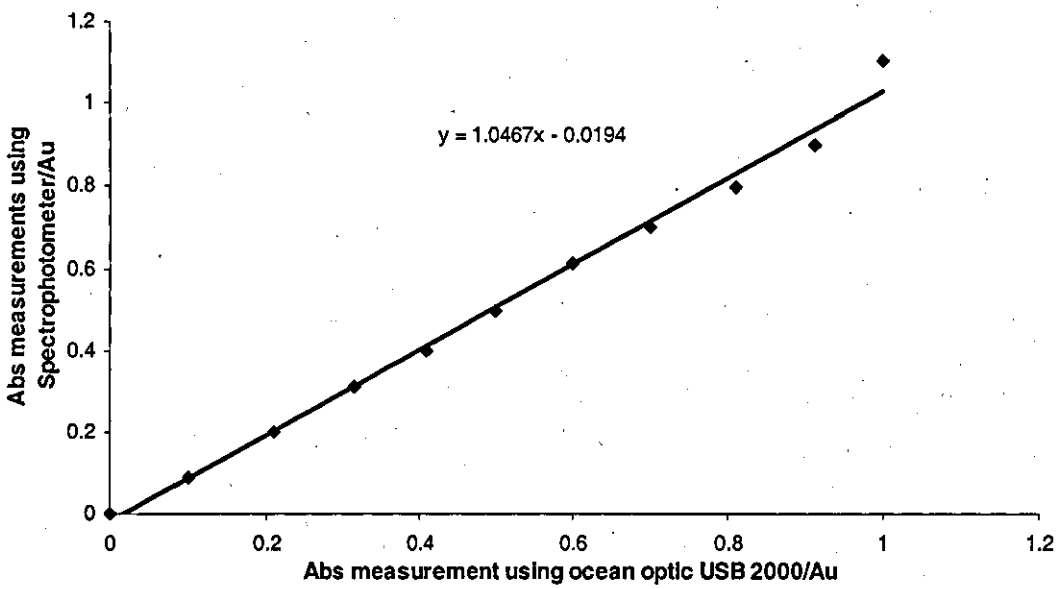

Figure 5.1: A graph showing the solution of anthracene in Methanol monitored at 355 nm, using the HP8453 spectrometer and using the ocean optics USB 2000 in the SCF Cell

Both set ups gave very similar results at 355nm, this was very necessary to establish, as all measurements need to be of the same value in order to obtain consistency of results. Figure 5.1 showed anthracene but also Naphthalene gave the same results and the slope of 1 indicates the desired 1:1 correspondence.

5.2 Anthracene in Supercritical Carbon Dioxide

Since some experiments would be carried out in super critical carbon dioxide, it was necessary to carry out experiments to show how the absorption measurements would relate with the conventional solvents.

The lamp intensity of the blank (methanol) was recorded initially which was then flushed out of the cell using oxygen gas. Once the methanol was removed, $scCO_2$ was then pumped into the system and a blank measurement was taken after that the solution of interest was introduced into the cell, as described in Section 4.6.6, and the solvent was removed by flushing a steady stream of oxygen gas through the cell. Liquid carbon dioxide was then pumped into the cell to the initial pressure and the system heated to the desired temperature, the absorbance of the lamp through the cell was then recorded.

When using anthracene it was observed that for every 1 mole of solution injected in the cell only a third of it was observed in the super critical carbon dioxide, this can be shown in figure 5.2

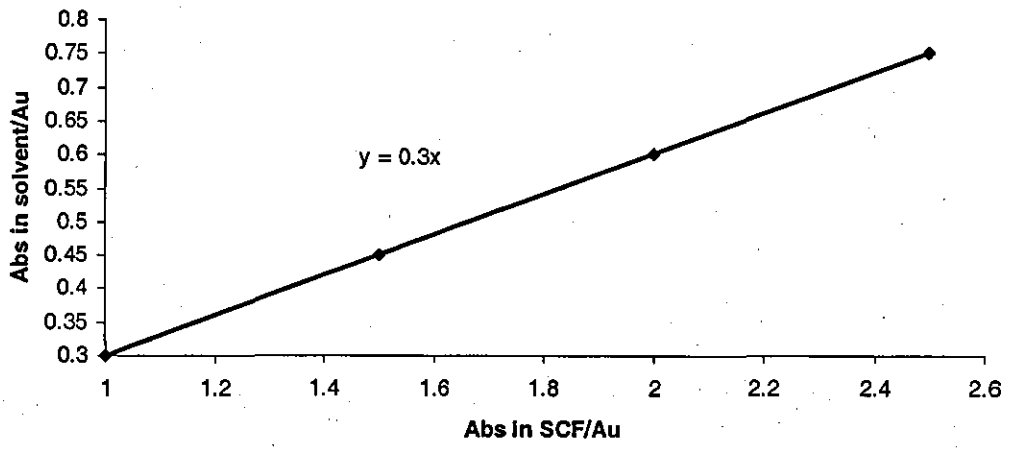

Figure 5.2: Relationship between anthracene in methanol and in $scCO_2$ in the home built set up

This phenomenon was only observed for anthracene, which is thought to be due to relatively large vapour pressure of anthracene, hence it is flushed out of the cell with

solvent. The other compounds showed consistency in both the conventional solvent and in super critical carbon dioxide, as shown in figure 5.3 with Methylene Blue

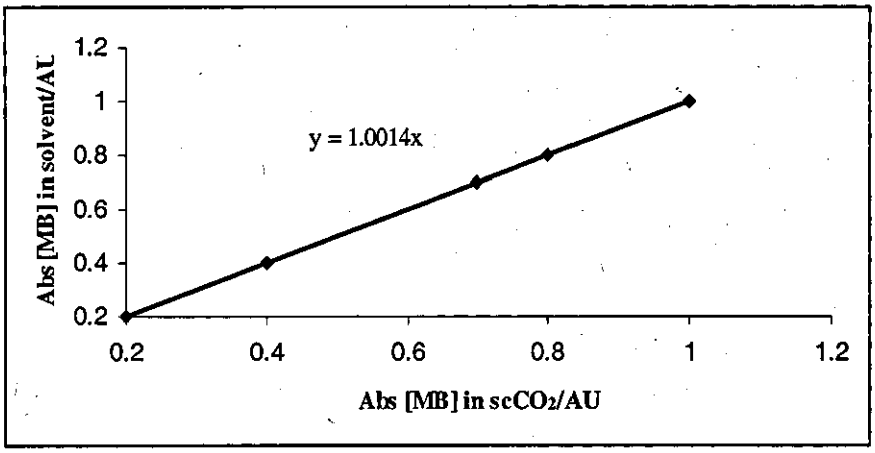

Figure 5.3: Relationship between MB in methanol and in $scCO_2$ in the set up

It has also been established that all these experiments required to be carried out within a window time frame of around 15 minutes, and this became clear that the stability of the compound could be seen within that time when we carried out the singlet oxygen quantum yields experiments, where the concentration of the compound was stable for the first 15 mins and then it slightly drops down as shown in figure 5.4

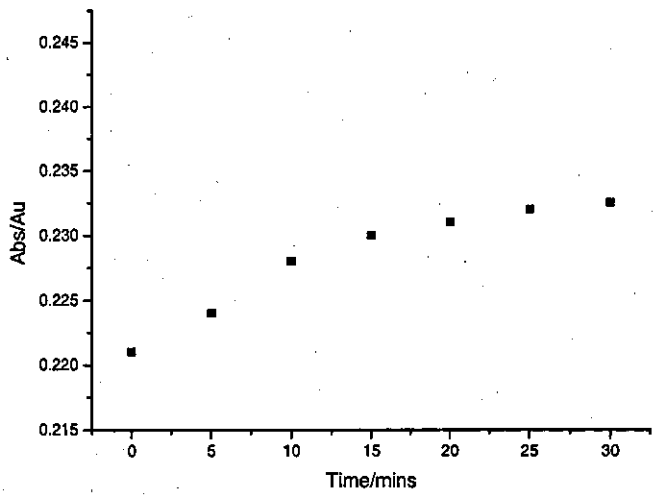

Figure 5.4: Stability of Anthracene shown over a period of time

This study has been seen to be reproducible on all other compounds, this is thought to be the main reason why previous studies were not in a position to obtain the required value of the singlet oxygen quantum yield, as they were not working within the required time frame where the compound exhibited some stability[1].

5.3 Validation of the photochemical method for Juglone production

Validation experiments were carried out to demonstrate the conditions necessary for the photochemical oxidation of 1, 5-dihydroxynaphthalene to Juglone; that is light and oxygen. The set up in figure 5.5 is similar to the section 4.6.6 with a few adjustments from the filter being moved to reduce radiation from light. To prevent irradiation of compounds (around 400-450 nm) a coloured light filter (filter A) was used (orange, >490 nm) as shown in figure 5.5. For monitoring purposes, an optical fibre (Ocean Optics USB 2000, with Ocean Optics Spectrasuite software) was used to measure absorbance. Neutral density light filters (filter B) were used after the cell to decrease the light intensity at the spectrometer; this was optimised for the region of interest, i.e. 400-450 nm.

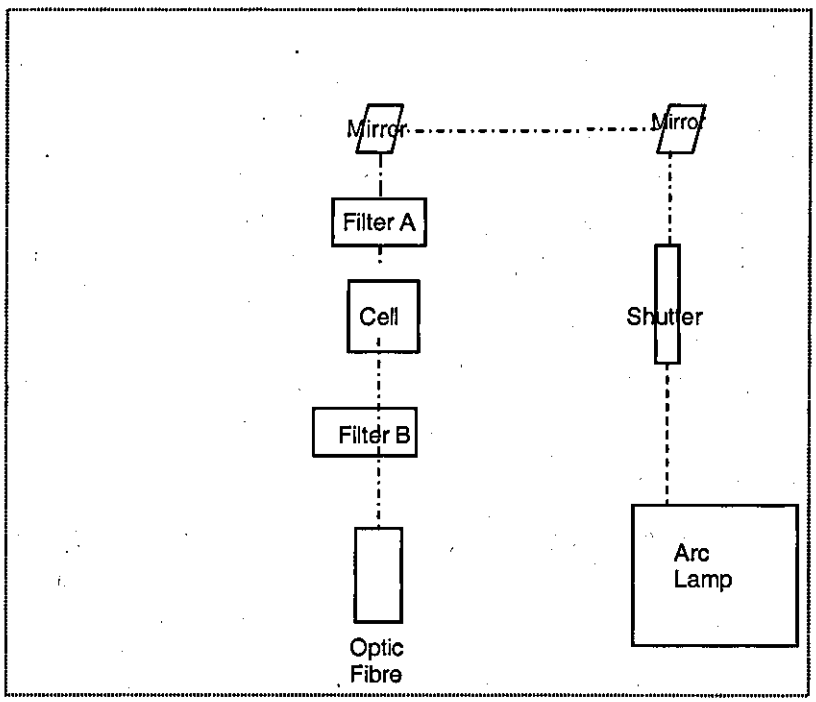

Figure 5.5: Schematic representation of reaction set-up for Juglone formation

5.3 Effects of Dihydroxnaphthalene in $scCO_2$

Dihydroxnaphthalene has been shown to be stable in supercritical carbon dioxide and this indicates that the reaction does proceed as expected and similar to the conventional solvent. This absorbance study was necessary and carried out with the experimental set up; detailed in section 4.2.1. For this measurement a different type of spectrometer was used to measure the DHDN peak, as with the USB 2000 ocean optics they were not able to follow at the 340 nm peak as this could be clearly seen later in figure 5.8 where the cut off point is seen after 350 nm in comparison to the figure 5.6; which shows the study of DHDN as a function of time.

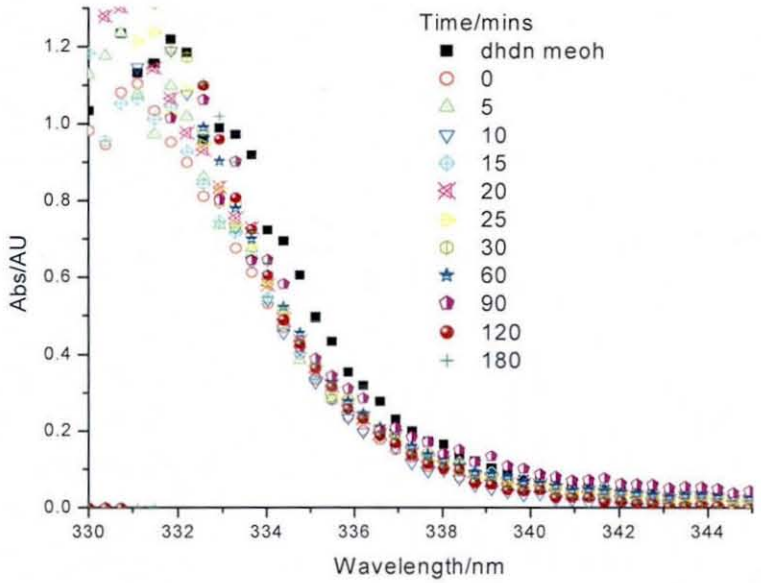

Figure 5.6: Dihydroxnaphthalene (DHDN) in supercritical carbon dioxide for 3 hours

5.4 Methylene Blue as a sensitiser

Methylene blue is one of the sensitisers which has shown great success to use in the production of Juglone, it has shown to work tremendously well in various studies[6-9] by using different solvents, although it is insoluble in hexane, it was found that it was soluble in $scCO_2$. Methylene blue (MB) was used as a sensitiser in the production of Juglone; it was observed to produce a higher yield in conventional solvent in various studies[9]. The relationship between dhdn in methanol and in supercritical carbon dioxide is nearly of the ratio of 1:1 and so is the relationship of the concentration of MB in

solvent and in super critical carbon dioxide with an approximately 5% decrease in 30 mins.

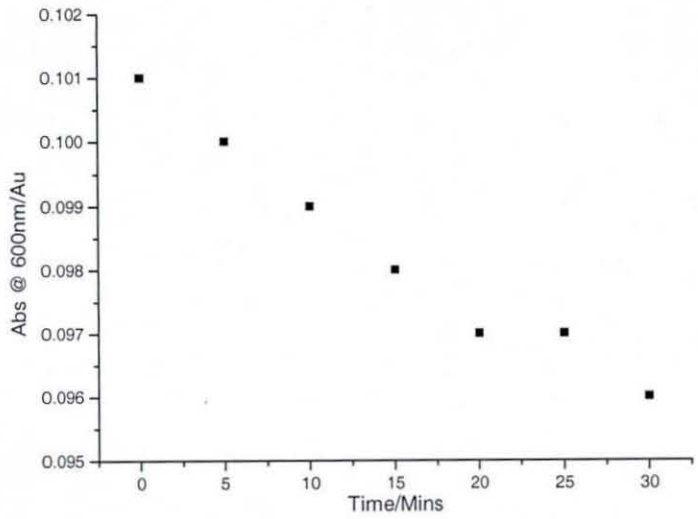

Figure 5.7: Shows Abs measurements of MB in $scCO_2$ for 30 mins at 100 Mpa and 35 °C

5.5 Stability of anthracene in $scCO_2$

A study of Anthracene in $scCO_2$ was carried out and it was observed that the concentration of Anthracene was unstable in $scCO_2$, as shown in figure 5.8 and 5.9. The absorbance was observed to decrease with time and this suggested that it could be due to the fact that it sublimes, and that the reaction needs to be done within the time frame of an half an hour, as after the half hour time frame a rapid reduction in absorbance was seen as shown in figure 5.7

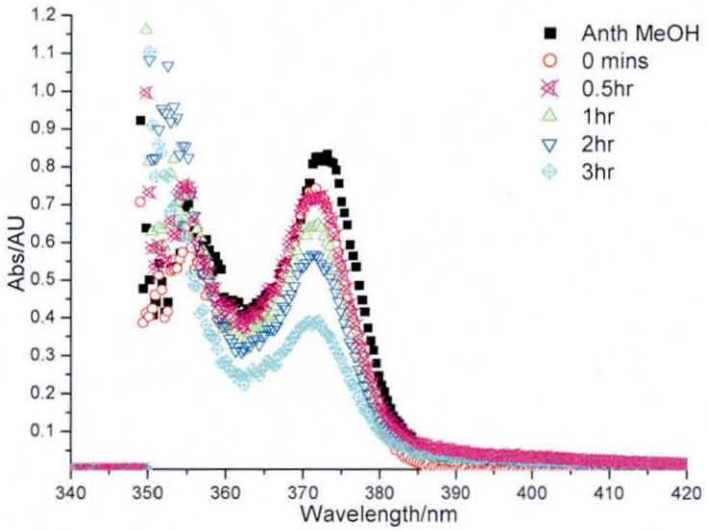

Figure 5.8: Anthracene in super critical carbon dioxide for 3 hours

On using Anthracene as a sensitiser, it was observed that the absorbance decreases this could be due to sublimation reaction in the first hour, therefore the production of Juglone should only be followed in the first hour only at the maximum, this will then avoid any errors but ideally all reactions should be monitored only within the half an hour time frame.

Detection of solutions using an optical fibre coupled to an Ocean Optics USB2000 photodiode array spectrophotometer at an integration time which was set at 100 ms to reduce noise level, provided a similar correlation to that observed with the spectrophotometer when measuring absorbance.

Absorption measurements were performed using the home built set up as detailed in section 4.2.1 as this set up was made so as to be able to measure the absorption measurements in super critical carbon dioxide which otherwise were not possible on the spectrophotometer, in which measurements were done directly from the supercritical fluids cell and not from the cuvette.

The absorbance measurements of anthracene in supercritical carbon dioxide were performed by removing the solvent from the cell by flowing oxygen at a flow rate of 200 cm^3 min^{-1} for 5 minutes whilst heating the cell at a temperature of 318 K and then pressurising the cell with carbon dioxide to 200 MPa. On addition of the super critical

carbon dioxide, it was seen that the absorption intensity reduces from 1 to 0.4 as shown on figure 5.9 and the wavelength has decreased from around 373 nm in methanol to around 370 nm in the supercritical carbon dioxide, this is found to be due to the fact that carbon dioxide is less polar than most solvents. This difference in absorption measurements of solvents and supercritical carbon dioxide could be used as a benchmark in calculating the final absorption required when using supercritical carbon dioxide as a solvent in a compound.

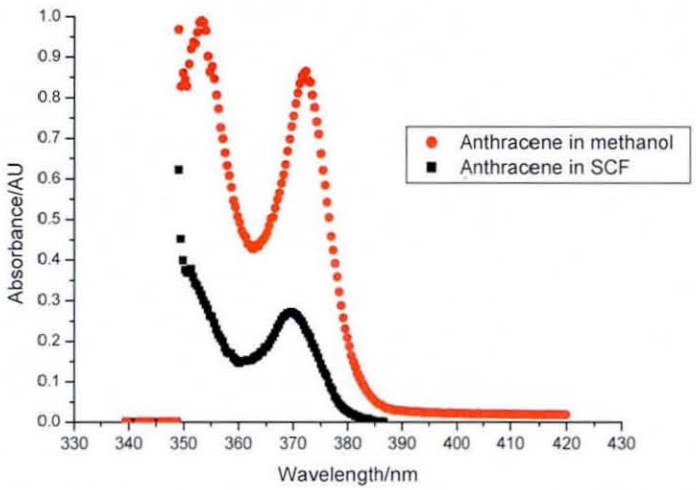

Figure 5.9: Absorption measurements of Anth in methanol and in $scCO_2$ in the cell

The absorbance measurements were found to be stable within the time window of 30 mins. This stability was observed for both the Anthracene and the Perinapthenone as shown in figure 5.9. This result could also contribute to why the previous studies[1] have obtained values of greater than one of singlet oxygen quantum yield in super critical carbon dioxide. A normalised graph shown in figure 5.10 was done just to ensure that the peaks are the same for both the conventional solvent and for the $scCO_2$ solvents, a very slight shift was seen and this was thought to be due to instrumentation.

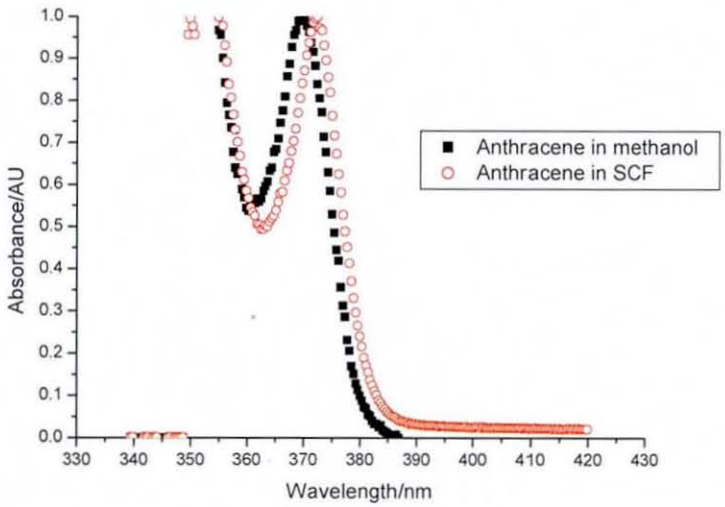

Figure 5.10: Normalised Absorption measurements of anthracene in MeOH and $scCO_2$

Absorbance measurements of Perinapthenone (PrN) and anthracene (Anth) were measured in supercritical carbon dioxide cell and the results were plotted as shown in figure 5.12. It is clear that both PrN and Anth are both stable over the 30 min timescale.

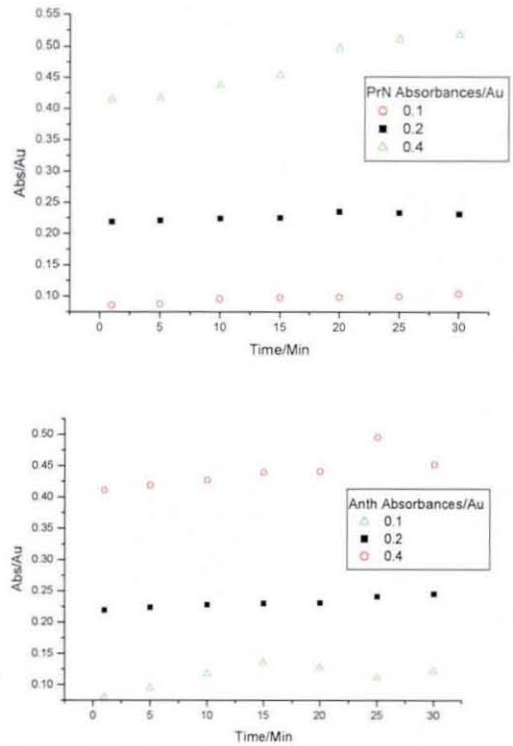

Figure 5.12: Absorbance measurements of Perinapthenone and Anthracene in $ScCO_2$

5.6 Conclusions

It was possible to characterise the equipments enabling the fluorescence of quantum yields to be obtained, it was from validating these equipments that it was possible to obtain the correct values compared to the previous study[1] which when the same study was conducted a very high value of singlet oxygen quantum yield in super critical carbon dioxide fluid was achieved. The discrepancies between the absorption measurements of solution introduced and in cell and that which was carried out using the either an HP8453 UV-Visible spectrophotometer or a Perkin-Elmer Lambda Bio 40 UV-Vis spectrophotometer was the same but with anthracene it was noticed that there was a drop in absorption measurements of almost a third in the $scCO_2$ in comparison to the conventional solvent this was attributed to be due to the sublimation of anthracene. However this was not seen for other compounds like MB and Perinapthenone. Dhdn was shown to be stable too.

References

1. Patel, M. Thesis, Loughborough University **2005**.
2. Worrall, D.R., Abdel-Shafi, A.A.; Wilkinson, F.; *J. Phys. Chem.A* **2001** ;105: 1270-1276.
3. Abdel-Shafi, A.A.; Wilkinson, F.; Worrall, D.R.; *Chem. Phys. Lett.* **2001**; 343: 273-276.
4. Abdel-Shafi, A.A.; Worrall, D.R.; *J. Photochem. and Photobio A*: **2007** ;186: 263–269.
5. Schiel, C.; Oelgemöller, M.; Ortner, J.; and Mattay, J.; *Green Chem.,* **2001**, 3, 224-228.
6. Mattay, J.; and Oelgemöller, M.; in *CRC Handbook of Organic Photochemistry and Photobiology, 2nd Edition*, ed. W. M. Horspool and F. Lenci, CRC Press, Boca Raton, **2004**, p. 88-03-88-45.
7. Oelgemöller, M.; Jung, C.; Ortner, J.; Mattay, J.; and Zimmermann, E.; *Green Chem.,* **2005**, 7, 35-38.
8. Suchard, O.; Kane, R.; Roe, B.J.; Zimmermann, E.; Jung, C.; Waske, P.A.; Mattay, J.; and Oelgemöller, M.; *Tetrahedron*, **2006**, 62, 1467-1473.
9. Oelgemöller, M.; Healy, N.; de Oliveira, L.; Jung, C.; and Mattay, J.; *Green Chem.*, **2006**, **8**, 831- 834.
10. Abdel-Shafi, A.A. and Worrall, D.R.; *J. Photochem. Photobiol. A.*, **2007**, 186, 263-269.
11. Abdel-Shafi, A.A.; Wilkinson, F.; and Worrall, D.R.; *Chem. Phys. Lett.*, **2001**, 343, 273-280.
12. Worrall, D.R.; Abdel-Shafi, A.A.: and Wilkinson, F.; *J. Phys. Chem. A*, **2001**, 105, 1270- 1276.

Chapter 6

Flavins

6.0 Introduction

This chapter will be looking at the study of a few types of flavins in different solvents and measure their fluorescence quenching, fluorescence lifetimes and triplet-triplet spectra. Additionally an investigation will be carried out to see if there will be any effect of adding bromobenzene to the triplet-triplet spectra of 6,9 Mall in both water and methanol

6.1 Photophysics of Flavins

Flavin photophysics has been the subject of intense research recently[1-5], as they play an important role in living organisms and are involved in a very wide range of biological processes. A number of important photobiological and photochemical processes, such as phototropism, phototaxis, and photodynamic have prompted the study[6-10] of flavin excited states, especially with respect to singlet oxygen quantum yields with different flavins as photosensitisers. Flavins possess the yellow chromophore characteristic of flavoproteins enzymes occurring widely in animals and plants, making observation of their spectral and photophysical properties the best tool to evaluate the physical properties of binding sites of flavoproteins. The parent molecule from which all other variants, e.g.vitamin B2 (riboflavin), flavin mononucleotide (FMN) and flavin adenine dinucleotide (FAD) derive, is Lumiflavin (7, 8, 10-trimethyl-10H-benzo[g]pteridine-2, 4-dione). Flavoenzymes are among the most structurally and functionally diverse families of redox proteins[11-12], since they catalyse an enormous range of biotransformations and electron transfer processes using a single redox unit, the flavin. These redox events can have either one- or two electron mechanisms, and one of the best known members of this family is riboflavin (vitamin B2, 10-(2,3,4,5-tetrahydroxypentyl)-7,8-dimethylbenzo[g]pteridine-2,4 (3H,10H)-dione), which plays an important role as part of a healthy diet.

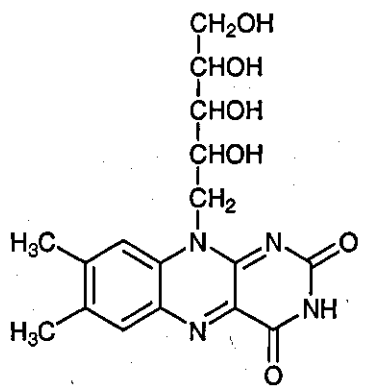

Rf Riboflavin

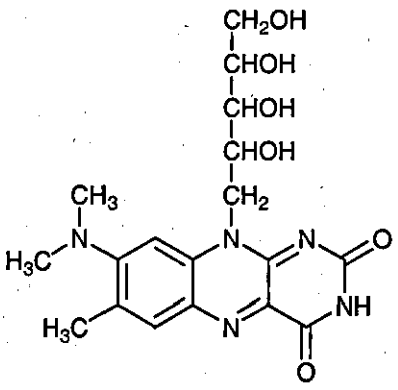

RR Roseoflavin

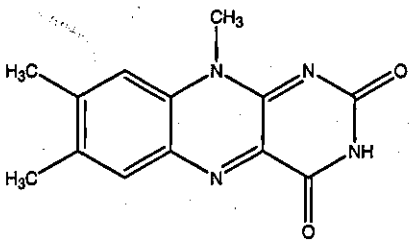

Lumiflavin

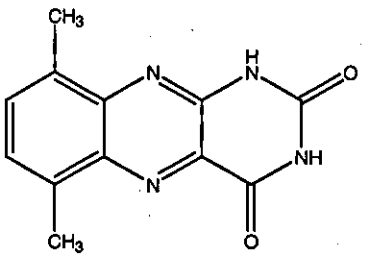

6,9 Mall

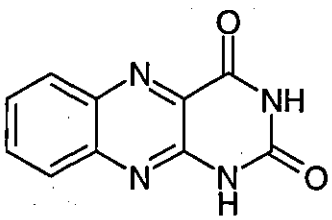

Alloxazine

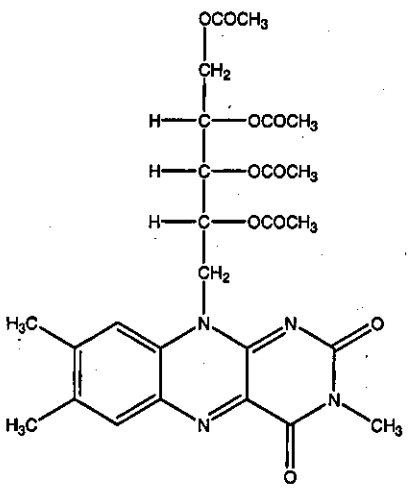

3-methyl-riboflavin tetraacetate, (3TARF).

Figure 6.1: Structures of different types of Flavins

Spectral and photophysical properties of riboflavin in methanol, DMSO, and water (pH of 4–8), including fluorescence quantum yields, fluorescence lifetimes, and quantum yield of triplet formation, have been determined [4-5].

Polymerization of 2-hydroxyethyl methacrylate photoinitiated by riboflavin in presence of triethanolamine has also been examined [9-10] and studies [7–10] of the electron transfer reactions of riboflavin in methanol. It has also been proposed that riboflavin can be induced in the process of photosensitized degradation of ethylene glycol [11]. The Singlet oxygen producing capacity of riboflavin in water was examined under UVA [12].

It has been recognised that riboflavin is an efficient photosensitiser that can act via radical species (Type I mechanism) or via the generation of singlet oxygen (Type II mechanism), [14-16]. Several reviews have given data regarding quantum yields of singlet oxygen formation photosensitized by flavins including riboflavin [17–19]. In this study the following properties have been determined for the first time which include; Fluorescence Quenching and Fluorescence Quantum yields including various Flavins triplet-triplet spectra.

6.2 Fluorescence Quenching of Flavins

Fluorescence Quenching of Flavins was done using bromobenzene and the ground state absorbance spectrum of Lf (standard, I^0) in acetonitrile was measured as detailed in section 4.6.1. Its absorbance at 355 nm was 0.098 and the fluorescence spectrum of this solution excited at 355 nm produced an area under the curve of 6.907×10^7 calculated using the micro Cal origin programme version 6.1. The fluorescence quenching constants of 3TARF, BR and 1R in methanol are 2.38×10^9, 2.69×10^9 and 8.13×10^8 l mol^{-1} s^{-1} respectively, which were calculated in this study using equation 6.1. These values were obtained using a Stern-Volmer relation as shown below, given that the lifetimes (τ_0) of the compounds were measured to be: $5.4 \pm 0.1 \times 10^{-9}$s for 3TARF, $4.8 \pm 0.1 \times 10^{-9}$s for BR and $6.3 \pm 0.1 \times 10^{-9}$s for 1R ±0.1

$$\frac{I^0}{I} = 1 + k_q \tau_0 [Q] \qquad 6.1$$

I^0 = Initial peak intensity of the fluorescence without a quencher

I = Intensity peak of fluorescence with a quencher

k_q= Quenching constant (l $mol^{-1}s^{-1}$)

τ_0= Lifetime of the excited state in the absence of the quencher Q (s)

[Q]= Concentration of the quencher (mol l^{-1})

Compound	Fluorescence k_q/l $mol^{-1}s^{-1}$	Lifetimes/ns
BR	$2.69 \pm 0.01 \times 10^9$	4.8
3TARF	$2.38 \pm 0.01 \times 10^9$	5.4
1R	$8.13 \pm 0.01 \times 10^8$	6.3

Table 6.1: Fluorescence quenching constants and lifetime values of different Flavins

Although there is no theoretical data to compare these values with, the values obtained seem to obey the Stern-Volmer relation and gave a linear plot of Stern-Volmer with an intercept at approximately to one. BR was observed to have the highest fluorescence quenching constant followed by 3TARF and the 1R, whilst the reverse is seen in their lifetimes with IR having the longest lifetime followed by 3TARF and then BR.

6.3 Fluorescence Quantum yield measurements of different Flavins in different solvents

The quantum yields of different Flavins in different solvents were measured as detailed in section 4.6.2 and the results tabulated as shown in tables 6.2-6.5, which were used together with the equation 6.2 to calculate the values of quantum yields of fluorescence (Φ_2) of 3TARF, 1R and BR.

3TARF in	Abs at 355 nm	Area Under Curve/Au
Methanol	0.085	4.413×10^7
Ethanol	0.099	2.729×10^7
Acetonitrile	0.082	4.019×10^7
Distilled Water	0.099	3.806×10^7

Table 6.2: Absorbance and area under curve measurements of 3TARF

BR in	Abs at 355 nm	Area Under Curve/Au
Methanol	0.109	4.296×10^7
Ethanol	0.095	3.096×10^7
Acetonitrile	0.105	4.857×10^7
Distilled Water	0.079	9.277×10^6

Table 6.3: Absorbance and area under curve measurements of BR

1R in	Abs at 355 nm	Area Under Curve/Au
Methanol	0.099	2.454×10^7
Ethanol	0.105	2.229×10^7
Acetonitrile	0.108	2.381×10^7
Distilled Water	0.085	7.978×10^6

Table 6.4: Absorbance and area under curve measurements of IR

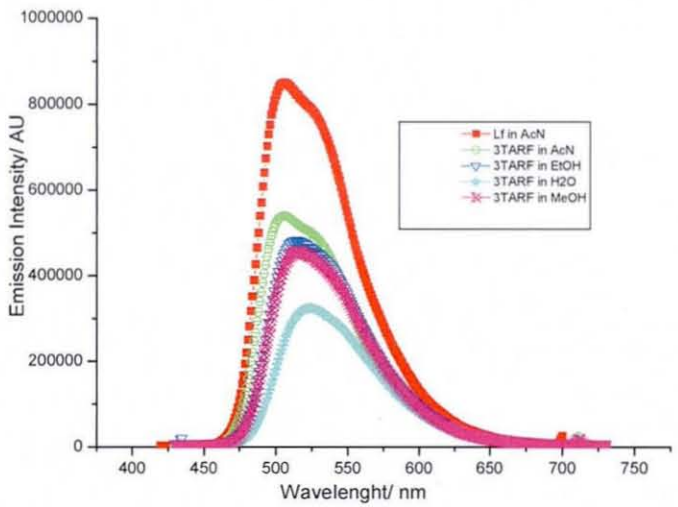

Figure 6.2: Area under the curve measurement of different Flavins in different solvents

$$\frac{\Phi_1}{\Phi_2} = \frac{I^1_{obs}}{I^2_{obs}} x \frac{I^2_{abs}}{I^1_{abs}} \qquad 6.2$$

I^1_{obs} = Area under Curve of Lf = 6.901×10^7

I^2_{obs} = Area under Curve of Compound

I^1_{abs} = Abs at 355nm of Lf = 0.100

I^2_{abs} = Abs at 355nm of Compound

$I^1_{obs} = 1\text{-}10^{-A}$

Φ_2 = Quantum yields of fluorescence

Φ_1 = 0.16 (Reference Quantum yield of fluorescence Lf)[13]

The following are the Quantum yields of fluorescence of the compounds (Φ_2) which were obtained from using the Equation 6.2.

	3 TARF	**BR**	**1R**
Methanol	0.09 ± 0.01	0.09± 0.01	0.06± 0.01
Ethanol	0.07 ± 0.01	0.07± 0.01	0.05± 0.01
Acetonitrile	0.11 ± 0.01	0.13± 0.01	0.05± 0.01
Distilled Water	0.09 ± 0.01	0.03± 0.01	0.02± 0.01

Table 6.5: Quantum yields of fluorescence of 3 TARF, BR and 1R

Experimental studies of 3TARF have shown two intense absorption bands which correspond to the two calculated lowest-energy absorptions[8]. In our study the quantum yields of fluorescence of BR and 1R in water obtained were very low and there are also additional recent reports on flavin chemistry in water[9-10]. Acetonitrile has shown to be the solvent which produces the highest quantum yield of fluorescence in the different Flavins in different solvents as shown in table 5. This could be explained on the basis of the proximity effect theory[11-12], which interprets the properties of such molecules as a result of vibronic interaction between the lowest π–π^* and n–π^* singlet states and also since most Flavins compounds are known to have closely spaced low-lying π–π^* and n–π^* excited states. The values in water are very low; this is attributed due to the fact that Flavins are partially soluble in water.

6.3.1 Measurements of fluorescence quantum yield of RR (Roseoflavin) in different solvents

Fluorescence quantum yield of RR was measured using the following formula

$$\Phi_x = \left(\frac{A_s}{A_x}\right)\left(\frac{\int_b^a (x)_x dx}{\int_b^a (x)_s dx}\right)\left(\frac{\eta_x}{\eta s}\right)^2 \Phi_s \qquad 6.3$$

Φ = Fluorescence quantum yield

$\int_b^a (x)_x dx$ = Area under corrected emission curve

A = absorbance

η = Refractive index of solvent used

Subscripts s and x refer to the standard and unknown samples respectively.

The standards used were of known fluorescence quantum yield and emission spectrum which covered the whole spectrum ranging from 250 nm – 700 nm so as to avoid as much errors as possible.

The standards used were Rhodamine 6g (Rh6G) and Acridine orange (AO) in different solvents at an absorbance of 0.1, which were then measured and recorded in different solvents as shown in the table 6:

Standards	**Solvent**	**Peak/nm**
Rh6G	Methanol	559
Rh6G2	Ethanol	558
Rh6G3	Acetonitrile	558
Rh6G4	Dioxane	556
Rh6G5	Water	555
AO1	Methanol	525
AO2	Ethanol	522
AO3	Acetonitrile	523
AO4	Dioxane	522
AO5	Water	555

Table 6.6: A List of standards used in different solvents at an absorbance = 0.1

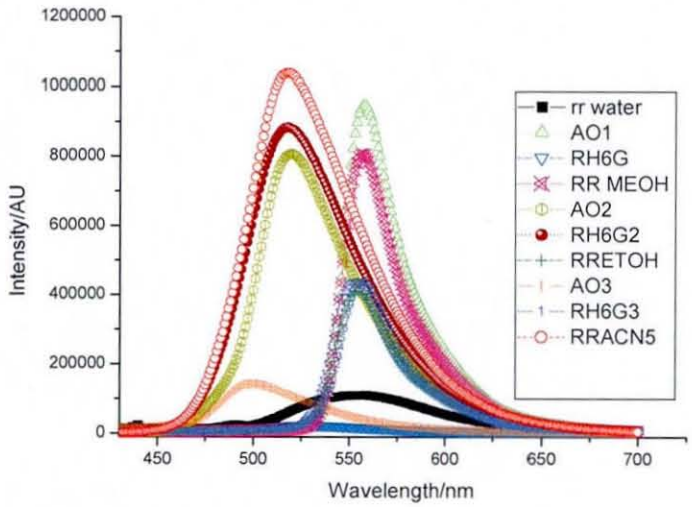

Figure 6.7: Standardised fluorescence graphs of RR solutions in different solvents and corresponding standard

Since the RR peaks were smaller and not very visible compared to their corresponding standards, the spectra were therefore normalised to one to show the peaks as shown in figure 6.

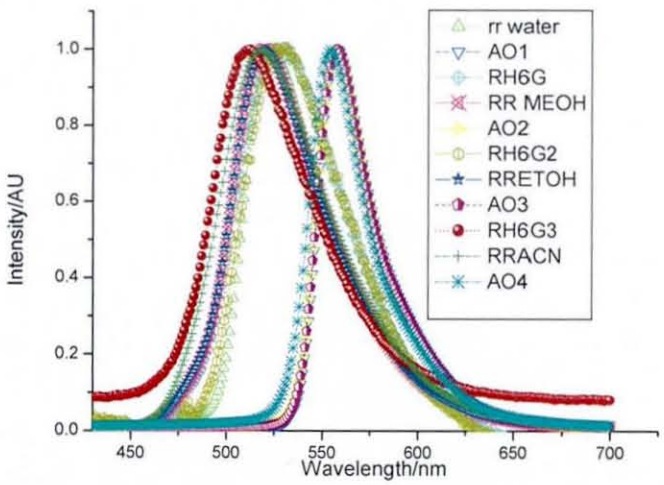

Figure 6.8: Normalised fluorescence graphs of RR in their solvents and corresponding standard

Since the fluorescence quantum yields of the standards were known and by using the fluorescence quantum yield equation above the quantum yield of RR in methanol, ethanol, and Acetonitrile are as follows: RR in ethanol is shown to have a higher quantum yield compared to other solvents whilst the lowest was observed in water.

RR in	Φ/sec	Peak/nm
Ethanol	0.591 ± 0.05	492
Methanol	0.539 ± 0.05	495
Dioxane	0.381 ± 0.05	478
1,2-DCE	0.361 ± 0.05	502
Acetonitrile	0.267 ± 0.05	477
Water	0.149 ± 0.05	503

Table 6.7: Fluorescence quantum yield of RR in methanol, ethanol, and Acetonitrile

Fluorescence quantum yield measurements of RR in the different solvents were measured in different solvents; the results were then tabulated as shown in table 6.7, not all the above solutions were able to be measured for lifetimes as the solutions in water, 1,2-DCE and dioxane have shown to have degraded with time therefore this can be concluded that the stability of RR in those solvents were unstable, this could be due to photodegradation which then influences the yield and the lifetimes[7]. Therefore the remaining solutions of RR were measured twice a few weeks later so as to confirm the quantum yield values obtained were consistent and an average (avg) was taken as shown in the table 6.8.

RR SOLVENT	Φ1	Φ2	Φ/avg
Methanol	0.015 ± 0.002	0.018 ± 0.002	0.017 ± 0.002
Ethanol	0.021 ± 0.002	0.027 ± 0.002	0.024 ± 0.002
Acetonitrile	0.093 ± 0.002	0.183 ± 0.002	0.138 ± 0.002

Table 6.8: Fluorescence quantum yields of RR in different solvents

This clearly illustrates the fluorescence quantum yield values of RR are not consistent in solutions and is unstable over a longer period of time. No fluorescence was observed for RR in dioxane, 1, 2DCE and water after storage for a few weeks as shown in table 6.8 in comparison to table to the values shown in table 6.7.

6.4 Fluorescence Lifetime measured using single Photon Counting

Fluorescence lifetime measurements of RR in different solvents were measured using the photon counting technique as detailed in section 4.6.5 and the results shown in table 6.9. Lifetime measurements of Roseoflavin (RR) in ethanol have shown to produce two

lifetime measurements, which suggest that RR is not stable in ethanol solvents which could be due to photodegradradation.

Solvent	τ /ns	Absorbance 420nm	Absorbance 337nm	Fluorescence peak/nm
Methanol	5.31 ± 0.01	0.0985	0.1945	532
Acetonitrile	2.89 ± 0.01	0.1033	0.2566	512
Ethanol	78%=5.2 ± 0.01 22%=25.8 ± 0.01	0.0899	0.1498	534

Table 6.9: Fluorescence lifetime measurements of RR in different solvents by photon counting

Roseoflavin absorbs light in the UV-Vis region and the absorption spectrum in methanol consists of several bands, on with the maximum at 258 nm (38.7×10^3 cm^{-1}) with a peak at 308 nm (32.6×10^3 cm^{-1}), and another at 493 nm (20.3×10^3 cm^{-1}). The fluorescence emission in methanol appears as a single weak band with maximum at 540 nm (18.5×10^3 cm^{-1}). The fluorescence lifetime for roseoflavin is in the nanosecond time range and was estimated theoretically as $\tau_F = 4.8$ ns in methanol and $\tau_F = 2.1$ ns in water. The transient absorption was excited using Nd:YAG third harmonics at 355 nm (5 mJ/pulse). Unfortunately, the transient absorption spectrum obtained was very weak, suggesting low triplet quantum yields or small T-T absorption coefficients.

The measurement of singlet oxygen quantum yields of Flavins and their derivatives as photosensitisers, based on measuring the emission at 1270 nm, which is highly specific to the $O_2(^1\Delta_g) \rightarrow O_2(^3\Sigma_g^-)$ transition, under laser excitation at 355 nm, of an air-equilibrated methanolic solution of the investigated compound. Supporting the results obtained in transient absorption, it was not possible to detect any signals attributable to singlet oxygen of RR. In contrast, most of previously examined isoalloxazines are efficient photosensitizers of singlet oxygen. Based on the experimental results, it was concluded that roseoflavin does not generate any singlet oxygen, in contrast to riboflavin, which reveals high quantum yields of singlet oxygen production ($\phi_\Delta = 0.51$). The difference between the two is the substituent in position C(8) of the isoalloxazine ring, thus, the NN-dimethyl substituent present in position 8 is probably the reason of such a drastic change in properties. Both the low triplet yields, as evidenced by the

flash photolysis results and undetectable singlet oxygen yields, and the low fluorescent yields, as compared to other flavin derivatives, point to the existence of other excited state deactivation channels acting in this substance due to the presence of the NN-dimethyl substituent in position 8.

6.5 Triplet-triplet spectra of different Flavins in different solvents

The triplet-triplet spectrum of 6,9 mall in water showed a peak which was in the range of 500 - 550 nm where it absorbs as shown in figure 6.9, this was achieved using the laser flash photolysis method as detailed in section 4.5. On addition of bromobenzene to 6,9 mall in water showed a more smooth spectrum which gave a peak of 500 nm as shown in figure 6.10. When methanol was added to 6,9 Mall for measurement of the spectrum it was seen to peak at around 475 nm and this stayed the same even after addition of bromobenzene as shown in figure 6.11 and 6.12 respectively.

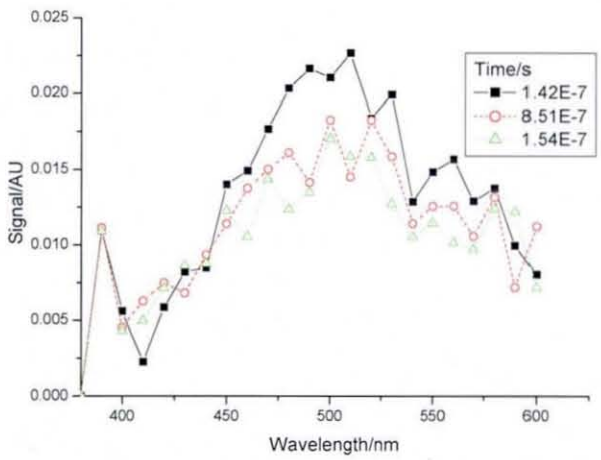

Figure 6.9: Triplet-triplet spectrum of 6,9 Mall in Methanol

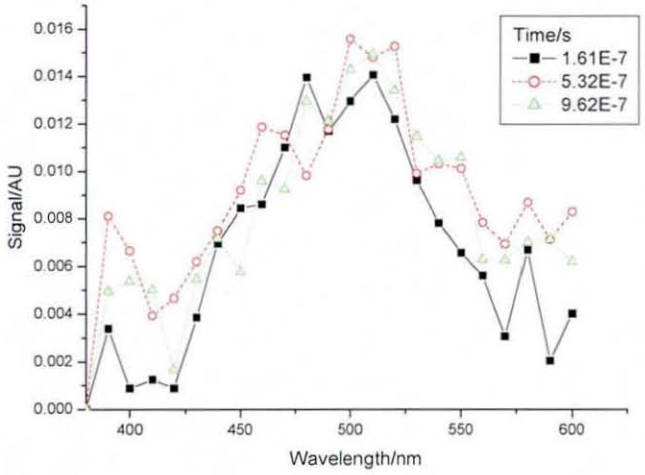

Figure 6.10: Triplet-triplet spectrum of 6,9 mall in water with bromobenzene (BrBz)

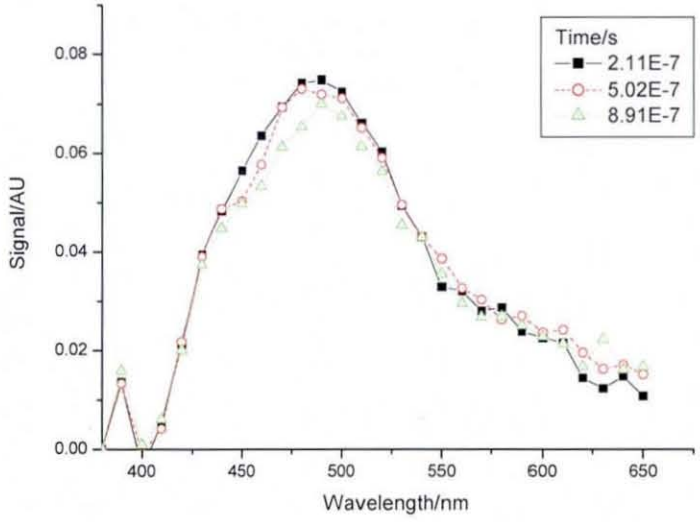

Figure 6.11: Triplet-triplet spectrum of 6,9 Mall in Water

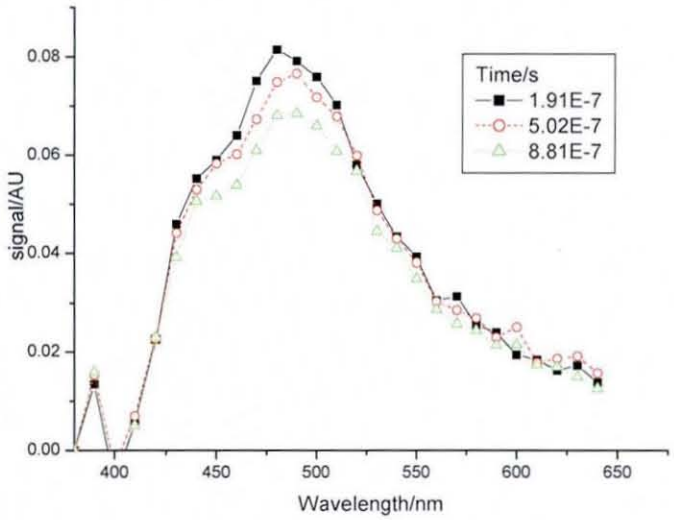

Figure 6.12: Triplet-triplet spectrum of 6,9 Mall in MeOH with Bromobenzene

Figures 6.9 - 6.12 have shown that there is a significant amount of triplet-triplet state in the different 6,9 Mall in water and in methanol but there was no significant increase on the addition of bromobenzene. The addition of bromobenzene to the Flavins was to increase the number of triplets formed due to the heavy atom effect enhancing the intersystem crossing.

6.6 Conclusions

The fluorescence quenching constants of 3TARF, BR and 1R in methanol are 2.38 x 10^9, 2.69 x 10^9 and 8.13 x 10^8 l mol^{-1} s^{-1} respectively, The fluorescence lifetimes (τ_0) of the compounds are 5.4 x 10^{-9}s for 3TARF, 4.8 x 10^{-9}s for BR and 6.3 x 10^{-9}s for 1R. Although there is no theoretical data to compare these values with, the values obtained seem to obey the Stern-Volmer relation and gave a linear plot of Stern-Volmer with an intercept at approximately one. BR was observed to have the highest fluorescence quenching constant followed by 3TARF and the 1R, whilst the reverse is seen in their lifetimes with IR having the longest lifetime followed by 3TARF and then BR.

The fluorescence quantum yield for RR in different solvents were of the value between 0.59 – 0.149 with the highest value in ethanol compared to other solvents whilst the least was observed in water. It must be noted that these RR are not very stable in the solvents studied and measurements must be carried out promptly (within a day or so).

Fluorescence lifetime measurements of RR in different solvents were measured using the photon counting technique and the results were in methanol 5.3 ns and 2.89 ns in Acetonitrile and 5.2 ns in ethanol. There is a significant amount of triplet-triplet state in the 6,9 Mall in water and in methanol but there was no significant increase on the addition of bromo benzene.

References

1. Sikorska E, Khmelinskii IV, Worrall DR, Koput J, Sikorski M. *J.Fluoresc.* **2004; 14:**57-64.

2. Sikorska E, Khmelinskii IV, Prukala W, Williams SL, Worrall DR, Bourdelande JL, et al. *J.Mol.Struct.* **2004** ;689:121-126.

3. Sikorska E, Herance JR, Bourdelande JL, Khmelinskii IV, Williams SL, Worrall DR, et al. *Journal of Photochemistry and Photobiology (1)A-Chemistry* **2005** ;170:267-272.

4. Insinska-Rak M, Sikorska E, Herance JR, Bourdelande JL, Khmelinskii IV, Kubicki M, et al. *Photochemical & Photobiological Sciences* **2005**;4:463-468.

5. Sikorska E, Khmelinskii I, Komasa A, Koput J, Ferreira LFV, Herance JR, et al. *Chemical Physics* **2005**;314:239-247.

6. Sikorska E, Khmelinskii I, Kubicki M, Prukala W, Hoffmann M, Machado IF, et al. *Journal of Physical Chemistry A* **2006** ;110:4638-4648.

7. Sikorska E, Khmelinskii IV, Bednarek A, Williams SL, Worrall DR, Herance JR, et al. Pol.J.Chem. **2004** ;78:2163-2173.

8. Sikorska E, Khmelinskii IV, Bourdelande JL, Bednarek A, Williams SL, Patel M, et al. Chem.Phys. **2004** ;301:95-103.

9. Insinska-Rak M, Sikorska E, Bourdelande JL, Khmelinskii IV, Prukala W, Dobek K, et al. *J.Mol.Struct.* **2006** ;783:184-190.

10. Sikorska E, Khmelinskii IV, Williams SL, Worrall DR, Herance JR, Bourdelande JL, et al. *J.Mol.Struct.* **2004** ;697:199-205

11. Sikorska E, Khmelinskii IV, Koput J, Sikorski M. *Journal of Molecular Structure-Theochem* **2004** ;676:155-160.

12. Sikorska E, Khmelinskii IV, Koput J, Bourdelande JL, Sikorski M. *J.Mol.Struct.* **2004; 697:**137-141.

13. Personal Correspondence. sikorski@amu.edu.pl

14. Sikorski M, Sikorska E, Koziolowa A, Moreno RG, Bourdelande JL, Steer RP, Wilkinson F. *Journal of Photochemistry and Photobiology.* **2001** ;60: 114-119.

15. Kowalczyk M, Sikorska E, Khmelinskii IV, Komasa J, Insinska-Rak M, Sikorski M. *Journal of Molecular Structure-Theochem* **2005** ;756:47-54.

16. Drossler, P.; Holzer, W.; Penzkofer, A.; Hegemann, P.; *Chem. Phys.* 286; **2003:** 409-420.

17. Islam, S.D.M.; Penzkofer, A.: Hegemann, P.; *Chem. Phys.* 291: **2003**; 97-114.

18. Melo, T.B.; Ionescu, M.A.; Haggquist, G.W.; Naqvi, K.R.; Spectrochim. Acta, Part A 55: **1999**; 2299-2307.

19. Porcal, G.; Bertolotti, S.G.; Previtah, C.M.; Encinas, M.V.; Phys. Chem. Chem. Phys. 5: **2003**; 4123-4128.

20. Encinas, M.V.; Rufs, A.M.; Bertolotti, S.; Previtali, C.M.; Macromolecules 34: **2001;** 2845-2847.

21. Bertolotti, S.G.; Previtali, C.M.; Rufs, A.M.; Encinas, M.V.; Macromolecules 32 (1999) 2920-2924.

22. Orellana, B.; Rufs, A.M.; Encinas, M.V.; Previtali, C.M.; Bertolotti, S. *Macromolecules* 32: **1999**; 6570-6573.

23. McGinnis, B.D.; Adams, V.D.; Middlebrooks, E.J.; *Environ. Int.* 25: **1999**; 953-959.

24. Joshi, P.C.; *J Indian. Biochem. Biophys.* 26: **1989**; 186-189.

25. Tatsumi, K; Ichikawa, H; Wada, S; *J. Contam. Hydrol.* 9: **1992**; 207-219.

26. Corbin, F.; *Int. J. Hematol.* 76: **2002**; 253-257.

27. Huvaere, K.: Olsen, K.; Andersen, M.L.; Skibsted, L.H.; Heyerick, A.; De Keukeleire, D.; *Photochem. Photobiol. Sci.* 3: **2004**; 337-340.

28. Min, D.B.; Boff, J.M.; *Comprehensive Rev. Food Sci Food Safety* 1: **2002**; 58-72.

29. Redmond, R.W.; Gamlin, J.N.; *Photochem. Photobiol.* 70: **1999**; 391-475.

30. Wilkinson, F.; Helman, W.P.; A.B. Ross, *J. Phys. Chem.* Ref. Data 24: **1995**; 663-1021.

31. Wilkinson, F.; Helman, W.P.; A.B. Ross, *J. Phys. Chem.* Ref. 22: **1993**; 113-262.

Chapter 7

Results and Discussions of Singlet Oxygen Quantum Yield

7.0 Introduction

The aim of this chapter is to examine the research which was done by a previous research student [1] who managed to obtain the value of the singlet oxygen quantum yield of more than one for anthracene in supercritical fluids carbon dioxide, although it's known that this is not possible. A mechanism was put forward, although this was less than satisfactory. Through the correct way of characterising the system and the set up as discussed in detail in section 4.6.6, in addition to working within the required time frame; values of less than one were achieved successfully. Hence, in this work the abnormality of the thesis of the previous student were corrected and successfully managed to measure values which can be regarded as correct. It is now possible, for the first time to examine in detail the effects of temperature and pressure on singlet oxygen quantum yield.

7.1 Anthracene

Anthracene is a solid polycyclic aromatic hydrocarbon consisting of three fused benzene rings derived from coal-tar or other residues of thermal pyrolysis, which is used in the artificial production of the red dye alizarin. It is also used in wood preservatives, insecticides, and coating materials. When pure it is colourless and has a violet fluorescence; it darkens when exposed to sunlight. It is obtained by the distillation of crude oils and the main use is in the manufacture of dyes.

Anthracene, also referred to as paranaphthalene or green oil, is the simplest tricyclic aromatic hydrocarbon colourless crystalline compound which exhibits blue (400-500 nm peak) fluorescence under UV light, which is insoluble in water but is quite soluble in carbon disulfide and somewhat soluble in ethanol, methanol, benzene, chloroform, and other organic solvents. It is readily oxidized to form anthraquinone, the parent compound of the alizarin series of dyes. A classic method for the preparation of anthracene in the laboratory is by cyclodehydration of o-methyl- or o-methylene-substituted diarylketones in the so-called Elbs reaction

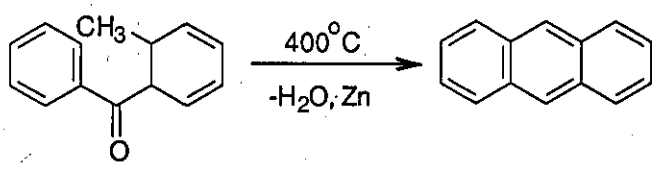

Anthracene has the ability to photodimerize with irradiation by UV light. This results in considerable changes in the physical properties of the material.

The dimer is connected by two covalent bonds resulting from the [4+4] cycloaddition. The dimer reverts to anthracene thermally or with UV irradiation below 300 nm. The reversible bonding and photochromic properties of anthracenes are the basis of many potential applications using poly and monosubstituted anthracene derivatives.

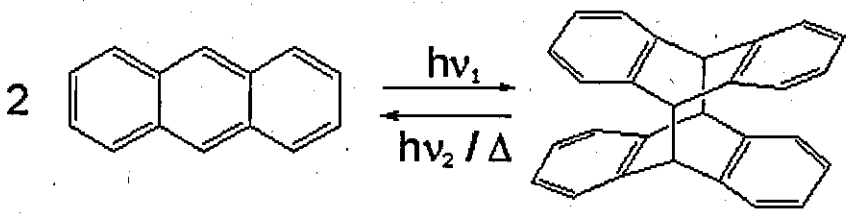

The reaction is sensitive to oxygen, in most other reactions of anthracene; the central ring is also targeted, as it is the most highly reactive. Electrophilic substitution occurs at the "9" and "10" positions of the centre ring, and oxidation of anthracene occurs readily, giving anthraquinone, $C_{14}H_8O_2$ (below).

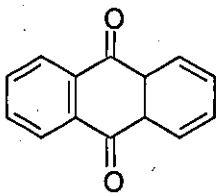

The reversible bonding and photochromic properties of anthracene is the basis of many potential applications using poly and monosubstituted anthracene derivatives, which are mostly used as intermediaries in pharmaceuticals[2], agricultural products[3], photographic products[4], thermosetting plastics, lubricating materials[5], and in other chemical industries[5].The reaction is sensitive to oxygen and light irradiation is known to induce photochemical transformations within it. Since anthracene is a polycyclic aromatic hydrocarbon (PAH), it exhibits high melting- and boiling-points, low vapour pressure, and very low water solubility, decreasing with increasing molecular weight whereas resistance to oxidation, reduction, and vaporisation increases. Vapour pressures tend to decrease with increasing molecular weight and these compounds are highly lipophilic and readily soluble in organic solvents. These properties have allowed the investigation of the various anthracene photophysics.

7.2 Determination of the Quantum yield of Triplet state production of Anthracene.

The quantum yield of Triplet formation (Φ_T) for anthracene was measured according to section 4.6.4 and was found to be 0.78 ±0.01. This value is a bit high compared to the expected value of 0.70-0.75, although it is within the expected experimental error. This value was obtained by using figure 7.1 and the equation below[4] from which the graph was plotted.

$$\frac{F'}{F} = \left(\frac{D_T F'}{D_T{}^0 F} - 1 \right) \Phi_T + 1$$

F' = Fluorescence intensity in the absence of a quencher

F = Fluorescence intensity in the presence of a quencher

$D_T{}^0$= Initial absorbance of the triplet state in the absence of a quencher

D_T= Initial absorbance of the triplet state in the presence of a quencher

Φ_T = Triplet quantum yield

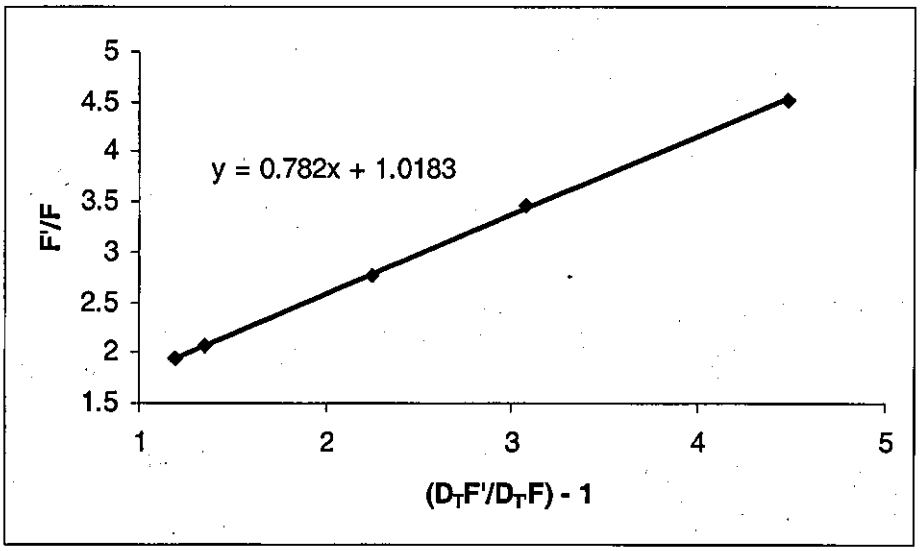

Figure 7.1: Quantum yield of triplet state production of Anthracene

7.3 Oxygen Quenching Constants (k_q) Measurements

Oxygen quenching constants (k_q) of the anthracene triplet in acetonitrile were measured using laser flash photolysis as detailed in section 4.5. The oxygen concentration was varied using gas ratios of nitrogen and oxygen, the results in table

7.1 clearly indicates that oxygen is a good quencher, and as the oxygen concentration is decreased, a decrease in decay rate constant is observed.

N_2 flow rate/ cm^3min^{-1}	O_2 flow rate/ cm^3min^{-1}	$k_{obs}/10^7\ s^{-1}$	$[O_2]/10^{-3}$ /M
10	90	1.85 ±0.01	8.2
30	70	1.61 ±0.01	6.4
50	50	1.41 ±0.01	4.6
70	30	1.15 ±0.01	2.7

Table 7.1: Anthracene gas proportion ratios and calculated values of k_{obs} and $[O_2]$

The values of the rate constant in table 7 are calculated using the equation below:

$k_{obs} = k_d + k_q[O_2]$

$k_{obs} = \frac{1}{t}\ (s^{-1})$

t = decay life time (s)

k_d = decay constant

k_q = quenching constant

$[O_2]$ = oxygen concentration (mol l^{-1})

The excited anthracene molecule loses its energy in the form of light rather than heat. In this nonradiative process, the anthracene either gets converted back to ground state (internal conversion) or to the lowest triplet state (intersystem crossing) and then to the ground state.

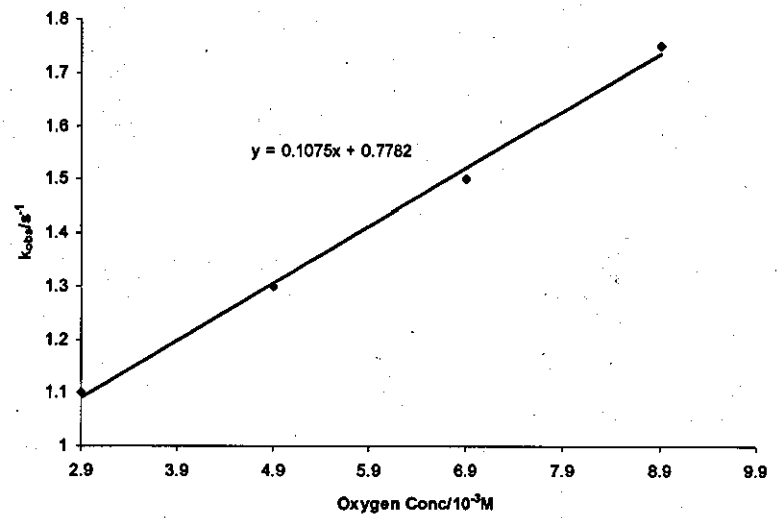

Figure 7.2: Fluorescence Quenching of anthracene via Oxygen

7.4 Singlet Oxygen Quenching Constants (k_q) Measurements

Anthracene singlet state quenching constant was measured as outlined in 4.6.7 and calculated using the Stern-Volmer equation as it was shown below. The flow rate of nitrogen was kept constant at 600 cm^3 min^{-1}, this ensured that most of the errors were minimised, as this was compared to the theoretical values calculated using the following equation[4].

$$\frac{I^0}{I} = 1 + k_q \tau_0 [Q]$$

I^0 = Initial peak intensity of the fluorescence without a quencher

I = Intensity peak of fluorescence with a quencher

k_q= Quenching Constant

τ_0= Lifetime of the excited state in the absence of the quencher Q = 5.1ns

[Q]= Concentration of the quencher

O_2 flow rate/ cm^3min^{-1}	I^0/I	$[O_2]/10^{-4}/M$
55	1.34	9.66
50	1.25	8.85
45	1.22	8.02
40	1.19	7.19
30	1.17	6.34
20	1.15	5.46
10	1.13	3.71

Table 7.2: Anthracene gas proportion ratios and calculated values of I^0/I and $[O_2]$

Therefore as observed above the higher the increase of oxygen flow the higher the values I^0/I, which corresponds to the Stern-Volmer equation where the oxygen concentration is proportional to the I^0/I values

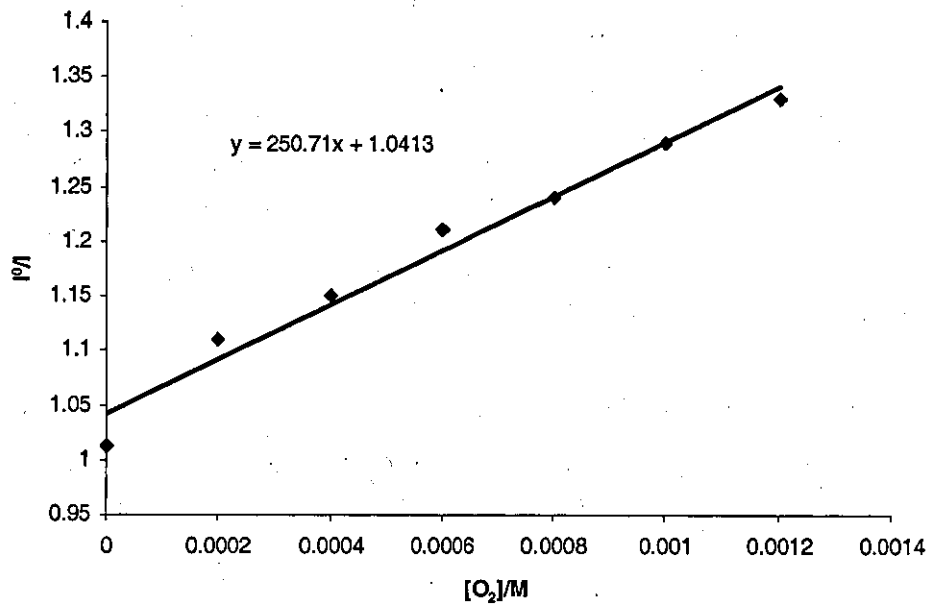

Figure 7.3: Shows a Stern-Volmer plot for fluorescence quenching of anthracene in acetonitrile by $[O_2]$

The experimental k_q value obtained was 4.8 ±0.01 $x10^{10}$ l mol^{-1} s^{-1}, since this value is higher than the theoretical value which is 2 ±0.1 $x10^{10}$ l mol^{-1} s^{-1}, it was therefore decided to perform an alternative measurement based on fluorescence lifetimes to check this value. These were measured using single photon counting.

7.5 Oxygen Quenching of anthracene fluorescence studied by Photon Counting

The quenching of the anthracene singlet state by oxygen was measured using single photon counting as detailed in section 4.6.5. The results obtained of the quenching constant through photon counting as shown in figure 7.4 were similar to the intensity and the theoretical values. Since there was a positive correlation in the two different methods used in obtaining a similar k_q it is therefore approved this to be a dynamic/collisional quenching as it depopulates the excited state without allowing fluorescence emission. The decrease in fluorescence intensity equates to the decrease in fluorescence lifetime as given on the Stern-Volmer equation.

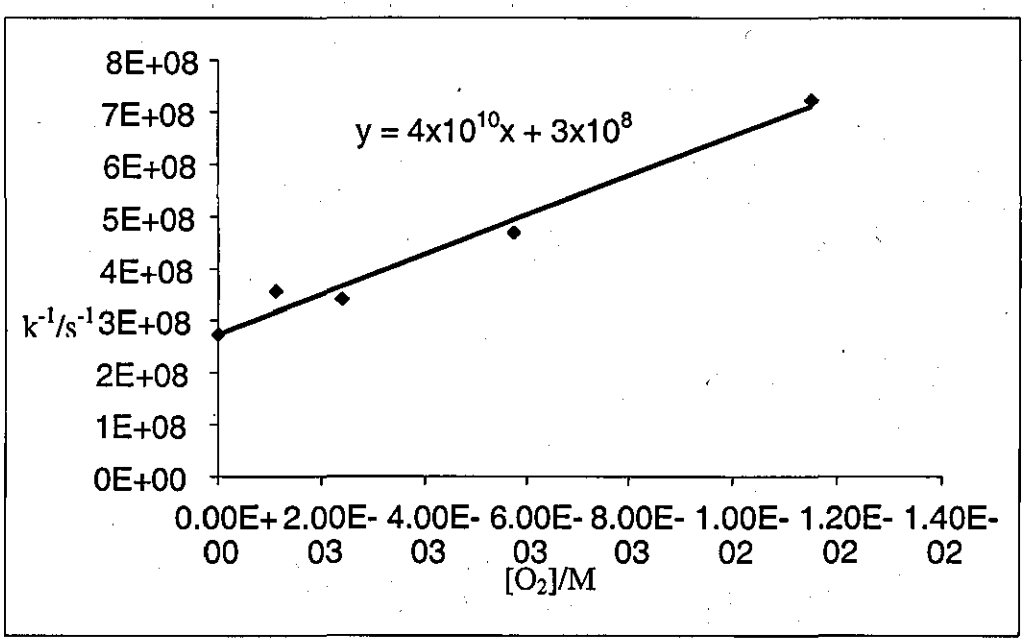

Figure 7.4: Fluorescence quenching of anthracene in acetonitrile by oxygen measured using single photon counting

The value of $4x10^{10}$ l mol^{-1} s^{-1} obtained using photon counting seems to correlate to the experimental value obtained using the Stern-Volmer equation, it is therefore assumed to be the correct one.

7.6 Singlet oxygen Quantum Yields at different temperatures and pressure in $scCO_2$

The quantum yield of singlet oxygen formation is determined by the detailed procedure shown in section 4.6.7 and the following equation:

$$\Phi_\Delta = \frac{\text{Concentration of singlet oxygen produced}}{\text{Number of photons absorbed}}$$

Once singlet oxygen ($^1\Delta_g$) is formed it decays back to the triplet ground state, via phosphorescence and intersystem crossing, as shown in figure 7.5

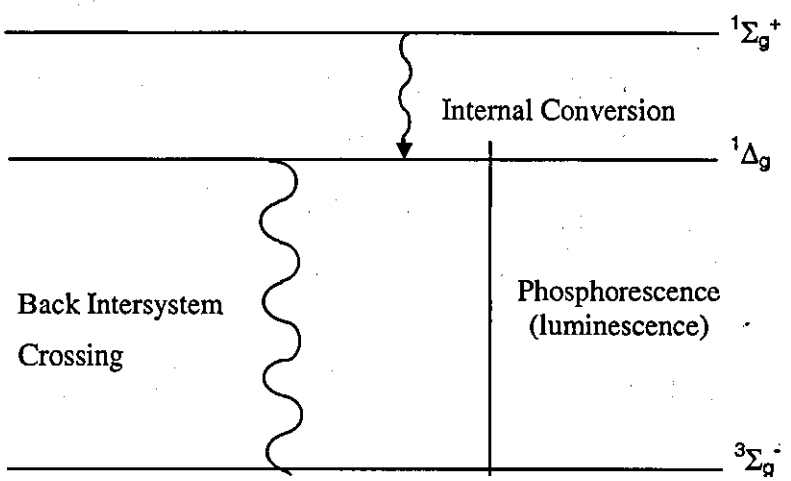

Figure 7.5: Decay processes from the singlet excited states of oxygen

The quantum yield can be obtained from a plot of luminescence intensity, I_Δ, versus the laser intensity, I_o, according to the following equation;

$$I_\Delta = I_o (1\text{-}10^{-A}) \Phi_\Delta$$

Singlet oxygen luminescence intensity can be obtained by monitoring singlet oxygen decay at 1270 nm, by fitting a plot of singlet oxygen intensities versus time, with a single exponential affords by extrapolating the initial luminescence intensity and the decay rate constant. Experiments were performed as a function of laser energy and fitting a plot of singlet oxygen luminescence intensity versus laser energy with a straight line, through the origin, affords a gradient, m, corresponding to;

$$m = (1\text{-}10^{-A}) \Phi_\Delta$$

Constructing a similar plot for a compound with known single oxygen quantum yield, gives:

$$\frac{m_u}{m_s} = \frac{\Phi_{\Delta u}\,(1\text{-}10^{-A})_u}{\Phi_{\Delta s}\,(1\text{-}10^{-A})_s}$$

Where s and u represent the sensitiser and the unknown respectively.

Since it is not possible to measure the singlet oxygen luminescence intensity in an absolute sense, the gradient m, is only proportional to $(1\text{-}10^{-A})$ multiplied by the quantum yield, Φ_Δ, and not actually equal to it.

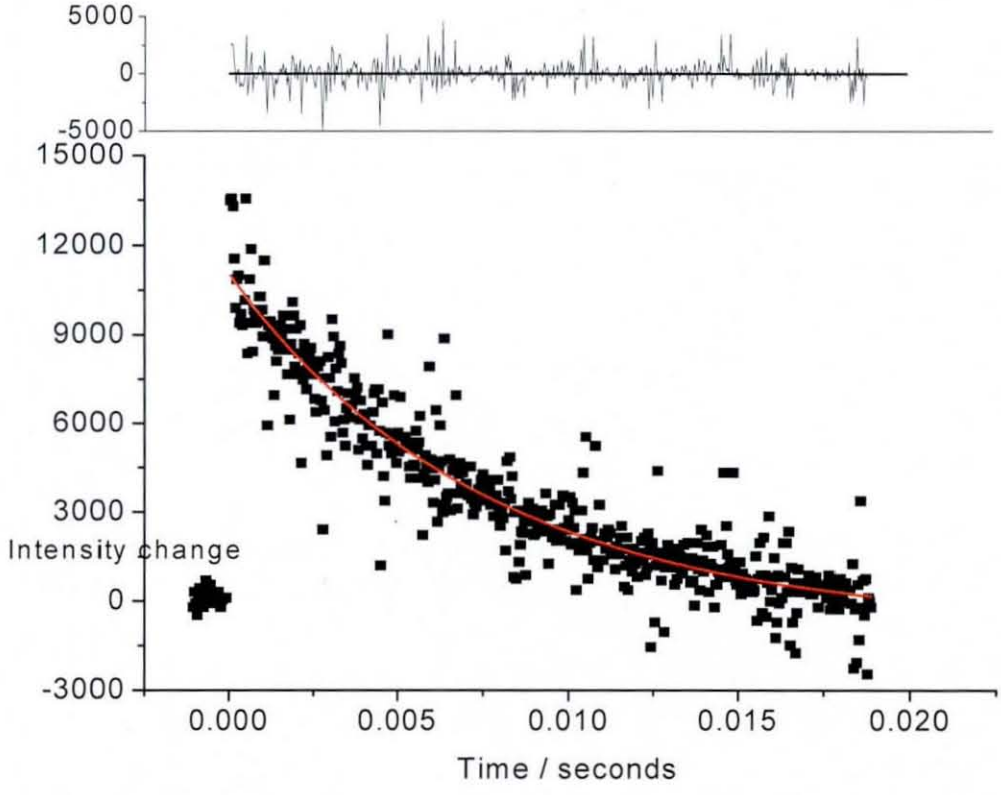

Figure 7.6: Typical Singlet Oxygen Decay trace at 1270 nm, sensitised with Perinaphthenone at 355nm

The singlet oxygen quantum yield, ϕ_Δ, was measured relative to perinaphthenone as a standard sensitiser, for which ϕ_Δ is reported to be 0.95 ± 0.05[2].

Singlet oxygen quantum yields were also obtained for anthracene in supercritical fluid carbon dioxide. Solubility experiments revealed that the concentrations of

anthracene altered in the supercritical cell with temperature and pressure, as discussed in detail in section 4.6.6. Therefore the absorbance of each sensitiser, including the reference sensitiser (perinaphthenone) was measured at each temperature and pressure during the experiment. It was seen that as the concentration of the solution was increased there is a decrease in singlet oxygen quantum yield which is thought could be due to aggregation, as shown in figure 7.7 and 7.8 respectively.

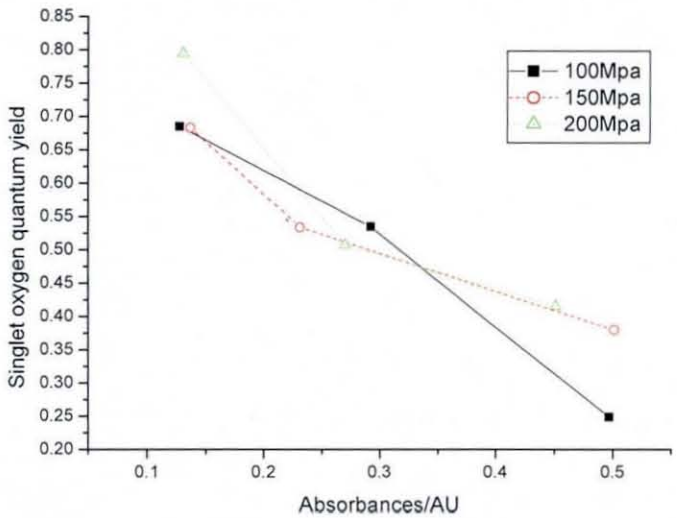

Figure 7.7: A plot to show the relationship between the concentrations of the anthracene with the singlet oxygen quantum yield in supercritical carbon dioxide at various pressures at 318K

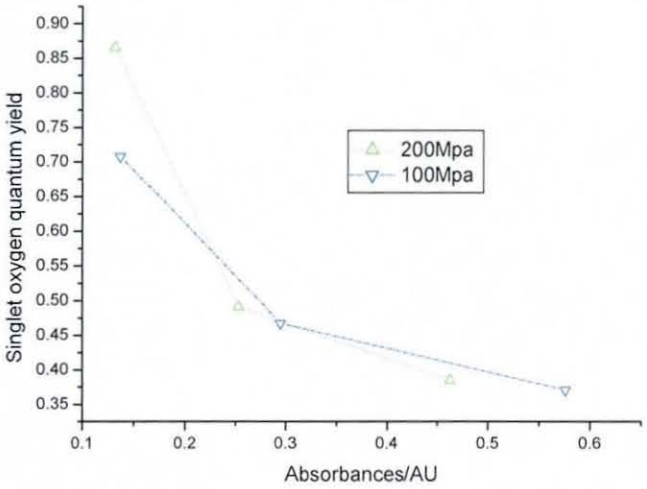

Figure 7.8: A plot to show the relationship between the concentrations of the anthracene with the singlet oxygen quantum yield in supercritical carbon dioxide at various pressures at 308K

The values obtained for the singlet oxygen quantum yield of Anthracene in supercritical carbon dioxide range between 0.2-0.8, but they are within the range of

the quantum yield Φ = 0.78 for the formation of either the triplet state or the singlet molecular oxygen of anthracene[3]. Increase in pressure increases the singlet oxygen quantum yield of anthracene as seen in table 7.3, but increase in concentration decreases the singlet oxygen quantum yield of anthracene. The value for the singlet oxygen quantum yield was previously obtained to be more than one but it is known that this is not possible. Through the correct way of characterising the system set up has been discussed in detail in section 4.6.6 and to work within the required time values of less than one were achieved successfully with errors of 0.05. Hence, the abnormality of the thesis of the previous student has been corrected.

Pressure = 100MPa, Temperature = 318.5K

Absorbance in Supercritical CO2		**ΦΔu**
Perinaphthenone	**Anthracene**	
0.525	0.497	0.249
0.321	0.292	0.535
0.133	0.127	0.685

Pressure = 150MPa, Temperature = 318.5K

Absorbance in Supercritical CO2		**ΦΔu**
Perinaphthenone	**Anthracene**	
0.545	0.501	0.379
0.247	0.231	0.533
0.143	0.136	0.683

Pressure = 200MPa, Temperature = 318.5K

Absorbance in Supercritical CO2		**ΦΔu**
Perinaphthenone	**Anthracene**	
0.421	0.451	0.415
0.231	0.270	0.507
0.123	0.130	0.795

Pressure = 200MPa, Temperature = 308.5K

Absorbance in Supercritical CO2		ΦΔu
Perinaphthenone	Anthracene	
0.495	0.463	0.385
0.298	0.253	0.491
0.139	0.132	0.866

Pressure = 100MPa, Temperature = 308.5 K

Absorbance in Supercritical CO2		ΦΔu
Perinaphthenone	Anthracene	
0.563	0.576	0.371
0.312	0.295	0.467
0.143	0.137	0.708

Table 7.3: Anthracene singlet oxygen quantum yield in supercritical carbon dioxide using Perinaphthenone as a reference sensitiser at different pressures and temperatures

In general, an increase in pressure appears to result in a small increase in the quantum yield, which becomes less apparent at the higher temperatures and therefore can be explained in terms of an increase in solvent density. Chemical reactions in solution are generally accompanied by changes in activation volume, known as their reaction volumes[5].

The activation volume is interpreted according to the transition state theory, as the difference between the partial molar volumes of the transition state and the sums of the partial volumes of the reactants at the same temperature and pressure[6]. The activation volume is not equal for all reactions, as a result increased pressure may favour one reaction over the others and therefore it is possible to control/enhance selectivities for the desired product by working at the desired temperature and pressure. In order to react, the molecules must get within certain proximity of each other; known as the transition state volume. To reach this volume work has to be done by the solvent to push the molecules together, if the molecules occupy a larger combined volume than the transition volume. If the molecule occupies a smaller combined volume than required to react, work has to be done by the molecules to move further apart. Therefore in terms of rates of reaction, if the transition state volume of the encounter complex, was larger than the volume occupied by the molecules an increase in pressure would cause the solvent to push the molecules

together, resulting in a reduced rate of reaction. Conversely if the transition state volume was smaller than the volume occupied by the molecules an increase in pressure would result in an increased rate of reaction.

Singlet oxygen quantum yield values for anthracene reported in normal solution range from to 0.57 to 1.12 given in Table 7.4.

Φ_Δ	$[O_2]$	Solvent
0.57	1.2×10^{-3}	Benzonitrile [12]
0.58	1.3×10^{-4}	CH_3CN [13]
0.68	O_2	C_6H_6 [6]
0.70	O_2	CS_2 [14]
0.74	air	C_6H_6 [15]
0.75	O_2	CCl_4 [14]
0.88	1.9×10^{-3}	C_6H_6 [11]
1.00	O_2	$C_6H_5CH_3$ [16]
1.12	9.0×10^{-3}	C_6H_6 [11]

Table 7.4: Reported literature values for singlet oxygen quantum yields for anthracene in solution

Previous studies [11] obtained a value of 1.12 ± 0.09 by assuming that quenching of the anthracene singlet state leads to the production of singlet oxygen, and quote a value of 0.46 for the fraction of excited states quenched that produce singlet oxygen, f_Δ^s. However, recent publications suggest that this is not possible since the T_2 state

of anthracene lies below the S_1 state and thus quenching of S_1 leads to production of the T_2 state via intersystem crossing, vide infra.

For quenching of the first excited singlet state by oxygen, it is necessary to consider the following five spin allowed and two spin forbidden processes as shown in scheme 1.

$$S_1 + O_2 ({}^3\Sigma_g^-) \longrightarrow T_1 + O_2 ({}^1\Sigma_g^+) \quad \text{(i)}$$

$$S_1 + O_2 ({}^3\Sigma_g^-) \longrightarrow T_1 + O_2 ({}^3\Sigma_g^-) \quad \text{(ii)}$$

$$S_1 + O_2 ({}^3\Sigma_g^-) \longrightarrow T_1 + O_2 ({}^1\Delta_g) \quad \text{(iii)}$$

$$S_1 + O_2 ({}^3\Sigma_g^-) \longrightarrow T_2 + O_2 ({}^3\Sigma_g^-) \quad \text{(iv)}$$

$$S_1 + O_2 ({}^3\Sigma_g^-) \longrightarrow S_0 + O_2 ({}^3\Sigma_g^-) \quad \text{(v)}$$

$$S_1 + O_2 ({}^3\Sigma_g^-) \longrightarrow S_0 + O_2 ({}^1\Sigma_g^+) \quad \text{(vi)}$$

$$S_1 + O_2 ({}^3\Sigma_g^-) \longrightarrow S_0 + O_2 ({}^1\Delta_g) \quad \text{(vii)}$$

Scheme 1: Possible pathways for singlet state quenching by molecular oxygen [17]

The four enhanced ISC pathways (i-iv) lead to the formation of the first or the second excited sensitiser triplet state and either the ground state (${}^3\Sigma_g^-$), or two lowest lying excited singlet states of oxygen (${}^1\Sigma_g^+$, ${}^1\Delta_g$). The three enhanced internal conversion processes (v-vii) generate the sensitiser ground state (S_o) and either O_2 (${}^3\Sigma_g^-$), O_2 (${}^1\Sigma_g^+$), or O_2 (${}^1\Delta_g$).

Quenching by oxygen is more complex than simply quenching of T_1 since other excited states exist that may be quenched by oxygen.

One study [18] found that in the absence of strong charge transfer interactions enhanced IC cannot compete efficiently with spin allowed ISC, either due to a large energy gap (process v), or due to the spin forbidden nature of such transitions (processes vi and vii). Process i has not been previously observed since the S_1-T_1 gap must exceed 158 $kJmol^{-1}$

Hence, the four enhanced intersystem crossing processes ii-v, have been identified to be the routes by which oxygen quenches the S_1 state as shown in scheme 1. The

different routes of intersystem crossing lead from the initially formed excited complex $^3(S_1{}^3\Sigma)$ to the product complexes $^3(T_1{}^3\Sigma)$, $^3(T_1{}^1\Delta)$, $^3(T_2{}^3\Sigma)$ and $^3(S_0{}^3\Sigma)$, which can then further dissociate, as shown in figure 7.9.

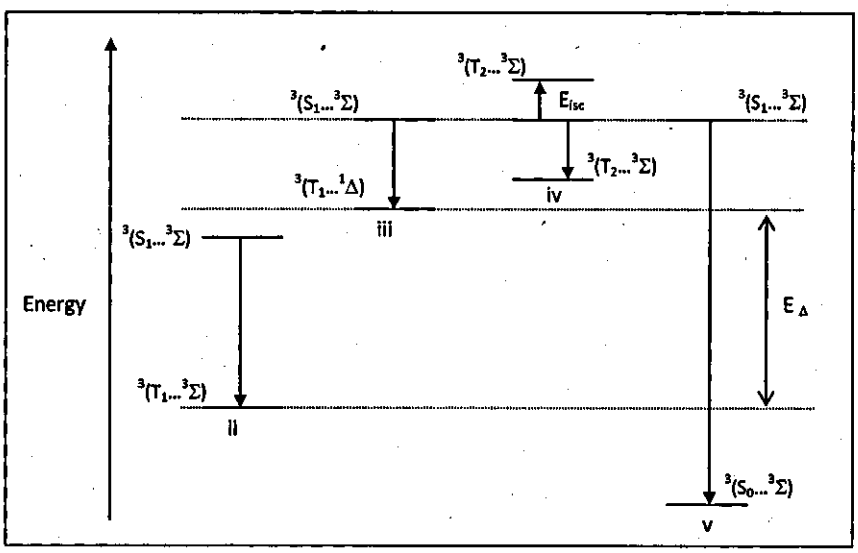

Figure 7.9: Most Probable routes for quenching of single states by Oxygen

In order to observe quenching of the singlet state, which results in the production of singlet oxygen, certain criteria must be satisfied. Firstly the S_1-T_1 gap must be greater than 94 kJmol^{-1}. The singlet state of anthracene lies 318 kJmol^{-1} above the ground state and the triplet state correspond to energy of 178 kJmol^{-1}, which results in an energy gap of 140 kJmol^{-1}, and therefore theoretically under these conditions singlet oxygen could be formed. However, the energy of the charge transfer state and of the second excited triplet state T_2 need to be considered. When the sensitiser is an easily oxidisable molecule charge transfer interactions with oxygen strongly influence the rate and efficiency of singlet oxygen formation. The oxidation potential of anthracene is 1.20 V [20] and the free energy change for complete energy transfer ΔG_{CET} is –128 kJmol^{-1} for the singlet state [21], when ΔG_{CET} is high and positive very little quenching proceeds *via* the charge transfer state. In this case the ΔG_{CET} value is negative which means that energy transfer proceeds predominantly through a charge transfer state as shown in figure 7.10. The energy of the charge transfer state of anthracene is 191 kJmol^{-1}, which is much lower than the anthracene singlet state. An energy gap of 11 kJmol^{-1} is not large enough to produce singlet oxygen. However, the energy of the second excited triplet state also requires

consideration. The T_2 state of anthracene lies 312 $kJmol^{-1}$ above the ground state which is energetically lower than the singlet state (318 $kJmol^{-1}$), since the charge transfer state lies below the T_2 state, quenching simply produces the T_2 state. Therefore quenching of the anthracene singlet state results in production of the T_2 state via intersystem crossing; and not via energy transfer to the oxygen molecule as shown previously for a range of meso-substituted anthracenes [19].

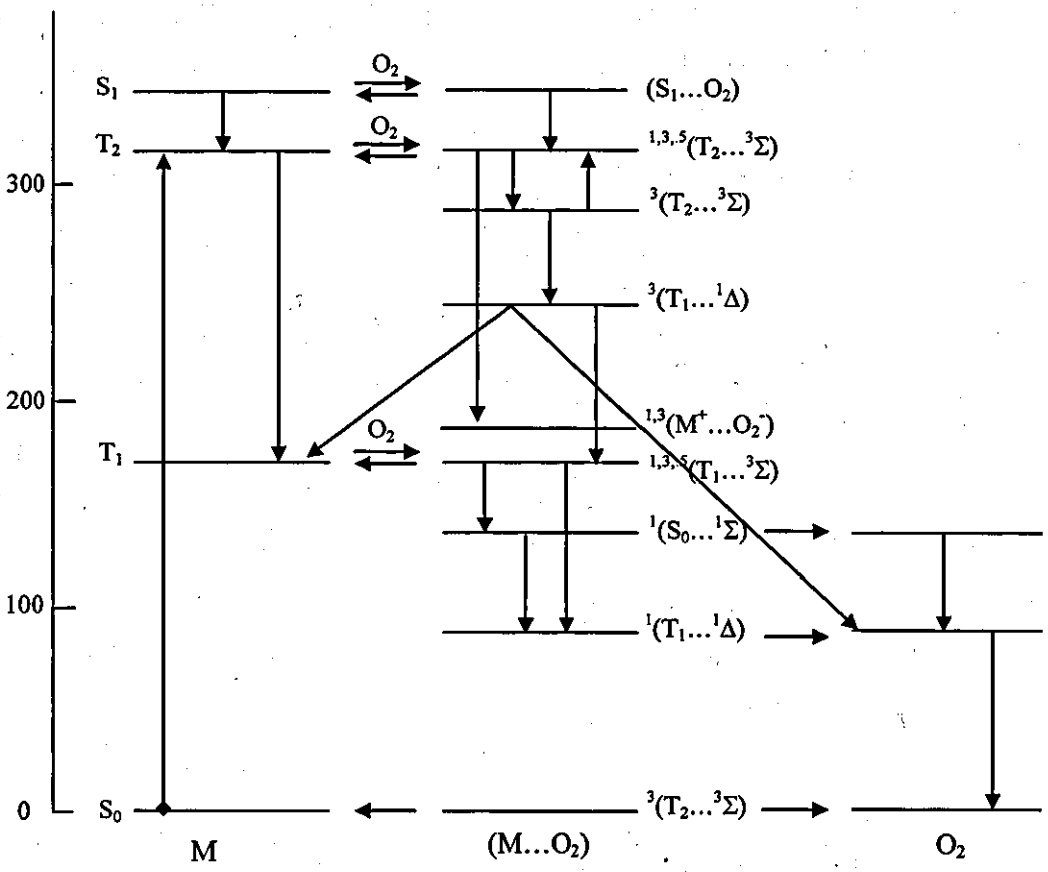

Figure 7.10: Energy level diagram to show energy transfer between anthracene excited states and molecular oxygen

Conclusions

The detection of the decay constant for singlet oxygen in super critical carbon dioxide was made possible after constructing the set up shown in the section 4.6.7 and obtained a range of values of the singlet oxygen quantum yield of anthracene which are within the expected value of less than one which have not been reported before.

The values obtained for the singlet oxygen quantum yield of anthracene in supercritical carbon dioxide range between 0.2-0.8, which are reasonable values in the context of known anthracene photophysics. Increase in pressure increases the singlet oxygen quantum yield of anthracene, but increase in concentration decreases the singlet oxygen quantum yield of anthracene, and it is this explanation which explains the observed dependencies.

In general, an increase in pressure appears to result in a small increase in the quantum yield, which becomes less apparent at the higher temperatures and therefore can be explained in terms of an increase in solvent density. Chemical reactions in solution are generally accompanied by changes in activation volume, known as their reaction volumes[5]

References

1. http://www.iss.com/resources/tech3/ accessed 20/08/06
2. Schmidt, R.; Tanielian, C; Dunsbach, R; and Wolff, C.; *J Photochem. Photobiol A.* **1994**; 79:1-2
3. Komorowski, S.; Grabowski, Z; and Zielenkiewicz, W; *J Photochem.* **1985;** 30: 141-51
4. Horrocks, R.; Medinger, T; and Wilkinson, F; *Chem Comms.* **1965;** 452-452.
5. Qin, J.; Eyring, M.; van Eldik, R.; Johnston, K. P.; Goates, R. S.; Lee, M.L., *J. Phys. Chem.*, 99, **1995**; 13461-13466
6. Okamoto, M.; Wada, O.; Tanaka, F.; Hiryama, S., *J. Phys. Chem. A,* **2001**; 105: 566-571
7. Larson, R.A.; Stackhouse, P.L.; Crowley, T.L.; *Environ. Sci. Technol.***1992;** 26**:** 1792–1798.
8. Insińska-Rak, M.; Sikorska, E.; Bourdelande, J.; Khmelinskii, I.; Prukała, W.; Dobek, K.; Karolczak, J.; Machado, I.; Ferreira, L. V.; Dulewicz, E.; Komasa, A.; Worrall, D.; Kubicki, M.; Sikorski, M. *Journal of Photochemistry and Photobiology A: Chemistry* **2007**; *186*: 14-23.
9. Ahmad, I.; Fasihullah, Q; Vaid, F.H.M.; J. *Photochem. Photobiol.B78* **2005**; 229–234.
10. Holzer, W; Shirdel, J; Zirak, P; Penzkofer, A; Hegemann, P; Deutzmann, R; Hochmuth, E; *Chem. Phys.* 308 **2005**; 69–78.
11. Lim, E.C ; *J. Phys. Chem.* 90 **1986**; 6770–6777.
12. Lai, T.I; Lim, B.T.; Lim, E.C.; *J. Am. Chem. Soc.* 104, **1982**; 7631–7635.
13. Stevens, B.; Marsh, K. L.; Baltrop, J. A., *J. Phys. Chem.*, **85, 1981**; 3079-3082.
14. Darmanyan, A.P.; *Chem. Phys. Lett.* **96, 1983**; 383-389.
15. Arai, T., Karatsu, T.; Tsuchiya, M; Sakuragi, H.; Tokumaru, K.; *Chem. Phys. Lett.*, **149, 1988**; 161-166.
16. Bowen, E. J.; *Discuss. Faraday Soc.* **1953**; 143-146.
17. Terazima, M.; Tonooka, M.; Azumi, T., *Photochem. Photobiol.*, **54, 1991**; 59-66.
18. Darmanyan, A.P., *Khim. Fiz.*, **6, 1987**; 1192-1198.
19. Sweitzer, C.; Schmidt, R., *Chem. Rev.*, **103, 2003**; 1685-1757.
20. Stevens, B; Small, R. D., Jr. *Chem. Phys. Lett.*, **61, 1977**; 233-257.
21. Stevens, B.; Mills, L. E., *Chem. Phys. Lett.*, **15, 1972**; 381-387.

Chapter 8

Juglone

8.0 Photooxygenation and green Chemistry

Juglone (5-hydroxy-1,4-naphthoquinone) is a natural product which is formed in nature by air oxidation of related hydroquinones found in the black walnut tree[1]. Derivatives of Juglone have been isolated from blue spirea and Chinese catalpa[2]. Juglone is of interest due to its alleopathic effects[1-3] (inhibits growth of plants) as well as its use as a preservative in non-alcoholic drinks[4]. However, the main chemical interest in Juglone is its use as a synthon, as it acts as a building block for many valuable compounds[1, 3, 5-9] and are also key intermediate in the pharmaceutical and agrochemical industry. Some Juglone-derived biologically active compounds include frenolicin B[10], (+)-nocardione A[11-12], Juglomycin A[13], Urdamycinone B[14-15] and the anti-inflammatory (AP-1 inhibitor) K1115-A[16-17]. Conventionally Juglone is prepared by oxidation with strong and often hazardous oxidizing agents, but a greener and safer convenient alternative is the use of dye-sensitized photooxygenation as shown in scheme 8.1.

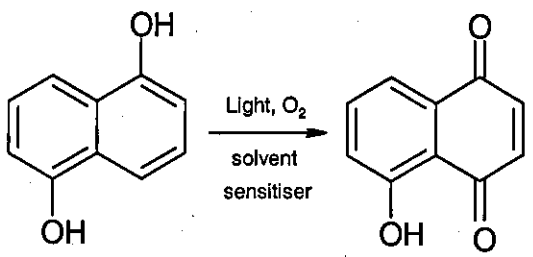

Scheme 8.1: Light photooxygenation of 1, 5-dihydroxynaphthaline

Juglone is considered a fine chemical (is a precursor to many processes and is not prepared in industrial quantities) and as a result is quite expensive. Its price in Sigma-Aldrich is £96 per 5 g, while the cost of the common starting material 1,5-dihydroxynaphthalene is £34.30 per 500 g (based on prices in September 2008). Assuming 100% conversion of 1, 5-dihydroxynaphthalene to Juglone, this indicates that Juglone is 155 times more valuable than its precursor and its for this reason that a simple and high-yielding conversion of 1, 5-dihydroxynaphthalene to Juglone is highly

desirable; from the cheap and commercially available 1,5-dihydroxynaphthalene by oxidation. The reaction proceeds via a [4+2] cycloaddition followed by a breakdown of the endoperoxide intermediate as shown in scheme 8.2.

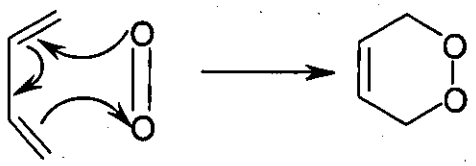

Scheme 8.2: Mechanism of the [4+2]-cycloaddition of singlet oxygen

In Type I photooxygenations a substrate in the excited state reacts with triplet state oxygen, which is then incorporated into the product. Type II photooxygenations involve the light initiated formation of singlet oxygen and subsequent reactions of this reactive species. There are three main Type II photooxygenation reactions: ene-reactions, [2+2]-cycloadditions and [4+2]-cycloadditions as shown in scheme 8.3

$$\text{sens} \xrightarrow{h\upsilon} {}^1\text{sens}^* \xrightarrow{ISC} {}^3\text{sens}^* \xrightarrow{{}^3O_2} \text{sens}^* + {}^1O_2$$

Scheme 8.3: Dye-sensitised generation of singlet oxygen

In light induced dye-sensitisation a photon of the correct wavelength causes excitation of the sensitiser to the singlet state, which then undergoes inter-system crossing to form the longer lived triplet state sensitiser as discussed in detailed in the singlet oxygen chapter 7. Upon interaction with molecular oxygen energy transfer occurs to yield singlet oxygen. This highly reactive species can then undergo a range of photochemical reactions, using sensitisers such as Methylene Blue (MB) and Rose Bengal (RB), their relatively high quantum yields may be obtained for singlet oxygen formation ($\Phi(CH_3OH)_{RB} = 0.8$ and $\Phi(CH_3OH)_{MB} = 0.51$). Production of singlet oxygen has been shown to be efficient in supercritical carbon dioxide, and the lifetime has been demonstrated to be long in comparison with conventional solvents [4,5] being 5.1 ms at 150 kg cm^{-2} and 41°C [1]. In this study, dye sensitised singlet oxygen has been utilised to effect the transformation of 1, 5-dihydroxynaphthalene to Juglone in supercritical fluid carbon dioxide, monitoring the production of Juglone *in situ* using UV-visible

spectrophotometer. A number of sensitisers soluble in supercritical fluid carbon dioxide are investigated which include; Anthracene (Anth), Alloxazine (All), Rose Bengal (RB) and Methylene Blue (MB).

The maximum absorbance of Rose Bengal is in the region 500 – 600 nm, which corresponds to approximately 170 $kJmol^{-1}$ of energy. This enables excitation of the sensitiser to its singlet state, from which it undergoes intersystem crossing to its triplet state (94 $kJmol^{-1}$), which can then selectively transfer energy to molecular oxygen.

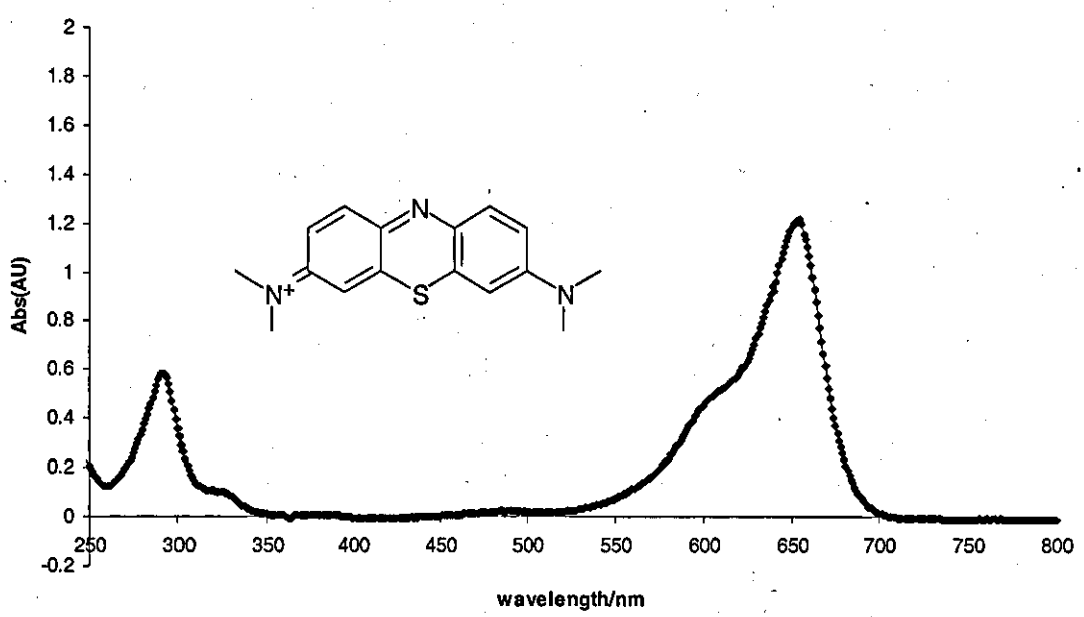

Figure 8.1: Absorbance spectrum of Methylene Blue in methanol

Whilst the maximum absorbance of Methylene Blue; is in the region 600 - 700 nm. In a similar process to that of rose Bengal, the dye is excited to its singlet state before intersystem crossing to the triplet state (140 $kJmol^{-1}$). Once in the triplet state, the dye can readily transfer energy to molecular oxygen.

8.1 Photochemical Synthesis

In general synthetic photochemistry has had little impact in industry, although some examples of photochemical process exist[18-20]. This low impact is attributed to the high running costs of the commonly used light sources (energy demands and cooling), such as mercury or halogen lamps. The typical energy demand of a medium pressure

mercury lamp (400 W) is 1343 kJ h^{-1}. Of the electrical energy supplied, less than half is converted to light energy, resulting in a large quantity of wasted energy. Over time the lamps degenerate and although they draw the same energy the quality of the light produced decreases significantly. The limited lifetime of such lamps is a contributor to the high cost of photochemical processes (installation, maintenance and particularly operational costs). In addition, while UV light may cause desirable photochemical transformations, in many cases filtering of the light source is needed to prevent unwanted side reactions. Therefore, the percentage of the light generated that contributes to the desired chemical reaction may be very low making such photochemical processes very inefficient. Recent interest in light emitting diodes (LEDs) has offered an alternative to these costly and inefficient light sources[21]. These are small, versatile and available in a large number of wavelengths, allowing for selectivity of the light source. In addition, there is minimal heat generation so little or no cooling is needed.

The efficiency of a photochemical process may be expressed using the quantum yield (Φ), which is the amount of reactant consumed or product formed divided by the amount of photons absorbed. In an ideal system all photons lead to a photochemical transformation and so the quantum yield is one. However, for practical applications a quantum yield of greater than 0.3 is considered very efficient. Exceptions to this are photo-initiated free radical chain reactions, where quantum yields of far greater than one may be obtained.

Another factor that limits the perceived greenness of photochemical processes is the typical reaction conditions, in particular the solvents used and the concentration of the solutions. Many photochemical transformations are carried out in benzene or acetonitrile, as these solvents are less reactive towards free radicals. However, these are less favourable solvents due to their toxicity[22]. Photochemical reactions, in particular on the large-scale, tend to use rather dilute reaction mixtures. The amount of photons absorbed by a reaction mixture is directly related to the concentration of the reaction mixture and is expressed by the Beer-Lambert Law

$A = \varepsilon c l$

Where A is absorbance, c is concentration, l is path length (through the reaction mixture) and ε is the molar absorption coefficient (wavelength dependent constant). In scale-up, this is a particular disadvantage as the light must irradiate a far larger quantity of reaction mixture and it is difficult to reproduce the same l value as the smaller scale synthesis. Consequently, the concentration of the reaction mixture is usually quite low, to enable light penetration of the entire reaction mixture.

Despite the disadvantages, there are several examples in the literature of 'green' photochemical transformations. The potential of photochemistry as a "clean" technology has been discussed previously[23], with outlines that perceives disadvantages of photochemistry and some approaches to avoid these issues and various research[24-26] have demonstrated the application of photochemistry as a green technology. In particular, use of solar light in photooxygenation and photoacylation reactions provides an effective green route to fine chemicals[27-29]. In addition, elimination of halogenated solvents and use of catalytic amounts of sensitiser give a process that adheres to the twelve principles of green chemistry.

8.2 Synthesis of Juglone

Due to the favourable absorption of most dyes within the visible spectrum, photooxygenation reactions have been subjected to concentrated sunlight and served as model systems for environmentally friendly and benign 'Green Photochemistry'. The photooxygenation of 1, 5-dihydroxynaphthalene was studied with moderately concentrated light and 5-hydroxy-1,4-naphthoquinone (Juglone) was obtained in good yields. Since Juglone is a valuable product, as a result it is desirable to develop an efficient method for its synthesis and its rate of formation, mostly looking at the oxidation of 1, 5-dihydroxynaphthalene using a variety of oxidising agents. 1,5-dihydroxynaphthalene is a desired starting material as it is cheap and commercially available. Other syntheses involve the use of 1, 8 dihydroxynaphthalene[30] or 1,8-amidonaphthol[31]. 5-acetoxy-1-naphthol also yields Juglone under photooxygenation conditions[32]. The earliest reported synthesis of Juglone was in 1887 by Bernthsen and Semper[33], where 1,5-dihydroxynaphthalene was converted to Juglone using chromic

acid (aqueous solution of potassium dichromate and sulphuric acid) at room temperature for 24 hours. In this study it was reported that Juglone was isolated in yields of 26-37%.

The first reported photochemical synthesis of Juglone was reported by Griffith in 1976[34], using methylene blue as a sensitiser and irradiation using a tungsten lamp, to get Juglone in 70% yield. An investigation by Duchstein and Wurm looked at the effect of different sensitisers (sensitiser-free, methylene blue, rose Bengal and 9,10-dicyanoanthracene), solvents (methanol and acetonitrile) and wavelengths (> 360 nm and < 360 nm) on the yield of this reaction[35-36]. The optimised conditions were found to be the use light > 360 nm for a solution of methylene blue in acetonitrile. This was found to give Juglone in yields of 70-75% following 8 hours of irradiation[37]. Recent studies[26-30] has reported the synthesis of Juglone under artificial and solar conditions, reporting yields of up to 88%[28]. Other studies of Juglone in the literature have looked at the kinetics of the reaction of 1, 5 dihydroxynaphthalene with singlet oxygen[38-40]. The mostly used sensitisers are: Rose Bengal[26-28], Methylene blue[34-35] and Tetraphenylporphyrin (TPP)[28, 43]. Although TPP is the most effective singlet oxygen generator[21], it is less commonly used than rose bengal due to solubility difficulties. TPP is primarily soluble in halogenated or nonpolar solvents and virtually insoluble in alcohols[27]. Methylene blue gave a good Juglone production, which is in line with the singlet oxygen quantum yields of the three sensitisers ($\Phi\ (CH_3OH)_{RB}$ = 0.80, $\Phi(C_6H_6)_{TPP}$ = 0.66 and $\Phi(CH_3OH)_{MB}$ = 0.5. Since it was possible to obtain a good yield of Juglone from these sensitisers, the aim of this research is to try and perform this project using supercritical carbon dioxide as a solvent, which will provide even greener photochemistry, and to follow its rate of formation spectroscopically.

8.3 Mechanism of the Photooxygenation of 1,5-dihydroxynaphthalene

The reaction of singlet oxygen with 1,5-dihydroxynaphthalene is an example of a photo-Diels Alder reaction ([4+2]-cycloaddition), in which 1,5-dihydroxynaphthalene functions as a diene and singlet oxygen as a dienophile. The photo-Diels Alder reaction

produces an endoperoxide, which subsequently undergoes the loss of water to yield the 1,4-naphthoquinone. The general mechanism suggests that the conversion of the endoperoxide to the naphthoquinone is spontaneous. Croux attributes this to the instability of the endoperoxide, but does not speculate further on the mechanism. However, Murtinho proposes that intramolecular acid catalysis occurs (supported by deuterium isotope studies[40]), causing conversion of the endoperoxide to the hydroperoxide.

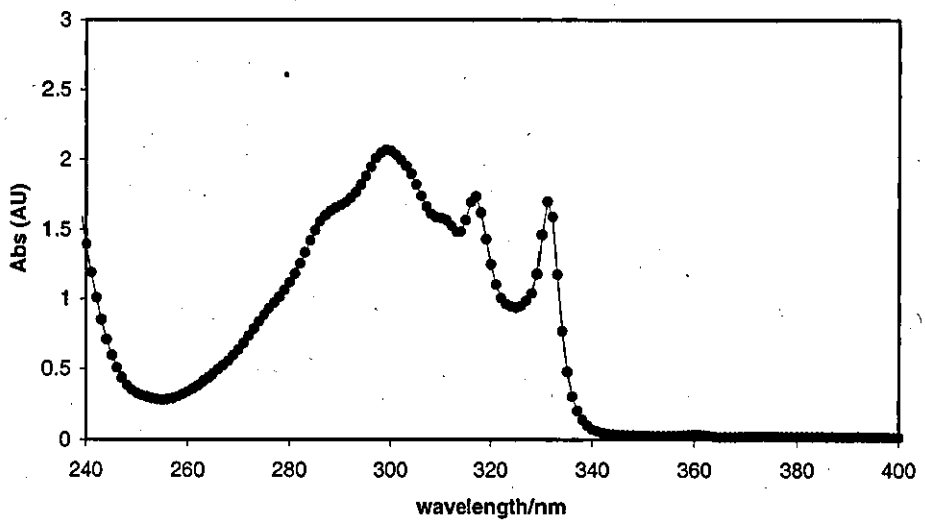

Figure 8.2: Spectrum of 1,5 -Dihydroxnaphthalene

8.4 Characterisation of Juglone

The use of different sensitisers will be investigated, using Rose Bengal, Methylene blue, Anthracene and Alloxazine, to identify the most suitable sensitiser for this system. Methanol will be used as the solvents for introduction into the set up, which will then be pumped out using oxygen for reactions using $scCO_2$. The product formed in these reactions was further analysed by NMR and IR and it was found to be very similar to the pure Juglone as shown in the appendix section, much appreciation goes to Will Simpson; for performing the two analysis detailed in section 8.4.1 and 8.4.1.2.

8.4.1 NMR Analysis

The ^{1}H NMR has been assigned as Juglone (scheme 8.1) which confirms that the Juglone has been formed as shown in the Appendix section (page vi) which is similar to the standard pure Juglone (page vii). Standard, δH ($CDCl_3$), 7.58 (1H, m, Ar-H), 7.22 (1H, m, Ar-H), 6.90 (1H, s, Ar-H), 1.50 (2H,s, R-CH-CH-R). Sample, δH ($CDCl_3$), 7.19 (3H, s, Ar-H), 1.51 (2H, s, R-CH-CH-R). Note, small peaks in the sample NMR indicate small levels of impurity, possibly a small quantity of methylene blue remaining.

8.4.1.2 IR Analysis

The standard IR and sample IR spectrums show four large, similar peaks suggesting the same compound is present as shown in the appendix section (page vii). These are 400-800 cm^{-1} (C-H, aromatic 750-900 cm^{-1}), 1000-1100 cm^{-1} (C-O, alcohol 1040-1060 cm^{-1}), 1400-1500 cm^{-1} (C=O, ketone, 1665-1725 cm^{-1}) (influenced by conjugation/ring size) and 2800-3600 cm^{-1} (O-H, alcohol 3200-3400 cm^{-1}).

8.4.2 Dark room studies

The conditions required for the production of Juglone are sensitiser, air bubbling as well as light. A reaction was carried out without light and no Juglone was formed. This unambiguously proves that only under light irradiation is this oxidation possible, hence Juglone formation. However, it has been reported[3] that under very basic conditions (phosphate buffer of $Na_2HPO/NaOH$ at pH 12) the Juglone anion has known to spontaneously synthesis in the dark (Scheme 5.2).

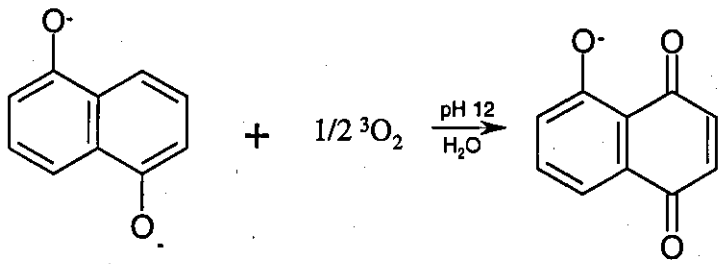

Scheme 8.1: Spontaneous dark synthesis of Juglone

8.4.2.1 Sensitiser-free studies and pure Juglone comparisons

Using a range of light sources has shown that a small amount of self-sensitisation occurs. This self sensitisation is greater when ultraviolet light (UV) is used (Mercury lamp and Rayonet (300 nm) than when visible light is used (halogen lamps). This is consistent with observations by Duchstein[41], who noted that yields of Juglone of up to 20% were obtained using light >360 nm (halogen lamp), with yields of 12-15% for light < 360 nm (high pressure mercury lamp).

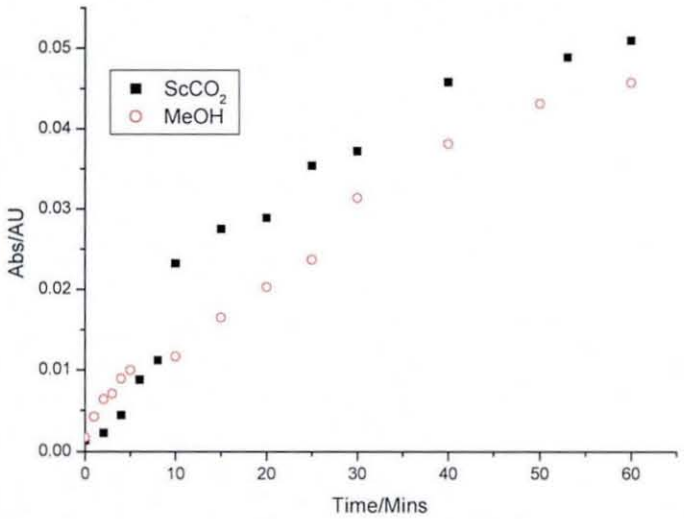

Figure 8.3: A graph showing the rate of formation of Juglone in the absence of sensitiser in both methanol and $scCO_2$ with a UV lamp

1,5-dihydroxynaphthalenes are known to be good self-sensitisers at 337 nm[38] and Murtinho reports yields of up to 28% using Tungsten lamps[42]. The UV-vis spectrum of 1,5-dihydroxynaphthalene (technical grade) shows that the starting material does not absorb at wavelengths greater than 350 nm. An absorbance band with a maximum at 300 nm may enable excitation of the molecule under UV irradiation, leading to self-sensitisation. Little self-sensitisation is observed when a halogen lamp is used. Solar irradiation provides light of 300 nm to greater than 700 nm, thus the diol may be excited under solar conditions.

A study of solvents for Juglone synthesis was carried out previously[27]. This showed that photooxygenation in *t*-amyl alcohol produces more oxidation product than in *i*-propyl alcohol or acetone, in a shorter length of time. As *t*-amyl alcohol is a longer

chain alcohol, with physical properties similar to those of *t*-butyl alcohol, it is expected that the singlet oxygen lifetime is about 31 μs or even longer (Table 8. 1). It is greater than that in the shorter chain alcohols (methanol, ethanol and *i*-propyl alcohol) and so greater yields may be achieved for photooxygenation in *t*-amyl.

Solvent	**$^1O_2$ lifetime (μs)**
Acetone	34-65
Ethyl acetate	45-50
Methanol	9.5-10.4
Ethanol	9.7-15.3
i-Propyl alcohol	22
t-Butyl alcohol	31
Dichloromethane	59-100

Table 8.1: Singlet oxygen lifetimes in selected solvents[18], alcohols

It has been observed that when reaction solutions of the same concentration in conventional solvents and in supercritical carbon dioxide are compared, higher absorbance values are noted for the supercritical carbon dioxide as shown in figure 8. 4.

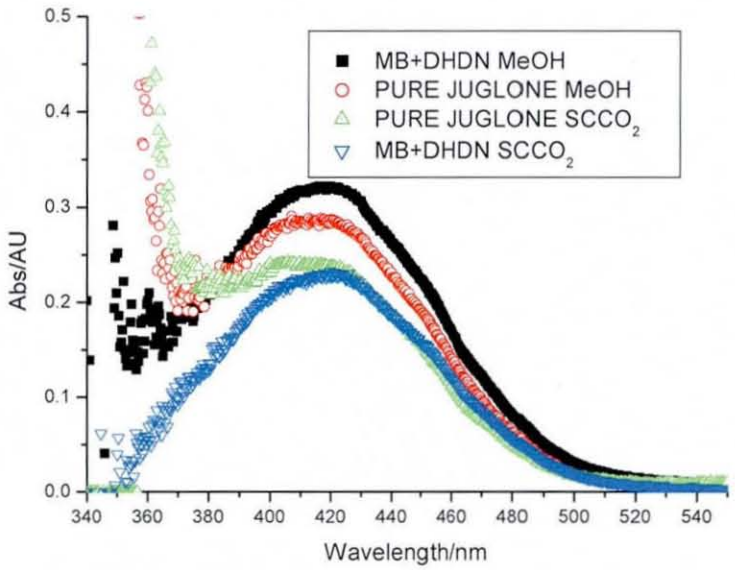

Figure 8.4: Comparison of pure Juglone with Juglone formed from DHDN in both $scCO_2$ and methanol

This has been attributed to the formation of 'clusters' of additional density. These are short lived formations but may cause an increase in absorbance of localised sample.

8.5 Effects of Oxygen on the formation of Juglone

Singlet oxygen is known to have a longer lifetime in gaseous state; therefore a study in using the mixture of gases was investigated instead of pure oxygen only as detailed in section 4.7. This was necessary to follow the reaction of the production of Juglone using a mixture of various concentrations of gases in comparison to the pure oxygen at different pressures. Figure 8.5 shows the production of Juglone using Anthracene and dhdn in supercritical carbon dioxide with the ratio of 60% nitrogen and 40% oxygen and a correlation was observed with the various pressures; as the pressure increases the production of Juglone decreases.

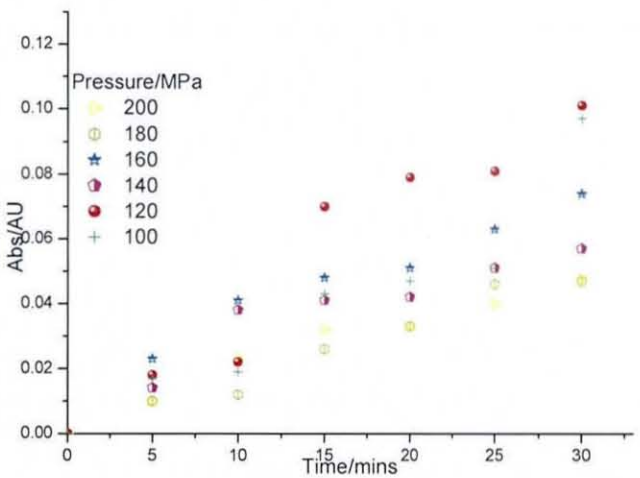

Figure 8.5: Production of Juglone in $scCO_2$ with a mixture of 60% N_2 and 40%O_2 at various pressures

Figure 8.6 shows two similar solutions of the same concentration but one has been oxygen bubbled through it and the other one is only air equilibrated. The plot indicates not much difference has been observed, therefore proves the fact that the limiting factor is not the amount of oxygen in solution but the concentration of Methylene Blue and the rate at which it can produce the singlet oxygen state. This is not surprising as the Methylene Blue concentration is a factor of 3 lower than the oxygen concentration in

the air equilibrated solution and therefore making the Methylene Blue the limiting reagent. It was observed that there was no correlation in the production of Juglone with pure oxygen and also with a mixture of gases at different pressures. Since pure oxygen is known to have a longer fluorescence lifetime

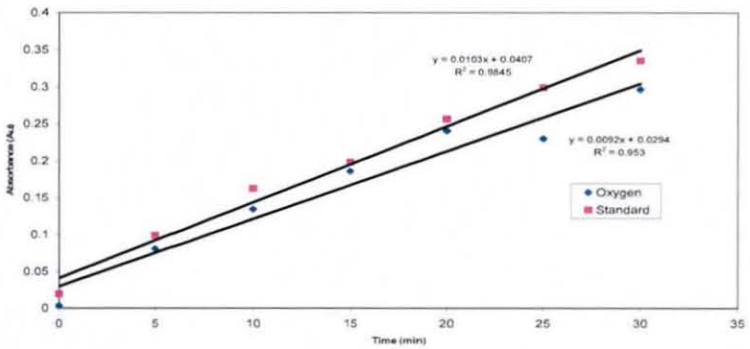

Figure 8.6: Comparison between the air equilibrated solution vs. pure oxygen.

8.6. Solvent and sensitiser study

Different solutions mixtures of 1,5-dihydroxynaphthalene (dhdn) were illuminated in the presence of different sensitizers and different solvents as detailed in section 4.7. The results were tabulated for which were in favour to produce Juglone and which were not as shown in Table 8.2. Mostly the ones which did not manage to produce Juglone was due to the fact that the sensitiser would not dissolve in the solvent and the ones which managed to dissolve did not produce the expected peak as the pure Juglone.

Solvents	Sensitiser	Juglone
MeOH	MB	yes
MeOH	Tris pp Ru	No
MeOH	RB	yes
MeOH	Hematotrophyn	yes
MeOH	Anthracene	yes
Acetone	MB	yes
Acetonitrile	MB	yes
DCM	MB	yes
Chloroform	MB	Yes
Dichloro ethane	MB	NO
Iso propanol	MB	yes
propanol	MB	yes
Dioxane	MB	NO
Ethanol	MB	yes
Ethyl Acetate	MB	Yes
Hexane	MB	NO
$scCO_2$	MB and RB	Yes

Table 8.2: A table showing the production of Juglone using different sensitisers and different solvents

The formation of Juglone using conventional solvents was investigated and the results in Table 8.2 can be used for comparison of the reaction rate and evaluation of the effectiveness of supercritical carbon dioxide as a suitable reaction solvent in comparison to other solvents investigated. Figure 8.7 provides information with regarding the use of MB as a sensitiser in methanol for the synthesis Juglone, whereby figure 8.8 follows the synthesis of Juglone using different solvents and different sensitisers.

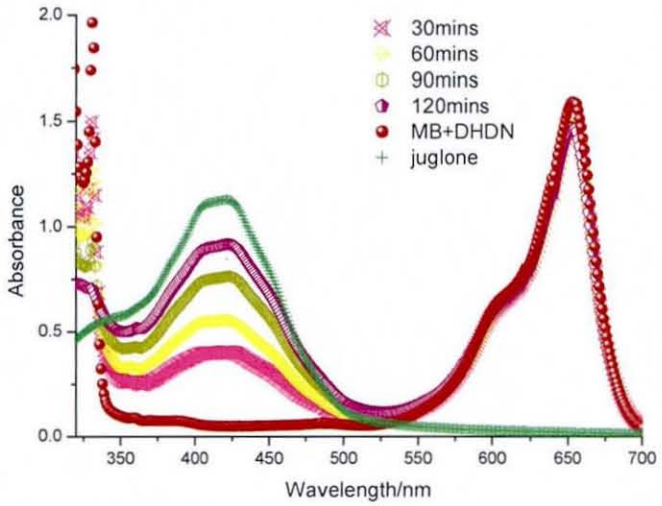

Figure 8.7: Juglone synthesis from Methylene blue and 1,5-dihydroxynaphthalene

The synthesis of Juglone from 1,5-dihydroxynaphthalene has shown to increase in yield with time and a correct amount of sensitiser. On using Methylene blue as a sensitiser the colour of the reaction mixture was observed to turn from dark green/blue during the experimental period to brown which is due to the result of the production of Juglone.

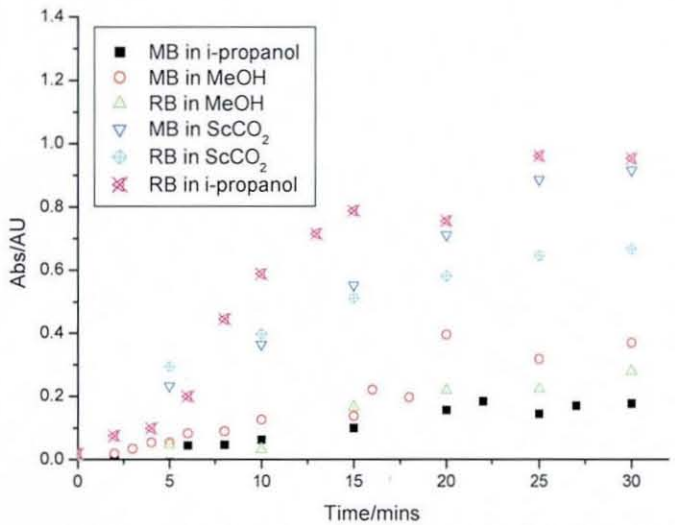

Figure 8.8: A graph showing the production of Juglone in different solvents and with different sensitisers

The formation of Juglone in different solvents and different sensitisers has been shown to produce Juglone in various rates as shown in figure 8.8, with RB in i-propanol

having produced more Juglone, this is in line with other studies as well which showed the same trend and then followed by $scCO_2$ which produced more Juglone. The higher production of Juglone in $scCO_2$ is thought to be due to the fact that $scCO_2$ has a longer singlet oxygen lifetime than the other solvents.

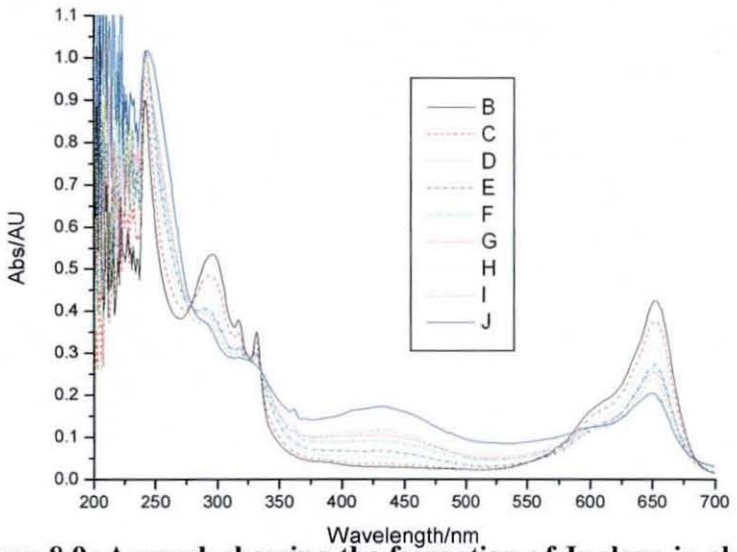

Figure 8.9: A graph showing the formation of Juglone in chloroform, using MB as a sensitiser and various concentration of dhdn

On using chloroform as a solvent, a peak was observed at the 300 nm wavelength, further investigation found out that it was the *leuco* form of MB which was being made, reflecting the detailed spectrum shown on the study in figure 8.9[45]

Whilst investigating the rate of Juglone production with different solvents an interesting additional reaction was noted when using initially chloroform, and subsequently isopropanol as a solvent. This was observed when the absorbance of methylene blue at 650 nm in the cell solution began to drop with time, whilst an additional peak at around 240 nm arose. The spectrum for MB in chloroform is shown, figure 8.9.

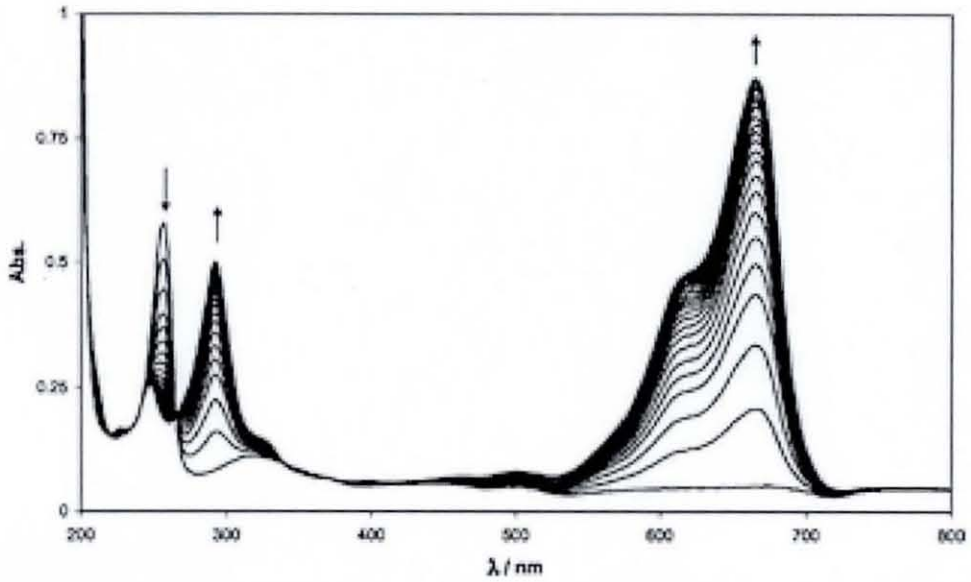

Figure 8.9.1: The absorbance peaks of methylene blue (650 nm, 290 nm) and leucomethylene blue (240 nm)[18].

A simple plot of the two absorbance peaks over time showed them to be rising and falling in proportion with one another, suggesting that the methylene blue was forming a new compound which absorbed in the near ultra-violet region. Initially this was thought to be a secondary singlet oxygen reaction, given that the singlet state is known to react with many organic compounds including aromatics and hetero-aromatics. However, why this should occur in some solvents and not others was not clear. With some additional research it became apparent that the new peak at 240 nm matched that of the *leuco* form of methylene blue, suggesting that the sensitiser was being reduced in the cell[18]. An illustration of the peaks associated with methylene blue and leucomethylene blue is shown in Figure 8.9.1.

8.7 Super critical Carbon Dioxide studies

Studies to evaluate the use of $scCO_2$ as a solvent for the Photooxygenation of 1,5-dihydroxynaphthalene to synthesise Juglone are done using different sensitisers like MB, RB, Anthracene and Alloxazine as detailed in section 4.6.6 and section 5.2. The synthesis of Juglone may be followed spectroscopically and their kinetics followed as a fraction of temperature and pressure.

Pure Juglone was initially used and pumped into the system in order to assess its solubility and validate it against methanol, and additional Juglone was pumped again in the set up at a higher pressure and the results could be seen in figure 8.10.

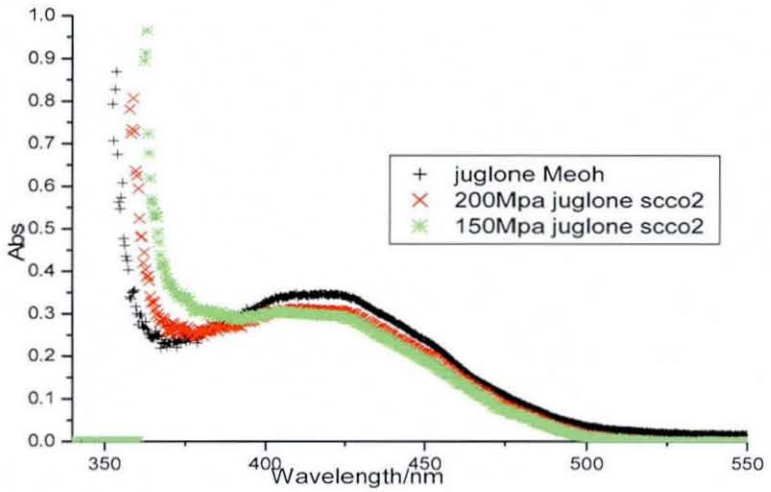

Figure 8.10: A graph of pure Juglone in 150 and 200 Mpa pressures in $scCO_2$ in comparison to methanol

The absorbance was measured over the range 350 nm- 600 nm, but the main area of interest was 400 nm – 450 nm (415 nm). Neutral density filters were used to decrease the intensity of the light reaching the optical fibre (after irradiation of the cell). Before commencing any monitoring study light and dark reference spectra were obtained. Pure Juglone spectra were also obtained at different pressure, it was noted that with the pure Juglone there was a decrease in absorbance as pressure was decreased, due to presumably to a decrease in solubility.

8.8. Anthracene as a sensitiser for Juglone production

Since Anthracene was studied and detailed in chapter 7 and known to be good sensitiser, was therefore used in the photooxygenation of dhdn. However, it was necessary to ensure that there was some comparison between the production of Juglone in the $scCO_2$ and in conventional solvents in order to follow the reaction successfully. It was possible to follow and monitor the production of Juglone using Anthracene as a sensitiser in different solvents and also in $scCO_2$ at 150 MPa and 313 K. Figure 8.10 shows the comparison of pure Juglone in both organic solvent and in $scCO_2$ in addition

to the Juglone produced through 1, 4 -dihdroxy naphthalene (dhdn) and Anthracene in both organic solvent and in $scCO_2$.

The irradiation of the mixture for a longer period at different pressure was studied, in order to observe if more of the product will be produced and investigate the relationship with pressure as shown in figure 8.11, although no apparent trend with the increase in pressure to the formation of Juglone using Anthracene as a sensitiser was observed.

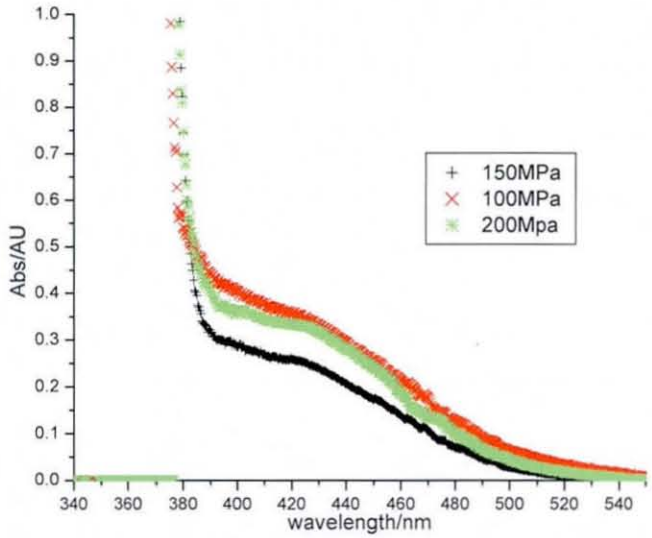

Figure 8.11: A graph showing the Juglone production in $scCO_2$ after 1hr of light irradiation with different pressures at a constant temperature of 35°C using Anthracene as a sensitiser

A study of Anthracene in $scCO_2$ was carried out, as expected the absorbance was noted to decrease with time; this is discussed in detail in section 5.2. On using Anthracene as a sensitiser, it was observed that a lot of it gets used up in the first half an hour, therefore the production of Juglone should only be followed in that time frame, this will then avoid any errors but ideally all reactions should be kept within the half an hour time frame.

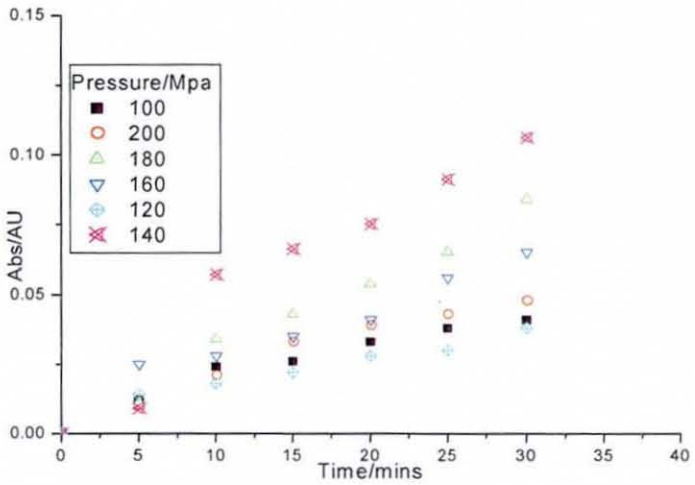

Figure 8.12: Production of Juglone in $scCO_2$ at various pressures at a constant temp of 313 K using Anthracene as a sensitiser.

8.9 Dihydroxnaphthalene in $scCO_2$

The stability of Dihydroxnaphthalene (DHDN) in $scCO_2$ was measured according to the method described in section 5.3. The DHDN stability over 30 mins is shown in figure 8.13, however a slight drop in the absorbance was observed over 30 mins period, hence the reactions were monitored over this time frame or less. The ocean optics USB 2000 used in the set up in figure 5.5 was only able to show the regions of above 350 nm and the kinetics were measured using the Juglone peak around 420 nm as shown in figure 8.11. Since the DHDN peak was around 330 nm a different spectrometer was used to validate the absorbance (stability), the values obtained are shown in figure 8.13.

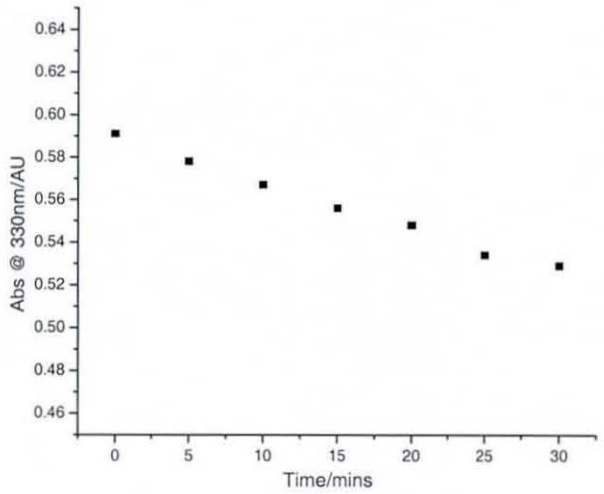

Figure 8.13: Dhdn in $scCO_2$ for 30mins at 100Mpa and 35°C

8.9.1 Rate of formation of Juglone as a function of initial [DHDN]

The formation of juglone from DHDN concentration increases with increasing DHDN concentration as shown in 8.14. The effect of solvent on Juglone formation is studied in detail later in section 8.9.2 but clearly figure 8.14 shows there is an increased rate of production of juglone when acetonitrile is used as a solvent. This is due to the fact the longer singlet oxygen lifetime in acetonitrile compared with $scCO_2$ and methanol.

This is attributable to the faster singlet oxygen lifetime in the $scCO_2$, which means that increase in the singlet oxygen is intercepted by DHDN in the acetonitrile. A detailed kinetic analysis is given later in Table 8.7, since the value of k_2 is lower in $scCO_2$ by as much as five times the value of singlet oxygen in Acetonitrile.

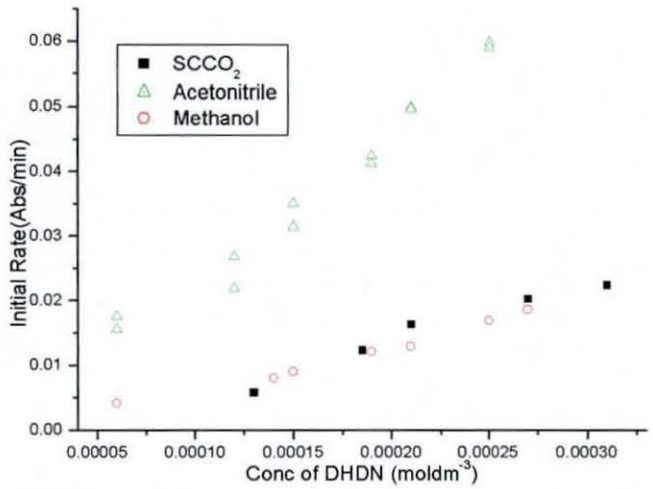

Figure 8.14: A graph showing the rate of production of juglone in various [DHDN] using MB as the sensitiser

8.9.2 Comparisons of the Effects of Dihydroxnaphthalene in MeOH and $scCO_2$

For Juglone formation to be understood, it was necessary to obtain the initial rates at which the dhdn is being consumed as the starting material in $scCO_2$, table 8.3 shows the different concentrations, absorbances and initial rates used as detailed in section 5.0 and 5.1.

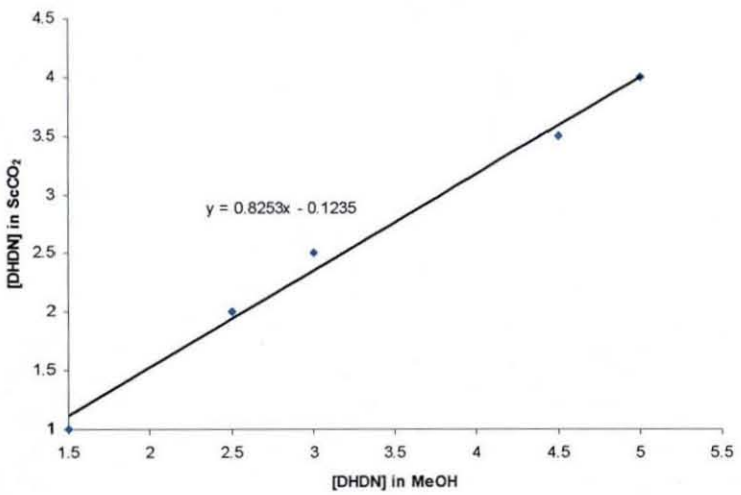

Figure 8.15: various [Dhdn $x10^{-4}$] in $scCO_2$ vs various [dhdn $x\ 10^{-4}$] in methanol

A plot of known concentration is shown in graph 8.15 and from this it could be seen that within the time frame of half an hour, only 10% of dhdn was consumed which

clearly shows that there is no much variation of dhdn concentration in methanol and in the super critical carbon dioxide.

From Table 8.3 it is clear that the higher the concentration the faster the initial rate hence more dhdn is being consumed.

Initial Abs/AU	Conc./M	Initial Rates/min^{-1}
0.31	0.000021	-0.0029 ±0.0001
0.42	0.000032	-0.0027 ±0.0001
0.53	0.000039	-0.0021 ±0.0001
0.61	0.000044	-0.0021 ±0.0001
0.69	0.000049	-0.0017 ±0.0001

Table 8.3: Various [Dhdn] in $scco_2$ with the initial rates within 30mins

8.10 Effects of increasing dhdn concentration on the initial rate of formation of Juglone

The higher the concentration of dhdn the higher and faster was on the formation of Juglone. Although the rates were higher in Acetonitrile as expected due to its higher singlet oxygen lifetime compared to methanol and $scCO_2$.

Conc of dhdn ($moldm^{-3}$)	Initial Rate in Methanol ($moldm^{-3}$ min^{-1})	Initial Rate in Acetonitrile ($moldm^{-3}$ min^{-1})	Initial Rate in scCO2 ($moldm^{-3}$ min^{-1})
6.0×10^{-4}	$3.51 \pm 0.02 \times 10^{-7}$	$1.16 \pm 0.03 \times 10^{-6}$	$2.72 \pm 0.01 \times 10^{-7}$
1.2×10^{-4}	$4.78 \pm 0.02 \times 10^{-7}$	$1.63 \pm 0.03 \times 10^{-6}$	$3.21 \pm 0.01 \times 10^{-7}$
1.5×10^{-4}	$6.65 \pm 0.02 \times 10^{-7}$	$2.61 \pm 0.03 \times 10^{-6}$	$4.33 \pm 0.01 \times 10^{-7}$
1.9×10^{-4}	$9.03 \pm 0.02 \times 10^{-7}$	$2.66 \pm 0.03 \times 10^{-6}$	$9.18 \pm 0.01 \times 10^{-7}$
2.1×10^{-4}	$1.05 \pm 0.02 \times 10^{-6}$	$3.12 \pm 0.03 \times 10^{-6}$	$1.22 \pm 0.01 \times 10^{-6}$
3.1×10^{-4}	$1.23 \pm 0.02 \times 10^{-6}$	$3.98 \pm 0.03 \times 10^{-6}$	$1.67 \pm 0.01 \times 10^{-7}$

Table 8.4: Effects of [DHDN] on the initial rates of formation of Juglone in different solvents, MB conc. was 1.2×10^{-4} M

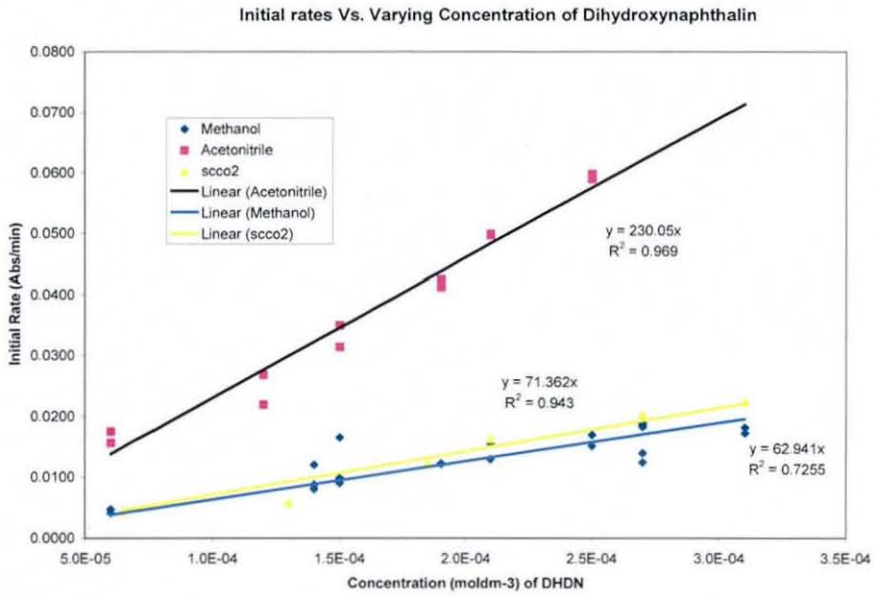

Figure 8.16: Effects of [DHDN] on the initial rates of formation of Juglone in different solvents, [MB] 1.2 x 10^{-4} M

8.11 Methylene Blue as a sensitiser

Methylene blue is one of the sensitisers which has shown great success to use in the production of Juglone, it has shown to work tremendously well in various studies[27-30] by using different solvents, although it is insoluble in hexane, it was found that it was soluble in $scCO_2$. Methylene blue was used as a sensitiser in the production of Juglone, it was observed to produce a higher yield in conventional solvent in various studies[27].

8.11.1 Effects on the rates of production of Juglone using MB as a sensitiser in both $scCO_2$ and MeOH

The production of Juglone using MB and Dhdn in super critical carbon dioxide was compared to that of the conventional solvent in methanol and was seen that a higher production of Juglone was obtained in $scCO_2$, this is thought to be due to the fact that there is less viscosity in $scco_2$ than in methanol and also the lifetime of singlet oxygen in $scCO_2$ is longer than in conventional solvent. The initial rates of reaction are double in $scCO_2$ compared to methanol (MeOH) as shown in Table 8.5

MeOH rates/min^{-1}	$scCO_2$ rates/min^{-1}	MB conc./M	Dhdn conc./M
0.0055	0.0102	0.000023	0.00026
0.0048	0.0106	0.000023	0.00054
0.0052	0.095	0.000046	0.00054
0.0007	0.0022	0.000023	.000013

Table 8.5: A table showing how the rates of reaction compare with the [MB] and [dhdn]

8.11.2 Comparison of MB in $scCO_2$ and in MeOH

Since an increase of MB concentration has not got that much effect in the production of Juglone, it was necessary to compare MB in a conventional solvent like methanol to the supercritical solvent like $scCO_2$. It was then observed as shown in figure 8.17 that there was not much difference.

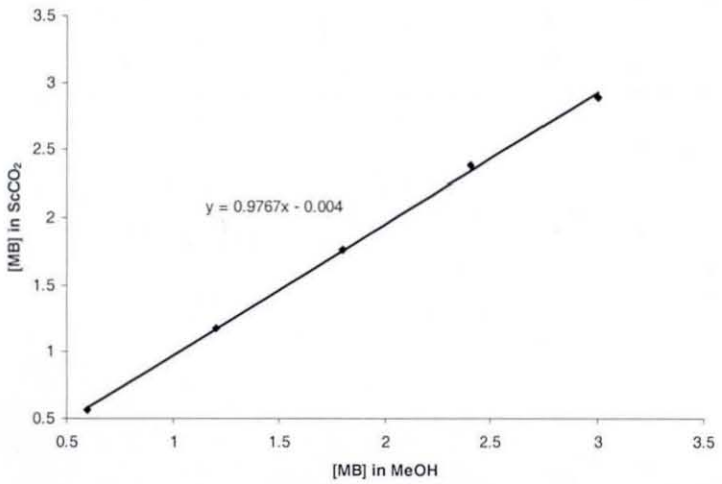

Figure 8.17: Various [MB] in $scCO_2$ vs. various [MB] in MeOH

The relationship between dhdn in methanol and in supercritical carbon dioxide is nearly of the ratio of 1:1. Similar to the relationship of the concentration of MB in solvent and in super critical carbon dioxide as discussed in section 5.1. The initial rates of the Juglone production in $scCO_2$ were higher that of the methanol even after varying the concentration of the sensitiser and dhdn, this also increases the production of Juglone in $scCO_2$.

8.11.3 Effects of MB on the initial rate of formation of Juglone

It is clear from the results that the higher the concentration of dhdn the faster the formation of Juglone. But for Juglone formation to be complete, it was necessary to determine what the effects of the concentration of the sensitiser are has to the product. As shown in table 8.6 the effects of increasing MB on the formation of Juglone was slight compared to the effect of increasing dhdn.

Concentration of M.B. (moldm-3)	Initial Absorbance of M.B. (AU)	Initial Rate in Methanol (Conc/min)	Initial Rate in Acetonitrile (Conc/min)	Initial Rate in $scCO_2$ (Conc/min)
2.30×10^{-6}	0.18	4.19×10^{-7}	1.0×10^{-6}	2.54×10^{-7}
4.60×10^{-6}	0.36	4.5×10^{-7}	1.2×10^{-6}	4.70×10^{-7}
6.00×10^{-6}	0.47	4.94×10^{-7}	1.4×10^{-6}	5.51×10^{-7}
1.20×10^{-5}	0.95	6.04×10^{-7}	2.0×10^{-6}	7.99×10^{-7}

Table 8.6: Effects of [MB] on the initial rates of formation of Juglone in different solvents, [DHDN] 1.3 X 10^{-4} M

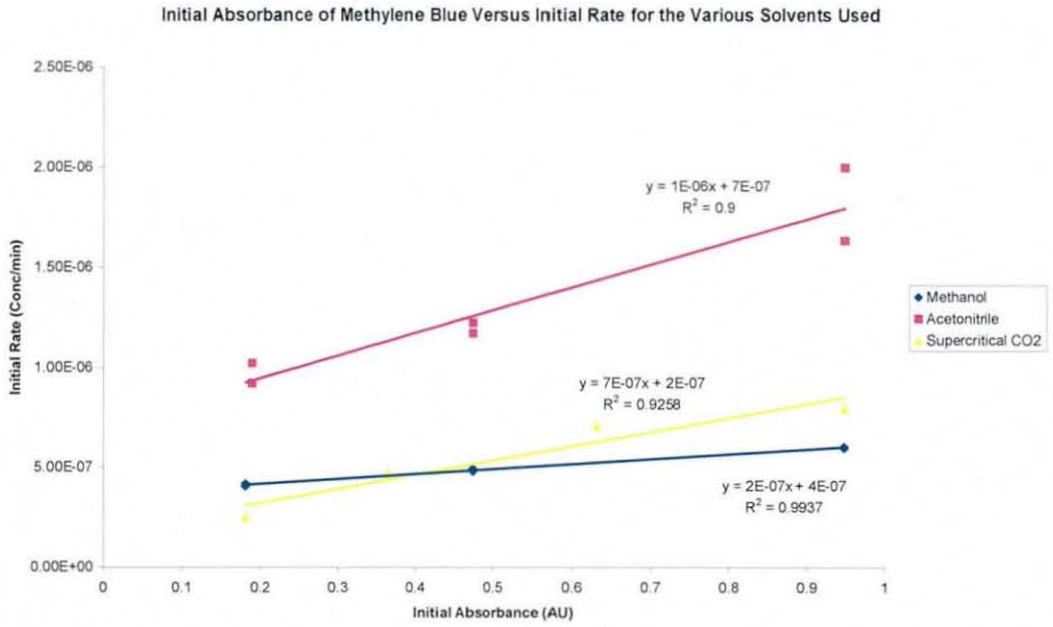

Figure 8.18: Effects of [MB] on the initial rates of formation of Juglone in different solvents, [DHDN] was 1.3 X 10^{-4}M

Table 8.5 and 8.6 also shows that the rate was slightly higher in Acetonitrile compared to MeOH and $scCO_2$ this is due to the fact Acetonitrile has a relatively long singlet oxygen lifetime. The singlet oxygen lifetime is $7.7x10^{-5}$ s in Acetonitrile where as in methanol it is only $9.0x10^{-6}$ s whilst the singlet oxygen lifetime of $scCO_2$ is 5.1 ms at 14.7 MPa and 314 K. The singlet oxygen lifetime is the longest in $scCO_2$ but its bimolecular rate constant (k_2 in table 8.7) is much lower than both acetonitrile and methanol hence the acetonitrile reacts with the 1,5-dihydroxynaphthalene to produce Juglone faster.

The reaction rates in Table 8.7 follows equation 1, therefore:

$$[DHDN] + {}^1O_2 \underset{k\text{-}d}{\overset{kd}{\rightleftharpoons}} [DHDN.....O_2] \xrightarrow{k_R} [J] \qquad \textbf{1}$$

If $k_R >> kd$, the rate would be diffusion controlled and therefore Debye-Huckel's equation would apply:

$$\text{Rate} = kd = \frac{8RT}{3\eta} \qquad \textbf{2}$$

If $k\text{-}d >> k_R$, the rate of the reaction would be reaction controlled and therefore:

$$\text{Rate} = K\,k_R \qquad \text{Where: } K = \frac{kd}{k-d} \qquad \textbf{3}$$

The rate of reaction will depend on the fraction of the singlet oxygen that reacts ($^1\Delta$) as follows

$$= \frac{k[DHDN]}{k_s + k[DHDN]} \qquad \textbf{4}$$

k_s is the reciprocal of the singlet oxygen lifetime. This means the rate of Juglone production would be:

$$\frac{d(J)}{dt} = k_2[DHDN][MB]\phi\Delta\frac{k[DHDN]}{k_s + k[DHDN]} \qquad \textbf{5}$$

As figure 8.18 is a straight line graph, and a plot of rate of production of Juglone against concentration of 1,5-dihydroxynaphthalene, then the gradient would equal:

$$= k_2[MB]\phi\Delta\frac{k[DHDN]}{k_s + k[DHDN]} \qquad \textbf{6}$$

For each of the three solvents, the fraction of singlet oxygen which would react at the lowest and highest concentration of 1,5-dihydroxynaphthalene have been calculated using equation 4. The fraction of singlet intercepted is determined from the rate constant k, which is calculated from the observed singlet oxygen lifetime in the presence of a sensitiser and the calculated values are shown in the table 8.7.

Solvent	Fraction of $^1\Delta$ O_2 that reacts (at highest [DHDN]	Fraction of $^1\Delta$ O_2 that reacts (at lowest [DHDN])	k_2 (highest [DHDN]) ($moldm^{-3}s^{-1}$)	k_2 (lowest [DHDN]) ($moldm^{-3}s^{-1}$)	Average k_2 ($moldm^{-3}s^{-1}$)
Methanol	0.017	0.0033	2.47×10^6	1.26×10^7	7.56×10^6
Acetonitrile	0.13	0.027	1.10×10^6	5.09×10^6	3.09×10^6
$scCO_2$	0.91	0.65	5.62×10^4	7.80×10^4	6.72×10^4

Table 8.7: Fraction of singlet oxygen that reacts and k_2 values for the three solvents

If the rate of reaction was diffusion controlled, then the average k_2 values would be similar to that of the diffusion coefficient. The diffusion coefficients for all three solvents are in the region of $1x10^{10}$ $mol^{-1}dm^3s^{-1}$. This shows that the rate of reaction is not diffusion controlled and therefore is reaction controlled (i.e. $k\text{-}d >> k_R$).

Chemical reactions in solution are generally accompanied by changes in volume, known their reaction volumes[41], which is interpreted according to the transition state theory, as the difference between the partial molar volumes of the transition state and the sums of the partial volumes of the reactants at the same temperature and pressure.

Changes in viscosity have been known to affect the activation volume; prominent among them are those reactions that are diffusion limited[42]. In order to react, the molecules must get within certain proximity of each other, known as the transition state volume. To reach this volume work either has to be done by the solvent to push the molecules together, or by the molecules to move further apart, thus doing work on the environment.

Partial molar volumes in liquids are only a few cm^3mol^{-1}, they can be very large and negative in SCFs, and as a result the pressure effect on the reaction rate constant can be

very significant. Partial molal volumes of solutes in supercritical fluids were reported to be small and positive at high pressures, but large and negative at low pressures in the highly compressible near-critical region. This was true for all the solutes studied[43-52] in both supercritical carbon dioxide and supercritical ethylene

8.11.4 Effect of the initial rate of formation of Juglone with the change in pressure and temperature using MB as a sensitiser in $scCO_2$

Further work to investigate the increase in pressure and temperature to the initial rates were done and although there seems to be an increase between the lower temperatures of 308 and 313k respectively, a slight decrease appeared at 318K and 323K as shown in figure 8.19. But this trend requires further thorough investigation with varieties of temperature and pressures, as the decrease in rate may be due to removing too much solvent from the cell hence removing the solution of MB and DHDN.

The concentration of the sensitiser only affects the rate of the reaction slightly, however adding more oxygen into the reaction does not affect the rate. This is because the concentration of Methylene Blue is much lower than that of the oxygen concentration. It has been found that the rate of Juglone production is reaction controlled and not diffusion controlled as the experimental rate constants (k_2) values are $1.26x10^5$ in methanol which is a lot lower than the theoretical value of $1.10x10^{10}$ $mol^{-1}dm^3s^{-1}$.

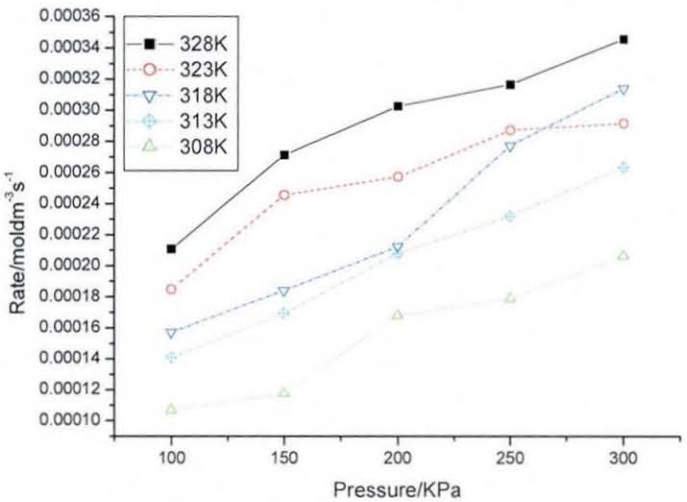

Figure 8.19: Effect of changing temperature and pressure on the initial kinetics rates of formation of Juglone using MB as a sensitser

An increase in the pressure has shown to increase the initial rates of reactions as shown in figure 8.19. The rate of production of Juglone in $scCO_2$ increases with increasing pressure and temperature, irrespective of sensitiser used at lower temperature and pressure, such a variation may be explained on the basis of the thermodynamics of encounter complex formation.

8.12 Effects of Rose Bengal as a sensitiser

The maximum absorbance of Rose Bengal is in the region 500 – 600 nm, which corresponds to absorbance of 170 kJ mol^{-1} of energy. This enables excitation of the sensitiser to its singlet state, from which it undergoes intersystem crossing to its triplet state (94 kJ mol^{-1}), which can then selectively transfer energy to molecular oxygen. The maximum absorbance of Methylene blue is in the region 600 - 700 nm. In a similar process to that of Rose Bengal, the dye is excited to its singlet state before intersystem crossing to the triplet state (140 kJ mol^{-1}), which can then produce Juglone at a more similar rate in comparison to MB, this study was also successful and could also be seen in a study [53-55].

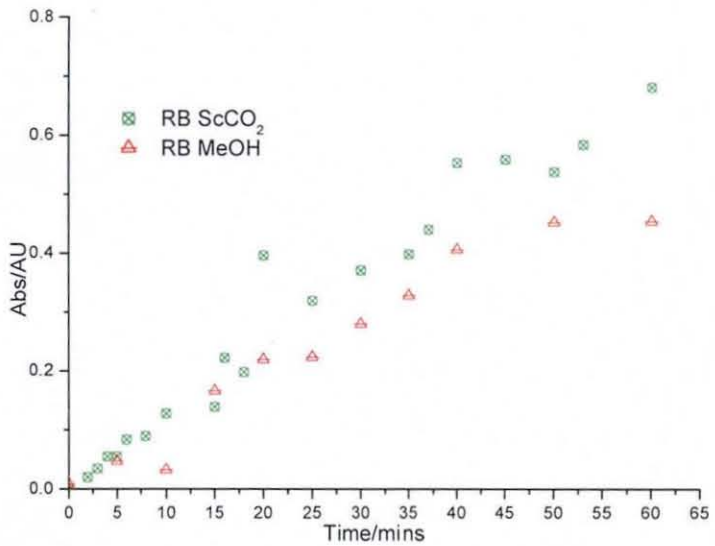

Figure 8.20: A graph showing the rate of formation of Juglone using RB as a sensitiser

Since it was seen that there was not much difference in the production of Juglone in both methanol and $scCO_2$, it was thought to investigate and see if there will be any

Since it was seen that there was not much difference in the production of Juglone in both methanol and $scCO_2$, it was thought to investigate and see if there will be any greater production when a combined study of both sensitisers were used to find the effects of the formation of Juglone, this did not have any impact on the formation as it stayed very much similar to if the sensitisers were used individually.

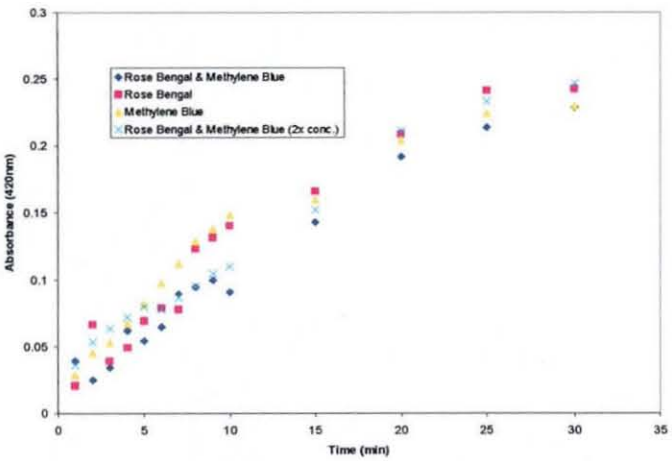

Figure 8.21: A graph showing the formation of Juglone with different sensitisers including a double sensitiser study

8.13 Effects of Alloxazine as a sensitiser

Flavins are derivatives of the dimethylisoalloxazine (7,8-dimethylbenzo[*g*]pteridine-2,4(3 *H*,10*H*)-dione) skeleton, with a substituent on the 10 position. Riboflavin (vitamin B2 being one of the best known members of this group), has a 10-D-ribityl group. There are also some most prominent members which are crucial coenzymes like: riboflavin, FMN and FAD, whilst Lumiflavin and Lumichromes are other representatives of Flavins. Iso- and alloxazines (alloxazines are well known as photochemical decomposition products of Flavins) are closely related compounds as shown in figure 6.1 in detail in section 6.1, yet their spectroscopic and photophysical properties are quite different. Alloxazine will be used as a sensitiser to follow the rates of formation of Juglone in both conventional solvents and in super critical carbon dioxide.

8.14 Effect of the initial rate of formation of Juglone with the change in pressure and temperature using Alloxazine as a sensitiser in $scCO_2$

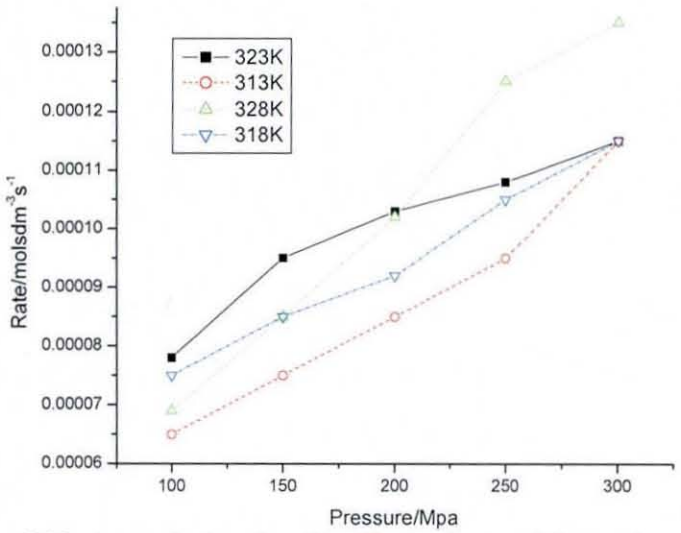

Figure 8.22: A graph showing the effects of rate of formation of Juglone using Alloxazine as a sensitiser at different temperature and pressures

Alloxazine was used as a sensitiser in both methanol and in $scCO_2$, the rates of formation of Juglone increases with an increase in pressure but there was no overall trend with the increase in temperature. The lifetimes of the three sensitisers used were measured and recorded in Table 8.8 and 8.9 respectively, with Alloxazine showing the longest lifetime.

	Singlet Oxygen Lifetimes in Acetonitrile/μs		
T/K	**MB**	**Anthracene**	**Alloxazine**
313	45.3	59.2	63.7
318	44.7	64.1	55.9
323	42.7	58.7	37.3
328	49.3	38.5	44.9

Table 8.8: Singlet Oxygen Lifetimes in Acetonitrile/μs

sensitiser	Pressure/Mpa	Temp/K	Av. Lifetime/μs
MB	100	313	37.6
MB	150	318	41.1
MB	200	323	40.2
MB	250	328	43.1
Anthracene	100	313	65.4
Anthracene	150	318	49.2
Anthracene	200	323	53.7
Anthracene	250	328	63.5
Alloxazine	100	313	40.4
Alloxazine	150	318	52.7
Alloxazine	200	323	64.7

Table 8.9: Singlet Oxygen Lifetimes in scco2 at different temperatures and pressures

Since light and sensitiser are the major factor in the production of Juglone a copy of the xenon arc lamp output spectrum, in figure 8.23 was analysed and it showed that where light absorption for flavins as a sensitiser is lower than for MB and RB hence the better production of Juglone with the latter than the former.

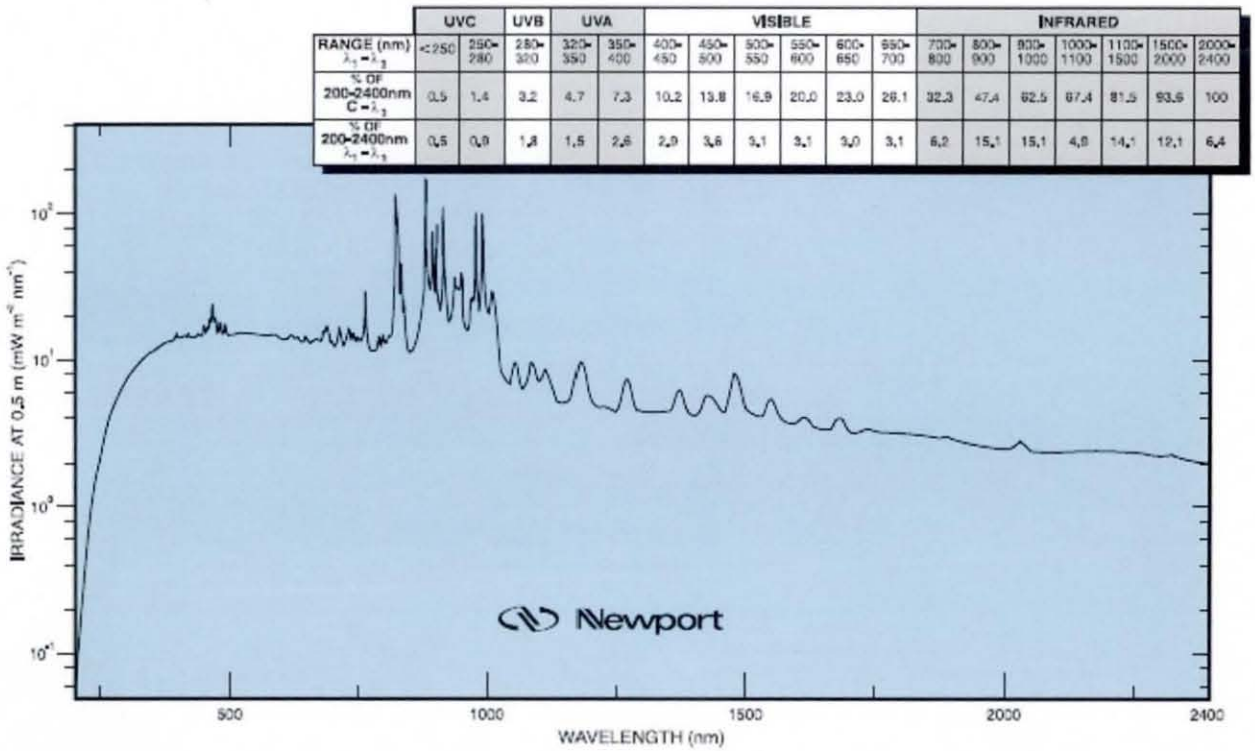

Figure 8.23: Showing a Standard Xenon arc lamp output showing constant output throughout the absorbance area of the sensitisers

9.0 Conclusions

Comparison of the [MB] and [DHDN] in methanol and in $scCO_2$ were similar, which implies that the stability of the Juglone production is good in the cell.

Acetonitrile was the best solvent to carry out the reaction with as the initial rate is faster than in methanol and in $scCO_2$, this is due to its long singlet oxygen lifetime and the high rate constant. Likewise $scCO_2$ has a longer singlet oxygen lifetime than Acetonitrile but the rate is limited by its low rate constant. It is believed that the reason the rate constant is higher in both methanol and Acetonitrile is due to the polar behaviour of the solvents compared to $scCO_2$, in which the polar solvent helps in stabilizing the intermediate that forms.

The concentration of the sensitiser only affects the rate of the reaction slightly as it's used up in the catalytic form, however adding more oxygen into the reaction does not affect the rate. This is because the concentration of Methylene Blue is much lower than that of the oxygen concentration. It has been found that the rate of Juglone production is reaction controlled and not diffusion controlled as the experimental rate constants (k_2) values are 1.26×10^5 in methanol which is a lot lower than the theoretical value of 1.10×10^{10} $mol^{-1}dm^3s^{-1}$. Furthermore it has also been found out that Rose Bengal, Anthracene and Alloxazine can also be used in the formation of Juglone as sensitisers in both $scCO_2$ and in conventional solvents. Comparison of the [MB] and [DHDN] in methanol and in $scCO_2$ were similar, which implies that the stability of the Juglone production is good in the cell.

The rate of production of Juglone in $scCO_2$ increases with increasing pressure and temperature, irrespective of sensitiser used at lower temperature and pressure, such a variation may be explained on the basis of the thermodynamics of encounter complex formation.

The effect of 1, 5-dihydroxynaphthalene concentration on the initial rate in the solvents; methanol, Acetonitrile and Supercritical carbon dioxide are similar. Acetonitrile shows a faster initial rate than methanol, which may be explained in part on the basis of the longer singlet oxygen lifetime[6], although the enhancement is less than may be expected on the basis of a simple dependence on lifetime. In supercritical fluid carbon dioxide,

the rate is significantly lower than may be expected on the basis of the Acetonitrile data, suggesting a perturbation of second order rate constant.

The concentration of the sensitiser only affects the rate of the reaction slightly, however adding more oxygen into the reaction does not affect the rate. This is because the concentration of sensitiser is much lower than that of the oxygen concentration. It has been found that the rate of Juglone production is reaction controlled and not diffusion controlled as the experimental rate constants (k_2) values are 1.26×10^5 in methanol which is a lot lower than the theoretical value of 1.10×10^{10} $mol^{-1}dm^3s^{-1}$.

References

1. Tundo, P.; Anastas, P.T; Black, D.S.; Breen, J.; Collins, T.; Memoli, S.; Miyamoto, J.; Poliakoff, M.; and Tumas, W.; *Pure Appl. Chem.*, **2000**, 72, 1207-1228.
2. Anastas, P.T.; and Warner, J.C.; *Green Chemistry: Theory and Practice*, Oxford University Press, Oxford England ; New York, **1998**.
3. Constable, D.J.C.; Dunn, P.J.; Hayler, J.D.; Humphrey, G.R.; Leazer Jr., J.L.; Linderman, R.J.; Lorenz, K; Manley, J.; Pearlman, B.A.; Wells, A; Zaks, A.; and Zhang, T.Y.; *Green Chem.*, **2007**, 9, 411-420.
4. Lancaster, M.; *Green Chemistry: an Introductory Text*, Royal Society of Chemistry, Cambridge, **2002**.
5. Albini, A. and Fagnoni, M.; in *Green Chemical Reactions*, ed. P. Tundo and V. Esposito, Springer, Dordrecht ; London, **2008**, p. 173-189.
6. Braslavsky, S.E.; Acuna, A.U.; Adam, W.; Amat, F.; Armesto, D.; Atvars, T.D.Z.; Bard, A.; Bill, E.; Bjoern, L.O.; Bohne, C.; Bolton, J.; Bonneau, R.; Bouas-Laurent, H.; Braun, A.M.; Dale, R.; Dill, K.; Doepp, D.; Duerr, H; Fox, M.; Gandolfi, T.; Grabowski, Z.R.; Griesbeck, A.; Kutateladze, A.; Litter, M.; Lorimer, J.; Mattay, J.; Michl, J.; Miller, R.J.D.; Moggi, L.; Monti, S.; Nonell, S.; Ogilby, P.; Olbrich, G.; Oliveros, E.; Olivucci, M.; Orellana, G.; Prokorenko, V.; Naqvi, K. R.; Rettig, W.; Rizzi, A.; Rossi, R.A.; San Roman, E.; Scandola, F.; Schneider, S.; Thulstrup, E.W.; Valeur, B.; Verhoeven, J.; Warman, J.; Weiss, R.; Wirz, J.; and Zachariasse, K.; *Pure Appl. Chem.*, **2007**, 79, 293-465.
7. Coyle, J.D.; *Introduction to Organic Photochemistry*, Wiley, Chichester West Sussex; New York, **1986**.
8. Cowan, D.O.; and Drisko, R.L.; *Elements of Organic Photochemistry*, Plenum Press, New York, **1976**.
9. Rohatgi-Mukherjee, K.K.; *Fundamentals of Photochemistry*, Wiley, New York, **1978**.
10. Mori, T. and Inoue, Y; *Synthetic Organic Photochemistry*, ed. A. G. Griesbeck and J. Mattay, Marcel Dekker, New York, **2005**, p. 417-452.

11. Müller, A.M.; Lochbrunner, S.; Schmid, W.E.; and Fuss, W.; *Angew. Chem. , Int. Ed. Engl.*, **1998**, 37, 505-507.
12. Müller, A.M.; Lochbrunner, S.; Schmid, W.E.; and Fuss, W; *Angew. Chem.*, **1998**, 110, 520-522.
13. Liu, R.S.H. and Hammond, G.S.; *Chem. Eur. J.*, **2001**, 7, 4536-4544.
14. Wagner, P.J.; *Synthetic Organic Photochemistry*, ed. A. G. Griesbeck and J. Mattay, Marcel Dekker, New York, **2005**, p. 11-39.
15. Griesbeck, A.G.; *Synthetic Organic Photochemistry*, ed. A. G. Griesbeck and J. Mattay, Marcel Dekker, New York, **2005**, p. 89-139.
16. Armesto, D.; Ortiz, M.J.; and Agarrabeitia, A.R.; *Synthetic Organic Photochemistry*, ed. A. G. Griesbeck and J. Mattay, Marcel Dekker, New York, **2005**, p. 161-187.
17. Hutchison, J.; in *Photochemistry in Organic Synthesis*, ed. J. D. Coyle, Royal Society of Chemistry, London, **1986**, p. 314-333.
18. Kautsky, H. and de Bruijn, H.; *Naturwissenschaften*, **1931**, 19, 1043.
19. Khan, A. and Kasha, M..; *J. Chem. Phys.*, **1963**, 39, 2105-2106.
20. Foote, C.S. and Wexler, S.; *J. Am. Chem. Soc*, **1964**, 86, 3880-3881.
21. Foote, C.S. and Wexler, S.; *J. Am. Chem. Soc.*, **1964**, 86, 3879-3880.
22. Corey, E.J. and Taylor, W.C.; *J. Am. Chem. Soc*, **1964**, 86, 3881-3882.
23. Aubry, J.M.; *J. Am. Chem. Soc.*, **1985**, 107, 5844-5849.
24. Aubry. J.M. and Cazin, B; *Inorg. Chem.*, **1988**, 27, 2013-2014.
25. Turro, N.J.; Ramamurthy, V; Liu, K.C.; Krebs, A.; and Kemper, R; *J. Am. Chem. Soc.*, **1976**, 98, 6758-6761.
26. Wasserman, H.H.; and Scheffer, J.R.; *J. Am. Chem. Soc.*, **1967**, 89, 3073-3075.
27. Khan, A.U.; *J. Phys. Chem.*, **1976**, 80, 2219-2228.
28. Schmidt, R.; *Photochem. Photobiol.*, **2006**, 82, 1161-1177.
29. Greer, A; *Acc. Chem. Res.*, **2006**, 39, 797-804.
30. Clennan, E.L.; *Synthetic Organic Photochemistry*, ed. A. G. Griesbeck and J. Mattay, Marcel Dekker, New York, **2005**, p. 365-390.
31. Bourne, R.A.; Han, X.; Poliakoff, M.; and George, M.W.; *Angew. Chem. Int. Ed.* **2009**, 48, 5322-5325.

32. Bourne, R.A.; Han, X.; Poliakoff, M.; and George, M.W.; *Chem.Comm.*, **2008**, 4457-4459.

33. Prahl, S.; http://omlc.ogi.edu/spectra/PhotochemCAD/html/rosebengal.html, OMLC, Oregon Health and Sciences University, **1995**.

34. Prahl, S.; http://omlc.ogi.edu/spectra/mb/index.html, OMLC, Oregon Health and Sciences University, **1998**.

35. Prahl, S.; http://omlc.ogi.edu/spectra/PhotochemCAD/html/TPP.html, OMLC, Oregon Health and Sciences University, **1998**.

36. Murtinho, D.; Pineiro, M.; Pereira, M.M.; Gonsalves, A.M.D.; Arnaut, L.G.; Miguel, M.D.; and Burrows, H.D.; *J. Chem. Soc. , Perkin Trans. 2,* **2000**, 2441-2447.

37. Ribeiro, S.M.; Serra, A.C.; and Gonsalves, A.M.D.R.; *Tetrahedron,* **2007**, 63, 7885-7891.

38. Gerdes, R.; Bartels, O.; Schneider, G.; Wohrle, D.; and Schulz-Ekloff, G.; *Int. J. Photoenergy,* 1999, 1, 41-47.

39. Alfonsi, K.; Colberg, J.; Dunn, P.J.; Fevig, T.; Jennings, S.; Johnson, T.A.; Kleine, H.P.; Knight, C.; Nagy, M.A.; Perry, D.A. and Stefaniak, M; *Green Chem.*, **2008**, 10, 31-36.

40. Griesbeck, A.G. and Bartoschek, A.; *Chem. Commun.*, **2002**, 1594-1595.

41. Griesbeck, A.G.; El-Idreesy, T.T.; Fiege, M.; and Brun, R.; *Org. Lett.*, **2002**, 4, 4193-4195.

42. Fenical, W.H.; Kearns, D.R. and Radlick, P; *J. Am. Chem. Soc.*, **1969**, 91, 3396-3398.

43. Iesce, M.R.; in *Synthetic Organic Photochemistry*, ed. A. G. Griesbeck and J. Mattay, Marcel Dekker, New York, **2005**, p. 299-363.

44. Jähnisch, K. and Dingerdissen, U; *Chem. Eng. Technol.*, **2005**, 28, 426-427.

45. Braun, A.M.; Maurette, M.T. and Oliveros, E.; *Photochemical Technology*, Wiley, Chichester, West Sussex, England ; New York, **1991**.

46. Gollnick, K.; *Chim. Ind.*, **1982**, 63, 156-166.

47. Pfoertner, K.H.; *J. Photochem. Photobiol. , A,* **1990**, 51, 81-86.

48. Kreisel, G.; Meyer, S.; Tietze, D.; Fidler, T.; Gorges, R.; Kirsch, A.; Schaefer, B. and Rau, S.; *Chem. Ing. Tech.,* **2007**, 79, 153-159.

49. Ciana, C.L. and Bochet, C.G.; *Chimia,* **2007**, 61, 650-654.

50. Eissen, M. and Metzger, J.O.; *Chem. Eur. J.,* **2002**, 8, 3580-3585.

51. Albini, A.; Fagnoni, M.; and Mella, M.; *Pure Appl. Chem.,* **2000**, 72, 1321-1326.

52. Razzaq, T. and Kappe, C.O.; *ChemSusChem,* **2008**, 1, 123-132.

53. Protti, S.; Dondi, D.; Fagnoni, M.; and Albini, A.; *Pure Appl. Chem.,* **2007**, 79, 1929-1938.

54. Schiel, C.; Oelgemöller, M.; Ortner, J.; and Mattay, J.; *Green Chem.,* **2001**, 3, 224-228.

55. Mattay, J. and Oelgemöller, M; *CRC Handbook of Organic Photochemistry and Photobiology, 2nd Edition*, ed. W. M. Horspool and F. Lenci, CRC Press, Boca Raton, **2004**, p. 88-03-88-45.

56. Oelgemöller, M.; Jung, C.; Ortner, J.; Mattay, J.; and Zimmermann, E.; *Green Chem.,* **2005**, 7, 35-38.

Chapter 9

Conclusions

9. Conlusions

The fluorescence quenching constants of 3TARF, BR and 1R in methanol are 2.38 x 10^9, 2.69 x 10^9 and 8.13 x 10^8 l mol^{-1} s^{-1} respectively. The lifetimes (τ_0) of the compounds are 5.4 x 10^{-9} s for 3TARF, 4.8 x 10^{-9} s for BR and 6.3 x 10^{-9} s for 1R. Although there is no theoretical data to compare these values with, the values obtained seem to obey the Stern-Volmer relation and gave a linear plot of Stern-Volmer with an intercept at approximately to one. BR was observed to have the highest fluorescence quenching constant followed by 3TARF and the 1R, whilst the reverse is seen in their lifetimes with IR having the longest lifetime followed by 3TARF and then BR.

The fluorescence quantum yield for RR in different solvents were of the value between 0.59 – 0.149 with the highest value in ethanol compared to other solvents whilst the least was observed in water.

Lifetime measurements of RR in different solvents were measured using the photon counting technique and the results were in methanol 5.3 ns and 2.89 ns in Acetonitrile and 5.2 ns in ethanol. There is a significant amount of triplet-triplet state in the different 6,9 Mall in water and in methanol but there was no significant increase on the addition of bromobenzene.

The detection of the decay constant for singlet oxygen in super critical carbon dioxide was made possible after constructing the set up shown in section 6.6 and obtained a range of values of the singlet oxygen quantum yield of anthracene which are within the expected value of less than one which have not been reported before.

The values obtained for the singlet oxygen quantum yield of anthracene in supercritical carbon dioxide range between 0.2-0.8, which are reasonable values in the context of known anthracene Photophysics. Increase in pressure increases the singlet oxygen quantum yield of anthracene, but increase in concentration decreases the singlet oxygen quantum yield of anthracene. And it is this explanation which explains the observed dependencies.

In general, an increase in pressure appears to result in a small increase in the quantum yield, which becomes less apparent at the higher temperatures and therefore can be explained in terms of an increase in solvent density. An increase in concentration was

also observed with increasing pressure, since solvent density increases with pressure and therefore more anthracene dissolved.

Comparison of the [MB] and [DHDN] in methanol and in $scCO_2$ were similar, which implies that the stability of the Juglone production is good in the cell.
Acetonitrile was the best solvent to carry out the reaction with as the initial rate is faster than in methanol and in $scCO_2$, this is due to its long singlet oxygen lifetime and the high rate constant. Likewise $scCO_2$ has a longer singlet oxygen lifetime than Acetonitrile but the rate is limited by its low rate constant. It is believed that the reason the rate constant is higher in both methanol and Acetonitrile is due to the polar behaviour of the solvents compared to $scCO_2$, in which the polar solvent helps in stabilizing the intermediate that forms.

Acetonitrile shows a faster initial rate than methanol, which may be explained in part on the basis of the longer singlet oxygen lifetime, although the enhancement is less than may be expected on the basis of a simple dependence on lifetime. In supercritical fluid carbon dioxide, the rate is significantly lower than may be expected on the basis of the Acetonitrile data, suggesting a perturbation of second order rate constant.

The concentration of the sensitiser only affects the rate of the reaction slightly as it's used up in the catalytic form, however adding more oxygen into the reaction does not affect the rate. This is because the concentration of sensitiser is much lower than that of the oxygen concentration. It has been found that the rate of Juglone production is reaction controlled and not diffusion controlled as the experimental rate constants (k_2) values are 1.26×10^5 in methanol which is a lot lower than the theoretical value of $1.10 \times 10^{10}\ mol^{-1}dm^3s^{-1}$. Furthermore it has also been found out that Rose Bengal, Anthracene and Alloxazine can also be used in the formation of Juglone as sensitisers in both $scCO_2$ and in conventional solvents.

The rate of production of Juglone in $scCO_2$ increases with increasing pressure and temperature, irrespective of sensitiser used at lower temperature and pressure, such a variation may be explained on the basis of the thermodynamics of encounter complex formation. Nonetheless there was no apparent trend with the effects of varying temp

and pressure overall, whilst at higher temperature there seem to reduce it and at a temperature of 323K which is the highest there seem to reach the peak as all the rates were constant. This could be due to the fact that the initial rates of formation of Juglone have reached its optimum temperature and no more can be formed.
The effect of 1, 5-dihydroxynaphthalene concentration on the initial rate in the solvents; methanol, and Supercritical carbon dioxide are similar whilst for acetonitrile was longer due to its singlet oxygen lifetime.

Chapter 10

Further Work

10. Further Work

- Although singlet oxygen quantum yields have been measured for anthracene relative to Perinapthenone, it would be of use to measure a wider range of sensitisers to obtain relative yields, and to evaluate whether temperature and pressure dependences are specific or generic.

- It would be of interest if more work could be done for the other types flavins and using different solvent. It would also be of interest to obtain more triplet-triplet spectra for more flavins and to further investigate the effect of bromobenzene on the triplet yields.

- An in depth investigation could seek to discover the effect of conducting the juglone synthesis at different temperatures, pH or with more solvents. The study of pH could interesting when considering the theorised mechanism for the reaction as an excess of H^+ ions may scavenge the hydroxyl group when eliminated from the ring structure, slowing the rate of formation whilst a high pH may act conversely to speed the reaction up. There is also clearly more work to be done in investigating the effects of temperature and pressure on rates and yields, and more data on this would allow evaluation of activation volumes for the reaction in $scCO_2$.

Chapter 11

Appendix

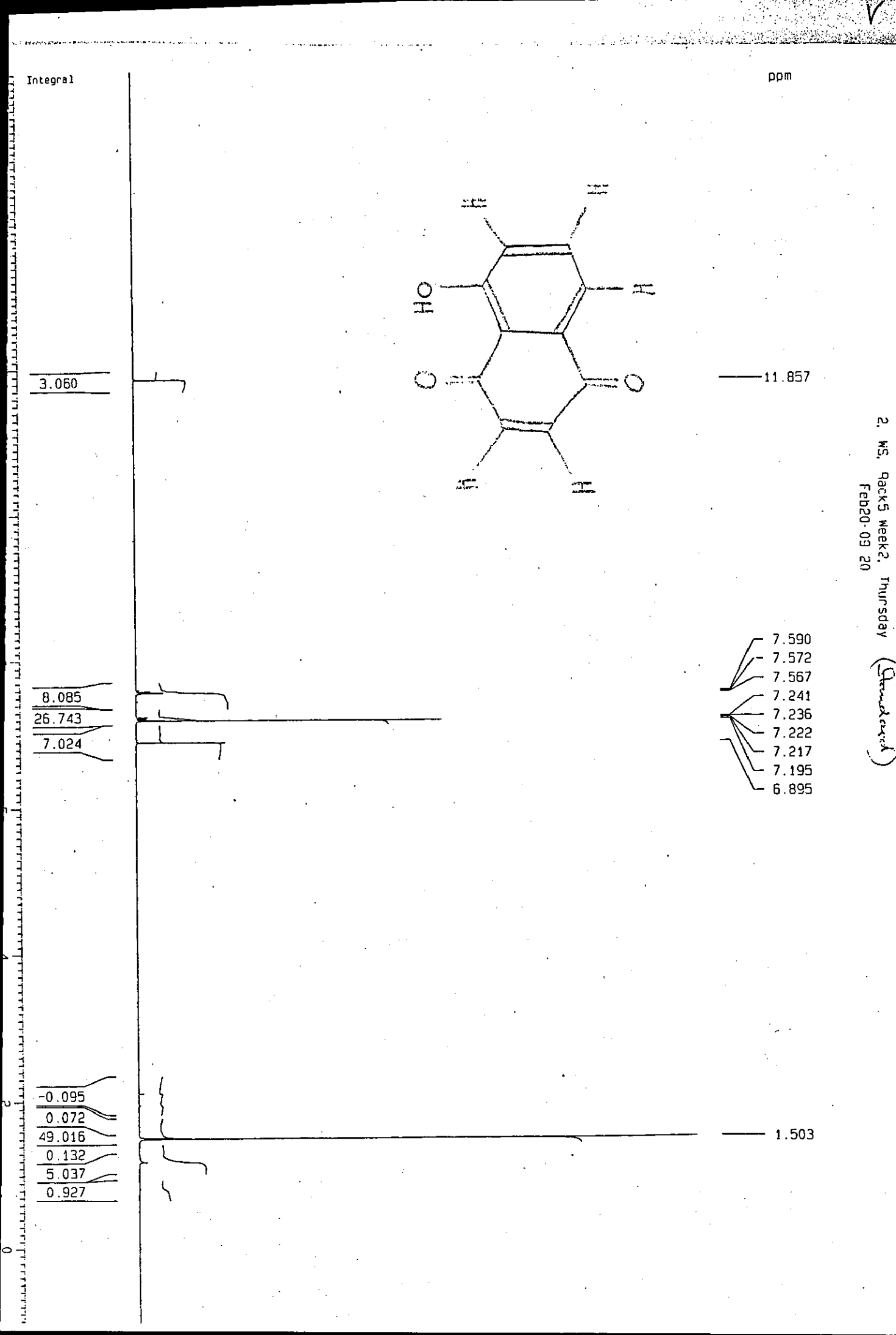
Integral
ppm
3.060
8.085
26.743
7.024
-0.095
0.072
49.016
0.132
5.037
0.927
11.857
7.590
7.572
7.567
7.241
7.236
7.222
7.217
7.195
6.895
1.503
2, WS, Pack5 Week2, Thursday
Feb20-09 20

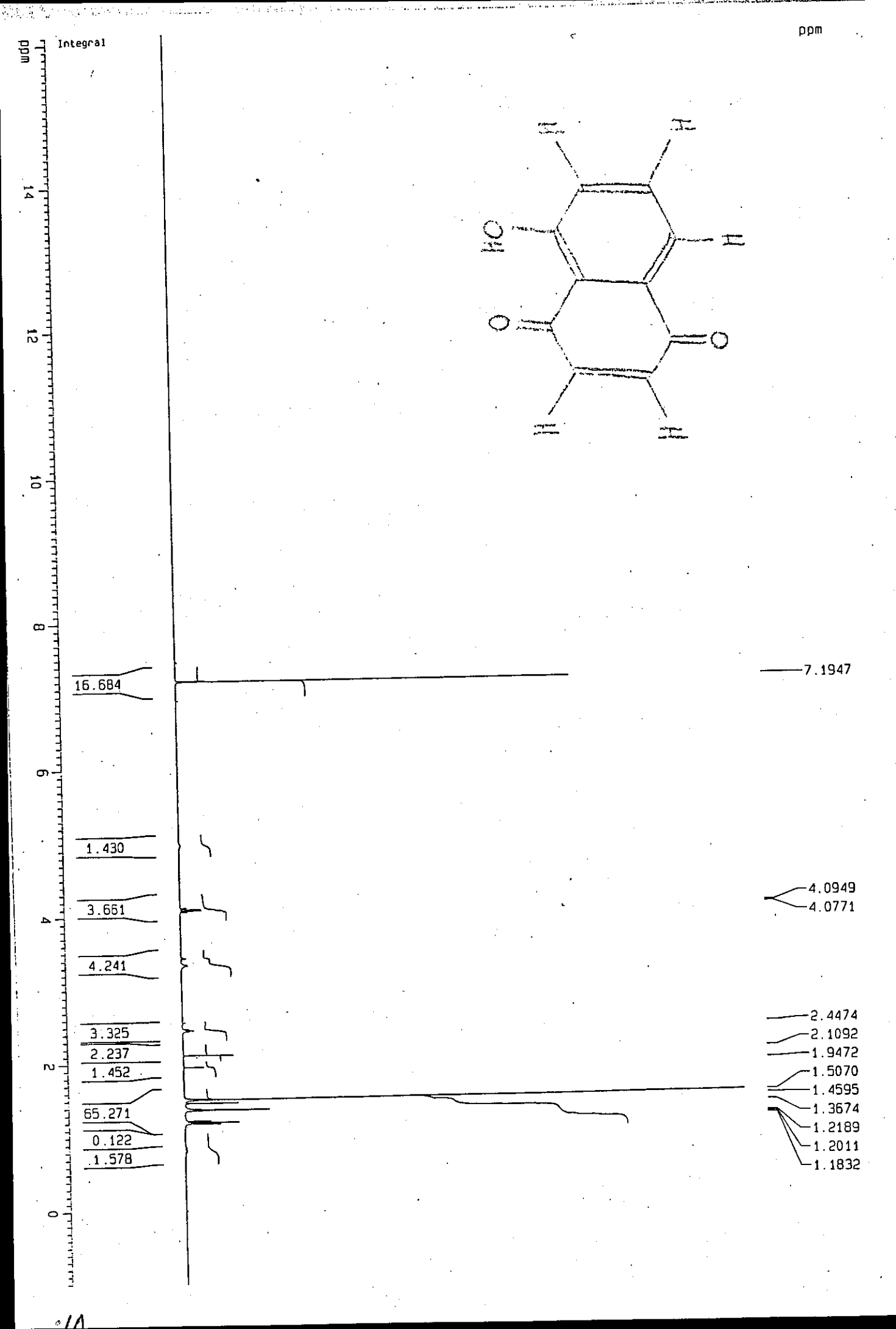
ppm
Integral
ppm
14
12
10
8
6
4
2
0
16.684
1.430
3.661
4.241
3.325
2.237
1.452
65.271
0.122
1.578
7.1947
4.0949
4.0771
2.4474
2.1092
1.9472
1.5070
1.4595
1.3674
1.2189
1.2011
1.1832
H
H
HO
H
O
O
H
H

ChemNMR H-1 Estimation

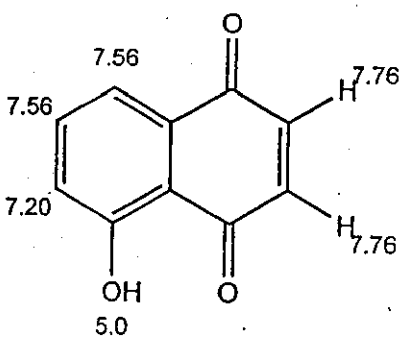

Estimation Quality: blue = good, magenta = medium, red = rough

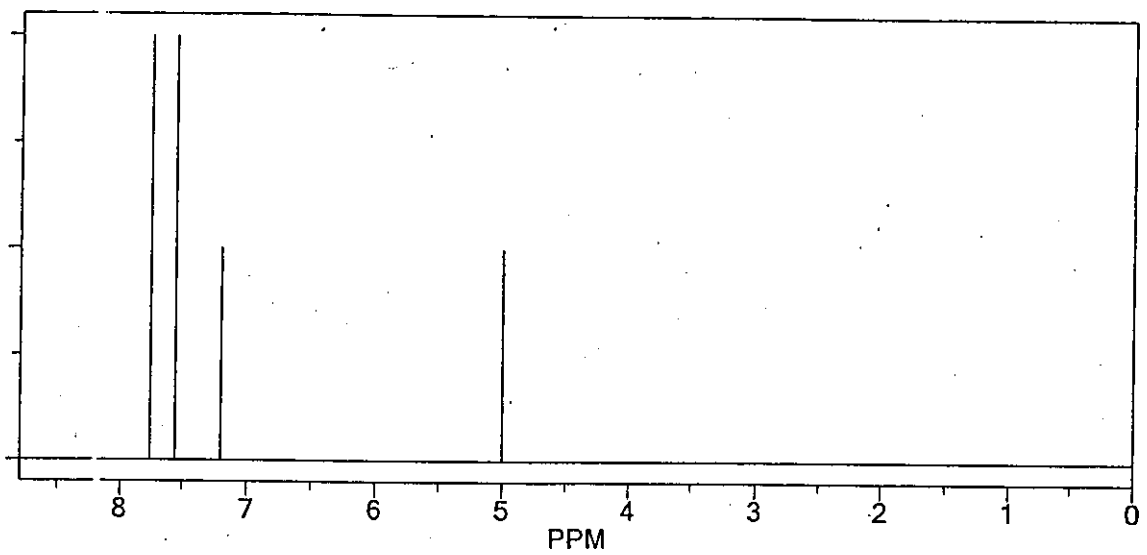

Protocol of the H-1 NMR Prediction:

Node	Shift	Base + Inc.	Comment (ppm rel. to TMS)
CH	7.56	7.26	1-benzene
		-0.17	1 -O
		0.28	1 -C=O
		0.19	1 -C=O
CH	7.20	7.26	1-benzene
		-0.53	1 -O
		0.19	1 -C=O
		0.28	1 -C=O
CH	7.56	7.26	1-benzene
		-0.44	1 -O
		0.19	1 -C=O
		0.55	1 -C=O
OH	5.0	5.00	aromatic C-OH
H	7.76	5.25	1-ethylene
		1.95	1 -C(=O)-1:C*C*C*C*C*C*1 gem
		0.56	1 -C(=O)-1:C*C*C*C*C*C*1 trans
H	7.76	5.25	1-ethylene
		0.56	1 -C(=O)-1:C*C*C*C*C*C*1 trans
		1.95	1 -C(=O)-1:C*C*C*C*C*C*1 gem

Juglone Standard IR. Spec. 19/02/09

viii.

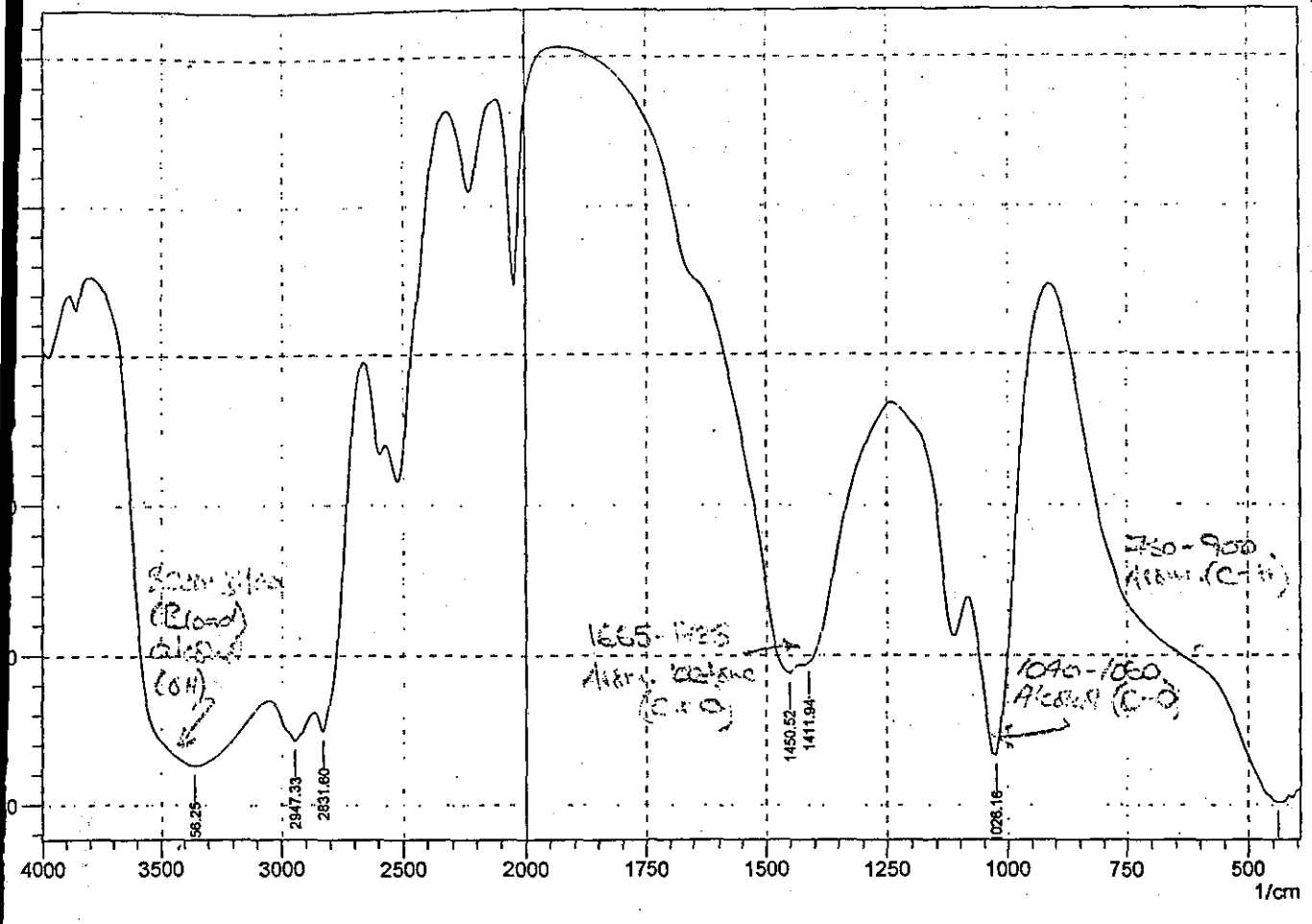

	Peak	Intensity	Corr. Intensity	Base (H)	Base (L)	Area	Corr. Area
	439.78	0.189	3.821	910.43	393.49	603.075	37.005
	1026.16	3.367	17.389	1080.17	918.15	140.75	36.423
	1411.94	9.345	0.758	1419.66	1242.2	131.211	0.483
	1450.52	8.777	1.846	1928.88	1435.09	248.912	1.722
	2831.6	4.924	4.975	2862.46	2669.57	174.477	13.208
	2947.33	4.294	2.207	3047.63	2870.17	225.292	14.913
	3356.25	2.637	15.83	3796.04	3055.35	856.804	263.293

Juglone sample IR Spec. 19/02/09

ix.

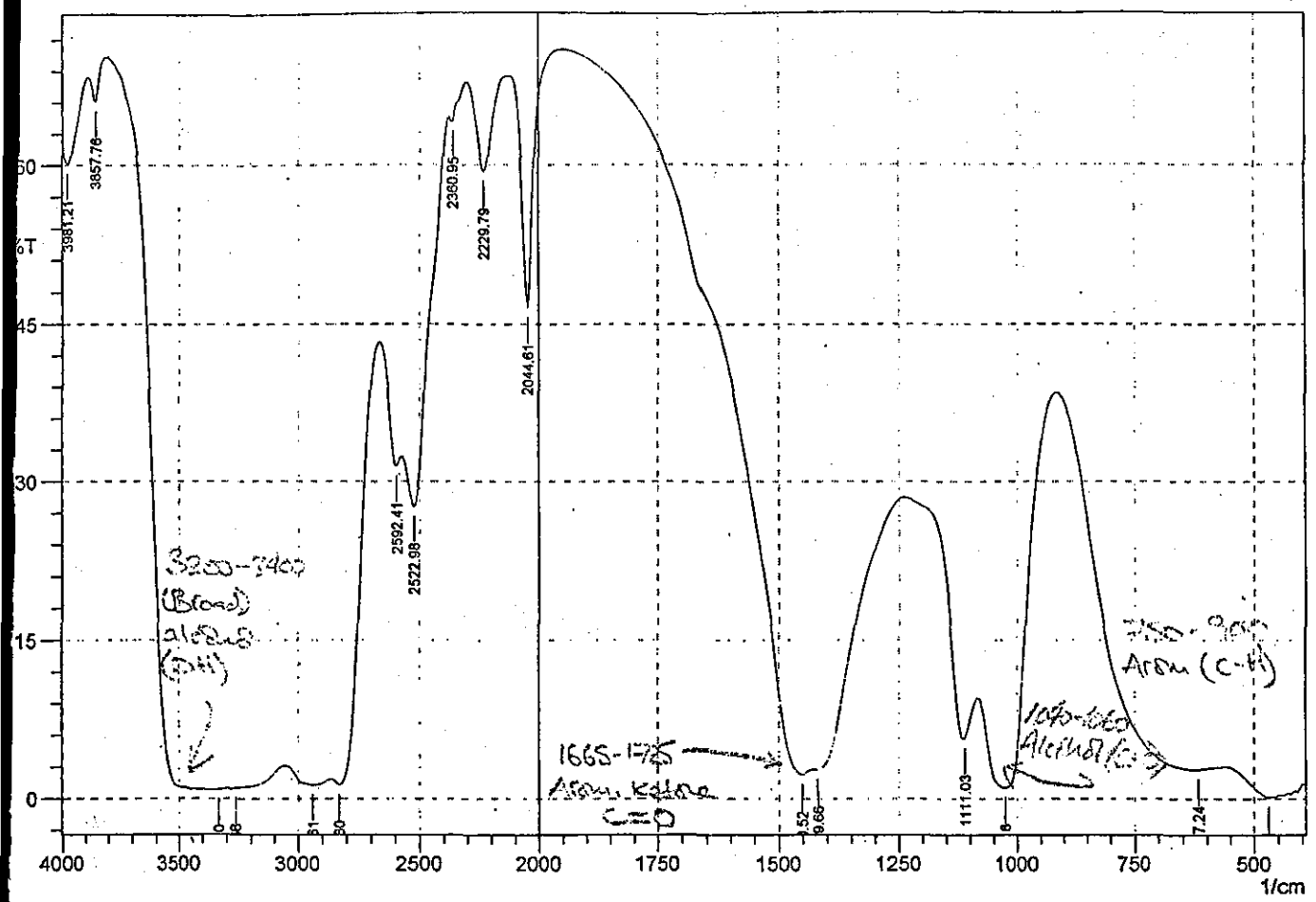

	Peak	Intensity	Corr. Intensity	Base (H)	Base (L)	Area	Corr. Area
	470.65	0.113	2.061	555.52	393.49	348.269	73.9
	617.24	2.755	5.814	910.43	563.23	395.533	58.73
	1026.16	1.035	18.043	1080.17	918.15	179.875	67.492
	1111.03	5.699	6.819	1234.48	1087.89	115.731	9.104
	1419.66	2.732	1.119	1427.37	1242.2	163.057	1.72
	1450.52	2.216	2.588	1944.31	1435.09	237.262	3.135
	2044.61	46.559	23.022	2121.77	1952.03	35.272	8.709
	2229.79	59.347	8.772	2299.22	2121.77	33.573	4.063
	2360.95	64.083	1.211	2376.38	2306.94	12.528	0.178
0	2522.98	27.56	12.833	2569.27	2384.1	72.039	10.203
1	2592.41	31.398	2.922	2661.85	2576.98	37.898	1.411
2	2831.6	1.313	7.186	2862.46	2669.57	201.516	21.562
3	2939.61	1.301	1.031	3055.35	2870.17	327.059	26.568
4	3263.66	1.023	0.077	3271.38	3063.06	376.101	13.736
5	3333.1	0.89	0.021	3340.82	3302.24	78.471	0.415
6	3857.76	66.043	3.239	3888.62	3819.18	11.564	0.585
7	3981.21	60.128	2.65	4004.35	3896.34	21.272	1.056

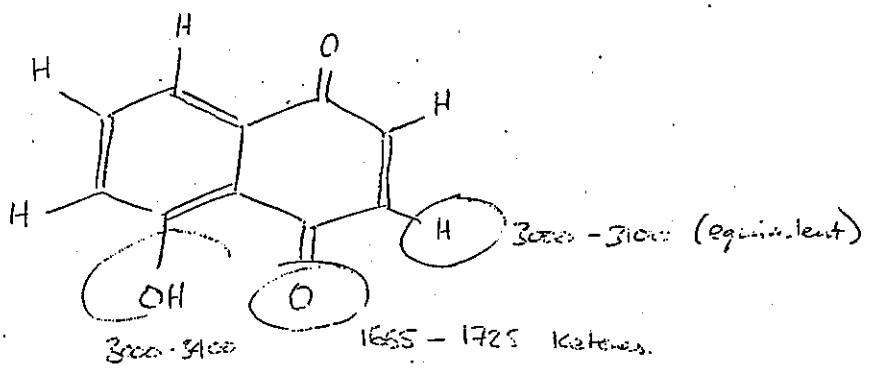

Posters Presentation

DYE SENSITISED PHOTOOXIDATION OF 1,5-DIHYDROXYNAPHTHALENE TO JUGLONE IN SUPERCRITICAL FLUID CARBON DIOXIDE

Nadya Muhammed and David R. Worrall

Department of Chemistry, Loughborough University, Loughborough, UK, LE11 3TU

Email: cmnm3@lboro.ac.uk

oduction

inetics of photo oxygenation of 1,5-dihydroxynaphthalene (DHDN) has been ed using a home built set up as shown in figure 1. The investigation was carried out if it is a suitable method to produce the much more expensive product Juglone. 5-xy1-4-naphthquinone (Juglone, **2**) which is an important intermediate in the naceutical and agrochemical industry[1]. Juglone is produced naturally in walnut trees, ver in industry it is conventionally produced using strong hazardous oxidizing s. A 'greener' and safer method of production of Juglone is dye-sensitized photo nation of cheap and commercially available 1,5-dihyrdoxnaphthalene (DHDN) **1** as n in scheme 1.

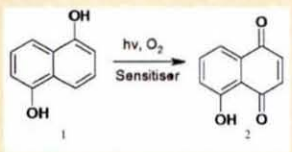

Scheme 1: Photo oxygenation of 1,5-dihydroxynaphthalene

eaction was carried out in conventional organic solvents such as methanol and nitrile in addition to supercritical carbon dioxide ($scCO_2$), to investigate weather the her' approach to chemistry can be applied and its rate of kinetics of formation was ved for this reaction. The progress of the reaction was monitored using the optic through the absorbance spectroscopy in the home built setup as shown in figure 1 .

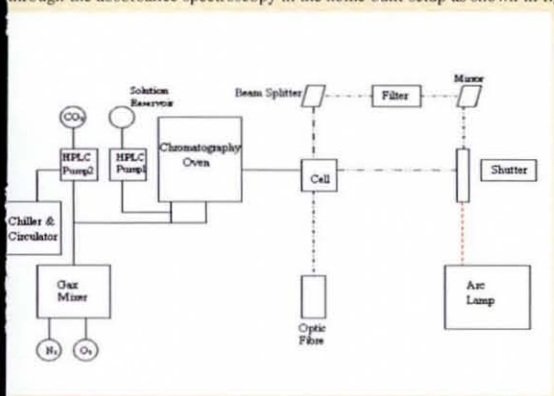

e 1: A schematic diagram of the set up used for the supercritical carbon dioxide.

sensitiser when irradiated with light produces and excites the oxygen into a singlet which in turn reacts with the 1,5-dihydroxynaphthalene to form Juglone. This is a n cleaner and cheaper way to produce Juglone than the industrial production of using g hazardous oxidizing agents. Many studies of this reaction have been carried out various sensitisers such as Methylene Blue (MB), Rose Bengal and other complex . Production of singlet oxygen in supercritical carbon dioxide, and the lifetime has demonstrated to be long in comparison with conventional solvents[3,4] being 5.1 ms at kg cm^{-2} and 41°C 1. In this study, we have utilised dye sensitised singlet oxygen to t the transformation of 1,5-dihydroxynaphthalene to juglone in supercritical fluid on dioxide, monitoring the production of juglone *in situ* using UV-visible trophotometry. A number of sensitisers soluble in supercritical fluid carbon dioxide vailable including anthracene and methylene blue. The effects of temperature and sure on the observed reaction rates have been studied and are discussed. Comparison ade with the equivalent reaction in conventional solvents.

sults and Discussion

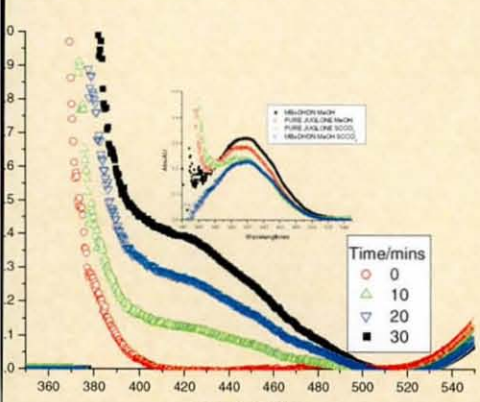

h 1: Juglone production in scCO2 using MB as a sensitiser and DHDN in scco2 at 100KPa and 308K
h 1 clearly shows the Juglone production increases with time, the reaction seem to be independent on the tiser and oxygen concentration, but does depend on the increase of DHDN. On the inset of graph 1 a parison of pure Juglone (Aldrich) is similar to the produced from the dye sensitized photo oxygenation.

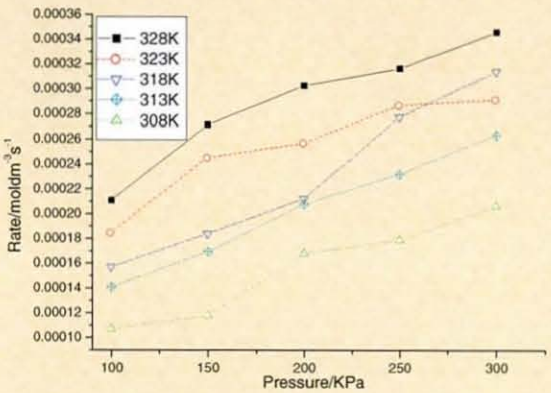

Graph 2: Effect of changing temperature and pressure on the initial kinetics rates of formation of Juglone in scCO2 using MB as a sensitiser

The rate of kinetics of the production of Juglone in scCO2 seem to increase with increasing pressure and temperature as shown in graph 2.

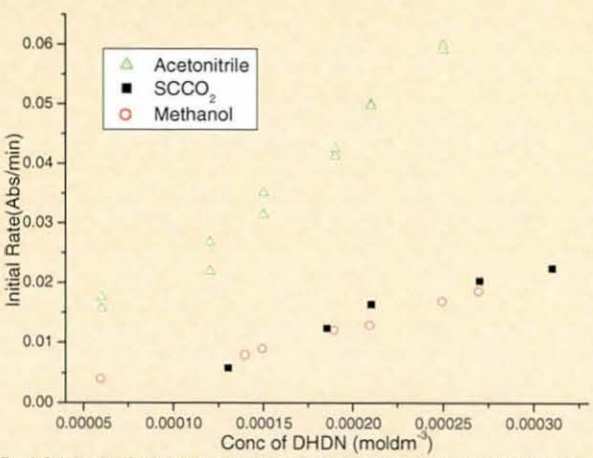

Graph 3: Increasing [DHDN] verses Initial rate for the solvents Methanol, Acetonitrile and scCO2.

The effect of 1, 5-dihydroxynaphthaline concentration on the initial rate in the solvents; methanol, Acetonitrile and Supercritical carbon dioxide is shown in graph 3. Which shows that using Acetonitrile as the solvent produced a much faster initial rates of formation of Juglone. Supercritical carbon dioxide was faster than methanol, this is due to the fact Acetonitrile has a higher singlet oxygen lifetime. The singlet oxygen lifetime is $7.7x10^{-5}$ seconds in Acetonitrile where as in methanol it is only $9.0x10^{-6}$ seconds, hence singlet oxygen last longer in Acetonitrile whereby there is more chance of it reacting with the DHDN to produce Juglone faster.

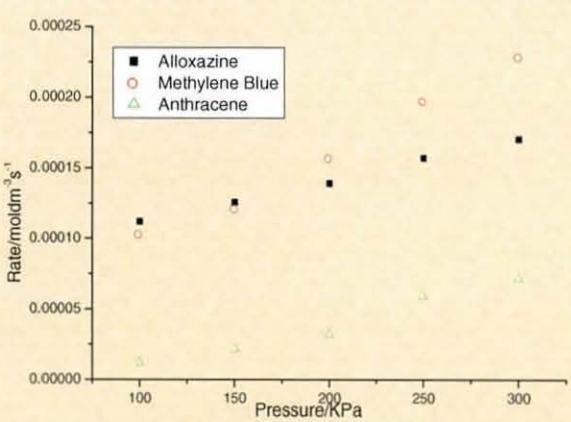

Graph 4: The rate of formation of Juglone using different sensitisers at 308K with different pressure in scco2

The rate of Juglone formation in scco2 is much slower when Anthracene is used as a sensitiser compared to Alloxazine and Methylene blue. This could be due to the fact that Anthracene

Conclusion

Juglone can be produced using the method shown in scheme 1 very effectively as [10], however we believe we are the first to study the kinetics of the reaction. The rate of production of Juglone increases as an increase in temperature and pressure increases. It has been found that the rate of Juglone production is reaction controlled and not diffusion controlled as the experimental K_2 values are $7.56x10^6$ $moldm^{-3}s^{-1}$ in methanol which is lower than the theoretical value of $1.10x10^{10}$ $moldm^{-3}s^{-1}$ [9].

ces: [1] M.Oelgemoller, C.Jung. *Green Chem*, **2005**, 7, 35. (1) D.R. Worrall, A. A. Abdel-Shafi and F. Wilkinson, *J. Phys. Chem. A*, 2001, **105**, 1270 (2)A. A. Abdel-Shafi and D. R. Worrall, *J. Photochem. Photobiol. A:Chem*, 2007, **186**, 263. [1] D. R. Worrall, F. Wilkinson, *J. Chem. Soc. Trans.* **1996**, 92, 1467. [2] D. R. [3] A.A. Abdel-Shafi, F. Wilkinson, D.R. Worrall, *Chem. Phys. Lett.* **2001**, 343, 273. [7] F. Wilkinson, *J. Phys. Chem. Reference Data*, **1993**, 22, 113. [9] S. L. Murov, I. Carmichael, G. L. Hug, *Handbook of Photochemistry*, Marcel Dekker, **1993**, 208.

Singlet Oxygen Quantum Yields of Anthracene in Supercritical Carbon Dioxide

David R. Worrall, & N. Muhammed
Department of Chemistry, Loughborough University, Loughborough, Leicestershire, LE11 3TU, UK.

1 INTRODUCTION

Singlet Oxygen has been implicated in various photodynamic oxidation reactions of industrial, biological and atmospheric importance, of which the few examples are photochemotherapy, photobleaching etc. Molecular oxygen exists as a triplet, $^3\Sigma g$, in its ground state. Quenching of aromatic molecules by oxygen forms the lowest lying excited singlet states of oxygen, $^1\Sigma g+$ (158 kJmol-1) and $^1\Delta g$ (94 kJmol^{-1}). Although the $^1\Sigma g+$ state may be formed initially, electronic to vibrational energy transfer rapidly occurs to deactivate it to the metastable and highly reactive $^1\Delta g$ state. The $^1\Delta g$ state is the active species in many important photo-processes and is more commonly known as **singlet oxygen** . Once singlet oxygen ($^1\Delta_g$) is formed it decays back to the triplet ground state, via phosphorescence and intersystem crossing.

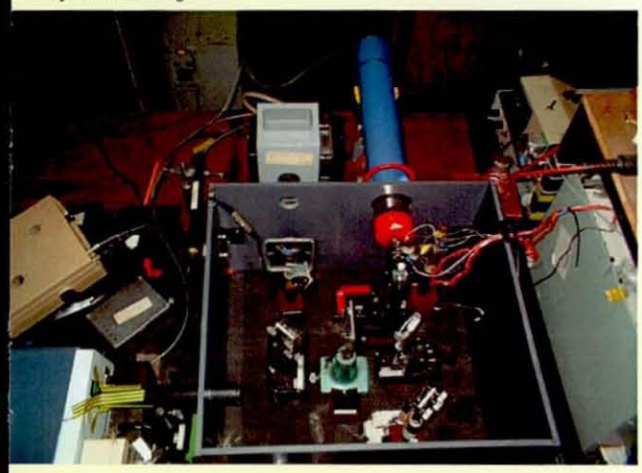

Figure 1: A picture of the home built apparatus used for measuring singlet oxygen quantum yield

The aim of this project is to measure Singlet oxygen quantum yields,ΦΔ, at varying temperatures and pressures, as a function of oxygen concentration, in supercritical fluid carbon dioxide using the home built set up as shown in pictorially in figure 1 and geometrically in figure2.

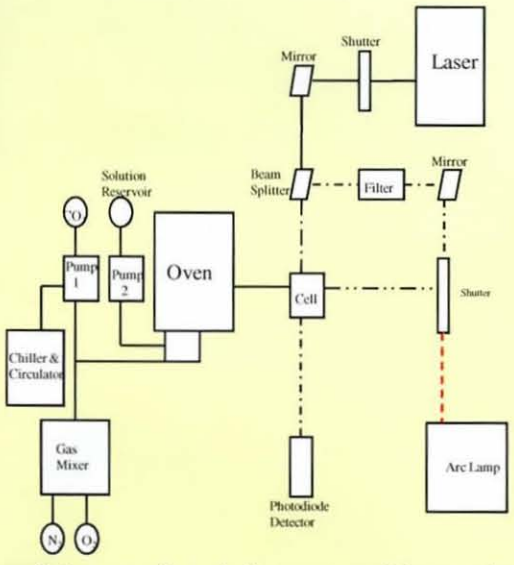

Figure 2: Geometry of home built apparatus used for measuring Singlet oxygen Quantum yield

2. SINGLET OXYGEN DETECTION

An EO-817P liquid nitrogen cooled germanium photodiode detector (North Coast Scientific), was employed to detect singlet oxygen. ΦΔ values were measured in supercritical carbon dioxide for anthracene relative to perinaphthenone as a standard sensitiser, known to be insensitive to changing solvent, for which ΦΔ is 0.95 ± 0.5 [1].

Utilising near-IR detection techniques it was possible to measure the phosphorescence of singlet oxygen at 1270nm, generated via energy transfer from perinapthenone and anthracene in supercritical carbon dioxide. An interference filter was interposed between sample and detector, to reduce detection of light scatter.

The quantum yield can be obtained from a plot of luminescence by fitting a plot of singlet decay versus time, with a single exponential affords the luminescence intensity and the decay rate constant. Experiments were performed as a function of laser energy and fitting a plot of singlet oxygen luminescence intensity versus laser energy with a straight line. The experimental setup was designed such that it was possible to measure the absorbance in the cell for each sensitiser allowing the mismatched ground state absorbances to be accounted for and corrected using the following equation.

$$\frac{m_u}{m_s} = \frac{\Phi_{\Delta u}}{\Phi_{\Delta s}}\left(\frac{1-10^{-A_s}}{1-10^{-A_u}}\right)$$

where s and u represent the sensitiser and the unknown respectively.

3. RESULTS AND DISCUSSIONS

The absorbance measurements were found to only be stable within the range of 10-15mins as shown in Fig 3, with the values being lower than in normal solvents.

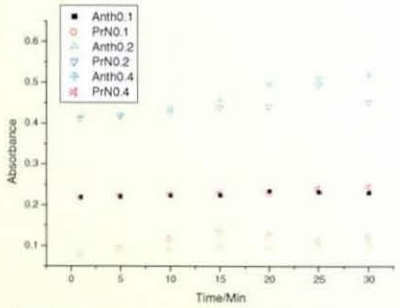

Figure 3: Absorbance measurements of Perinapthenone and anthracene In supercritical Carbon Dioxide at 355nm.

Absorbance in Supercritical CO_2		$\Phi_\Delta u$
Anthracene	Perinapthenone	
0.10	0.12	0.63
0.21	0.23	0.57
0.41	0.45	0.49

Table 1: Anthracene singlet oxygen quantum yield in supercritical carbon dioxide Using Perinapthenone as a reference sensitiser at 44.5°C and 200Kg/cm^2

4 CONCLUSIONS AND FURTHER WORK

The values obtained for the singlet oxygen quantum yield in supercritical carbon dioxide shows some variations which needs further investigation, but they are within the range of the quantum yield Φ=0.69 for the formation of either the triplet state or the singlet molecular oxygen of anthracene [2]. Further investigations with temperature and pressure change are also required as the values shown in Table 1 were obtained on a constant temperature and pressure of 44.5oC and 200Kg/cm^2.

5 REFERENCES

[1]. R.Schmidt, C. Tanielian, R. Dunsbach and C. Wolff, J Photochem. Photobiol A: Chem 79 (1-2) (1994) 11

[2]. S.Komorowski, Z. Grabowski, and W. Zielenkiewicz, J Photochem. 30 (141-51) (1985)

6 ACKNOWLEDGEMENTS

Dr D.R.Worrall, Dr S.Williams, Loughborough University and Engineering and Physical Sciences Research Council